IEC TS 62153-4-1

Edition 1.1 2020-05
CONSOLIDATED VERSION

TECHNICAL SPECIFICATION

colour inside

Metallic communication cable test methods – Part 4-1: Electromagnetic compatibility (EMC) – Introduction to electromagnetic screening measurements

IEC TS 62153-4-1:2014-01+AMD1:2020-05 CSV(en)

IEC Central Office
3, rue de Varembé
CH-1211 Geneva 20
Switzerland

Tel.: +41 22 919 02 11
info@iec.ch
www.iec.ch

About the IEC
The International Electrotechnical Commission (IEC) is the leading global organization that prepares and publishes International Standards for all electrical, electronic and related technologies.

About IEC publications
The technical content of IEC publications is kept under constant review by the IEC. Please make sure that you have the latest edition, a corrigendum or an amendment might have been published.

IEC publications search - webstore.iec.ch/advsearchform
The advanced search enables to find IEC publications by a variety of criteria (reference number, text, technical committee,…). It also gives information on projects, replaced and withdrawn publications.

IEC Just Published - webstore.iec.ch/justpublished
Stay up to date on all new IEC publications. Just Published details all new publications released. Available online and once a month by email.

IEC Customer Service Centre - webstore.iec.ch/csc
If you wish to give us your feedback on this publication or need further assistance, please contact the Customer Service Centre: sales@iec.ch.

Electropedia - www.electropedia.org
The world's leading online dictionary on electrotechnology, containing more than 22 000 terminological entries in English and French, with equivalent terms in 16 additional languages. Also known as the International Electrotechnical Vocabulary (IEV) online.

IEC Glossary - std.iec.ch/glossary
67 000 electrotechnical terminology entries in English and French extracted from the Terms and definitions clause of IEC publications issued between 2002 and 2015. Some entries have been collected from earlier publications of IEC TC 37, 77, 86 and CISPR.

IEC TS 62153-4-1

Edition 1.1 2020-05
CONSOLIDATED VERSION

TECHNICAL SPECIFICATION

colour inside

Metallic communication cable test methods – Part 4-1: Electromagnetic compatibility (EMC) – Introduction to electromagnetic screening measurements

INTERNATIONAL
ELECTROTECHNICAL
COMMISSION

ICS 33.100.10

ISBN 978-2-8322-8341-7

IEC TS 62153-4-1

Edition 1.1 2020-05

REDLINE VERSION

colour inside

Metallic communication cable test methods – Part 4-1: Electromagnetic compatibility (EMC) – Introduction to electromagnetic screening measurements

IEC TS 62153-4-1:2014-01+AMD1:2020-05 CSV(en)

CONTENTS

FOREWORD 7
1 Scope 9
2 Normative references 9
3 Symbols interpretation 10
4 Electromagnetic phenomena 12
5 The intrinsic screening parameters of short cables 14
5.1 General 14
5.2 Surface transfer impedance, Z_T 14
5.3 Capacitive coupling admittance, Y_C 15
5.4 Injecting with arbitrary cross-sections 17
5.5 Reciprocity and symmetry 17
5.6 Arbitrary load conditions 17
6 Long cables – coupled transmission lines 17
7 Transfer impedance of a braided wire outer conductor or screen 25
8 Test possibilities 31
8.1 General 31
8.2 Measuring the transfer impedance of coaxial cables 31
8.3 Measuring the transfer impedance of cable assemblies 32
8.4 Measuring the transfer impedance of connectors 32
8.5 Calculated maximum screening level 32
9 Comparison of the frequency response of different triaxial test set-ups to measure the transfer impedance of cable screens 37
9.1 General 37
9.2 Physical basics 37
9.2.1 Triaxial set-up 37
9.2.2 Coupling equations 39
9.3 Simulations 41
9.3.1 General 41
9.3.2 Simulation of the standard and simplified methods according to EN 50289-1-6, IEC 61196-1 (method 1 and 2) and IEC 62153-4-3 (method A) 41
9.3.3 Simulation of the double short circuited methods 47
9.4 Conclusion 55
10 Background of the shielded screening attenuation test method (IEC 62153-4-4) 55
10.1 General 55
10.2 Objectives 56
10.3 Theory of the triaxial measuring method 56
10.4 Screening attenuation 61
10.5 Normalised screening attenuation 63
10.6 Measured results 64
10.7 Comparison with absorbing clamp method 66
10.8 Practical design of the test set-up 67
10.9 Influence of mismatches 68
10.9.1 Mismatch in the outer circuit 68
10.9.2 Mismatch in the inner circuit 70

11 Background of the shielded screening attenuation test method for measuring the screening effectiveness of feed-throughs and electromagnetic gaskets (IEC 62153-4-10) 73
11.1 General 73
11.2 Theoretical background of the test Fixtures and their equivalent circuit 74
11.3 Pictures and measurement results 77
11.3.1 Characteristic impedance uniformity 77
11.3.2 Measurements of shielding effectiveness 79
11.3.3 Calculation of transfer impedance 81
11.4 Calculation of screening attenuation for feed-through when the transfer impedance Z_T is known 83
12 Background of the shielded screening attenuation test method for measuring the screening effectiveness of RF connectors and assemblies (IEC 62153-4-7) 84
12.1 Physical basics 84
12.1.1 Surface transfer impedance Z_T 84
12.1.2 Screening attenuation a_S 85
12.1.3 Coupling attenuation a_C 85
12.1.4 Coupling transfer function 85
12.1.5 Relationship between length and screening measurements 86
12.2 Tube in tube set-up (IEC 62153-4-7) 87
12.2.1 General 87
12.2.2 Procedure 87
12.2.3 Measurements and simulations 89
12.2.4 Influence of contact resistances 90
Annex A (normative) Mixed mode S-parameter 92
A.1 General 92
A.2 Definition of mixed mode S-parameters 92
A.3 Mixed mode S-parameter nomenclature 93
A.4 Termination 95
A.5 Reference impedance of a VNA 96
A.6 TP-connecting unit 96
Annex B (informative) Example derivation of mixed mode parameters using the modal decomposition technique 98
Bibliography 102

Figure 1 – Total electromagnetic field $(\vec{E}_t, \vec{H}_t)$ 13
Figure 2 – Defining and measuring screening parameters – A triaxial set-up 14
Figure 3 – Equivalent circuit for the testing of Z_T 16
Figure 4 – Equivalent circuit for the testing of $Y_c = j\,\omega C_T$ 16
Figure 5 – Electrical quantities in a set-up that is matched at both ends 16
Figure 6 – The summing function $S\{L \cdot f\}$ for near and far end coupling 21
Figure 7 – Transfer impedance of a typical single braid screen 21
Figure 8 – The effect of the summing function on the coupling transfer function of a typical single braid screen cable 22
Figure 9 – Calculated coupling transfer functions T_n and T_f for a single braid – $Z_F = 0$ 22
Figure 10 – Calculated coupling transfer functions T_n and T_f for a single braid – $\mathrm{Im}(Z_T)$ is positive and $Z_F = +0{,}5 \times \mathrm{Im}(Z_T)$ at high frequencies 23

Figure 11 – Calculated coupling transfer functions T_n and T_f for a single braid – Im(Z_T) is negative and Z_F = –0,5 × Im(Z_T) at high frequencies 24
Figure 12 – $L \cdot S$: the complete length dependent factor in the coupling function T 25
Figure 13 – Transfer impedance of typical cables 26
Figure 14 – Magnetic coupling in the braid – Complete flux 27
Figure 15 – Magnetic coupling in the braid – Left-hand lay contribution 27
Figure 16 – Magnetic coupling in the braid – Right-hand lay contribution 27
Figure 17 – Complex plane, Z_T = *Re* Z_T + j *Im* Z_T, frequency *f* as parameter 28
Figure 18 – Magnitude (amplitude), | Z_T (*f*) | 28
Figure 19 – Typical Z_T (time) step response of an overbraided and underbraided single braided outer conductor of a coaxial cable 29
Figure 20 – Z_T equivalent circuits of a braided wire screen 30
Figure 21 – Comparison of signal levels in a generic test setup 33
Figure 22 – Triaxial set-up for the measurement of the transfer impedance Z_T 37
Figure 23 – Equivalent circuit of the triaxial set-up 38
Figure 24 – Simulation of the frequency response for *g* 42
Figure 25 – Simulation of the frequency response for *g* 42
Figure 26 – Simulation of the frequency response for *g* 43
Figure 27 – Simulation of the frequency response for *g* 43
Figure 28 – Simulation of the 3 dB cut off wavelength (L/λ_1) 44
Figure 29 – Interpolation of the simulated 3 dB cut off wavelength (L/λ_1) 44
Figure 30 – 3 dB cut-off frequency length product as a function of the dielectric permittivity of the inner circuit (cable) 45
Figure 31 – Measurement result of the normalised voltage drop of a single braid screen on a solid PE dielectric in the triaxial set-up 46
Figure 32 – Measurement result of the normalised voltage drop of a single braid screen on a foam PE dielectric in the triaxial set-up 47
Figure 33 – Triaxial set-up (measuring tube), double short circuited method 48
Figure 34 – Simulation of the frequency response for *g* of a cable having solid PE dielectric (ε_{r1}=2,3) 49
Figure 35 – Simulation of the frequency response for *g* of a cable having foamed PE dielectric (ε_{r1}=1,6) 49
Figure 36 – Simulation of the frequency response for *g* of a cable having foamed PE dielectric (ε_{r1}=1,3) 50
Figure 37 – Simulation of the frequency response for *g* of a cable having PVC dielectric (ε_{r1}=5) 50
Figure 38 – Interpolation of the simulated 3 dB cut off wavelength (L/λ_1) 51
Figure 39 – 3 dB cut-off frequency length product as a function of the dielectric permittivity of the inner circuit (cable) 52
Figure 40 – Simulation of the frequency response for *g* 53
Figure 41 – Interpolation of the simulated 3 dB cut off wavelength (L/λ_1) 54
Figure 42 – 3 dB cut-off frequency length product as a function of the dielectric permittivity of the inner circuit (cable) 54
Figure 43 – Definition of transfer impedance 56
Figure 44 – Definition of coupling admittance 56
Figure 45 – Triaxial measuring set-up for screening attenuation 57

Figure 46 – Equivalent circuit of the triaxial measuring set-up 57
Figure 47 – Calculated voltage ratio for a typical braided cable screen 59
Figure 48 – Calculated periodic functions for ε_{r1} = 2,3 and ε_{r2} = 1,1 60
Figure 49 – Calculated voltage ratio-typical braided cable screen 60
Figure 50 – Equivalent circuit for an electrical short part of the length Δl and negligible capacitive coupling 62
Figure 51 – a_s of single braid screen, cable type RG 58, L = 2 m 64
Figure 52 – a_s of single braid screen, cable type RG 58, L = 0,5 m 65
Figure 53 – a_s of cable type HF 75 0,7/4,8 2YCY (solid PE dielectric) 65
Figure 54 – a_s of cable type HF 75 1,0/4,8 02YCY (foam PE dielectric) 66
Figure 55 – a_s of double braid screen, cable type RG 223 66
Figure 56 – Schematic for the measurement of the screening attenuation a_s 68
Figure 57 – Short circuit between tube and cable screen of the CUT 68
Figure 58 – Triaxial set-up, impedance mismatches 69
Figure 59 – Calculated voltage ratio including multiple reflections caused by the screening case 70
Figure 60 – Calculated voltage ratio including multiple reflections caused by the screening case 70
Figure 61 – Attenuation and return loss of a self-made 50 Ω to 5 Ω impedance matching adapter 71
Figure 62 – equivalent circuit of a load resistance connected to a source 72
Figure 63 – Cross-sectional sketch of a typical feed-through configuration 73
Figure 64 – Cross-sectional sketch of the test fixture with a feed-through connector (a) and EMI gasket (b) under test 74
Figure 65 – Equivalent circuit of the test fixture 75
Figure 66 –Two-port network 75
Figure 67 – TDR measurement of the text-fixture with inserted “Teflon-through” sample 77
Figure 68 – TDR step response from A (Input)-port of test fixture with inserted “Teflon-through” sample 78
Figure 69 – TDR step response from B (Output)-port of test fixture with inserted “Teflon-through” sample 78
Figure 70 – S-parameter measurement (linear sweep): “Teflon-through” sample 79
Figure 71 – S-parameter measurement (logarithmic sweep): “Teflon-through” sample 79
Figure 72 – S parameter test setup 80
Figure 73 – TDR test setup 80
Figure 74 – Test fixture assembled 80
Figure 75 – Detailed views of the contact area the test fixture and the secondary side of side opened 81
Figure 76 – S_{21} measurements 81
Figure 77 – S_{21} measurements of “Teflon-through” and “Sonnenscheibe” feed-through 82
Figure 78 – Transfer impedance ZT of a “Sonnenscheibe” feed-through based on the S_{21} measurement in Figure 77 82
Figure 79 – measurements of a conducting plastic gasket 83
Figure 80 – Z_T of the conducting plastic gasket based on the S_{21} measurement in Figure 79 83
Figure 81 – equivalent circuit of the set-up without DUT 83

Figure 82 – equivalent circuit of the set-up with inserted DUT 84
Figure 83 – Definition of Z_T 85
Figure 84 – Calculated coupling transfer function 86
Figure 85 – Principle test set-up for measuring the screening attenuation of a connector with the tube in tube procedure 87
Figure 86 – Principle test set-up for measuring the coupling attenuation of screened balanced or multipin connectors 88
Figure 87 – Principle preparation of balanced or multiconductor connectors for coupling attenuation 88
Figure 88 – Comparison of simulation and measurement, linear frequency scale 89
Figure 89 – Comparison of simulation and measurement, logarithmic frequency scale 90
Figure 90 – Measurement of the coupling attenuation of a CAT6 connector 90
Figure 91 – Contact resistances of the test set-up 91
Figure 92 – Equivalent circuit of the test set-up with contact resistances 91
Figure A.1 – Common two-port network 92
Figure A.2 – Common four port network 92
Figure A.3 – Physical and logical ports of a VNA 93
Figure A.4 – Nomenclature of mixed mode S-parameters 93
Figure A.5 – Balunless measuring of coupling attenuation, principle set-up with multiport VNA and standard head 94
Figure A.6 – Termination network 95
Figure A.7 – Termination of a screened symmetrical cable, principle 96
Figure B.1 – Voltage and current on balanced cable or cabling under test (CUT) 98
Figure B.2 – Voltage and current on unbalanced DUT 100

Table 1 – The coupling transfer function *T* (coupling function)[a] 19
Table 2 – Screening effectiveness of cable test methods for surface transfer impedance Z_T 35
Table 3 – Load conditions of the different set-ups 39
Table 4 – Parameters of the different set-ups 41
Table 5 – Cut-off frequency length product 45
Table 6 – Typical values for the factor *v*, for an inner tube diameter of 40 mm and a generator output impedance of 50 Ω 48
Table 7 – Cut-off frequency length product 51
Table 8 – Material combinations and the factor *n* 53
Table 9 – Cut-off frequency length product 54
Table 10 – Cut-off frequency length product for some typical cables in the different set-ups 55
Table 11 – Δa in dB for typical cable dielectrics 64
Table 12 – Comparison of results of some coaxial cables 67
Table 13 – Cable parameters used for simulation 89
Table A.1 – Measurement configurations unbalanced – balanced 94
Table A.2 – Measurement configurations balanced – balanced 95
Table A.3 – TP-connecting unit performance requirements (100 kHz to 2 GHz) 97

INTERNATIONAL ELECTROTECHNICAL COMMISSION

METALLIC COMMUNICATION CABLE TEST METHODS –

Part 4-1: Electromagnetic compatibility (EMC) – Introduction to electromagnetic screening measurements

FOREWORD

1) The International Electrotechnical Commission (IEC) is a worldwide organization for standardization comprising all national electrotechnical committees (IEC National Committees). The object of IEC is to promote international co-operation on all questions concerning standardization in the electrical and electronic fields. To this end and in addition to other activities, IEC publishes International Standards, Technical Specifications, Technical Reports, Publicly Available Specifications (PAS) and Guides (hereafter referred to as "IEC Publication(s)"). Their preparation is entrusted to technical committees; any IEC National Committee interested in the subject dealt with may participate in this preparatory work. International, governmental and non-governmental organizations liaising with the IEC also participate in this preparation. IEC collaborates closely with the International Organization for Standardization (ISO) in accordance with conditions determined by agreement between the two organizations.
2) The formal decisions or agreements of IEC on technical matters express, as nearly as possible, an international consensus of opinion on the relevant subjects since each technical committee has representation from all interested IEC National Committees.
3) IEC Publications have the form of recommendations for international use and are accepted by IEC National Committees in that sense. While all reasonable efforts are made to ensure that the technical content of IEC Publications is accurate, IEC cannot be held responsible for the way in which they are used or for any misinterpretation by any end user.
4) In order to promote international uniformity, IEC National Committees undertake to apply IEC Publications transparently to the maximum extent possible in their national and regional publications. Any divergence between any IEC Publication and the corresponding national or regional publication shall be clearly indicated in the latter.
5) IEC itself does not provide any attestation of conformity. Independent certification bodies provide conformity assessment services and, in some areas, access to IEC marks of conformity. IEC is not responsible for any services carried out by independent certification bodies.
6) All users should ensure that they have the latest edition of this publication.
7) No liability shall attach to IEC or its directors, employees, servants or agents including individual experts and members of its technical committees and IEC National Committees for any personal injury, property damage or other damage of any nature whatsoever, whether direct or indirect, or for costs (including legal fees) and expenses arising out of the publication, use of, or reliance upon, this IEC Publication or any other IEC Publications.
8) Attention is drawn to the Normative references cited in this publication. Use of the referenced publications is indispensable for the correct application of this publication.
9) Attention is drawn to the possibility that some of the elements of this IEC Publication may be the subject of patent rights. IEC shall not be held responsible for identifying any or all such patent rights.

This consolidated version of the official IEC Standard and its amendment(s) has been prepared for user convenience.

IEC TS 62153-4-1 edition 1.1 contains the first edition (2014-01) [documents 46/465/DTS and 46/492/RVC] and its amendment 1 (2020-05) [documents 46/726/DTS and 46/748/RVDTS].

In this Redline version, a vertical line in the margin shows where the technical content is modified by amendment 1. Additions are in green text, deletions are in strikethrough red text. A separate Final version with all changes accepted is available in this publication.

The main task of IEC technical committees is to prepare International Standards. In exceptional circumstances, a technical committee may propose the publication of a technical specification when

- the required support cannot be obtained for the publication of an International Standard, despite repeated efforts, or
- the subject is still under technical development or where, for any other reason, there is the future but no immediate possibility of an agreement on an International Standard.

Technical specifications are subject to review within three years of publication to decide whether they can be transformed into International Standards.

IEC TS 62153-4-1, which is a technical specification, has been prepared by IEC technical committee 46: Cables, wires, waveguides, R.F. connectors, R.F. and microwave passive components and accessories.

This first edition of technical specification IEC TS 62153-4-1 constitutes a technical revision. This edition includes the following significant technical changes with respect to IEC TR 62153-4-1:

a) comparison of the frequency response of different triaxial test set-ups to measure the transfer impedance of cable screens;
b) background of the shielded screening attenuation test method (IEC 62153-4-4);
c) background of the shielded screening attenuation test method for measuring the screening effectiveness of feed-throughs and electromagnetic gaskets (IEC 62153-4-10);
d) background of the shielded screening attenuation test method for measuring the screening effectiveness of RF connectors and assemblies (IEC 62153-4-7).

This publication has been drafted in accordance with the ISO/IEC Directives, Part 2.

A list of all parts of the IEC 62153 series, under the general title: *Metallic communication cable test methods*, can be found on the IEC website.

The committee has decided that the contents of the base publication and its amendment will remain unchanged until the stability date indicated on the IEC web site under "http://webstore.iec.ch" in the data related to the specific publication. At this date, the publication will be

- reconfirmed,
- withdrawn,
- replaced by a revised edition, or
- amended.

IMPORTANT – The 'colour inside' logo on the cover page of this publication indicates that it contains colours which are considered to be useful for the correct understanding of its contents. Users should therefore print this document using a colour printer.

METALLIC COMMUNICATION CABLE TEST METHODS –

Part 4-1: Electromagnetic compatibility (EMC) – Introduction to electromagnetic (EMC) screening measurements

1 Scope

This part of IEC 62153 deals with screening measurements. Screening (or shielding) is one basic way of achieving electromagnetic compatibility (EMC). However, a confusingly large number of methods and concepts is available to test for the screening quality of cables and related components, and for defining their quality. This technical specification gives a brief introduction to basic concepts and terms trying to reveal the common features of apparently different test methods. It is intended to assist in correct interpretation of test data, and in the better understanding of screening (or shielding) and related specifications and standards.

2 Normative references

The following documents, in whole or in part, are normatively referenced in this document and are indispensable for its application. For dated references, only the edition cited applies. For undated references, the latest edition of the referenced document (including any amendments) applies.

IEC 60096-1:1986, *Radio-frequency cables – Part 1: General requirements and measuring methods*[1]

IEC 60096-4-1, *Radio-frequency cables – Part 4: Specification for superscreened cables – Section 1: General requirements and test methods*[1]

IEC 60169-1-3, *Radio-frequency connectors - Part 1: General requirements and measuring methods - Section Three: Electrical tests and measuring procedures: Screening effectiveness*

IEC 61196-1:2005, *Coaxial communication cables - Part 1: Generic specification - General, definitions and requirements*

IEC 61726, *Cable assemblies, cables, connectors and passive microwave components - Screening attenuation measurement by the reverberation chamber method*

IEC 62153-4-2, *Metallic communication cable test methods - Part 4-2: Electromagnetic compatibility (EMC) - Screening and coupling attenuation - Injection clamp method*

IEC 62153-4-3, *Metallic communication cable test methods - Part 4-3: Electromagnetic compatibility (EMC) - Surface transfer impedance - Triaxial method*

IEC 62153-4-4, *Metallic communication cable test methods - Part 4-4: Electromagnetic compatibility (EMC) - Shielded screening attenuation, test method for measuring of the screening attenuation as up to and above 3 GHz*

IEC 62153-4-5, *Metallic communication cables test methods - Part 4-5: Electromagnetic compatibility (EMC) - Coupling or screening attenuation - Absorbing clamp method*

---

[1] This publication has been withdrawn.

IEC 62153-4-6, *Metallic communication cable test methods - Part 4-6: Electromagnetic compatibility (EMC) - Surface transfer impedance - Line injection method*

IEC 62153-4-7, *Metallic communication cable test methods - Part 4-7: Electromagnetic compatibility (EMC) - Test method for measuring the transfer impedance and the screening - or the coupling attenuation - Tube in tube method*

IEC 62153-4-9, *Metallic communication cable test methods – Part 4-9: Electromagnetic compatibility (EMC) – Coupling attenuation of screened balanced cables, triaxial method*

IEC 62153-4-10, *Metallic communication cable test methods - Part 4-10: Electromagnetic compatibility (EMC) - Shielded screening attenuation test method for measuring the screening effectiveness of feed-throughs and electromagnetic gaskets double coaxial method*

IEC/TR 62152:2009, *Transmission properties of cascaded two-ports or quadripols – Background of terms and definitions*

EN 50289-1-6: 2002, *Communication cables – Specifications for test methods Part 1-6: Electrical test methods – Electromagnetic performance*

CISPR 25, *Vehicles, boats and internal combustion engines – Radio disturbance characteristics – Limits and methods of measurement for the protection of on-board receivers*

3 Symbols interpretation

This clause gives the interpretation of the symbols used throughout this specification.

α_1, α_2 attenuation constants of primary and secondary circuit

a_s screening attenuation

a_{sn} normalized screening attenuation with phase velocity difference not greater than 10 % and 150 Ω characteristic impedance of the injection line (Z_s=150 Ω and $|\Delta v/v_1|$=10 % or $\varepsilon_{r1}/\varepsilon_{r2n}$=1,21)

c_o velocity of light in free space $c_o = 3 \times 10^8$ m/s

C_T through capacitance of the braided cable

CUT cable or component under test

E e.m.f.

f frequency

f far end

f_c cut-off frequency

f_{cf} far end cut-off frequency

f_{cn} near end cut-off frequency

Φ_1 the total flux of the magnetic field induced by the disturbing current I_1

Φ'_{12} the direct leaking magnetic flux

Φ''_{12} complete magnetic flux in the braid

I_1, U_1 current and voltage in the primary circuit (feeding system)

I_F current coupled by the feed through capacitance to the secondary system (measuring system)

ε_{r1} relative permittivity of the injection line (feeding system)

ε_{r2} relative permittivity of the cable (measuring system)

L cable length, coupling length

L_1 (external) inductance of the outer circuit

L_2 (external) inductance of the inner circuit

M'_{12} mutual inductance related to direct leakage of the magnetic flux Φ'_{12}

M''_{12} mutual inductance related to the magnetic flux Φ''_{12} (or ½ Φ''_{12}) in the braid

$$M'_{12} = \frac{\Phi'_{12}}{j\omega I_1} \text{ and } M''_{12} = \frac{1}{2} \cdot \frac{\Phi''_{12}}{j\omega I_1}$$

M_T effective mutual inductance per unit length for braided screens

$M_T = M'_{12} - M''_{12}$

where M'_{12} relates to the direct leakage of the magnetic flux and M''_{12} relates to the magnetic flux in the braid [24]

n near end

P_1 sending power

P_{2f} far end measured power

P_{2n} near end measured power

P_r radiated power in the environment of the cable, which is comparable to $P_{2n}+P_{2f}$ of the absorbing clamp method of 12.4 of IEC 61196-1:1995

P_s radiated power in the normalised environment of the cable under test (Z_s=150 Ω and $|\Delta v/v_1|$=10 % or $\varepsilon_{r1}/\varepsilon_{r2n}$=1,21)

R load resistance of secondary circuit (input resistance of receiver)

R_T screen resistance per unit length

T coupling transfer function

T_f far end transfer function

T_n near end transfer function

U'_2 the disturbing voltage induced by Φ'_{12}

U''_{rh} the disturbing voltage induced by ½ Φ''_{12} of the right hand lay contribution

U''_{lh} the disturbing voltage induced by ½ Φ''_{12} of the left hand lay contribution

U''_2 is equal to U''_{rh} and U''_{lh} (= the disturbing voltage induced by ½ Φ''_{12})

v phase velocity

v_1 phase velocity of the "primary" system (feeding system)

v_2 phase velocity of the "secondary" system (measuring system)

v_{r1} relative phase velocity of the "primary" system (feeding system)

v_{r2} relative phase velocity of the "secondary" system (measuring system)

Z_1 characteristic impedance of the "primary" system (feeding system or line (1))

Z_2 characteristic impedance of the cable under test (CUT) (measuring system or line (2))

Z_{1f} terminating impedance of the line (1) in the far end

Z_{2n} terminating impedance of the line (2) in the near end

Z_{2f} terminating impedance of the line (2) in the far end (in a matched set-up $Z_{1f} = Z_1$ and $Z_{2n} = Z_{2f} = Z_2$)

$$Z_{12} = \sqrt{Z_1 Z_2}$$

Z_a surface impedance of the braided cable

Z_F capacitive coupling impedance per unit length

Z_f capacitive coupling impedance

Z_T surface transfer impedance per unit length

Z_{Th} transfer impedance of a tubular homogeneous screen per unit length

Z_t surface transfer impedance

Z_{TEn} effective transfer impedance (= $| Z_F + Z_T |$) per unit length in the near end

Z_{TEf} effective transfer impedance (= $| Z_F - Z_T |$) per unit length in the far end

$Z_{TEn,f}$ effective transfer impedance (= $| Z_F \pm Z_T |$) per unit length in the near end or in the far end

Z_{TE} effective transfer impedance (= max $| Z_{TEn}, Z_{TEf} |$) per unit length

Z_{te} effective transfer impedance (= max $| Z_f \pm Z_t |$)

Z_{ten} normalized effective transfer impedance of a cable (Z_1 = 150 Ω and $| v_1 - v_2 | / v_2 \leq 10$ % velocity difference in relation to velocity of CUT

4 Electromagnetic phenomena

It is assumed that if an electromagnetic field is incident on a screened cable, there is only weak coupling between the external field and that inside, and that the cable diameter is very small compared with both the cable length and the wavelength of the incident field. The superposition of the external incident field and the field scattered by the cable yields the total electromagnetic field $(\vec{E}_t, \vec{H}_t)$ in Figure 1. The total field at the screen's surface may be considered as the source of the coupling: electric field penetrates through apertures by electric or capacitive coupling; also magnetic fields penetrate through apertures by inductive or magnetic coupling. In addition, the induced current in the screen results in conductive or resistive coupling.

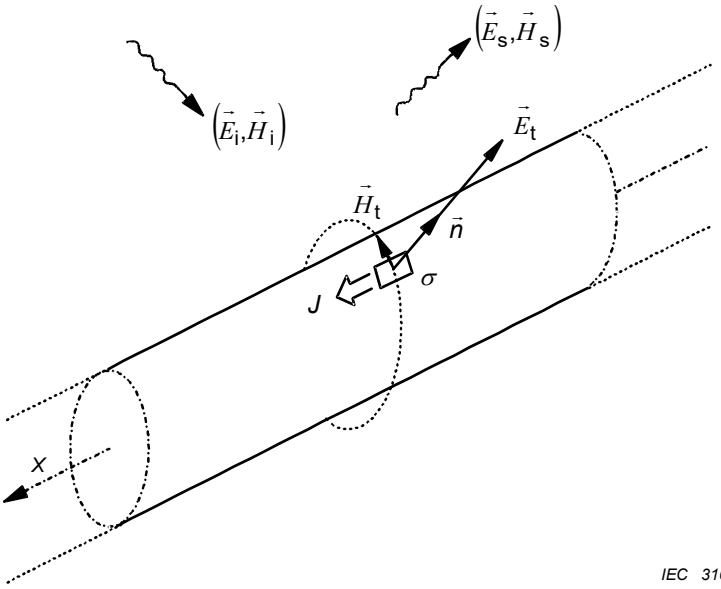

Key

$(\vec{E}_i,\vec{H}_i)$	incident electromagnetic field
$(\vec{E}_s,\vec{H}_s)$	scattered electromagnetic field
$(\vec{E}_t,\vec{H}_t)$	total electromagnetic field
x	positive axial cable direction
σ	induced surface charge density- (C/m^2)
$\vec{n}$	unit vector normal to the surface
ε_o, ε_r	permittivity, free space and relative

Figure 1 – Total electromagnetic field $(\vec{E}_t,\vec{H}_t)$

$$(\vec{E}_t,\vec{H}_t)=(\vec{E}_i,\vec{H}_i)+(\vec{E}_s,\vec{H}_s) \quad (1)$$

$$J=\vec{n}\cdot\vec{H}_t \quad (2)$$

$$\sigma=\vec{n}\cdot\vec{E}_t\varepsilon_o\varepsilon_r \quad (3)$$

where the symbols are described in the key of Figure 1.

As the field at the surface of the screen is directly related to density of surface current and surface charge, the coupling may be assigned either to the total field $(\vec{E}_t,\vec{H}_t)$ or to the surface current- and charge- densities (J and σ). Consequently, the coupling into the cable may be simulated by reproducing, through any suitable means, the surface currents and charges on the screen. Because the cable diameter is assumed to be small, the higher modes may be neglected and it is possible to use an additional coaxial conductor as the injection structure, as shown in Figure 2.

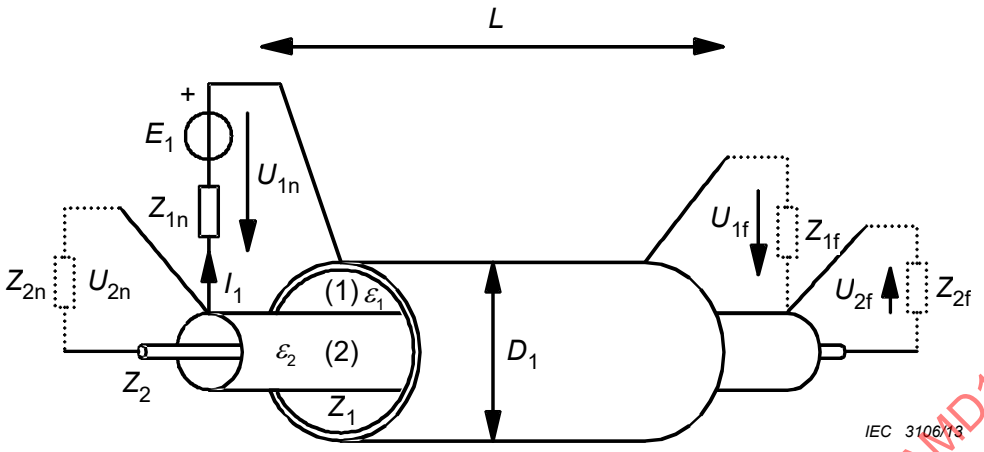

Key (for Figures 2,3,4,5)

(1), (2)	outer circuit (1), tube, respectively inner circuit (2), cable
$Z_{1,2}$	characteristic impedance of the outer circuit (1), tube, respectively inner circuit (2), cable
$\varepsilon_{1,2}$	dielectric permittivity of the outer circuit (1), tube, respectively inner circuit (2), cable
$\beta_{1,2}$	phase constant of the outer circuit (1), tube, respectively inner circuit (2), cable
$\lambda_{1,2}$	wave length of the outer circuit (1), tube, respectively inner circuit (2), cable
L	coupling length
D_1	diameter of injection cylinder-tube
V	voltmeter
A	ammeter
Z_{1n}, Z_{1f}	load resistance at the near end, respectively far end of the outer circuit (1), tube
Z_{2n}, Z_{2f}	load resistance at the near end, respectively far end of the inner circuit (2), cable
E_1	EMF of the generator
I_1, I_2	current in the outer circuit (1), tube, respectively inner circuit (2), cable
U_{1n}, U_{1f}	voltage at the near end, respectively far end of the outer circuit (1), tube
U_{2n}, U_{2f}	voltage at the near end, respectively far end of the inner circuit (2), cable

Figure 2 – Defining and measuring screening parameters – A triaxial set-up

Figure 2 shows the concept of a triaxial set-up. The outer circuit (1) is formed by an injection cylinder-tube and the screen under test, with an characteristic impedance Z_1. The inner circuit (2) is formed by the screen under test, and centre conductor, with an characteristic impedance Z_2. The screening at the ends of circuit (2) is not shown. Observe the conditions Z_{1f}, Z_{2n}, Z_{2f} and λ in Figure 3 and Figure 4. Also note that diameter of the injection cylinder tube (D1) shall be much smaller than the coupling length (L).

5 The intrinsic screening parameters of short cables

5.1 General

The intrinsic parameters refer to an infinitesimal length of cable, like the inductance or capacitance per unit length of transmission lines. Assuming electrically short cables, with $L << \lambda$ which will always apply at low frequencies, the intrinsic screening parameters are defined and can be measured as indicated in the subclauses 5.2 and 5.3.

5.2 Surface transfer impedance, Z_T

As shown in Figure 3, where Z_{1f} and Z_{2f} are zero, the surface transfer impedance (Z_T in Ω/m) is given:

$$Z_T = \frac{U_{2n}}{I_1 \cdot L} \tag{4}$$

where

Z_T is the transfer impedance,

U_{2n} is the voltage at the near end of the inner circuit (2),

L is the coupling length

I_1 is the current in the outer circuit (1).

The dependence of Z_T on frequency is not simple and is often shown by plotting log Z_T against log frequency. Note that the phase of Z_T may have any value, depending on braid construction and frequency range.

NOTE In circuit (2) of Figure 3, the voltmeter and short circuit may also be interchanged.

5.3 Capacitive coupling admittance, Y_C

As shown in Figure 4, where Z_{1f} and Z_{2f} are open circuit, the capacitive coupling admittance (Y_C in S/m) is given by:

$$Y_C = \mathrm{j} \cdot \omega C_T = \frac{I_2}{U_{1n} \cdot L} \tag{5}$$

where

Y_C is the coupling admittance

C_T is the through capacitance;

ω is the radian frequency;

j is the imaginary operator

L is the coupling length

I_2 is the current in the inner circuit (2).

The through capacitance C_T is a real capacitance and has usually a constant value up to 1 GHz and higher (with aperture $a << \lambda$).

While Z_T is independent of the characteristics of the coaxial circuits (1) and (2), C_T is dependent on those characteristics. There are two ways of overcoming this dependence:

a) The normalized through elastance K_T (with units of m/F) derived from C_T is independent of the size of the outer coaxial circuit (2), but it depends on its permittivity:

$$K_T = C_T / (C_1 \cdot C_2) \tag{6}$$

$$K_T \sim 1/(\varepsilon_{r1} + \varepsilon_{r2}) \tag{7}$$

where C_1 and C_2 are the capacitance per unit length of the two coaxial circuits.

b) The capacitive coupling impedance Z_F (with units of Ω/m) again derived from C_T is also independent of the size of the outer coaxial circuit (2) and, for practical values of ε_{r1}, is only slightly dependent on its permittivity:

$$Z_F = Z_1 Z_2 Y_C = Z_1 Z_2 \mathrm{j}\omega C_T \tag{8}$$

$$Z_F \sim \sqrt{(\varepsilon_{r1} \cdot \varepsilon_{r2})}/(\varepsilon_{r1} + \varepsilon_{r2}) \tag{9}$$

Compared with Z_T, Z_F is usually negligible, except for open weave braids. It may, however, be significant when Z_{2n} and $Z_{2f} >> Z_2$ (audio circuits).

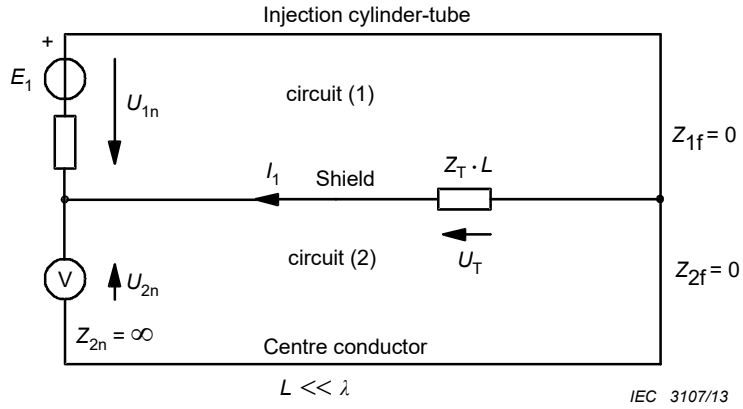

Key

See Figure 2.

Figure 3 – Equivalent circuit for the testing of Z_T

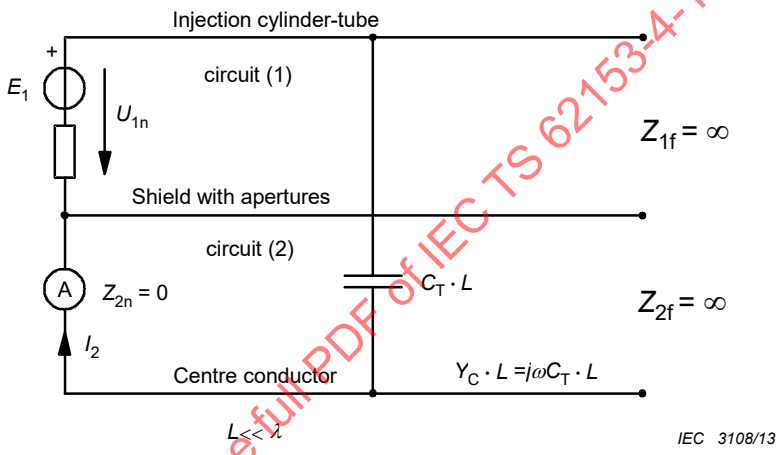

Key

See Figure 2.

Figure 4 – Equivalent circuit for the testing of $Y_c = j\ \omega C_T$

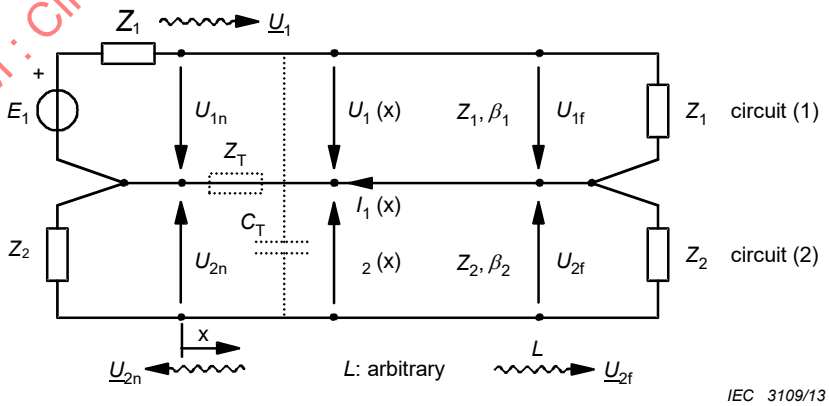

Key

See Figure 2.

NOTE Z_T and C_T are distributed (not correctly shown here). The loads Z_1, Z_2 at the ends may represent matched receivers.

Figure 5 – Electrical quantities in a set-up that is matched at both ends

5.4 Injecting with arbitrary cross-sections

A coaxial outer circuit (2) has been assumed so far in this report, but it is not essential because of the invariance of Z_T and Z_F. Using a wire in place of the outer cylinder, the injection circuit (2) becomes two-wire with the return via the screen of the cable under test. Obviously the charge and current distribution become non-uniform, but the results are equivalent to coaxial injection, especially if two injection lines are used opposite to each other, and may be justified for worst-case testing. Note that the IEC line injection test uses a wire.

5.5 Reciprocity and symmetry

Assuming linear shield materials, the measured Z_T and Z_F values will not change when interchanging the injection circuit (1) and the measuring circuit (2). Each of the two conductors of the two-line circuit can be interchanged, but in practice the set-up will have to take into account possible ground loops and coupling to the environment.

5.6 Arbitrary load conditions

When the circuit ends of Figure 3 and Figure 4 are not ideally a short or open circuit, Z_T and Z_F will act simultaneously. Their superposition is noticeable in the low frequency coupling of the matched circuit (1) and circuit (2) (see Figure 5 and Table 1).

6 Long cables – coupled transmission lines

The coupling over the whole length of the cable is obtained by summing up (integrating) the infinitesimal coupling contributions along the cable while observing the correct phase. The analysis utilizes the following assumptions and conventions:

– matched circuits considered with the voltage waves $\underline{U}_1$, $\underline{U}_{2n}$, $\underline{U}_{2f}$, see Figure 5,

– representation of the coupling, using the normalized wave amplitudes $U/\sqrt{Z}\left[\sqrt{Watt}\right]$, instead of voltage waves. i.e. the coupling transfer function, in the following denoted by "coupling function", will be defined as

$$T_n = \frac{\underline{U}_{2n}/\sqrt{Z_2}}{\underline{U}_1/\sqrt{Z_1}} \qquad (10)$$

$$T_f = \frac{\underline{U}_{2f}/\sqrt{Z_2}}{\underline{U}_1/\sqrt{Z_1}} \qquad (11)$$

The square of the coupling transfer function, $|T|^2$, is the ratio of the power waves travelling in circuits (2) and (1). Due to reciprocity and assuming linear screen (shield) materials, T is reciprocal, i.e. invariant with respect to the interchange of injection and measuring circuits (1) and (2). The quantity $|1/T|^2$ or in logarithmic quantities

$$a_s = -20 \times \log_{10}|T| \qquad (12)$$

may be considered as the "screening attenuation" of the cable, specific to the set-up.

Performing the straight forward calculations of coupled transmission line theory, the coupling function T, given in Table 1, is obtained. The term $S\{L \cdot f\}$ is the "summing function" S, being dependent on L and f. (The wavy bracket just indicates that the product $L \cdot f$ is the argument of the function S and not a factor to S). S represents the phase effect, when summing up the infinitesimal couplings along the line, and is:

$$S_{\underset{f}{n}}\{L\cdot f\} = \frac{\sin\frac{\beta L\pm}{2}}{\frac{\beta L\pm}{2}}\exp\left(-j\cdot\frac{\beta L+}{2}\right) \tag{13}$$

$$\beta L+ = (\beta_2 + \beta_1)\cdot L \tag{14}$$

$$\beta L\pm = (\beta_2 \pm \beta_1)\cdot L \tag{15}$$

$$\beta L\pm = 2\pi L f\cdot(1/v_2 \pm 1/v_1) \tag{16}$$

$$\beta L\pm = 2\pi L f\cdot\left(\sqrt{\varepsilon_{r2}} \pm \sqrt{\varepsilon_{r1}}\right)/c \tag{17}$$

subscript ± refers to near/far end respectively; i.e. + indicates the near end and – indicates the far end;

\+ refers to both near/far ends.

Note that weak coupling, i.e. $T << 1$, has been assumed. This case, including losses, is given in [1][2].

Equation (18) and the representation in Table 1 illustrate the contributions of the different parameters to the coupling function T:

$$T_{\underset{f}{n}} = (Z_F \pm Z_T)\cdot\frac{1}{\sqrt{Z_1\cdot Z_2}}\cdot\frac{L}{2}\cdot S_{\underset{f}{n}}\{L\cdot f, \varepsilon_{r1}, \varepsilon_{r2}\} \tag{18}$$

2 Figures in square brackets refer to the bibliography.

Table 1 – The coupling transfer function *T* (coupling function)[a]

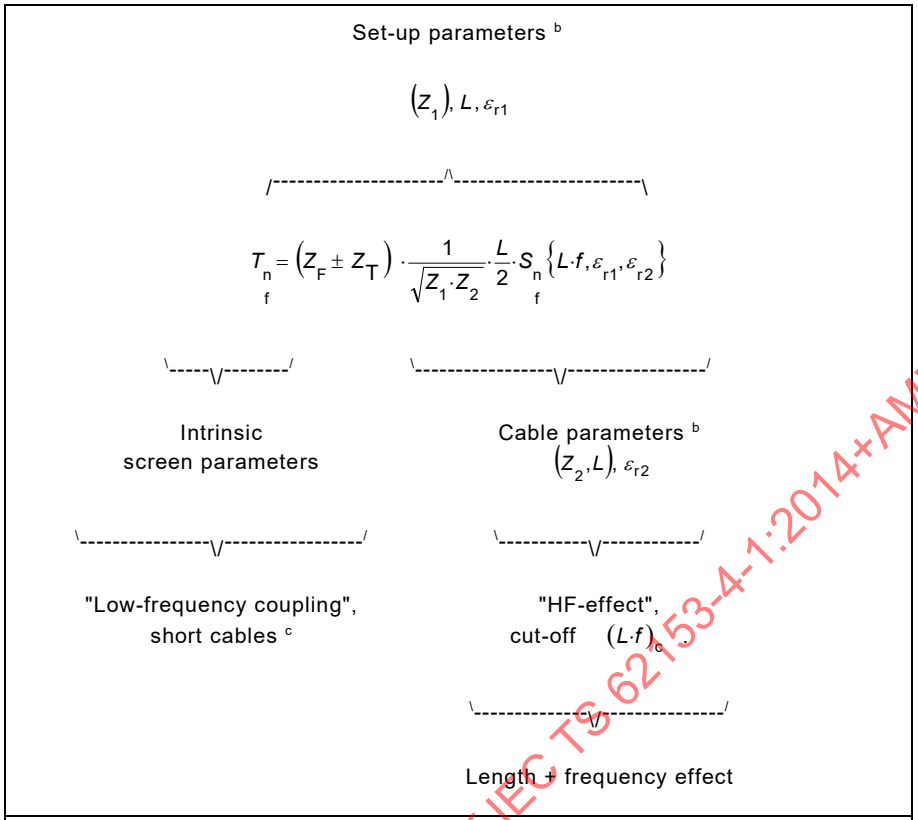

a T^2 is the power coupling from circuit (1) to circuit (2).
The stacked subscripts $\substack{n\\f}$ are associated to the stacked operation symbols ± in the obvious way: upper subscript → upper operation, lower subscript → lower operation.

b ε_{r1} and ε_{r2} contained in S as parameters.

c for $L << \lambda$: $S\{L \cdot f\} \rightarrow 1$.

Note especially the following points.

a) There may be a directional effect ($T_n \neq T_f$) in the whole frequency range if Z_F is not negligible. (But Z_F is usually negligible except with loose, single braid shields.)

b) Up to a constant factor, T is the quantity directly measured in a set-up.

c) For low frequencies, i.e. for short cables ($L << \lambda$), the trivial coupling formula is obtained that is directly proportional to L:

$$T_{\substack{n\\f}} = (Z_F \pm Z_T) \cdot \frac{1}{Z_{12}} \cdot \frac{L}{2} \tag{19}$$

where

$$Z_{12} = \sqrt{Z_1 \cdot Z_2}$$

d) The summing function $S\{L \cdot f\}$ is presented in Figure 6.

e) $S\{L \cdot f\}$ has a sin(*x*)/*x* behaviour. A cut-off point may be defined as $(L \cdot f)_c$:

$$(L \cdot f)_{c_{\substack{n\\f}}} = \frac{c}{\pi \left| \sqrt{\varepsilon_{r1}} \pm \sqrt{\varepsilon_{r2}} \right|} \tag{20}$$

f) The exact envelope of $S\{L \cdot f\}$ is

$$\operatorname{Env}\left|\underset{f}{S_n}\{L\cdot f\}\right| = \frac{1}{\sqrt{1+\dfrac{(L\cdot f)^2}{\underset{f}{(L\cdot f)^2_{cn}}}}} \tag{21}$$

g) The first minimum (zero) of $S\{L\cdot f\}$ occurs at

$$(L\cdot f)_{min} = \pi(L\cdot f)_c \tag{22}$$

h) As seen from Equations (13) and (21), below the cut-off points $\underset{f}{(L\cdot f)_{cn}}$ is $S\{L\cdot f\} \approx 1$ and above them it starts to oscillate and its envelope drops asymptotically 20 dB/decade,

$$\operatorname{Env}\left|\underset{f}{S_n}\{L\cdot f\}\right| \approx \frac{\left(\underset{f}{(L\cdot f)_{cn}}\right)}{(L\cdot f)} \tag{23}$$

i) S is symmetrical in L and f, i.e. L and f are interchangeable. For a fixed length a cut-off frequency f_c and vice versa, for a fixed frequency a cut-off length L_c may be defined. Substituting c/λ_o for f, we obtain the cut-off length as

$$\underset{f}{L_{c_n}} = \frac{\lambda_o}{\pi\left|\sqrt{\varepsilon_{r1}} \pm \sqrt{\varepsilon_{r2}}\right|} \tag{24}$$

j) The effect of S in the frequency range (L = constant) is illustrated in Figure 8. The coupling function is proportional to Z_T, only if $f < f_c$. Note also the typical values indicated for f_c.

k) The minima and maxima of S are not resonances, they are due to cancelling and additive effects of the coupling along the line.

l) The far end cut-off frequency is significantly influenced by the permittivity of the outer system (ε_{r1}). Selecting $\varepsilon_{r1} \to \varepsilon_{r2}$ we obtain $(L\cdot f)_{cf} \to \infty$, i.e. no cut-off at the far end. Due to practical aspects (tolerances, homogeneity, etc.), an ideal phase matching $(\varepsilon_{r1} \equiv \varepsilon_{r2})$ is not feasible.

m) The effects of Z_T and Z_F on the coupling transfer functions T_n and T_f are shown in Figure 8.

n) The total effect of L on the coupling is not contained in S alone, but in the product $L\cdot S\{L\cdot f\}$. The product $L\cdot S$ is presented in Figure 12 for f = constant. The coupling function T which can be measured in a set-up is proportional to L if $L < L_c$. However, for appropriately long cables ($L > L_c$), the maximum coupling is independent of L and we obtain a length independent shielding attenuation above the cut-off point $(L\cdot f)_c$. But we should remember that $(L\cdot f)_c$ as well as A_s are still dependent on the set-up parameters (ε_{r1}, Z_1).

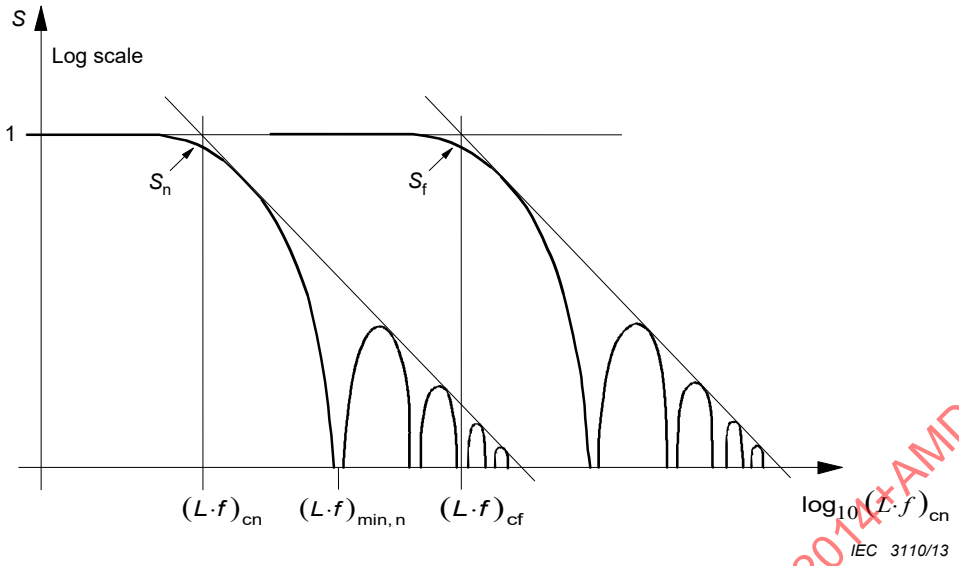

Key

$(L \cdot f)_{cn,f}$ cut-off point at near (n) respectively far (f) end

$S_{n,f}$ summing function at the (n) respectively far (f) end

NOTE $S_f > S_n$ above near end cut-off, yielding a directive effect.

Figure 6 – The summing function $S\{L \cdot f\}$ for near and far end coupling

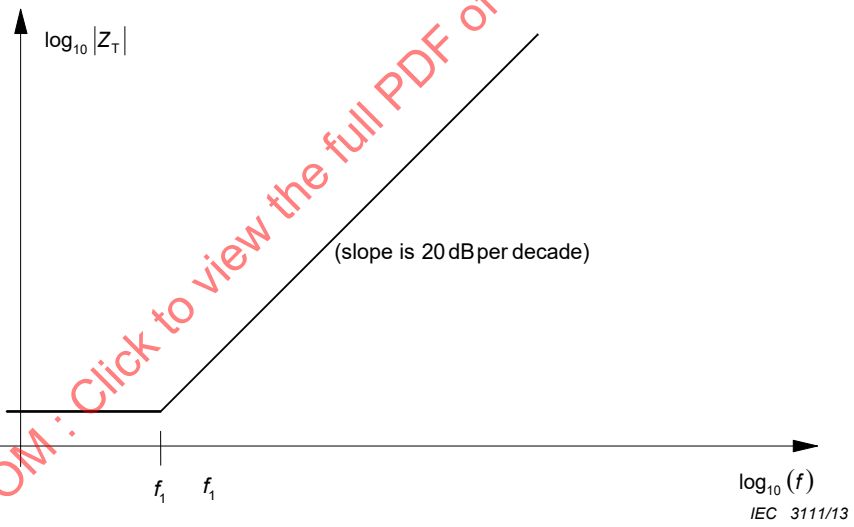

Key

$\log_{10}|Z_T|$ magnitude of the transfer impedance drawn on a logarithmic scale

$\log_{10}(f)$ frequency drawn on a logarithmic scale

f_1 frequency of the intersection of the DC resistance of the screen and the 20dB slope at higher frequencies

Figure 7 – Transfer impedance of a typical single braid screen

Figure 8 gives the result of adding (on a log scale) the frequency responses from Figure 6 and Figure 7. It is assumed the cable has a negligible capacitive coupling impedance Z_F ($Z_F << Z_T$).

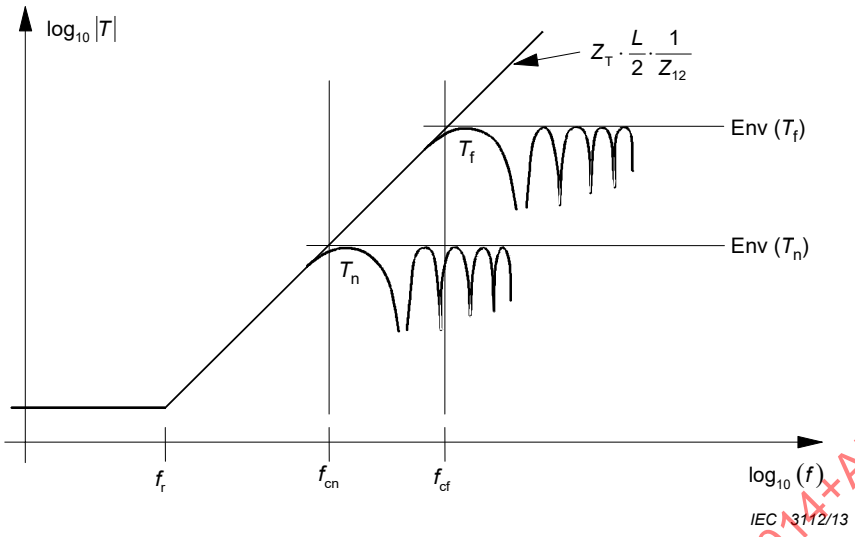

Key

$T_{n,f}$	coupling transfer function at the (n) respectively far (f) end
Env($T_{n,f}$)	envelope of the coupling transfer function at the (n) respectively far (f) end
$f_{cn,f}$	cut-off frequency at the (n) respectively far (f) end

Example: ε_{r1} = 1 (set-up), ε_{r2} = 2,2 (cable), L = 1 m; results in f_{cn} = 40 MHz; f_{cf} = 200 MHz

Figure 8 – The effect of the summing function on the coupling transfer function of a typical single braid screen cable

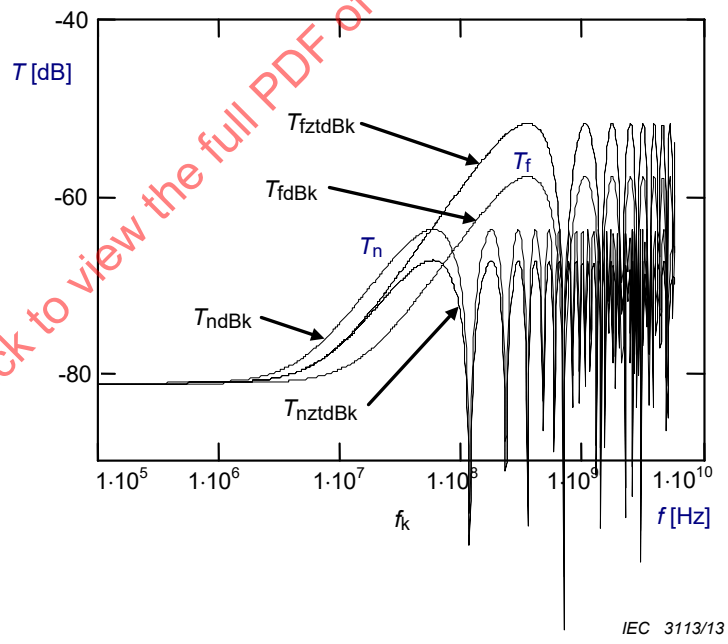

In calculations the following parameters are used:

Z_T (d.c.) =15 mΩ/m and Z_T (10 MHz) = 20 mΩ/m increasing 20 dB/decade (see Figure 7), cable length 1 m, and velocities of the outer and inner line: v_1 = 200 Mm/s and v_2 = 280 Mm/s corresponding to a velocity difference of 40 %.

Figure 9 – Calculated coupling transfer functions T_n and T_f for a single braid – Z_F = 0

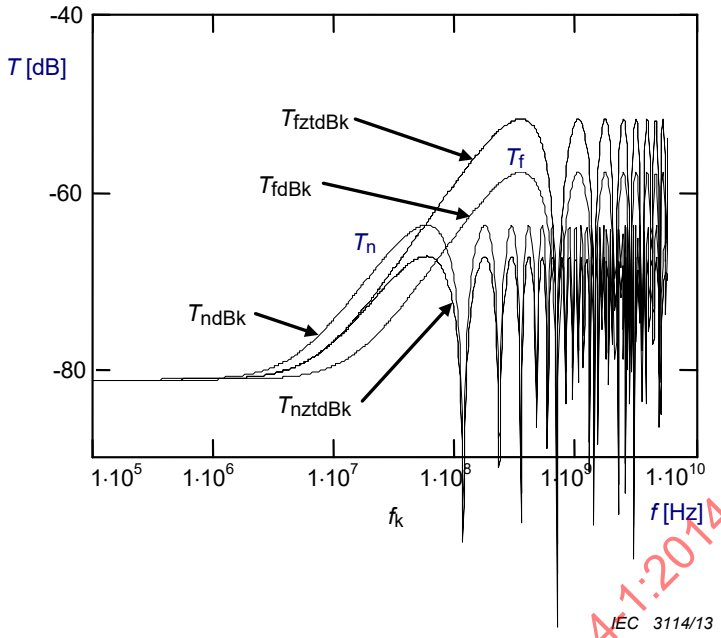

T_n is 3,5 dB higher and T_f is 6 dB lower than in reference Figure 9 because

$T_n \sim | Z_F + Z_T | = 1{,}5 \times Z_T$ and

$T_f \sim | Z_F - Z_T | = 0{,}5 \times Z_T$

Figure 10 – Calculated coupling transfer functions T_n and T_f for a single braid – Im(Z_T) is positive and Z_F = +0,5 × Im(Z_T) at high frequencies

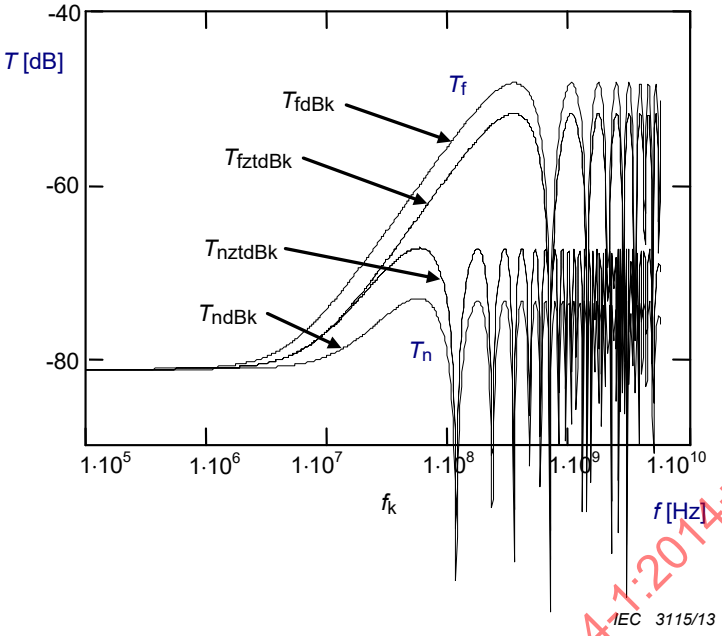

T_f is 3,5 dB higher and T_n is 6 dB lower than in reference Figure 9 because

$T_f \sim |Z_F - Z_T| = 1{,}5 \times |Z_T|$ and

$T_n \sim |Z_F + Z_T| = 0{,}5 \times |Z_T|$

Figure 11 – Calculated coupling transfer functions T_n and T_f for a single braid – Im(Z_T) is negative and $Z_F = -0{,}5 \times$ Im(Z_T) at high frequencies

In Figure 9, $Z_F = 0$ and Z_T is positive.

In Figure 10 and Figure 11, Z_F is significant ($Z_F = (1/2) \times Z_T$).

In Figure 11, the imaginary part of Z_T is negative at high frequencies.

The following notes apply to Figure 9 to Figure 11.

NOTE 1 T_n for near-end, T_f for far-end and dB means that $T_{n,f}$ are calculated in dB ($20 \times \log_{10} | T_{n,f} |$).

NOTE 2 T_n dB: near-end when $Z_F = (1/2) \times Z_T$ and T_{nzt} dB: near-end when $Z_F = 0$.

NOTE 3 T_f dB: far-end when $Z_F = (1/2) \times Z_T$ and T_{fzt} dB: far-end when $Z_F = 0$.

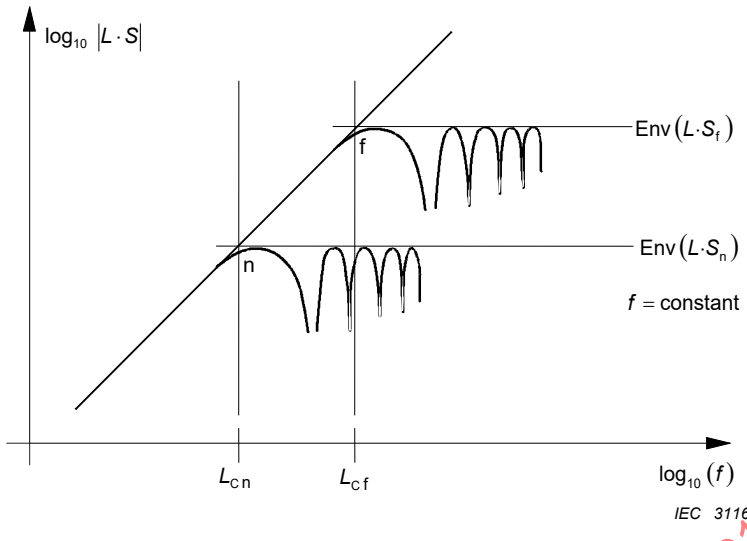

NOTE 1 For $L > L_c$, the maximum value of T is attained, i.e. the maximum coupling (or the screening attenuation) is not dependent on L.

NOTE 2 L_{cf} strongly depends on ε_{r1}.

NOTE 3 See also Table 1 and list item n)

Figure 12 – $L \cdot S$: the complete length dependent factor in the coupling function T

7 Transfer impedance of a braided wire outer conductor or screen

Typical transfer impedances of cables with braided wire screens are shown in Figure 13. The constant Z_T value at the low-frequency end is equal to the DC resistance of the screen, the 20 dB per decade rise at the high-frequency end is due to the inductive coupling through the screen and the dip at the middle frequencies is caused by eddy currents or skin effect of the braid. Some braided cables may behave anomalously having less than a 20 dB per decade rise at high frequencies. By using an extrapolation of 20 dB per decade we are in most cases on the conservative side. This extrapolation can be used up to several GHz.

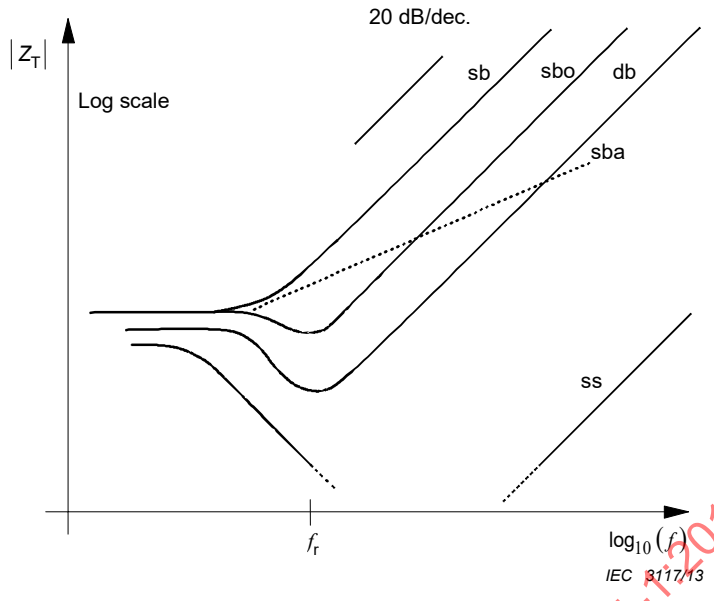

Key

f_r: typically 1....10 MHz
sb: single braid
sbo: single braid optimized
sba: single braid 'anomalous'
db: double braid
ss: superscreen

Figure 13 – Transfer impedance of typical cables

An electrically short piece of braided coaxial cable (2) is considered to be placed in a triaxial arrangement as in Figure 2.

It is assumed that the outer circuit (1) is the disturbing one. As stated, a braided cable has a transfer impedance Z_T that increases proportionally to frequency at high frequencies, because of the leakage of the magnetic field through holes in the braid.

The total flux of the magnetic field induced by the disturbing current I_1 is Φ_1. A part of it, Φ'_{12} leaks directly through the holes and includes a disturbing voltage U'_2 in the inner circuit. However, a part Φ''_{12} of Φ_1 flows in the braid and complicates the mechanism of the total magnetic leakage by the following additional phenomenon.

The braiding wires alternate between the outer and inner layer. It means that the inner and outer braid wires are likewise ingredients of both the inner (2) and outer (1) circuit of Figure 14.

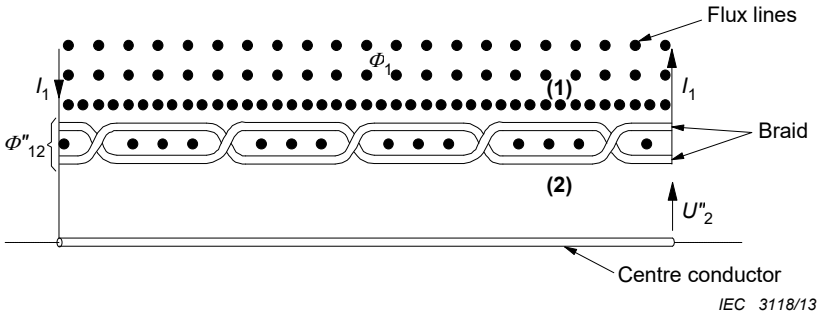

Figure 14 – Magnetic coupling in the braid – Complete flux

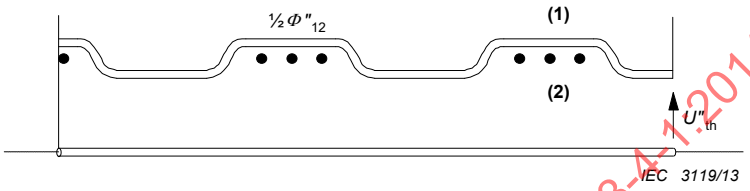

Figure 15 – Magnetic coupling in the braid – Left-hand lay contribution

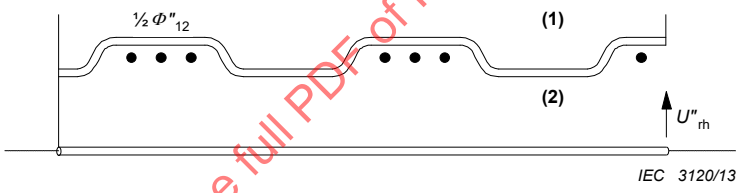

Figure 16 – Magnetic coupling in the braid – Right-hand lay contribution

Therefore it is necessary and unavoidable that Φ''_{12} is partly also in the inner circuit (see Figure 14). Both the left hand (lh) (see Figure 15) and right hand (rh) lay (see Figure 16) of the braiding wires bring into the inner circuit (2) an equal disturbing voltage U''_2 induced by Φ''_{12} / 2. The voltages are in parallel:

$$U''_{rh} = U''_{lh} = U''_2 = ½j\omega\Phi''_{12} \quad (25)$$

This phenomenon is similar to the "magnetic part" of the coupling through a homogeneous screen.

The two induced disturbing voltages oppose each other.

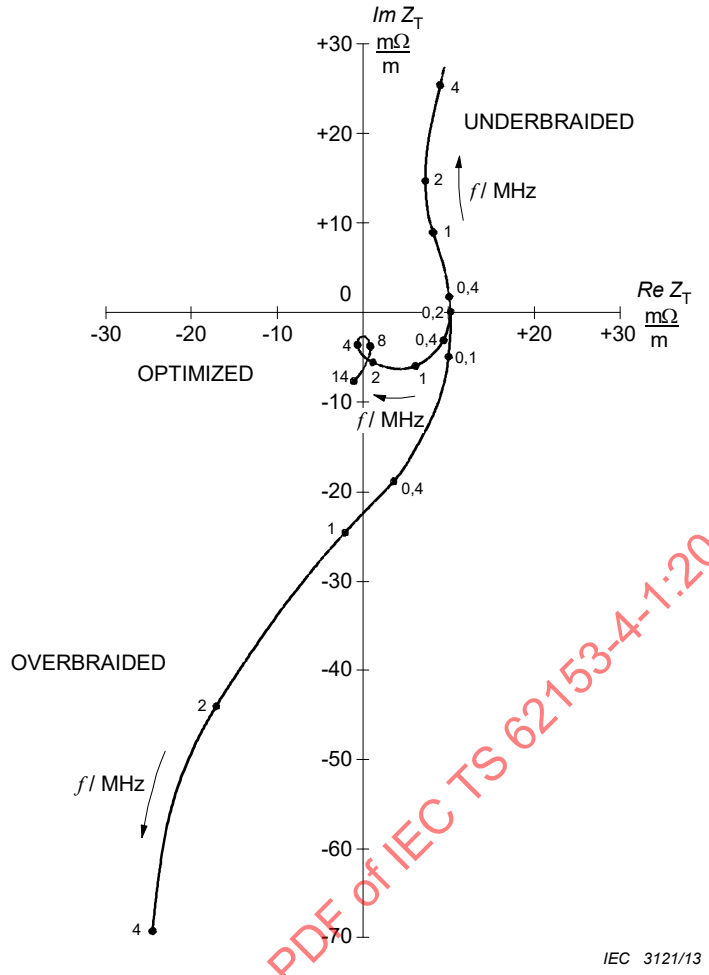

Figure 17 – Complex plane, Z_T = *Re* Z_T + j *Im* Z_T, frequency *f* as parameter

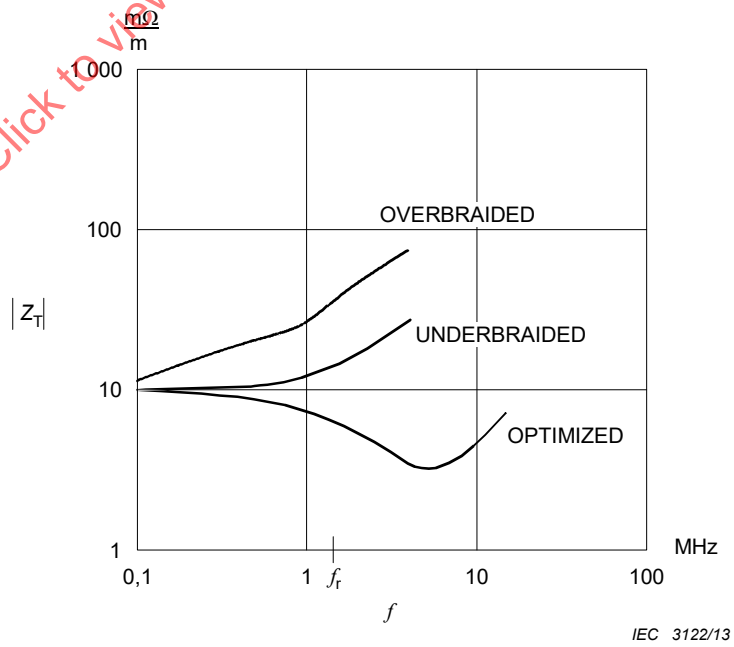

Figure 18 – Magnitude (amplitude), | Z_T (*f*) |

In Figure 17 and Figure 18, the d.c., resistance Z_T (d.c.), is set to the value of 10 mΩ/m.

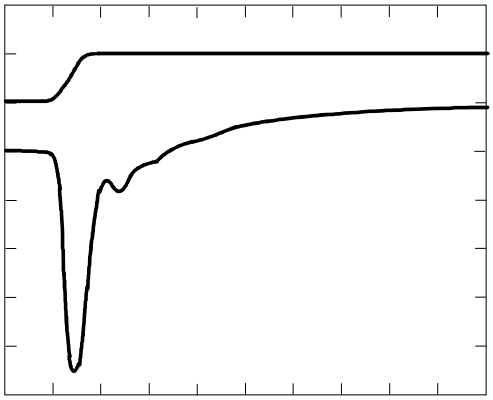

Figure 19a – Overbraided cable

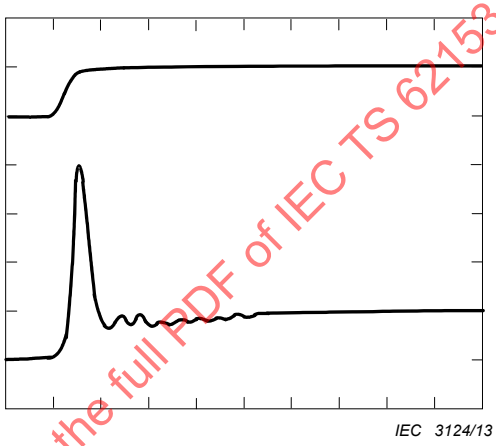

Figure 19b – Underbraided cable

Top trace: Injection step current (100 mA/div)

Time base: 50 ns/div

Amplifier gain: 30 dB, therefore Z_T (time) = 12,5 mΩ/m/div

Lower trace: The height of the spike corresponds to

a) – Z_T (3 MHz) = –4,7 × 12,5 mΩ/m = –59 mΩ/m;

b) – Z_T (3 MHz) = +4 × 12,5 mΩ/m = +50 mΩ/m.

Figure 19 – Typical Z_T (time) step response of an overbraided and underbraided single braided outer conductor of a coaxial cable

Braid optimization is based on these important physical facts. Both leakage phenomena can be described by mutual inductances:

$$M'_{12} = \frac{\Phi'_{12}}{\mathrm{j}\omega I_1} \tag{26}$$

$$M''_{12} = \frac{1}{2} \times \frac{\Phi''_{12}}{\mathrm{j}\omega I_1} \tag{27}$$

Clearly it is possible to make braided-wire screens where either M'_{12} or M''_{12} are dominant or where they cancel each other. Therefore, underbraided, overbraided or optimized braids may be considered. Figure 17 shows measured transfer impedances in the complex plane of such screens and the main transfer impedance components of a braided screen can be observed. From the optimized case, it can be concluded that at low frequencies the braid behaves approximately as a homogeneous tubular screen. The same can be concluded from Figure 18 where the transfer impedance amplitudes are shown as a function of frequency, but from it cannot be seen directly if the screen is underbraided or overbraided.

The transfer impedance of a braided wire screen consists of the following three main components (mentioned above).

a) At low and medium frequencies, the tubular screen coupling behaviour (Z_{Th}) varies with eddy currents and decreasing Z_T. In [2] it is stated that a good approximation for Z_{Th} is a tubular homogeneous screen [3] with the thickness of one wire diameter and the same d.c. resistance as the braid.

b) The mutual inductance M'_{12} is related to direct leakage of the magnetic flux Φ'_{12}.

c) The mutual inductance M''_{12} (negative) is related to the magnetic flux Φ''_{12} in the braid.

By adding these components, a good approximation is obtained for the transfer impedance Z_T of a braided wire screen:

$$Z_T \approx Z_{Th} + \mathrm{j}\,\omega\,(M'_{12} - M''_{12}) \tag{28}$$

and the first approximation of the equivalent circuit is shown in Figure 20a.

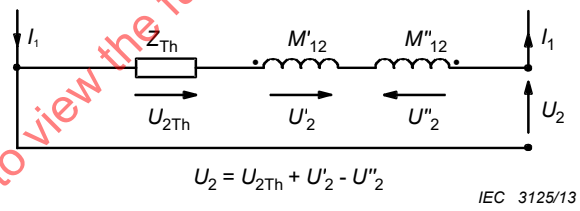

Figure 20a – Contributions to the transfer impedance

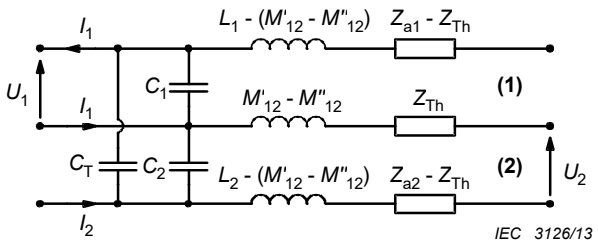

Figure 20b – Significant elements of circuits (1) and (2)

Figure 20 – Z_T equivalent circuits of a braided wire screen

A more complete equivalent circuit where the through capacitance C_T and surface impedances Z_a of the braided cable are incorporated is shown in Figure 20b. L_1 and L_2 are the (external) inductances of the outer and inner circuit.

Many attempts have been made to calculate the transfer impedance of a braided coaxial cable. Most of the literature ([2], [4], [5]) have concentrated on models of braided screens and calculation of direct leakage of the magnetic field induced by I_1, and of M'_{12}. Satisfactory results have been achieved.

There exists very little literature ([6], [7]) on M''_{12} but the matter has been studied by experts of standardization bodies. Especially the calculation and stability of M''_{12} have been shown to be very problematic because of so many uncertain and unstable parameters, e.g. the resistance of the crossover points of the wires, which have an effect on the magnetic field distribution in the braid. Also the pressure of the jacket has an effect on the small space between the right hand lay and left-hand lay of the braided wires. Not to mention the number of wire ends per carrier and the braid angle and the tightness and optical coverage of the braid.

After understanding the magnetic coupling mechanisms, it is not surprising that the transfer impedances of braided wire screens vary considerably and are unstable for many braid and cable constructions whether or not they are optimized. It is also clear that a perforated tube cannot be used as a model for a braided screen.

It is clear that a loose highly optimized braid can have a very unstable Z_T during bending, twisting and/or pressing. An overbraided screen with a high filling factor or optical cover normally has a (pure) negative transfer impedance at high frequencies because of a large M''_{12} coupling through the mutual "space" between the left and right lays of the braid in comparison with a small leakage through the braid M'_{12}. Pressure on the jacket would improve the screening performance by diminishing the mutual "space" and decrease the Z_T.

The manufacture of a good stable optimized cable requires the control of braid parameters such as:

– braid angle, tension (and lubricant) of the strands;
– number of strand in a spindle;
– wire diameter;
– plating;
– pressure of the jacket on the braid in manufacturing.

8 Test possibilities

8.1 General

A number of test procedures are used to test cables for their screening properties, some of which will be found in IEC standards. Each procedure has benefits for some users which for historical reasons may not be widely appreciated. Table 2 summarizes the test procedures available, some of which will be discussed here, with special reference to their applicability to cables, cable assemblies and connectors.

8.2 Measuring the transfer impedance of coaxial cables

All tests listed in Table 2 can be used on coaxial cables, but if a single test is needed to cover frequencies above and below 100 MHz, tests 1, 4, 7, 9 and 10 can be dismissed. Of the others, those with 's' under 'grouping' (column 3) have better intrinsic isolation between measuring and injection circuits, while in those with 'o' under grouping the injection circuit is unscreened. The difference is the line interchange referred to in 4.5 above. One benefit of an unscreened injection line is that better access may be obtained for inspection of the cable under test, which may be useful if the sample is in any way flawed. The two test methods with unscreened injection lines are test 3 and test 8. The latter, with its wide frequency coverage is recommended for future testing.

8.3 Measuring the transfer impedance of cable assemblies

Even with a restricted frequency range, many of the tests listed in Table 2 are not suited to tests on cable assemblies. Tests 1, 4, and 6 are unsuitable because an electrically short sample may be needed to achieve the upper frequencies, while test 10 is still limited to frequencies above 100 MHz. Tests with screened injection wires (test 2 and test 5) are difficult to set up due to the varying cross section of the assembly, a difficulty which also applies to test 3. Such objections leave tests 7, 8 and 9. To set against its low (effective) upper frequency limit, with test 7 it is easy to distinguish between connector and cable contributions, so it is ideal in a diagnostic role. Test 9 works only above 30 MHz, which may be restrictive. Test 8 will require several measurements on each sample, as it is unreasonable to assume that a cable assembly has circular symmetry.

It is only fair to state that in any frequency domain test on cable assemblies where signal phase is not recorded, a test is only valid if the sample length is not varied (tests carried out on a sample of one length cannot be used to assess a sample of another length – whether it be longer or shorter). Of the transfer impedance tests being discussed, only test 7 can be used in this way.

Multi-conductor cable assemblies are more complex, because the 'core' cannot be considered to be coaxial. A test for such cable assemblies has not yet been addressed.

8.4 Measuring the transfer impedance of connectors

In principle, all the tests in Table 2 can be used on coaxial connectors.

As with tests on cable assemblies, there is much benefit to be gained from using a test with an unscreened injection circuit, though other tests will remain in the standard, because they have become accepted. If it is possible to distinguish the screening of a connector from that of the attached cable, this will considerably ease the test procedure.

Multi-pin connectors are far more numerous and varied than coaxial connectors. However, non-circular connectors cannot be tested by the means implied by the test procedures of Table 2, though by suitable variation test 7 and test 10 would become appropriate. This problem is under study.

NOTE These methods give only an outline for measurement of symmetrical multicore cables, multipin connectors and cable assemblies made with these components.

The problems to be addressed come from the fact that:

a) a connector is electrically short, while the parameters of a cable are distributed, and it may be electrically long;

b) multi-core cables rarely have circular symmetry. This applies both physically and to the signal paths on their conductors;

c) most multi-pin connectors have no circular symmetry; nor are they equally spaced from other conductors, which might couple to them;

d) economics will dictate that a cable assembly test should apply to other assemblies using the same components, even though of differing overall length.

8.5 Calculated maximum screening level

It is important to know the exact theoretical limitation of the test equipment. By knowing the limitations, it is possible to calculate the maximum measurable screening effectiveness. This should be calculated to check the strengths and weaknesses of the test setup or even to optimize the test setup.

The following test equipment specifications are required for the calculation:

- minimum input (noise floor);
- maximum input;

- amplification/attenuation;
- maximum output.

Figure 21 gives a comparison of the different signal levels in a generic test setup. The maximum screening is the difference between the maximum obtainable input signal to the DUT and the minimum detectable signal from the DUT, in this case 131 dB. The noise floor level (*NL*) of the measuring system must be low enough to allow the measurement. In this case, lower than –122 dBm. Measurements at the noise floor result in a maximum error of 3 dB. When measured 6 dB above the noise floor, the error is only about 1 dB.

The triaxial tube column is divided in two to show both the loss in the tube and the actual maximum screening.

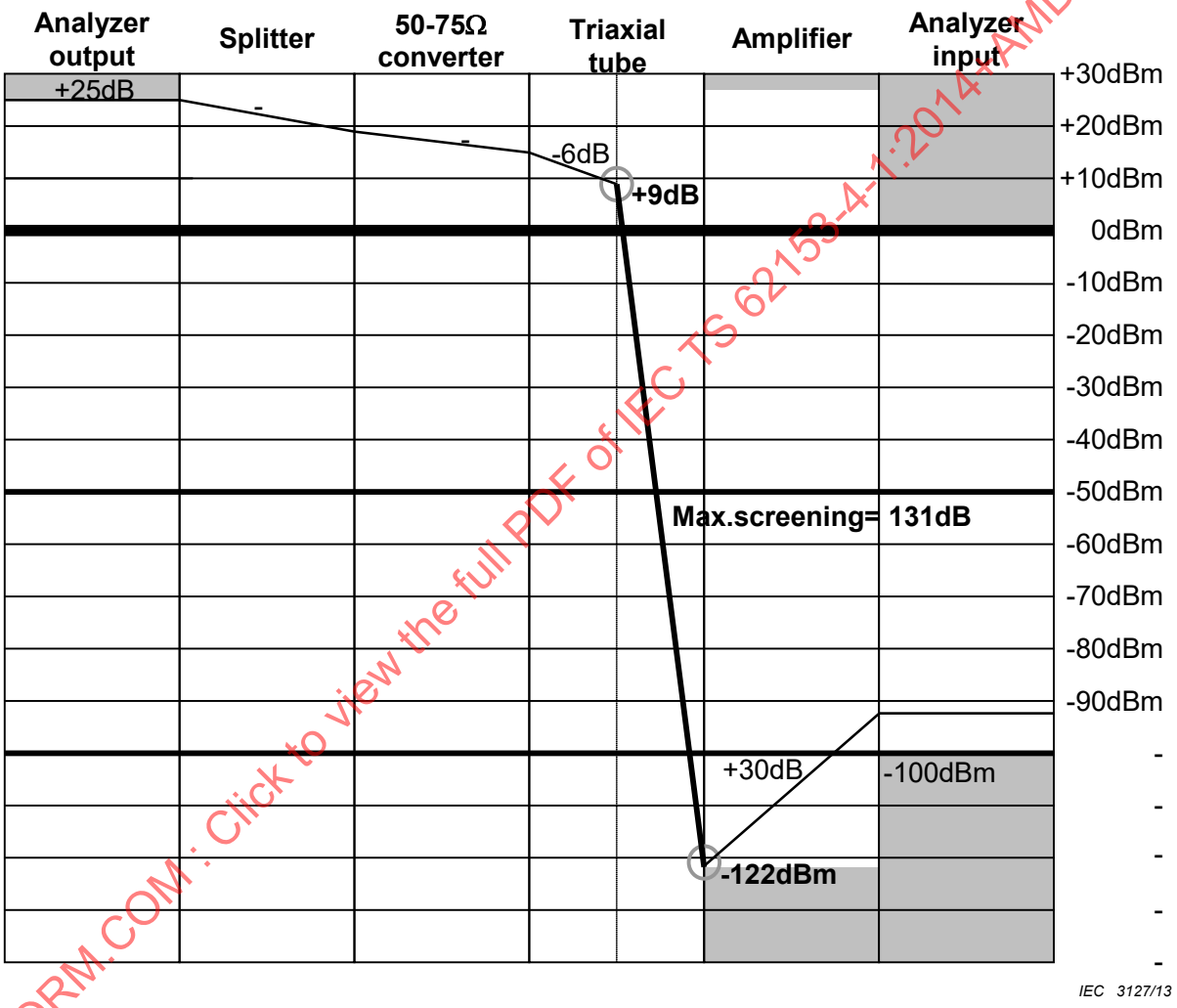

Figure 21 – Comparison of signal levels in a generic test setup

Taking into consideration the noise level of 1 Hz bandwidth at room temperature being –173 dBm, (increase 10 × log(bandwidth) dB) and adding the noise figure of the amplifier, we get the theoretical noise level of the test setup. Assuming that the amplifier in the Figure 21 example has a noise figure of 11 dB, we can then calculate that the bandwidth (Δf) of the network analyzer shall be smaller than 10 kHz.

This can be expressed as a general formula:

$$NL = (-173 + F + 10 \times \log_{10} \Delta f) \quad (29)$$

where

NL is the noise floor level of receiving side of the measuring system in dBm;

F is the noise figure of the pre amplifier in dB;

Δf is the bandwidth of the receiver in Hz.

Table 2 – Screening effectiveness of cable test methods for surface transfer impedance Z_T

	Short title	Reference	Grouping (see Note 1)	Frequency range		Injection N or F (see Note 2)	Advantages or shortcomings
				Possible	Actually used		
1	IEC triaxial	IEC 62153-4-3	kf s	d.c. to 50 MHz	10 kHz to 30 MHz	F	Rigid test rig or flexible (milked on braid)
2	Terminated triaxial (Simons)	Figure A5 of IEC 60096-1:1986 [32]	m s	10 kHz to 1 GHz	100 kHz to 500 MHz	N F	Flexible test jig relies on ferrites
3	Braid injection (Fowler)	[9]	m o	d.c. to 500 MHz	10 kHz to 500 MHz	N F	Flexible test needs good screening on measuring system
4	Quadraxial	[10]	m s	100 kHz to 50 MHz	100 kHz to 1 GHz	N	Deep resonances make use above 50 MHz theoretically impossible. The test has been used for assessing screening at frequencies up to 1 GHz
5	Matched T triaxial (Staegar)	IEC 60169-1-3 [11]	m s	1 kHz to 12 GHz	100 MHz to 10 GHz 10 kHz to 100 MHz	N F	Rigid test jig needs good screening
6	ERA triaxial (Smithers)	[12]	kf s	d.c. to 400 MHz	10 kHz to 300 MHz	F	Very short CUT requires amplifier or phase locked loop
7	Line injection (time domain)	IEC 60096-4-1 [33] [13]	m o	d.c. to 100 MHz	1 kHz to 80 MHz (note 3)	N F	Very easy to use. Needs good screening in measuring amplifier
8	Line injection (frequency domain)	IEC 62153-4-6 [14]	m o	d.c. to 20 GHz	10 kHz to 3 GHz	N F	Flexible and cheap measuring set-up, equipment needs to be well shielded
9	Open screening attenuation test method (absorbing clamp)	IEC 62153-4-5	m o	30 MHz to 2,5 GHz	30 MHz to 1 GHz 300 MHz to 2,5 GHz	N F	Poor sensitivity. Measuring of a_S is dependent on the surroundings
10	Reverberation chamber method	IEC 61726 [15]	kn kf	0,1 GHz →	0,3 GHz to 40 GHz	N & F	Flexible in use, but a complex and expensive computer controller with sophisticated test software needed
11	Shielded screening attenuation test method	IEC 62153-4-4 [16] (note 4)	m s	d.c. to 5 GHz	10 kHz to 3 GHz	F	High-sensitivity measurements can be made without a screened room. Transfer impedance and screening attenuation can be measured with one set-up
12	Open multipin connector screening test method	[17]	o	d.c. to 1 GHz	10 kHz to 700 MHz	N	Low cost and flexible

Short title	Reference	Grouping (see Note 1)	Frequency range		Injection N or F (see Note 2)	Advantages or shortcomings
			Possible	Actually used		
13 Coupling attenuation measurements of balanced cables, cable-assemblies, connecting hardware						
13.1 Current clamp injection method	IEC 62153-4-2		50 MHz to 1 GHz	50 MHz to 1 GHz		High sensitivity but a screened room is recommended
13.2 Shielded triaxial test method	IEC 62153-4-9 [22]		d.c. to 3 GHz	d.c. to 1 GHz		High-sensitivity measurements can be made without a screened room
13.3 Absorbing clamp method	IEC 62153-4-5 IEC 62153-4-11 IEC 62153-4-12 IEC 62153-4-13		50 MHz to 2,5 GHz	50 MHz to 2,5 GHz		Poor sensitivity
14 Shielded screening attenuation, test method for measuring the transfer impedance Z_T and the screening attenuation a_S of RF connectors up to and above 3 GHz; tube in tube method	IEC 62153-4-7	m s	d.c. to 20 GHz	d.c. to 3 GHz		High-sensitivity measurements can be made without a screened room Transfer impedance and Screening attenuation with one test set-up
15 Shielded screening attenuation test method for measuring the screening effectiveness of feedtroughs and electromagnetic gaskets – double coaxial method	IEC 62153-4-10	m s	d.c. to 4 GHz	d.c. to 3 GHz		High-sensitivity measurements can be made without a screened room

NOTE 1 Grouping by condition of 'primary circuit':

kn = short circuit at near end;

kf = short circuit at far end;

m = matched with characteristic impedance;

o = open on unscreened;

s = screened or shielded.

NOTE 2 N denotes near end feeding of primary relative to secondary circuit. F denotes far end feeding of primary relative to secondary circuit.

NOTE 3 Effective frequencies tested. Actually pulse with T_R = 3,5 ns and duration up to 160 µs.

NOTE 4 Secondary circuit near end short circuited.

9 Comparison of the frequency response of different triaxial test set-ups to measure the transfer impedance of cable screens

9.1 General

Different triaxial test set-ups for the measurement of the transfer impedance exist as described in EN 50289-1-6 and the IEC 62153-4 series. All of them are based on the same principle but are using different load conditions. In one method for example the cable under test is matched, while in the other the cable is short circuited at the far end. Furthermore, generator and receiver may be interchanged in the different set-ups. The following investigation analyses the frequency response of the different set-ups and their influence on the cut-off frequency up to which the transfer impedance could be measured.

9.2 Physical basics

9.2.1 Triaxial set-up

9.2.1.1 General

The triaxial set-up is of the “triple coaxial” form, see Figure 22 and Figure 23. A short length of the screen under test forms both, the inner conductor of the outer system and at the same time the outer conductor of the inner system. The coupling between the two coaxial systems is caused by the transfer impedance and the capacitive coupling admittance of the screen. The matching circuit, load resistor and series resistor are used to change the load conditions of the set-up. Also the generator and receiver may be interchanged between the different methods.

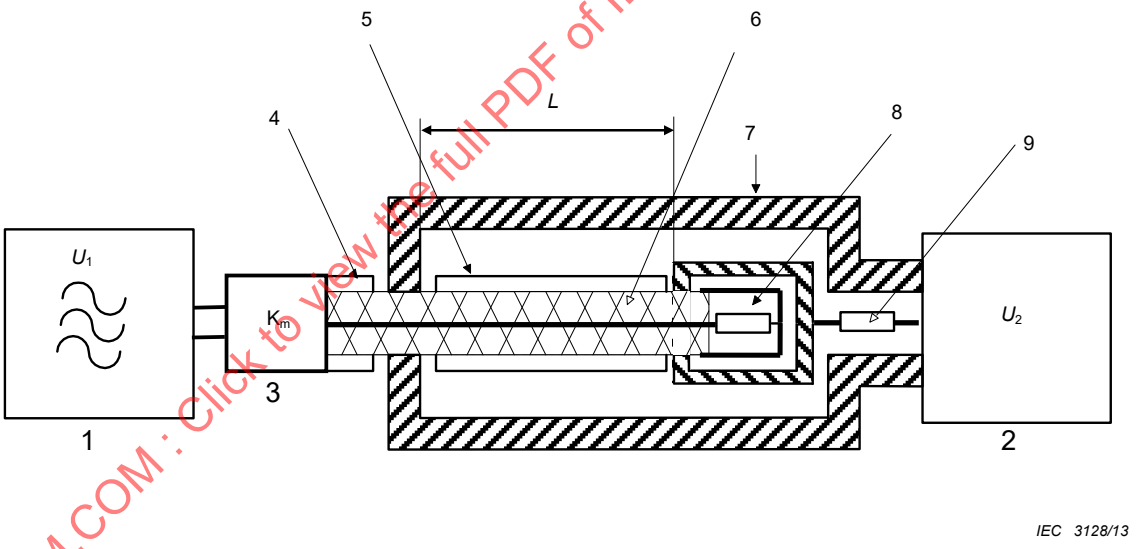

Key

1	Signal generator	6	Cable screen
2	Calibrated receiver or network analyzer	7	Tube
3	Matching circuit	8	Terminating resistor
4	Cable under test	9	Series resistor
5	Cable sheath		

Figure 22 – Triaxial set-up for the measurement of the transfer impedance Z_T

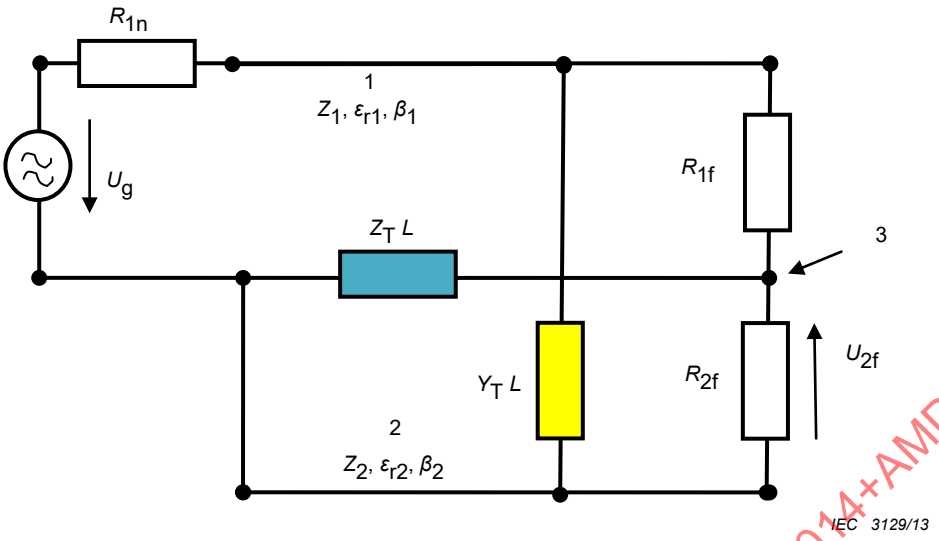

Key

1	inner circuit, cable
2	outer circuit, tube
3	screen
$Z_{1,2}$	characteristic impedance of the inner circuit, cable, respectively outer circuit, tube
$\varepsilon_{1,2}$	dielectric permittivity of the inner circuit, cable, respectively outer circuit, tube
$\beta_{1,2}$	phase constant of the inner circuit, cable, respectively outer circuit, tube
L	coupling length
Z_T	transfer impedance
Y_T	capacitive coupling admittance
R_{1n}	load resistance at the near end of the inner circuit, cable. Equal to the output impedance of the generator respectively input impedance of the receiver including an eventually used feeding resistor
R_{1f}	load resistance at the far end of the inner circuit, cable. Depending on the used method either equal to the characteristic impedance of the cable or a short circuit.
R_{2f}	load resistance at the far end of the outer circuit, tube. Equal to the output impedance of the generator respectively input impedance of the receiver including an eventually used feeding resistor
U_g	EMF of the generator
U_{2f}	voltage at the far end of the outer circuit

Figure 23 – Equivalent circuit of the triaxial set-up

9.2.1.2 Load conditions of the different set-ups

EN 50289-1-6 is using a method, where the cable under test and the far end of the secondary circuit are matched. The signal is fed to the cable under test and the disturbing voltage is measured at the far end of the outer circuit. A simplified method is to neglect the matching resistor at the far end of the outer circuit, which results in a higher dynamic range.

IEC 61196-1 describes two methods:

Method 1: Feeding through a resistance, where the signal is fed via a resistance into the outer circuit and the disturbing voltage is measured at the far end of the cable under test.

Method 2: Direct feeding, where the signal power is fed directly into the outer circuit and the disturbing voltage is measured at the far end of the cable under test.

With the revision of IEC 61196-1, the standard IEC 62153-4-3 has been published which also describes several methods:

Method A “Matched-Short” is equal to EN 50289-1-6.

Method B “Short-Short” is the double short circuited method, where the load resistance of the cable is replaced by a short circuit, thus having two short circuits in the set-up. One is at the near end of the outer circuit (between the cable screen and the tube) and the other is at the far end of the cable. The advantage of this method is the simplification of the sample preparation. A short circuit is easier to make than to solder a resistor, especially if the sample is a multi-conductor cable. Furthermore, the measurement sensitivity is improved. Compared to the “matched-short” method, the dynamic range is improved by about 16 dB. In the “milked on braid” method, an additional braid, the measuring braid, is pulled over the cable sheath instead of using the measuring tube. The advantage is that the sample could be bent under test, however the preparation is more laborious than with the measuring tube.

The load conditions of the different methods are given in Table 3. The impedance of the outer circuit, Z_2 is varying with the diameter of the screen under test. Using the measuring tube Z_2 is in general higher, and in the “milked on braid” method Z_2 is lower, than the input impedance of the receiver.

Table 3 – Load conditions of the different set-ups

Method	Generator	Receiver	R_{1n}/Z_1	R_{1f}/Z_1	Z_2/R_{2f}
EN 50289-1-6					
Standard	IC	OC	1	1	0,71
simplified	IC	OC	1	1	1…5 depending on the tube diameter
IEC 61196-1					
Method 1: feeding through a resistance	OC	IC	1	1	0,71
Method 2: direct feeding	OC	IC	1	1	1…5 depending on the tube diameter
IEC 62153-4-3 Double short circuit methods					
With tube	OC	IC	1*	0	1…5 depending on tube diameter
With milked on braid	IC	OC	1*	0	0,1…0,4 depending on screen and sheath diameter of the cable
IC: inner circuit (cable under test) OC: outer circuit (tube)					
* only if the cable impedance is equal to the generator impedance. For other cable impedances, the value may vary, e.g. 0,67 for cables with an impedance of 75 Ω.					

9.2.2 Coupling equations

The equations for the coupling between the inner circuit and outer circuit for any load conditions are described in [18] and [19]. By taking into account the short circuit at the near end of the outer circuit (between the cable screen and the measuring tube), neglecting the attenuation of the disturbing and disturbed line, assuming non ferromagnetic materials and introducing further variables, the following equations are defined.

$$\frac{u_{2f}}{u_q} = \frac{L}{R_{1f} + R_{1n}} \cdot [Z_T \cdot g + Z_F \cdot h] \quad (30)$$

$$g = \frac{1}{N} \cdot \frac{1}{1-n^2} \cdot \frac{j}{x} \cdot \{ r \cdot [\cos x - \cos nx] - j \cdot n \cdot \sin nx + j \cdot \sin x \} \quad (31)$$

$$h = \frac{1}{N} \cdot \frac{1}{1-n^2} \cdot \frac{j}{x} \cdot \{ n \cdot r \cdot [\cos x - \cos nx] - j \cdot \sin nx + j \cdot n \cdot \sin x \} \quad (32)$$

$$N = \left\{ \cos x + \frac{j \cdot \sin x}{r + w} \cdot [1 + r \cdot w] \right\} \cdot \{ \cos nx + j \cdot v \cdot \sin nx \} \quad (33)$$

$$x = \beta_1 \cdot L = 2\pi \cdot \frac{L}{\lambda_1} \quad (34)$$

$$n = \frac{\beta_2}{\beta_1} = \frac{\lambda_1}{\lambda_2} = \sqrt{\frac{\varepsilon_{r2}}{\varepsilon_{r1}}} \quad (35)$$

$$r = \frac{R_{1f}}{Z_1} \quad (36)$$

$$v = \frac{Z_2}{R_{2f}} \quad (37)$$

$$w = \frac{R_{1n}}{Z_1} \quad (38)$$

where

$Z_{1,2}$ is the characteristic impedance of the inner circuit (cable) respectively outer circuit (tube);

$\varepsilon_{1,2}$ is the dielectric permittivity of the inner circuit (cable) respectively outer circuit (tube);

$\beta_{1,2}$ is the phase constant of the inner circuit (cable) respectively outer circuit (tube);

$\lambda_{1,2}$ is the wave length in the inner circuit (cable) respectively outer circuit (tube);

L is the coupling length;

Z_T is the transfer impedance;

Y_T is the capacitive coupling admittance;

$R_{1,n}$ is the load resistance at the near end of the inner circuit (cable). Equal to the output impedance of the generator respectively input impedance of the receiver including an eventually used feeding resistor;

$R_{1,f}$ load resistance at the far end of the inner circuit (cable). Depending on the used method either equal to the characteristic impedance of the cable or a short circuit.

The factors g and h (see Equations (31) and (32)) describe the frequency response of the test set-up. At low frequencies, when $\lambda >> L$, the factors g and h are equal to 1. However, with increasing frequency, the factors g and h start to oscillate and thus also the measurement results. The maximum frequency to which the transfer impedance could be measured without oscillations, caused by the set-up, is defined as the 3 dB deviation from the linear interpolation of the measurement results. Or in other words, the maximum frequency is reached when the factor g respectively h becomes $> \sqrt{2}$ respectively $< 1/\sqrt{2}$.

9.3 Simulations

9.3.1 General

For the following investigations, simulations have been chosen rather than a pure mathematical solution because they are easier to grasp and clearly illustrate the differences in the set-ups given in Table 4. In general, the capacitive coupling can be neglected compared to the magnetic coupling ($Z_F << Z_T$). i.e. the cut-off frequency is mainly determined by the frequency behaviour of the factor *g*. Thus the following simulations are limited to the factor *g*.

Due to the reciprocity of the materials, it is possible to interchange the generator and receiver without changing the results. Thus the standard EN 50289-1-6 method gives the same results as IEC 61196-1, method 1: "feeding through a resistance" and the simplified EN 50289-1-6 method gives the same results as IEC 61196-1, method 2: "direct feeding".

Table 4 – Parameters of the different set-ups

Method	$w=R_{1n}/Z_1$	$r=R_{1f}/Z_1$	$v=Z_2/R_{2f}$	$n=\sqrt{\varepsilon_{r2}}/\sqrt{\varepsilon_{r1}}$
EN 50289-1-6, IEC 62153-4-3 method A				
Standard	1	1	0,71	0,66 (0,45)...0,91
Simplified	1	1	1...5 depending on the tube diameter	
IEC 61196-1				
Method 1: feeding through a resistance	1	1	0,71	0,66 (0,45)...0,91
Method 2: direct feeding	1	1	1...5 depending on the tube diameter	
IEC 62153-4-3 Double short circuit methods				
With tube	1[a]	0	1...5 depending on tube diameter	0,66 (0,45)...0,91
With milked on braid	1[a]	0	0.1...0,4 depending on screen and sheath diameter of the cable	1,02...2,0

[a] only if the cable impedance is equal to the generator impedance. For other cable impedances, the value may vary, e.g. 0,67 for cables with an impedance of 75 Ω.

In the tube methods, the factor *n* is given by the dielectric permittivity of the cable (inner circuit) as the dielectric permittivity of the outer circuit is nearly independent on the sheath material and can be assumed to be 1. However, in the "milked on braid method", the factor *n* is dependent on both the dielectric permittivity of the cable insulation and the sheath, as the "measuring braid" is directly put on the sheath of the sample. The values for the factor *n* are given for typical insulation materials (PE, foam PE, PTFE ...). The values in brackets are given for an insulation material of PVC, which may be used in multi-pair/conductor cables. For the "milked on braid" method, typical combinations of insulation and sheath materials (PE/PVC, PE/LSZH, PTFE/FEP...) are taken into account, resulting in a value $n > 1$.

9.3.2 Simulation of the standard and simplified methods according to EN 50289-1-6, IEC 61196-1 (method 1 and 2) and IEC 62153-4-3 (method A)

In EN 50289-1-6, IEC 61196-1 method 1: "feeding through a resistance" and IEC 62153-4-3 method A: "Matched-Short", the factor $v=Z_2/R_{2f}$ is specified at $1/\sqrt{2}$. The following simulations show that this factor is a good compromise with respect to the maximum frequency to which the transfer impedance could be measured.

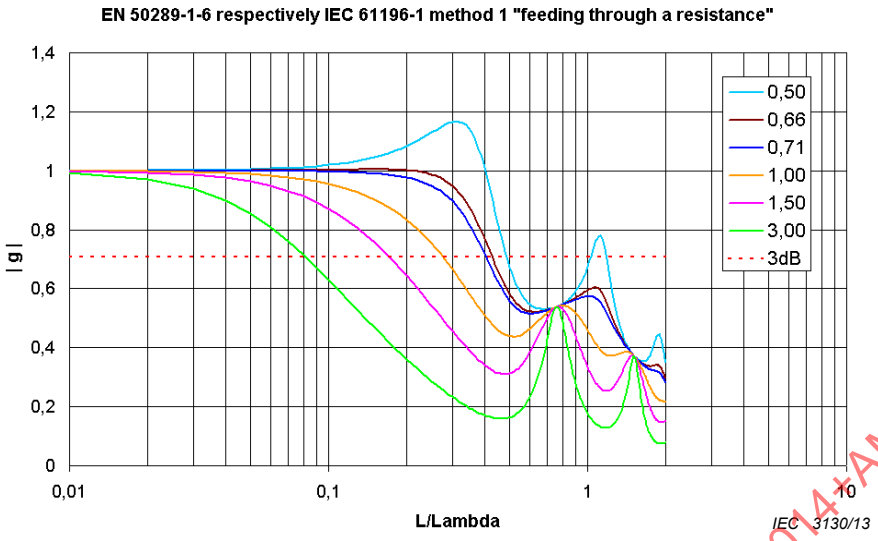

Key

Coloured lines correspond to indicated factors of $v=Z_2/R_{2f}$.

Simulation parameters		
ε_{r1}	ε_{r2}	n
2,3 (solid PE)	1,0	0,569

Figure 24 – Simulation of the frequency response for *g*

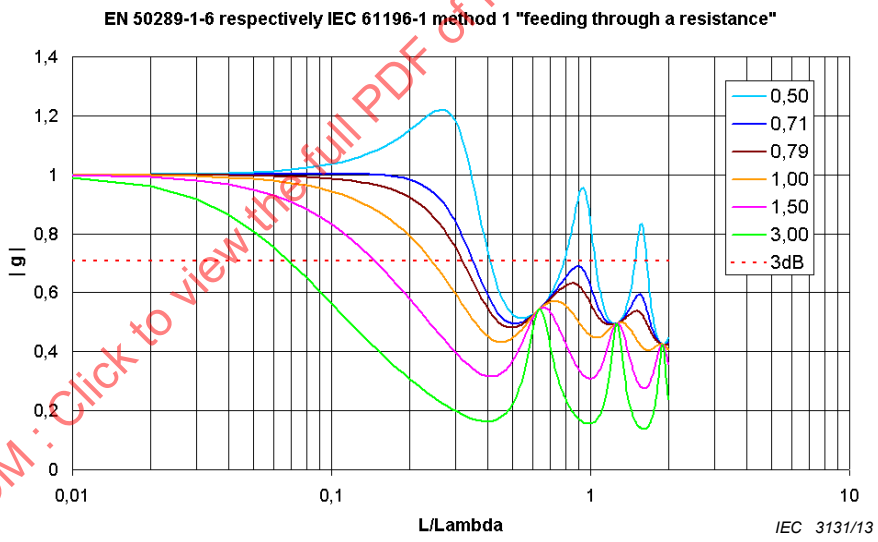

Key

Coloured lines correspond to indicated factors of $v=Z_2/R_{2f}$.

Simulation parameters		
ε_{r1}	ε_{r2}	n
1,6 (foam PE)	1,0	0,791

Figure 25 – Simulation of the frequency response for *g*

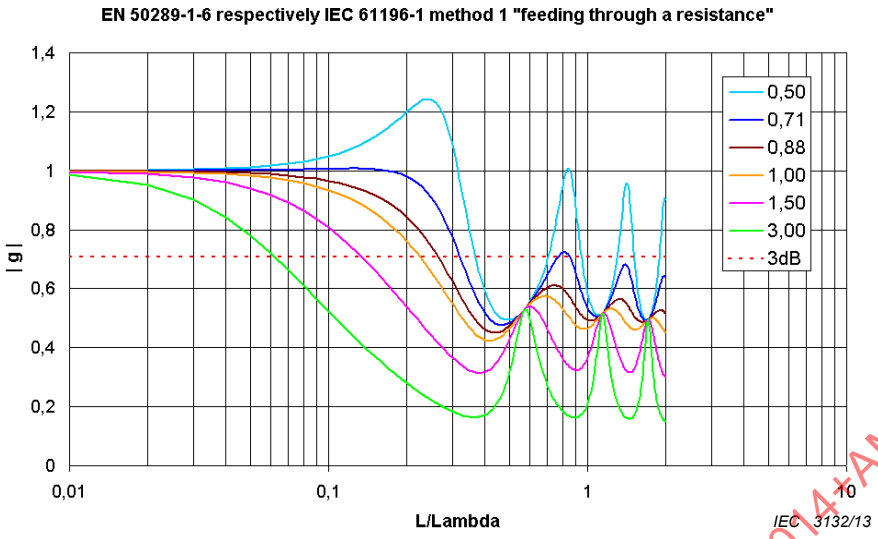

Key

Coloured lines correspond to indicated factors of $v=Z_2/R_{2f}$.

Simulation parameters		
ε_{r1}	ε_{r2}	n
1,3 (foam PE)	1,0	0,877

Figure 26 – Simulation of the frequency response for *g*

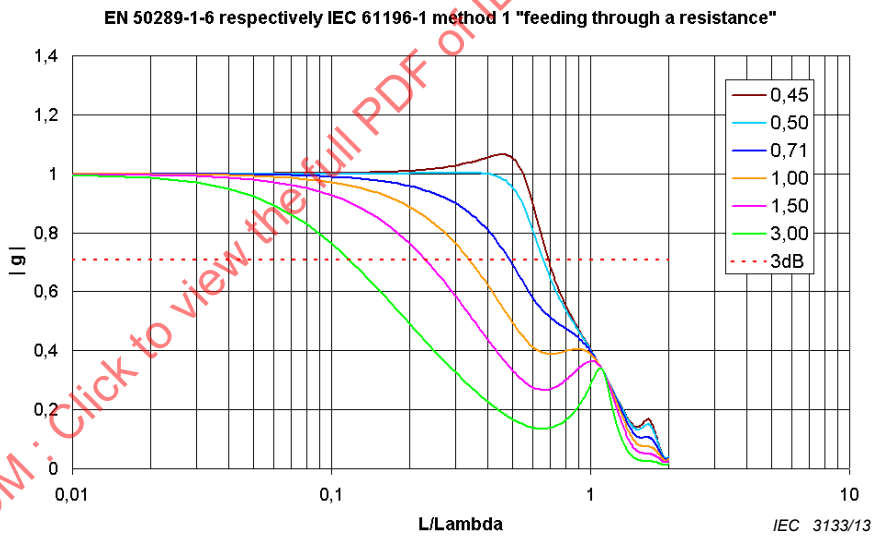

Key

Coloured lines correspond to indicated factors of $v=Z_2/R_{2f}$.

Simulation parameters		
ε_{r1}	ε_{r2}	n
5 (PVC)	1,0	0,447

Figure 27 – Simulation of the frequency response for *g*

The highest frequencies (respectively shortest wavelengths) are obtained if the factor $v=1/\sqrt{2}$ respectively $v=n$, whichever is smaller. In Figure 24 and Figure 27, the highest frequency is obtained for $v=n$ (=0,659 respectively 0,447). But in Figure 25 and Figure 26, the highest frequency is obtained for $v=1/\sqrt{2}=0,71$. Below that value, the factor g overshoots, i.e. becomes higher than one. Above that value, the cut-off frequency is decreasing.

Figure 28 gives the calculated, by iteration, 3 dB cut-off wavelength (L/λ_1) at which the factor $|g|$ becomes $1/\sqrt{2}$. The graph is given as a function of the factor $n=\sqrt{\varepsilon_{r2}}/\sqrt{\varepsilon_{r1}}$ and for different factors $v=Z_2/R_{2f}$. The curves show a linear behaviour and could be interpolated by straight line.

This has been done in Figure 29 for $v=1/\sqrt{2}$, $v=1$, $v=1{,}8$ and $v=3{,}6$. The factor $v=1/\sqrt{2}$ corresponds to the set-up according to EN 50289-1-6, IEC 61196-1 method 1 "feeding through a resistance" and IEC 62153-4-3 method A "Matched-Short". The other values of the factor v correspond to the simplified set-up, i.e. direct feeding. For common diameters of the measuring tube (around 40 mm) and common cable screen diameter (2 mm to 9 mm), the impedance in the outer circuit is 90 Ω to 180 Ω and $v=1{,}8\ldots3{,}6$.

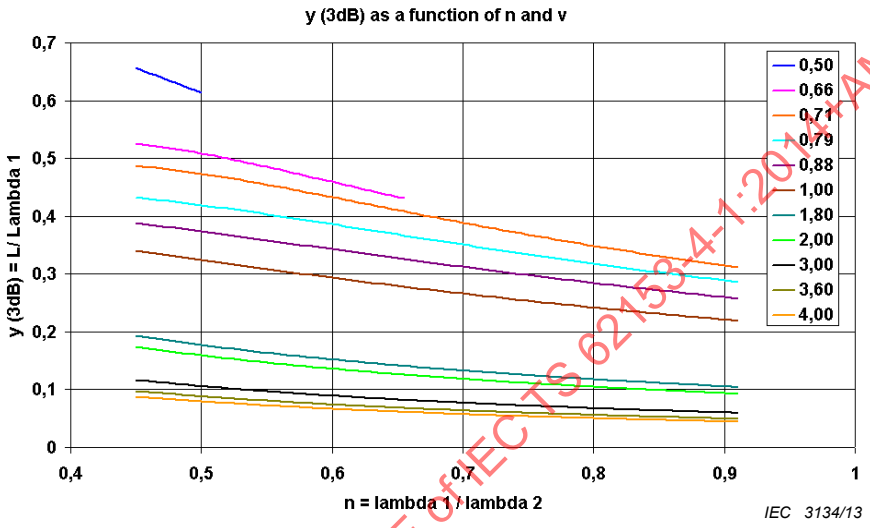

Key

Coloured lines correspond to indicated factors of $v=Z_2/R_{2f}$.

Figure 28 – Simulation of the 3 dB cut off wavelength (L/λ_1)

The graphs for $v=0{,}5$ and $v=0{,}66$ are only given for n up to 0,5 respectively 0,66 because otherwise the factor g oversoots as described above.

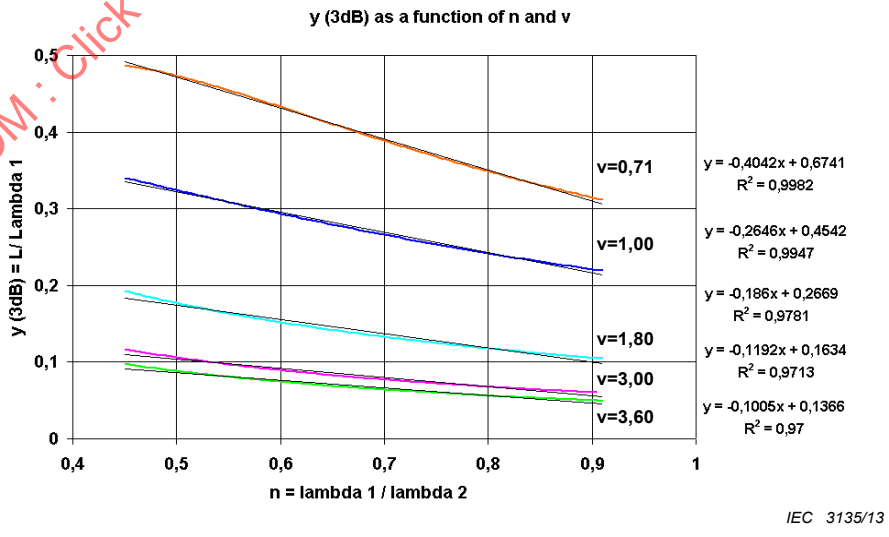

Key

Coloured lines correspond to indicated factors of $v=Z_2/R_{2f}$.

Figure 29 – Interpolation of the simulated 3 dB cut off wavelength (L/λ_1)

The linear interpolation equation is used to derive an equation to calculate the cut-off frequency length product up to which the transfer impedance could be measured in a given triaxial test set-up.

Table 5 – Cut-off frequency length product

Triaxial test set-up	v	Cut-off equation
EN 50289-1-6 IEC 61196-1 method 1 “feeding through a resistance IEC 62153-4-3 method A “matched-short”	v=1/√2	$(f \cdot L)_{3\ dB} \approx \left[\frac{200}{\sqrt{\varepsilon_{r1}}} - \frac{120}{\varepsilon_{r1}}\right] \cdot MHz \cdot m$
Simplified EN 50289-1-6 IEC 61196-1 method 2 “direct feeding”	v=1	$(f \cdot L)_{3\ dB} \approx \left[\frac{135}{\sqrt{\varepsilon_{r1}}} - \frac{80}{\varepsilon_{r1}}\right] \cdot MHz \cdot m$
	v=1,8	$(f \cdot L)_{3\ dB} \approx \left[\frac{80}{\sqrt{\varepsilon_{r1}}} - \frac{55}{\varepsilon_{r1}}\right] \cdot MHz \cdot m$
	v=3	$(f \cdot L)_{3\ dB} \approx \left[\frac{50}{\sqrt{\varepsilon_{r1}}} - \frac{35}{\varepsilon_{r1}}\right] \cdot MHz \cdot m$
	v=3,6	$(f \cdot L)_{3\ dB} \approx \left[\frac{40}{\sqrt{\varepsilon_{r1}}} - \frac{30}{\varepsilon_{r1}}\right] \cdot MHz \cdot m$

The equations given in Table 5 are drawn in the graphs of Figure 30.

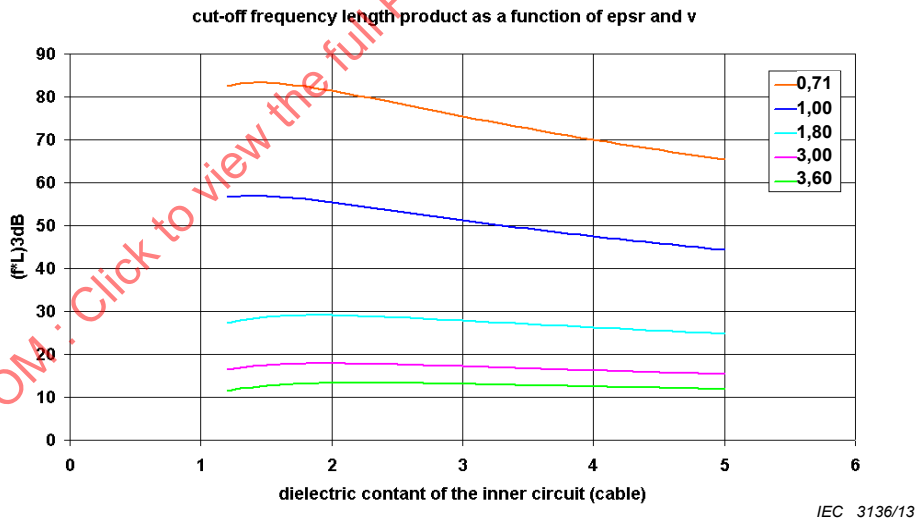

Key

Coloured lines correspond to indicated factors of $v=Z_2/R_{2f}$.

Figure 30 – 3 dB cut-off frequency length product as a function of the dielectric permittivity of the inner circuit (cable)

For example, if a cable with a PE insulation – dielectric permittivity of, ε_{r1} = 2,3, and a screen diameter of 3,5 mm is measured in a triaxial set-up according to EN 50289-1-6 or IEC 61196-1 method 1 “feeding through a resistance” with v=0,71, then the cut-off frequency length product is about 80 MHz·m. Therefore for a coupling length of 0,5 m, the maximum frequency to which the transfer impedance could be measured is around 160 MHz.

If the same cable is measured in a triaxial set-up according to IEC 61196-1 method 2 “direct feeding” or the simplified set-up according to EN 50289-1-6 where v=3, then the cut-off frequency length product is about 18 MHz·m. For a coupling length of 0,5 m, the maximum frequency to which the transfer impedance could be measured is around 36 MHz.

Figure 31 and Figure 32 show the measurement results of the normalised voltage drop – i.e. the attenuation caused by the series resistor has been taken into account – in the triaxial set-up for different factors of v. Both figures show the results of the same screen design, however one with a solid PE insulation (ε_{r1}=2,3), the other with a foam PE insulation (ε_{r1}=1,6). The measurement results confirm the simulations. From the equations given in Table 5 one obtains cut-off frequency length products for v=3 of about 18 MHz·m and for v=1 of about 55 MHz·m for both the solid PE and the foam PE. This is also found from the measurement results.

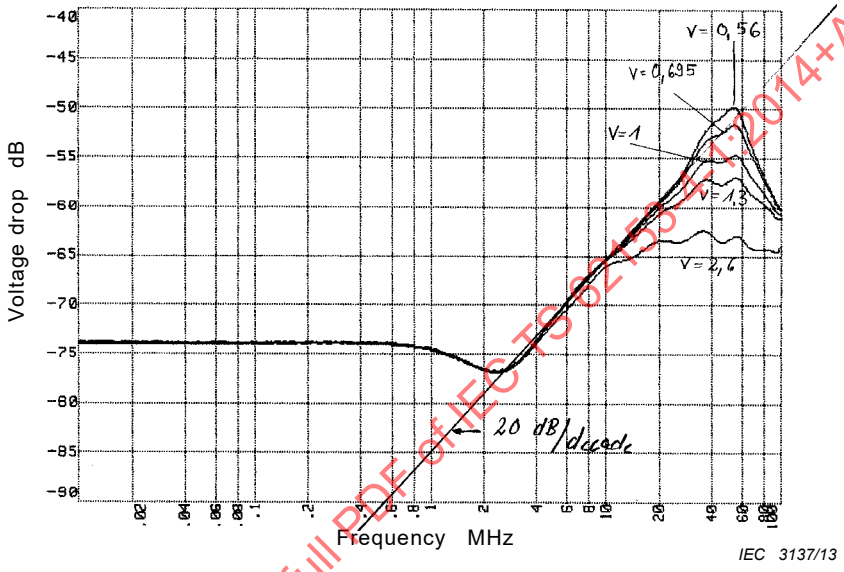

Key

Indicated lines correspond to factors of $v=Z_2/R_{2f}$

Measurement set-up parameters				
ε_{r1}	ε_{r2}	n	Z_2	L
2,3 (PE)	1,0	0,659	130 Ω	1 m

Figure 31 – Measurement result of the normalised voltage drop of a single braid screen on a solid PE dielectric in the triaxial set-up

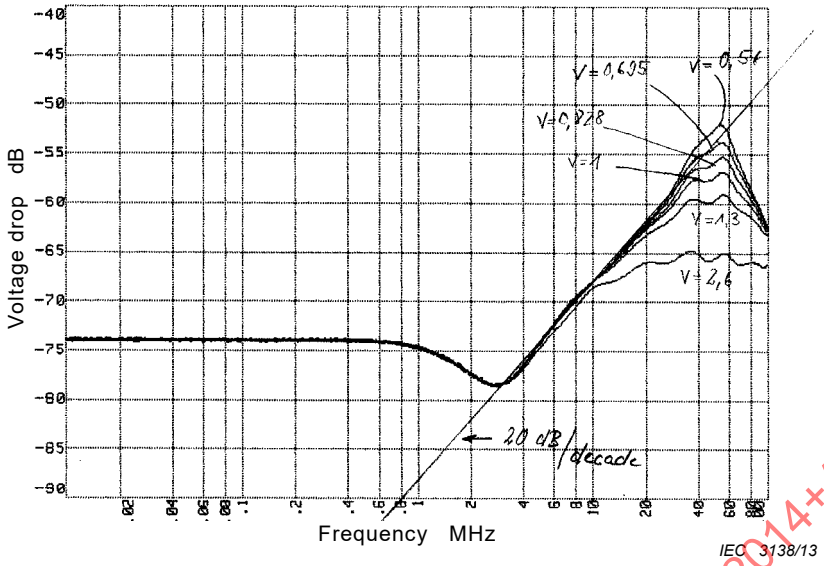

Key

Indicated lines correspond to factors of $v = Z_2/R_{2f}$

Measurement set-up parameters				
ε_{r1}	ε_{r2}	n	Z_2	L
1,6 (foam PE)	1,0	0,791	130 Ω	1 m

Figure 32 – Measurement result of the normalised voltage drop of a single braid screen on a foam PE dielectric in the triaxial set-up

9.3.3 Simulation of the double short circuited methods

9.3.3.1 General

For the double short circuited methods, one has either a measuring tube or a “milked on braid”. When using a measuring tube, the dielectric permittivity of the outer circuit (tube) is nearly independent on the sheath material and could be assumed to be 1. However in the “milked on braid” method, the dielectric permittivity is given by the sheath material. Thus the factor n is different for both methods. Also the impedance of the outer circuit is different for both methods, first due to the different dimensions, second due to the different permittivities.

9.3.3.2 Simulation of the double short circuited method using a measuring tube

The double short circuited method using a measuring tube is shown in Figure 33. The outer circuit is fed over a fixed – i.e. the same value for all cable types – feeding resistor, the value of which is equal to the output impedance of the generator (e.g. 50 Ω). Thus the load impedance of the outer circuit at the far end is equal to 2 times the output impedance of the generator. The factor v is then only dependent on the diameters of the screen and of the measuring tube.

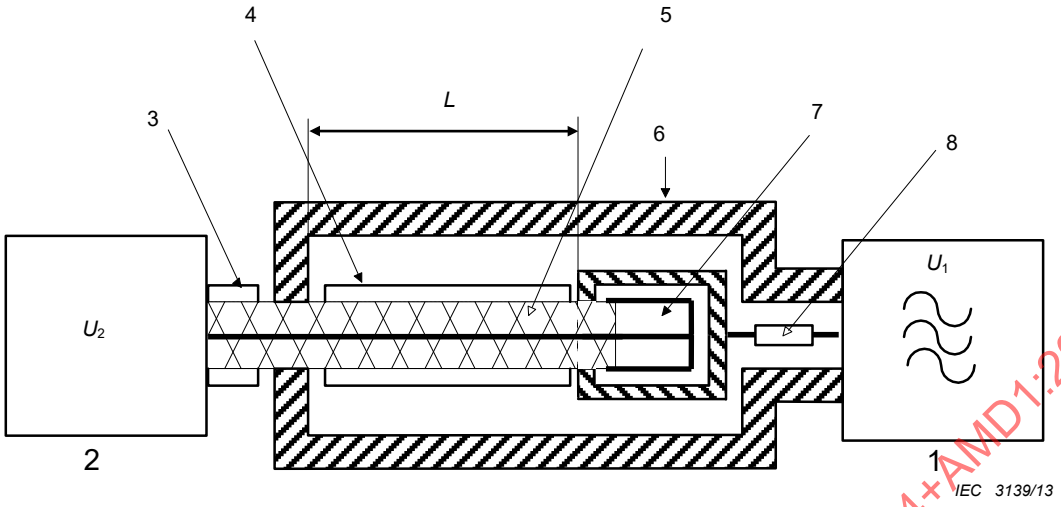

Key

1 signal generator
2 calibrated receiver or network analyzer
3 cable under test
4 cable sheath
5 cable screen
6 tube
7 short circuit
8 series resistor (50 Ω)

Figure 33 – Triaxial set-up (measuring tube), double short circuited method

Table 6 – Typical values for the factor *v*, for an inner tube diameter of 40 mm and a generator output impedance of 50 Ω

Screen diameter mm	**Z_2** Ω	***v*= Z_2/R_{2f}**
9	89	0,89
8	97	0,97
5	125	1,25
3,5	146	1,46
2	180	1,80

Those values have been used in the following simulations. The graphs in Figure 34 to Figure 37 show the simulated frequency response for different dielectric permittivities of the cable and for the different factors of *v* given in Table 6.

Figure 38 plots the results of calculation by iteration for the 3 dB cut-off wavelength (L/λ_1) at which the factor $|g|$ becomes $1/\sqrt{2}$. The curves have then been interpolated by straight lines.

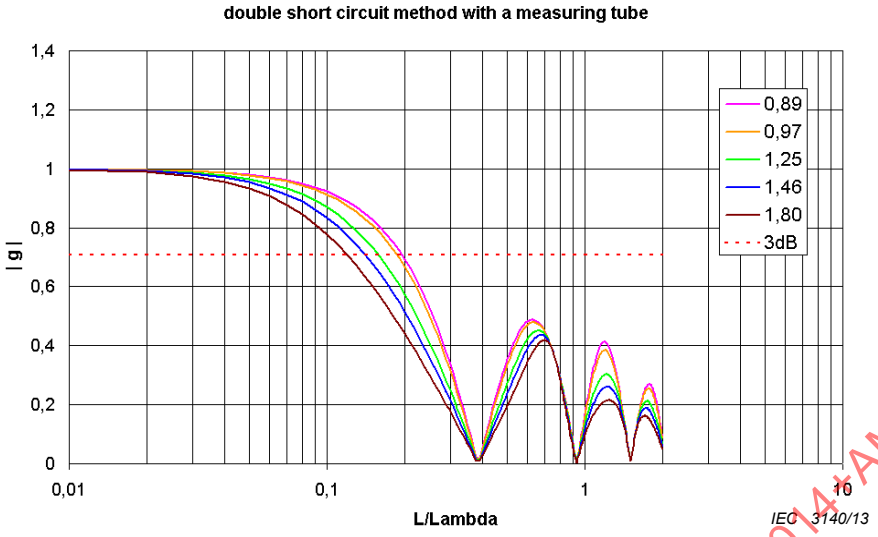

Key

Coloured lines correspond to indicated factors of $v=Z_2/R_{2f}$.

Simulation parameters		
ε_{r1}	ε_{r2}	n
2,3 (solid PE)	1,0	0,659

Figure 34 – Simulation of the frequency response for *g* of a cable having solid PE dielectric (ε_{r1}=2,3)

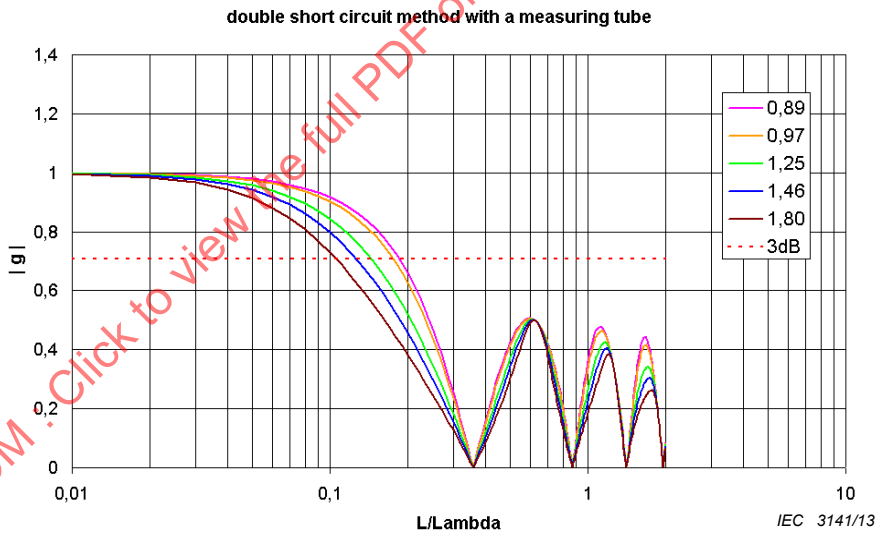

Key

Coloured lines correspond to indicated factors of $v=Z_2/R_{2f}$.

Simulation parameters		
ε_{r1}	ε_{r2}	n
1,6 (foam PE)	1,0	0,791

Figure 35 – Simulation of the frequency response for *g* of a cable having foamed PE dielectric (ε_{r1}=1,6)

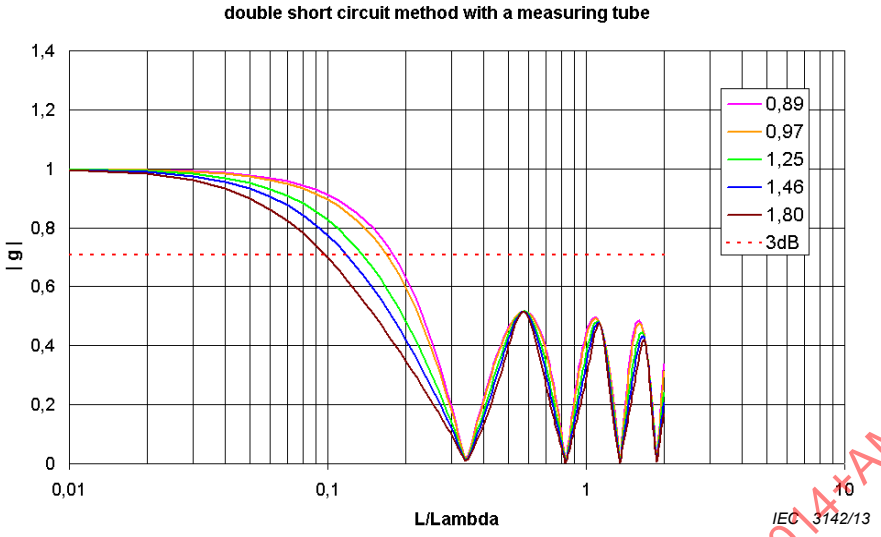

Key

Coloured lines correspond to indicated factors of $v = Z_2/R_{2f}$.

Simulation parameters		
ε_{r1}	ε_{r2}	n
1,3 (foam PE)	1,0	0,877

Figure 36 – Simulation of the frequency response for *g* of a cable having foamed PE dielectric (ε_{r1}=1,3)

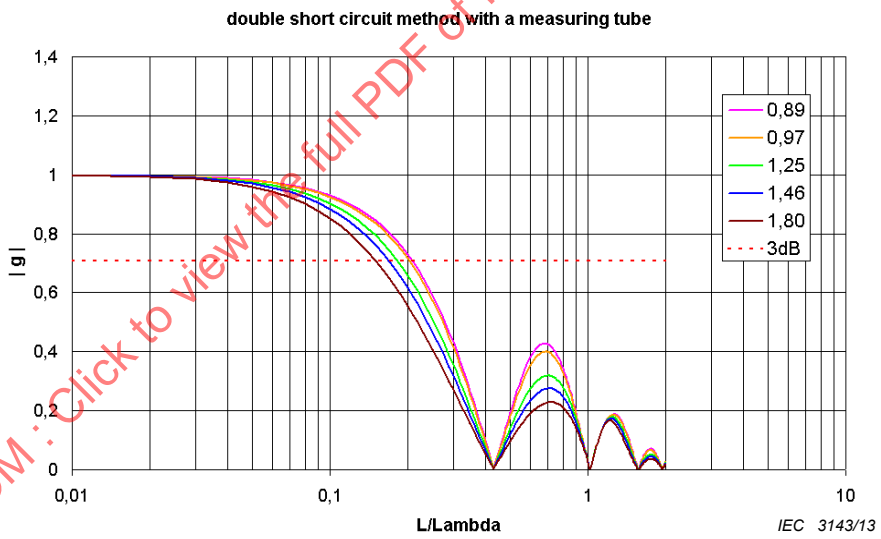

Key

Coloured lines correspond to indicated factors of $v = Z_2/R_{2f}$.

Simulation parameters		
ε_{r1}	ε_{r2}	n
5 (PVC)	1,0	0,447

Figure 37 – Simulation of the frequency response for *g* of a cable having PVC dielectric (ε_{r1}=5)

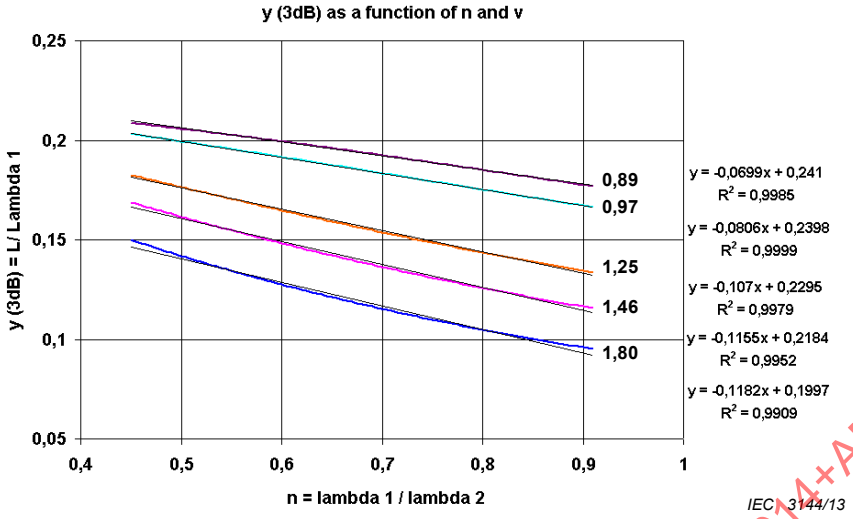

Key

Coloured lines correspond to indicated factors of $v=Z_2/R_{2f}$.

Figure 38 – Interpolation of the simulated 3 dB cut off wavelength (L/λ_1)

From the found linear interpolation, one can derivate following equations to calculate the cut-off frequency length product, to which the transfer impedance could be measured in the "double short circuit" triaxial set-up using a measuring tube.

Table 7 – Cut-off frequency length product

v=0,89	$(f \cdot L)_{3\ dB} \approx \left[\frac{70}{\sqrt{\varepsilon_{r1}}} - \frac{20}{\varepsilon_{r1}}\right] \cdot \text{MHz} \cdot \text{m}$
v=0,97	$(f \cdot L)_{3\ dB} \approx \left[\frac{70}{\sqrt{\varepsilon_{r1}}} - \frac{25}{\varepsilon_{r1}}\right] \cdot \text{MHz} \cdot \text{m}$
v=1,25	$(f \cdot L)_{3\ dB} \approx \left[\frac{68}{\sqrt{\varepsilon_{r1}}} - \frac{32}{\varepsilon_{r1}}\right] \cdot \text{MHz} \cdot \text{m}$
v=1,46	$(f \cdot L)_{3\ dB} \approx \left[\frac{65}{\sqrt{\varepsilon_{r1}}} - \frac{35}{\varepsilon_{r1}}\right] \cdot \text{MHz} \cdot \text{m}$
v=1,80	$(f \cdot L)_{3\ dB} \approx \left[\frac{60}{\sqrt{\varepsilon_{r1}}} - \frac{35}{\varepsilon_{r1}}\right] \cdot \text{MHz} \cdot \text{m}$

The equations given in Table 7 are plotted in the graphs of Figure 39. For example, if a cable with a PE insulation – dielectric permittivity of ε_{r1}=2,3 – is measured in a triaxial set-up with v=1,46 (screen diameter=3,5 mm, tube diameter=40 mm), then the cut-off frequency length product is about 27 MHz·m.: i.e. for a coupling length of 0,5 m, the maximum frequency to which the transfer impedance could be measured is around 60 MHz. If the same cable is measured in a triaxial set-up according to IEC 61196-1 method 2 "direct feeding" or the simplified set-up according to EN 50289-1-6 where v=3, then the cut-off frequency length product is about 18 MHz·m: i.e. for a coupling length of 0,5 m, the maximum frequency to which the transfer impedance could be measured is around 36 MHz. That is to say, that the

double short circuit method (using a measuring tube) facilitates the sample preparation, has a 6 dB higher dynamic range and also allows to measure the transfer impedance up to higher frequencies, compared to the simplified EN 50289-1-6 or IEC 61196-1 method 2 "direct feeding".

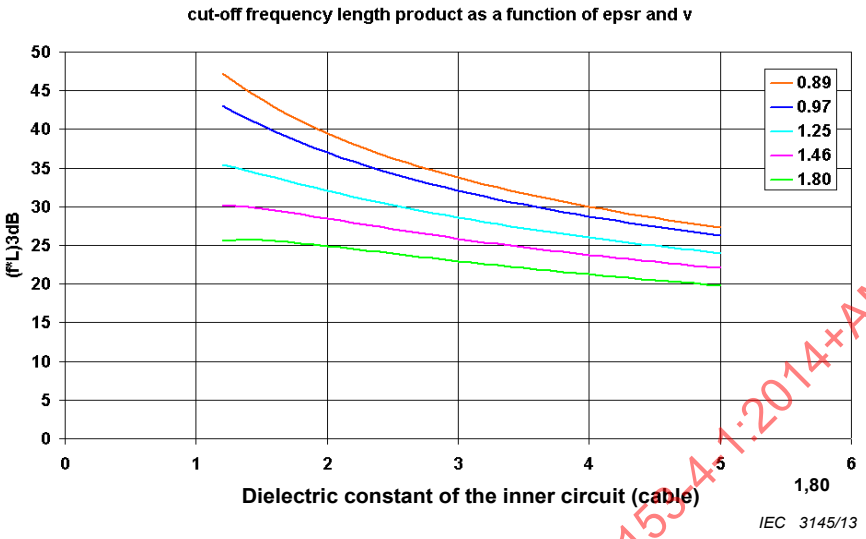

Key

Coloured lines correspond to indicated factors of $v=Z_2/R_{2f}$.

Figure 39 – 3 dB cut-off frequency length product as a function of the dielectric permittivity of the inner circuit (cable)

9.3.3.3 Simulation of the double short circuited method using a "milked on braid"

In the "milked on braid" method, a measuring braid is used instead of a measuring tube. The measuring braid is put directly over the sheath of the sample. Thus the dielectric permittivity of the outer circuit is given by the dielectric permittivity of the sheath (ε_{r2}=2…5), and the impedance of the outer circuit is given by the dielectric constant and the diameter over the sheath of the sample.

In this method, the inner circuit is fed over a 10 dB attenuation pad instead of a 50 Ω feeding resistor while using a measuring tube. However, using a 10 dB attenuation pad instead of a feeding resistor doesn't affect the cut-off frequency, as described below.

For cable screen diameters between 1 mm to 10 mm, sheath thickness between 0,2 mm to 1 mm and ε_{r2} between 2 and 5, the impedance in the outer circuit is between 5 Ω and 20 Ω, i.e. v between 0,1 and 0,4.

A closer look on the coupling equations (Equation (30) to Equation (38)) shows that for small values of the factor v and at low frequencies, the frequency response of the test set-up (factor g) becomes nearly independent of it. The worst case with respect to the 3 dB cut-off is reached if v=0. This is drawn out in the equations below and in Figure 40. Thus, in the following, the simulations are done for v=0.

$$N = \left\{ \cos x + \frac{\mathrm{j} \cdot \sin x}{r + w} \cdot \left[1 + r \cdot w \right] \right\} \cdot \left\{ \cos nx + \mathrm{j} \cdot v \cdot \sin nx \right\} \tag{39}$$

for small values of v, i.e. v<<1 and low frequencies, i.e. x<<1 one gets

$$N = \left\{\cos x + \frac{\mathrm{j}\cdot\sin x}{r+w}\cdot\left[1+r\cdot w\right]\right\}\cdot\left\{e^{\mathrm{j}\cdot nx} - \mathrm{j}\cdot(1 - v\cdot\sin nx)\right\} \tag{40}$$

$$\approx \left\{\cos x + \frac{\mathrm{j}\cdot\sin x}{r+w}\cdot\left[1+r\cdot w\right]\right\}\cdot\left\{e^{\mathrm{j}\cdot nx} - \mathrm{j}\right\}$$

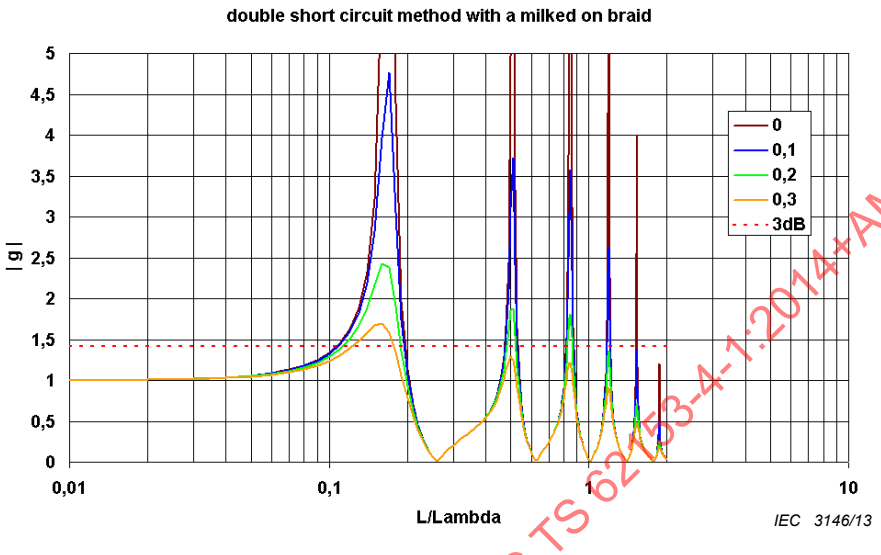

Key

Coloured lines correspond to indicated factors of $v=Z_2/R_{2f}$.

Simulation parameters		
ε_{r1}	ε_{r2}	n
2,3 (PE)	5 (PVC)	1,474

Figure 40 – Simulation of the frequency response for *g*

Taking into account typical combinations of insulation and sheath materials (PE/PVC, PE/LSZH, PTFE/FEP…), one gets values for the factor n between 1,02 and 2. Those values in Table 8 have been used for the iteration of the 3 dB cut-off wavelength (L/λ_1) shown in Figure 41.

Table 8 – Material combinations and the factor *n*

ε_{r1}	ε_{r2}	$n=\sqrt{\varepsilon_{r2}}/\sqrt{\varepsilon_{r1}}$
2,3 (PE)	5 (PVC)	1,47
	3 (LSZH)	1,14
1,6 (foam PE)	5 (PVC)	1,77
	3 (LSZH)	1,37
1,3 (foam PE)	5 (PVC)	1,96
	3 (LSZH)	1,52
2,0 (PTFE)	2,1 (FEP)	1,02
1,3 (expanded PTFE)	2,1 (FEP)	1,27

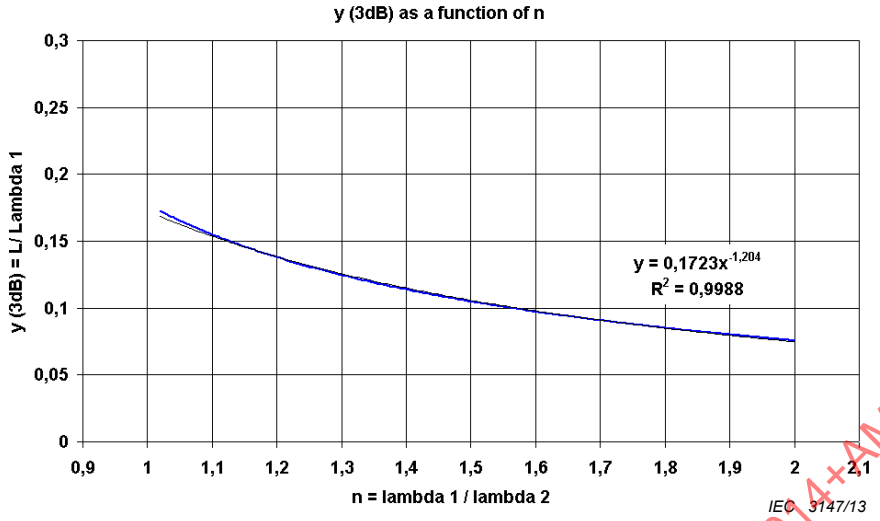

Key

Plotted line is for $v=Z_2/R_{2f} << 1$.

Figure 41 – Interpolation of the simulated 3 dB cut off wavelength (L/λ_1)

From the interpolation, one can derive following equation given in Table 9 for the 3 dB cut-off frequency length product. The equation in Table 9 is plotted in Figure 42.

Table 9 – Cut-off frequency length product

$v<<1$	$(f \cdot L)_{3\,\mathrm{dB}} \approx \left[\frac{50 \times n^{-1,204}}{\sqrt{\varepsilon_{r1}}}\right] \cdot \mathrm{MHz} \cdot \mathrm{m}$

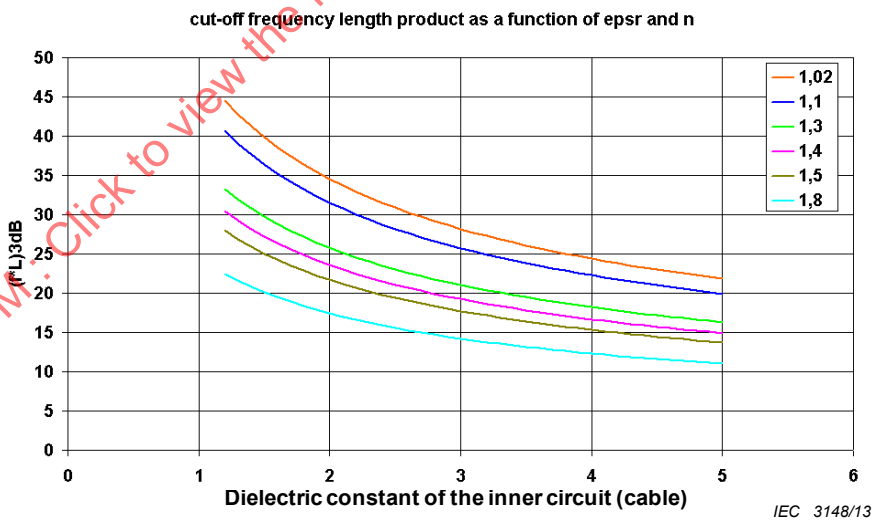

Key

Coloured lines correspond to indicated factors of $n=\sqrt{\varepsilon_{r2}}/\sqrt{\varepsilon_{r1}}$, for $v=Z_2/R_{2f} << 1$.

Figure 42 – 3 dB cut-off frequency length product as a function of the dielectric permittivity of the inner circuit (cable)

For example, a cable with PE insulation and PVC sheath (n=1,47) with the dimensions of a RG 58 (screen diameter around 3,5 mm) measured with the “milked on braid” method results in a cut-off frequency length product of 20 MHz·m. The same cable measured in the double

short circuit method with a measuring tube results in a cut-off length product of 27 MHz·m. If measured in the simplified EN 50289-1-6 method respectively one gets a cut-off frequency length product of 18 MHz·m. Thus the major advantage of the “milked on braid” method is that it allows for bending of the sample under test.

9.4 Conclusion

The best compromise between a simple test set-up and the cut-off frequency is given for the “double short circuit” method using a measuring tube. It covers the usually required frequency range of 100 MHz (see Table 10) for the transfer impedance measurement (using a 30 cm tube) and has the highest dynamic range of all triaxial methods.

The “milked on braid” method has a limited frequency range, requires a long sample preparation but allows for bending of the sample under test.

The matched method according to EN 50289-1-6, IEC 62153-4-3 method A “matched-short” respectively IEC 61196-1 method 1 “direct feeding” has the highest cut-off frequency but also the lowest dynamic range. An additional error source in that method is the accuracy of the series resistor which might have unknown frequency behaviour and thus an unknown attenuation.

Table 10 – Cut-off frequency length product for some typical cables in the different set-ups

Cable type	Sheath	EN 50289-1-6 IEC 61196-1 method 1 IEC 62153-4-3 method A	Double short circuit method using a tube	Double short method using a milked on braid
RG 58 (ε_{r1}=2,3)	PVC	80 MHz·m (v=0,71)	28 MHz·m (v=1,46)	20 MHz·m (n=1,47)
	LSZH			28 MHz·m (n=1,14)
Thin Ethernet (ε_{r1}=1,6)	PVC	83 MHz·m (v=0,71)	30 MHz·m (v=1,46)	20 MHz·m (n=1,77)
	LSZH			28 MHz·m (n=1,37)
RG 214 (ε_{r1}=2,3)	PVC	80 MHz·m (v=0,71)	35 MHz·m (v=0,97)	20 MHz·m (n=1,47)
	LSZH			28 MHz·m (n=1,14)
RG 8 (ε_{r1}=1,3)	PVC	83 MHz·m (v=0,71)	42 MHz·m (v=0,97)	20 MHz·m (n=1,96)
	LSZH			26 MHz·m (n=1,52)

10 Background of the shielded screening attenuation test method (IEC 62153-4-4)

10.1 General

In many cases, above all in the lower frequency range, the screening effectiveness of cables is described by the transfer impedance Z_T. It is, for an electrically short length of cable, defined (see Figure 43) as the quotient of the longitudinal voltage measured on the secondary side of the screen to the current in the screen, caused by a primary inducing circuit, related to unit length [23]. Although the transfer impedance Z_T covers only the galvanic and magnetic couplings, it is common practice to use it also as a quantity which includes the effect of the coupling capacitance C_T through the cable screen [24]. In this case, it is named equivalent

transfer impedance Z_{TE} which includes the effects of galvanic, magnetic and capacitive coupling.

For the determination of the proper coupling capacitance there is, as standardised quantity, the capacitance coupling admittance Y_T. The coupling admittance (see Figure 44) for an electrically short peace of cable is defined as the quotient of the current in the screen caused by the capacitive coupling in the secondary circuit to the voltage in the primary circuit related to unit length [23].

With electrically short cables, where wave propagation can be neglected, the screening quantities related to unit length can directly be used to calculate an induced disturbing voltage. In the higher frequency range, the implications get similar complicated as the transmission characteristics of a simple line, dependent on the impedance and admittance per unit length as well as on the terminating resistors.

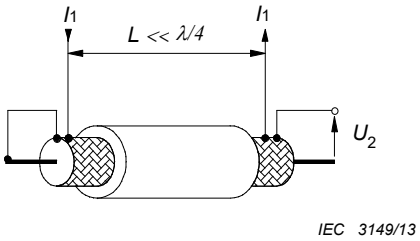

$$Z_T = \frac{U_2}{I_1 \cdot L}$$

Figure 43 – Definition of transfer impedance

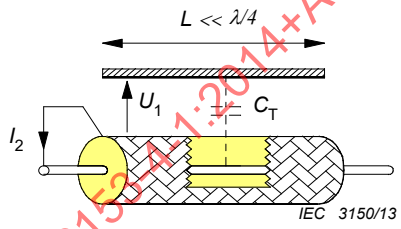

$$Y_T = \frac{I_2}{U_1 \cdot L} = \mathrm{j} \cdot \omega \cdot C_T$$

Figure 44 – Definition of coupling admittance

10.2 Objectives

It is desirable to measure and evaluate the screening efficiency of cable screens also in the wave propagation frequency range such that its characteristics can be directly applied. This requires a closer examination of the conditions of such applications.

In general, a system of electromagnetic induction consists of a transmission circuit in the cable, which is assumed to be fully defined, and of a surrounding transmission system, which is assumed to be universal with respect to the definition of cable screening. The screening effectiveness may be universally described by the maximum power output into the surroundings of the cable related to the power propagating in the cable. The power ratio is best expressed logarithmically as screening attenuation.

An often used procedure to determine the screening attenuation is the well-known “absorbing clamp method“ given in IEC 62153-4-5. The drawback of this method is that the set-up requires relatively much space, does not exclude environmental effects – unless the measuring area is enclosed in a shielded cabin –, and that the available absorbing clamp transformers considerably limit the measurement sensitivity.

It suggests itself to limit the free space such that the said problems don’t occur but wave propagation near the cable surface is not significantly changed. A triaxial measuring set-up is the solution. It has a one-sided short circuit between the metal tube and the cable screen. Power is fed into the terminated inner circuit of the cable and the disturbing power is measured at the opposite end of the outer circuit.

10.3 Theory of the triaxial measuring method

On the basis of the known reversibility of primary and secondary measuring circuits, the proposed measuring set-up, presented in Figure 45, is similar to the triaxial set-up for measuring the transfer impedance. The benefits of feeding the inner system, which is

terminated by its characteristic impedance, are the matching of the generator and reflection free wave propagation over the cable length.

The characteristic impedance of the outer circuit depends on the diameter of the measuring tube and the cable design. The effect of the mismatch in the outer circuit is discussed later on.

The equivalent circuit using lumped circuit elements (shown in Figure 46) facilitates the understanding of the theoretical relationships.

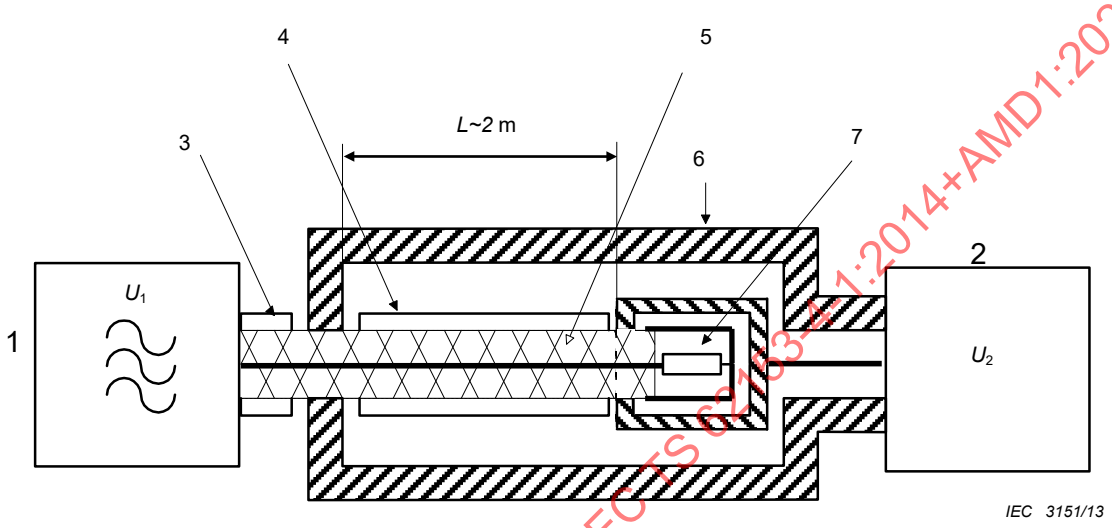

Key

1 signal generator
2 calibrated receiver or network analyzer
3 input voltage to cable under test
4 cable sheath
5 cable screen
6 tube
7 terminating resistor $R_1=Z_1$

Figure 45 – Triaxial measuring set-up for screening attenuation

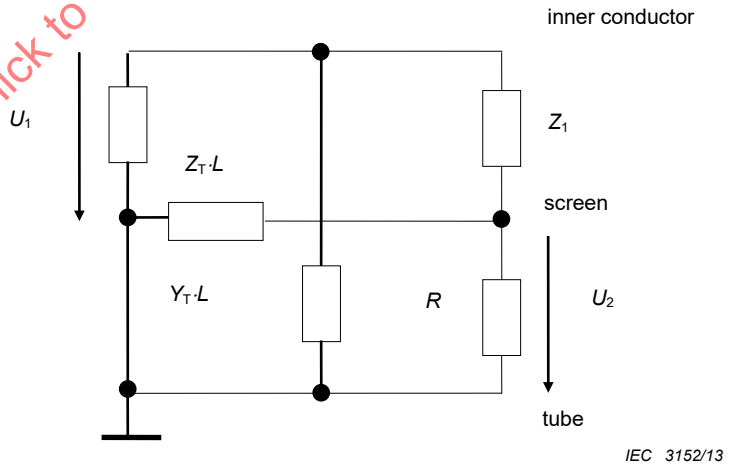

Figure 46 – Equivalent circuit of the triaxial measuring set-up

Based on the conditions of the objects to be measured, it is assumed that the transfer impedance Z_T is low and the reciprocal quantity of the coupling admittance Y_T is high in comparison with the characteristic impedances Z_1 and Z_2 and the load resistance R. Therefore, the feedback of the secondary circuit on primary circuit can be neglected.

When the frequency is low, one may consider the primary circuit shown in Figure 46 as a voltage divider and read the disturbing voltage ratio directly. The one-sided short circuit in the measuring circuit prevents the efficiency of the capacitance coupling admittance Y_T.

$$\frac{U_2}{U_1} \approx \frac{Z_T \cdot L}{Z_1} \tag{41}$$

In the high frequency range, where wave propagation has to be considered, one may expect the transfer impedance to be proportional to the frequency in most cases. Therefore it is expedient to use the following equation:

$$Z_T = R_T + j \cdot \omega M_T \approx j \cdot \omega M_T \tag{42}$$

and consider the effective mutual inductance per unit length M_T at high frequencies as an approximated constant quantity as it is usually done with the through capacitance C_T.

It is common practice to describe the capacitive coupling in the form of the capacitive coupling impedance Z_F, which is nearly invariant with respect to the geometry of the outer circuit (tube). [24], [27].

$$Z_F = Z_1 Z_2 Y_T = Z_1 Z_2 \cdot j \cdot \omega C_T \tag{43}$$

Furthermore, the attenuation constants α_1 and α_2 of the circuits may generally be neglected as, for example, the value of nearly 1 dB/m of the common cable type RG 58 at 3 GHz is relatively small compared to the usual measuring uncertainty.

In the relevant literature it is common practice to describe wave propagation in the form of phase constant [24], [25]. If the ratio between effective length and wave length is used instead of the phase constant, the periodic phenomena become clearer. With wave length λ_0 in free space or λ_1, λ_2 in the circuits 1 and 2, the following relation exists:

$$\beta_{1,2} \cdot L = 2\pi \cdot \sqrt{\varepsilon_{r1,2}} \cdot \frac{L}{\lambda_0} = 2\pi \frac{L}{\lambda_{1,2}} \tag{44}$$

According to the theory of wave propagation [25] and line crosstalk [26], a wave propagates in the matched inner circuit towards the matched end. In the outer circuit, a part of the induced wave propagates forwards to the measuring receiver and the other part is moving backwards to the short circuit. The total reflection at the short circuit reverses this backward wave and superposes it to the original forward wave, i.e. the sum can be obtained as measured value.

If the second circuit is matched at both ends, the backward wave would be measured at the generator end (near end) and the forward wave at the opposite end (far end) separately.

Hence equations for the near end are derived from [24]:

$$\frac{U_{2n}}{U_1} = \frac{Z_T + Z_F}{2Z_1} \frac{c_0}{j \cdot \omega\left(\sqrt{\varepsilon_{r1}} + \sqrt{\varepsilon_{r2}}\right)} \left\{1 - e^{-j2\pi\left(\sqrt{\varepsilon_{r1}} + \sqrt{\varepsilon_{r2}}\right)\frac{L}{\lambda_0}}\right\} \tag{45}$$

and for the far end:

$$\frac{U_{2f}}{U_1} = \frac{Z_F - Z_T}{2Z_1} \frac{c_0}{j \cdot \omega\left(\sqrt{\varepsilon_{r1}} - \sqrt{\varepsilon_{r2}}\right)} \cdot \left\{1 - e^{-j \cdot 2\pi\left(\sqrt{\varepsilon_{r1}} - \sqrt{\varepsilon_{r2}}\right)\frac{L}{\lambda_0}}\right\} \cdot e^{-j \cdot 2\pi \frac{L}{\lambda_2}} \quad (46)$$

Equations (47) and (48) are depicted in Figure 47 with the indicated parameters.

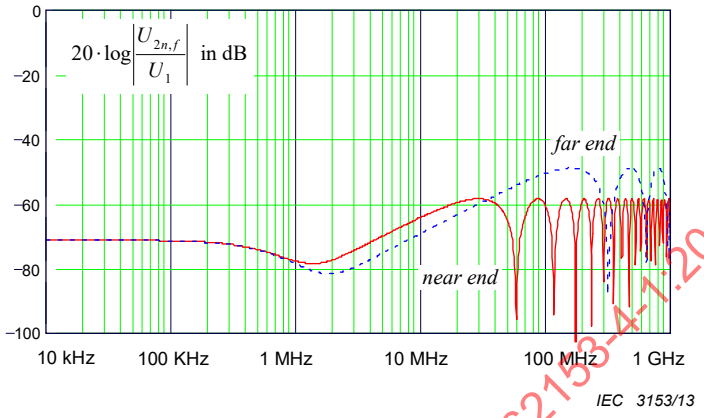

Calculation parameters

C_T	=	0,02	pF/m	M_T	=	0,4	nH/m
R	=	50	Ω	L	=	2	m
Z_1	=	50	Ω	ε_{r1}	=	2,3	
Z_2	=	120	Ω	ε_{r2}	=	1,1	

Figure 47 – Calculated voltage ratio for a typical braided cable screen

With a short circuit and an unmatched measuring receiver, these original voltage waves cause additional voltage portions. The sum of all voltage portions is zero at the shorted end (near end) and U_2 at the receiver end (far end). By use of the wave parameter and reflection factors or terminating resistors, it is possible to calculate all voltage portions and the voltage U_2 from the primary induced voltage waves, see Equation (45) and Equation (46):

$$\left|\frac{U_2}{U_1}\right| \approx \left| \frac{Z_T - Z_F}{\sqrt{\varepsilon_{r1}} - \sqrt{\varepsilon_{r2}}} \left[1 - e^{-j \cdot \varphi_1}\right] + \frac{Z_T + Z_F}{\sqrt{\varepsilon_{r1}} + \sqrt{\varepsilon_{r2}}} \cdot \left[1 - e^{-j \cdot \varphi_2}\right] \right| \cdot \left| \frac{1}{\omega \cdot Z_1} \right| \left| \frac{c_0}{2 + (Z_2 / R - 1) \cdot \left(1 - e^{-j\,\varphi_3}\right)} \right| \quad (47)$$

or in consideration of Equations (42) and Equation (43)

$$\left|\frac{U_2}{U_1}\right| \approx \left| \frac{M_T / Z_1 - C_T Z_2}{\sqrt{\varepsilon_{r1}} - \sqrt{\varepsilon_{r2}}} \left[1 - e^{-j \cdot \varphi_1}\right] + \frac{M_T / Z_1 + C_T Z_2}{\sqrt{\varepsilon_{r1}} + \sqrt{\varepsilon_{r2}}} \left[1 - e^{-j \cdot \varphi_2}\right] \right| \cdot \left| \frac{c_0}{2 + (Z_2 / R - 1) \cdot \left(1 - e^{-j \cdot \varphi_3}\right)} \right| \quad (48)$$

where

$$\varphi_1 = 2\pi\left(\sqrt{\varepsilon_{r1}} - \sqrt{\varepsilon_{r2}}\right)\frac{L}{\lambda_0} \qquad \varphi_2 = 2\pi\left(\sqrt{\varepsilon_{r1}} + \sqrt{\varepsilon_{r2}}\right)\frac{L}{\lambda_0} \qquad \varphi_3 = \varphi_2 - \varphi_1 = 4\pi\sqrt{\varepsilon_{r2}}\,\frac{L}{\lambda_0}$$

Calculated results for a typical braided cable screen are given in Figure 49. Another way to obtain the related induced voltage is given in [21].

The functional equation (see Figure 48)

$$\left|1 - e^{-j\cdot\varphi}\right| = \left|2 \times \sin(\varphi/2)\right| \quad \text{with } \varphi = \varphi_1, \varphi_2, \varphi_3 \tag{49}$$

shows that the equation of the voltage ratio contains three periodic partial functions of the ratio effective length L to wave length λ_0:

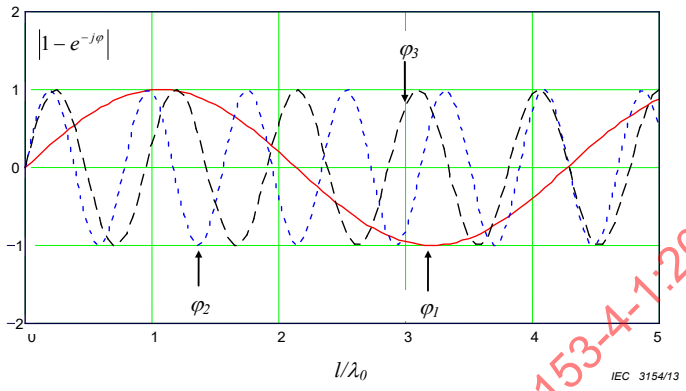

Figure 48 – Calculated periodic functions for ε_{r1} = 2,3 and ε_{r2} = 1,1

For low frequencies, when $L << \lambda_0$ and, consequently, $\sin(\varphi) \approx \varphi$, Equation (48) changes into Equation (42), the result of the common measuring method for the transfer impedance.

An example of the theoretical curve of the voltage ratio is shown in Figure 49 in two diagrams: The left one, a) with a logarithmic scale to extend the lower frequency range and the right one b) with a linear scale up to very high frequencies.

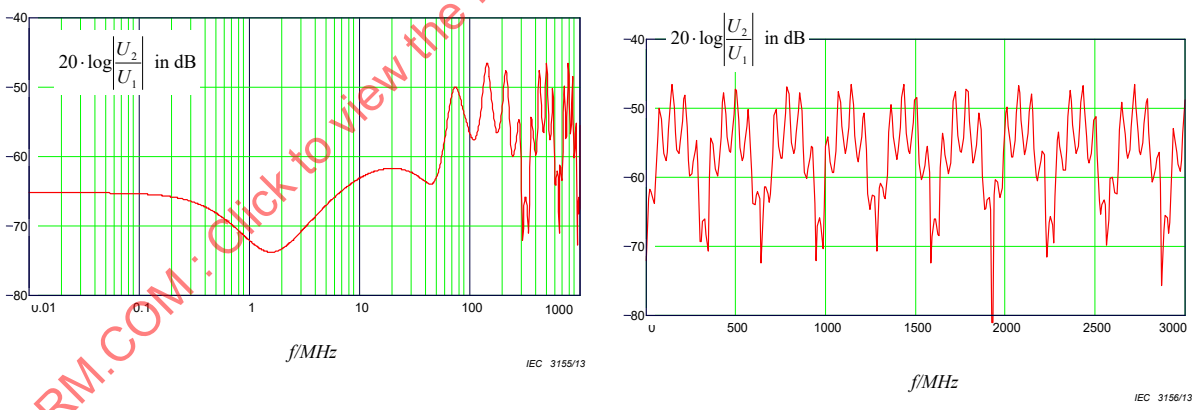

a) Logarithmic frequency scale

b) Linear frequency scale

Calculation parameters

C_T	=	0,02	pF/m	M_T	=	0,4	nH/m
R	=	50	Ω	L	=	2	m
Z_1	=	50	Ω	ε_{r1}	=	2,3	
Z_2	=	120	Ω	ε_{r2}	=	1,1	

Figure 49 – Calculated voltage ratio-typical braided cable screen

It is not useful to specify the induced power for an exact length of cable at a single frequency, anywhere between a minimum and maximum of the function. Only the periodic maximum voltage is important for the evaluation of the screening effectiveness. In the outer circuit, the wave propagation shall be nearly the same as in free space. Therefore, the characteristic

impedance Z_2 is higher than the common input resistance R of the measuring receiver, i.e. 50 Ω or sometimes 75 Ω.

Consequently, periodic maximum values of the voltage ratio are obtained from Equation (47) and Equation (48), which are independent of the input resistance of the receiver R and of effective cable length L:

$$\left|\frac{U_2}{U_1}\right|_{\max} \approx \frac{C_0}{\omega Z_1} \cdot \left| \frac{Z_T - Z_F}{\sqrt{\varepsilon_{r1}} - \sqrt{\varepsilon_{r2}}} + \frac{Z_T + Z_F}{\sqrt{\varepsilon_{r1}} + \sqrt{\varepsilon_{r2}}} \right| \tag{50}$$

or in consideration of Equation (42) and Equation (43):

$$\left|\frac{U_2}{U_1}\right|_{\max} \approx \left| \frac{M_T / Z_1 - C_T Z_2}{\sqrt{\varepsilon_{r1}} - \sqrt{\varepsilon_{r2}}} + \frac{M_T / Z_1 + C_T Z_2}{\sqrt{\varepsilon_{r1}} + \sqrt{\varepsilon_{r2}}} \right| \cdot c_0 \tag{51}$$

At first sight, C_T, Z_2, ε_{r2} and Z_F appear as random quantities which depend on freely chosen dimensions of the measuring tube. In reality, however, the voltage ratio is independent of the characteristic impedance of the outer circuit since $C_T \cdot Z_2$ and Z_F are practically invariant with respect to the dimensions of the measuring tube [24], [27]. Furthermore, the influence of the cable sheath on the resulting relative permittivity ε_{r2} is negligible if the design of the measuring tube takes into account the requirement for a wave propagation which is approximately the same as in the free space; in consequence $\varepsilon_{r2} \approx 1{,}0$.

The periodic maximum value is independent of the effective length L and frequency f or wave length λ. A measured frequency response would hint at a frequency-related quantity rather than the pure mutual inductance M_T.

As it is seen from Figure 48 and Figure 49, the envelope rise is reached with the first maximum of the wide period at:

$$\frac{\lambda_0}{L} \leq 2 \cdot \left| \sqrt{\varepsilon_{r1}} - \sqrt{\varepsilon_{r2}} \right| \quad \text{or} \quad f > \frac{C_0}{2 \cdot L \cdot \left| \sqrt{\varepsilon_{r1}} - \sqrt{\varepsilon_{r2}} \right|} \tag{52}$$

In this frequency range, Z_T can be calculated if Z_F is negligible:

$$|Z_T| \approx \frac{\omega \cdot Z_1 \cdot |\varepsilon_{r1} - \varepsilon_{r2}|}{2 \cdot c_0 \cdot \sqrt{\varepsilon_{r1}}} \cdot \left|\frac{U_2}{U_1}\right|_{\max} \tag{53}$$

10.4 Screening attenuation

The screening attenuation is defined as the logarithmical ratio of the maximum power in the secondary (outer) circuit to the power propagating in the primary (inner) circuit.

$$a_s = -10 \times \log_{10}\left(\mathrm{Env} \left| \frac{P_{r,\max}}{P_1} \right| \right) \tag{54}$$

The power coupled into the outer circuit depends on Z_2 although the peak voltage is independent of it. Thus a normalised value of the characteristic impedance of the outer circuit Z_s must be defined. It is common practice to define Z_s = 150 Ω [24].

In the standardised "absorbing clamp method" (see IEC 62153-4-5), the outer circuit is matched with Z_2, and the radiated power is the sum of the near end and far end crosstalk. From the comparison of that measuring circuit with the measuring circuit of the triaxial method results the relation of the measured power to the radiated power.

The equivalent circuit for an electrical short part of the length ΔL and for a negligible capacitive coupling illustrates the circumstances in Figure 50.

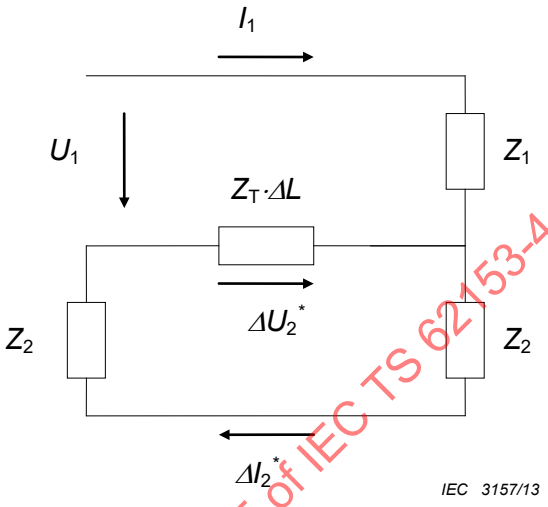

Figure 50 – Equivalent circuit for an electrical short part of the length Δl and negligible capacitive coupling

The power in the primary circuit is:

$$P_1 = U_1 \cdot I_1 = \frac{U_1^2}{Z_1} = I_1^2 \cdot Z_1 \tag{55}$$

The power in the secondary circuit, which is coupled by the transfer impedance Z_T is

$$P_2{}^* = \Delta U_{2^*} \cdot \Delta I_{2^*} \quad \Delta U_{2^*} = I_1 \cdot Z_T \cdot \Delta L \tag{56}$$

$$\Delta I_2^* = \frac{\Delta U_2^*}{2 \cdot Z_2} \tag{57}$$

Thus

$$\frac{P_2^*}{P_1} = \frac{\left(\Delta U_2^*\right)^2}{2 \cdot Z_2} \cdot \frac{1}{I_1^2 \cdot Z_1} = \frac{\left(Z_T \cdot \Delta L\right)^2}{2 \cdot Z_1 \cdot Z_2} \tag{58}$$

If the secondary circuit is short circuited at one end and terminated by R at the other end, the power measured at R is

$$\frac{P_2}{P_1} = \frac{(Z_T \cdot \Delta L)^2}{Z_1 \cdot R} \tag{59}$$

Thus

$$\frac{P_2^*}{P_2} = \frac{R}{2Z_2} \tag{60}$$

or in the case of radiation due to the normalised characteristic impedance of the environment

$$\frac{P_r}{P_2} = \frac{P_{r,max}}{P_{2,max}} = \frac{R}{2Z_s} \tag{61}$$

Thus the screening attenuation is calculated by:

$$\begin{aligned} a_s &= 10 \times \log_{10} \left| \frac{P_1}{P_{r,max}} \right| = 10 \times \log_{10} \left| \frac{P_1}{P_{2,max}} \cdot \frac{2Z_s}{R} \right| \\ &= 10 \times \log_{10} \left| \left(\frac{U_1}{U_{2,max}} \right)^2 \cdot \frac{2Z_s}{Z_1} \right| \\ &= 20 \times \log_{10} \left| \frac{U_1}{U_{2,max}} \right| + 10 \times \log_{10} \left| \frac{300}{Z_1} \right| \end{aligned} \tag{62}$$

10.5 Normalised screening attenuation

From Equation (50), it is seen that the maximum voltage ratio and therefore the screening attenuation is a function of the velocity difference between the primary and secondary circuit. Therefore the test results may also be presented for normalised conditions where Z_s = 150 Ω and the velocity difference $|\Delta v/v_1|$ = 10 % or $\varepsilon_{r1}/\varepsilon_{r2,n}$ = 1,21.

The normalised screening attenuation is calculated by:

$$a_{s,n} = 20 \times \log_{10} \left| \frac{\omega \cdot \sqrt{Z_1 \cdot Z_s} \cdot \left| \sqrt{\varepsilon_{r1}} - \sqrt{\varepsilon_{r2,n}} \right|}{Z_T \cdot c_0} \right| \tag{63}$$

With respect to Equation (50), Equation (62) and Equation (63) and assuming negligible Z_F, the difference Δa of the normalised and the measured screening attenuation is given by:

$$\Delta a = a_{sn} - a_s = 20 \times \log_{10} \left(\sqrt{2} \cdot \frac{\left| 1 - \sqrt{\frac{\varepsilon_{r2,n}}{\varepsilon_{r1}}} \right|}{\left| 1 - \frac{\varepsilon_{r2,t}}{\varepsilon_{r1}} \right|} \right) \tag{64}$$

where $\varepsilon_{r2,t} \approx 1{,}1$ is the relative dielectric permittivity of the outer circuit (tube) during measurement.

Table 11 shows the difference Δa for typical cable dielectric.

Table 11 – Δa in dB for typical cable dielectrics

Outer circuit (tube) $\varepsilon_{r2,n}$	Cable dielectric ε_{r1}	Δa in dB
1,9	2,3	–12
1,7	2,1	–11
1,3	1,6	–8
1,1	1,3	–2

10.6 Measured results

The measured screening attenuation of common types of cables shows the validity of the theoretical basis. The voltage ratio U_2/U_1 is measured by means of a network analyser having an internal resistance of 50 Ω. The screening attenuation a_s is presented in Figures 51 to Figure 55 for three types of cables as a function of frequency.

- RG 58 according to MIL-C-17 with single copper braid;
- HF 75 0,7/4,8 2YCY with a dielectric of solid PE and a single copper braid;
- HF 75 1,0/4,8 02YCY with a dielectric of foamed PE and a single copper braid;
- RG 223 according to MIL-C-17 with double copper braid.

The theoretical relations of the transitions from low to medium and high frequencies – appearing in the calculated curve in Figure 47 – become most evident with the single copper braid (see Figure 51). Here the voltage ratio is independent of the frequency up to approximately 0,4 MHz but proportional to the effective length of the measuring tube like the transfer impedance. At high frequencies, higher than about 100 MHz, super-positioned periodic functions occur showing maximum values of approximately equal magnitude independent of frequency and effective length. The frequency at which the superposition appears is reciprocal to the effective length just as the frequency spacing of the peak values (see Figure 51 and Figure 52). In contrast to the effective length of 2 m, the effective length of 0,5 m does not allow to plot the screening envelope curve with sufficient accuracy any more, due to the wide spacing of the long period maximum values.

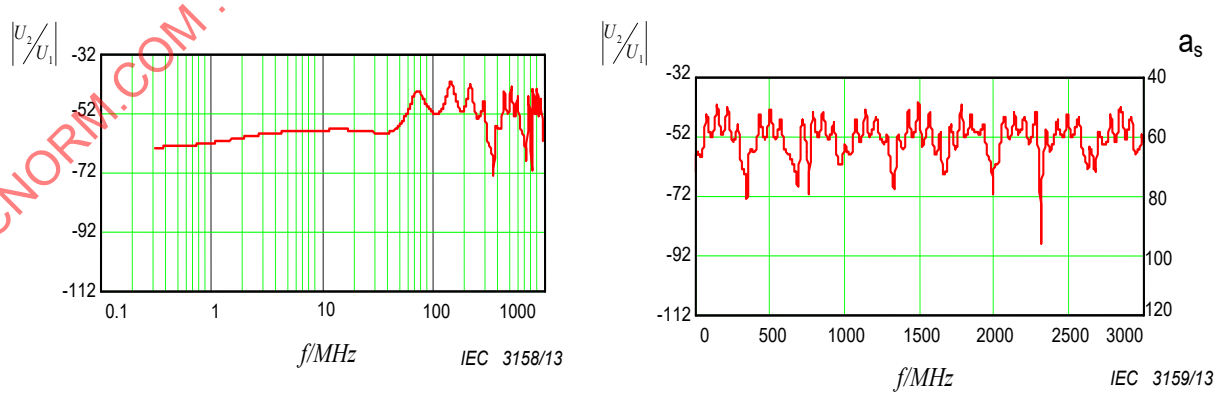

Logarithmic voltage ratio $|U_2/U_1|$ in dB (left hand scale) and screening attenuation as (right hand scale)
Coupling length L = 2 m.

Figure 51 – a_s of single braid screen, cable type RG 58, L = 2 m

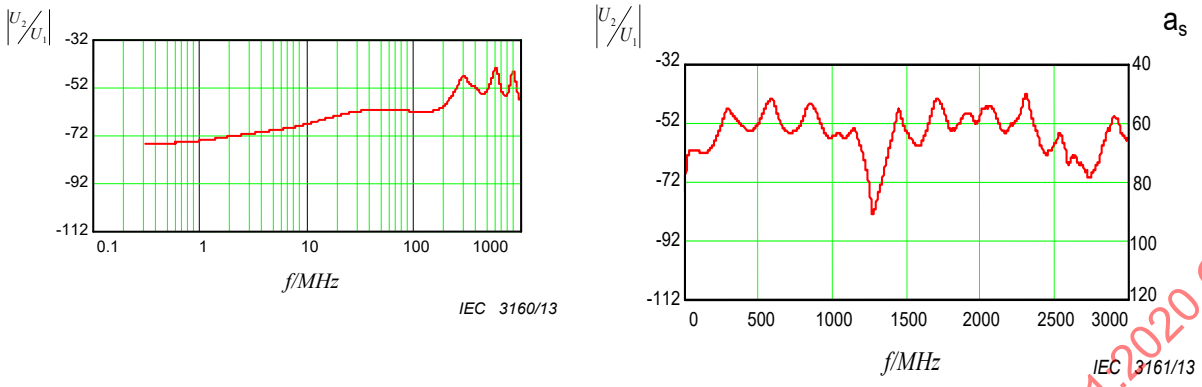

Logarithmic voltage ratio $|U_2/U_1|$ in dB (left hand scale) and screening attenuation as (right hand scale)
Coupling length L = 0,5 m.

Figure 52 – a_s of single braid screen, cable type RG 58, L = 0,5 m

The periodic frequency spacing in the measured curve and the screening attenuation are dependent on the velocity difference between primary and secondary circuit (Equation (47) and Equation (50)). This theoretical relation becomes most evident in Figure 53 and Figure 54 where the cable screens of both cables are equal, but the relative permittivities of the cable dielectric ε_{r1} and thus the velocity difference in the test set-up differ. In Figure 53 we have ε_{r1}=2,3 and a velocity difference $|\Delta v/v_1| \approx 45$ whereas in Figure 54 ε_{r2}=1,7 and $|\Delta v/v_1| \approx$ 24 %. Thus, in Figure 54, we have a larger frequency spacing of the wide period and also a lower screening attenuation. But the normalised screening attenuation of both cable screens is equal, $a_s \approx 43$ dB.

For the cable with double copper braid (see Figure 55), the theoretical relations become apparent only if the measurement is very accurate and the receiver is sensitive enough for low induced voltage. Apart from its level and distinct function of frequency, the screening attenuation of the double copper braid is obviously similar to that of the single copper braid.

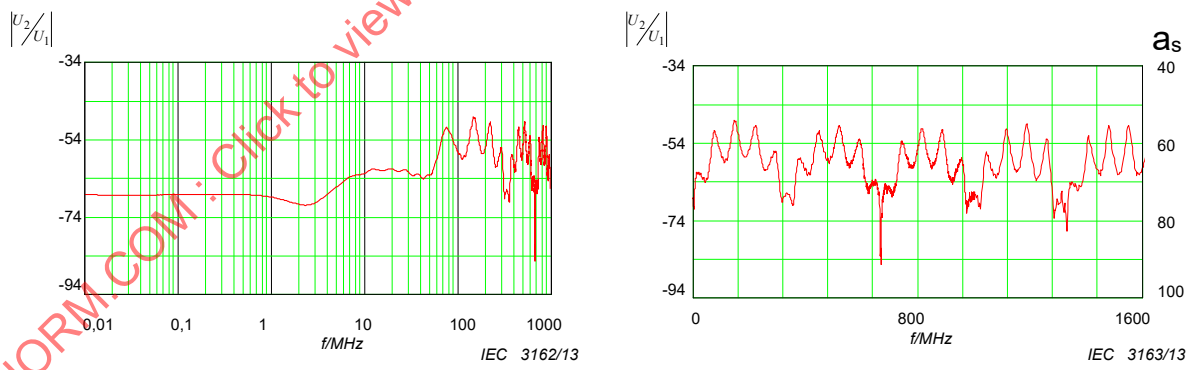

Logarithmic voltage ratio $|U_2/U_1|$ in dB (left hand scale) and screening attenuation as (right hand scale)
ε_{r1}=2,3, $|\Delta v/v_1|$=45 %, coupling length L = 2 m.

Figure 53 – a_s of cable type HF 75 0,7/4,8 2YCY (solid PE dielectric)

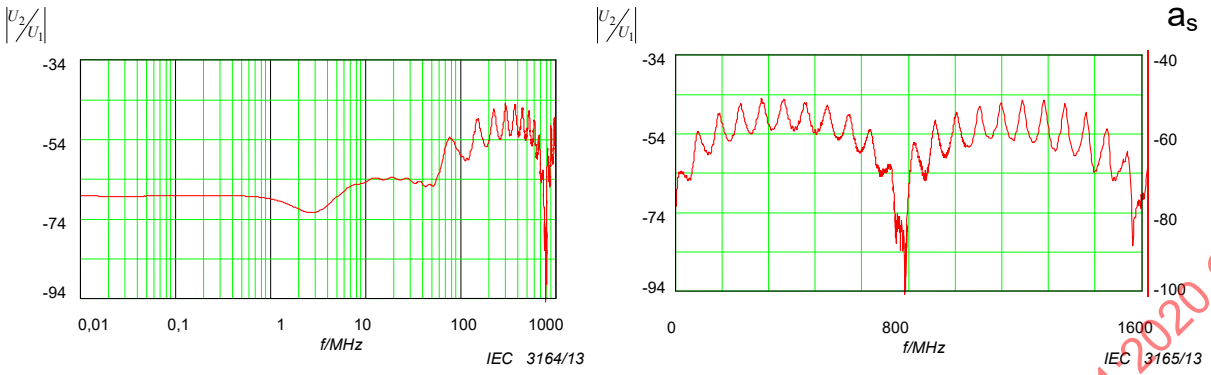

Logarithmic voltage ratio $|U_2/U_1|$ in dB (left hand scale) and screening attenuation as (right hand scale), ε_{r1}=1,7, $|\Delta v/v_1|$=24 %, coupling length L = 2 m.

Figure 54 – a_s of cable type HF 75 1,0/4,8 02YCY (foam PE dielectric)

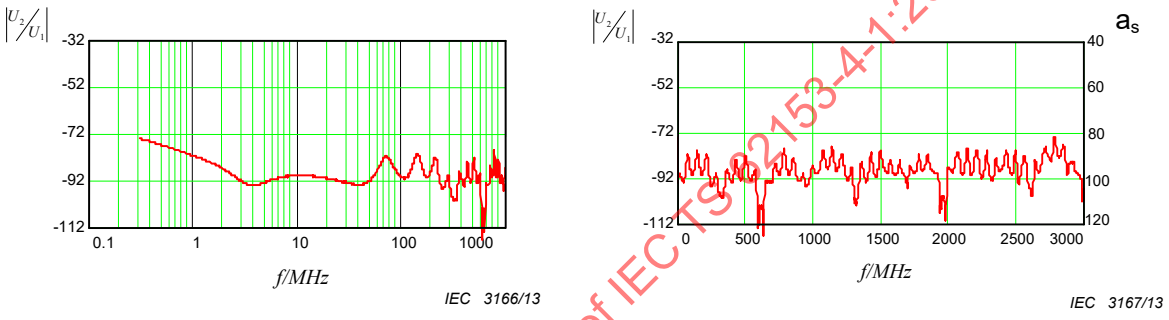

Logarithmic voltage ratio $|U_2/U_1|$ in dB (left hand scale) and screening attenuation as (right hand scale)
Coupling length L = 2 m.

Figure 55 – a_s of double braid screen, cable type RG 223

10.7 Comparison with absorbing clamp method

In the absorbing clamp method according to IEC 62153-4-5, in principle, the current on the outside of the cable under test is measured. The matched outer circuit is directly induced by the inner circuit. The power in the outer circuit is related to the current by calibration.

Table 12 gives a comparison of results of some coaxial cables with different screen designs. They show a maximum difference of 3 dB.

Table 12 – Comparison of results of some coaxial cables

	Screening attenuation a_S in dB		
Cable type, screen	**Frequency** GHz	**Absorbing clamp method**	**Triaxial method**
RG 58,	0,2	51	48
single	0,8	52	50
braid	3,0	-	50
RG 214,	0,2	51	50
single	0,8	54	51
braided	3,0	-	53
RG 214,	0,2	79	79
double	0,8	82	81
braid	3,0	-	83
RG 223,	0,2	86	88
double	0,8	90	90
braid	3,0	-	83

10.8 Practical design of the test set-up

The set-up to measure the screening attenuation a_S is in principle the set-up to measure the attenuation of RF devices, where the voltage ratio U_2/U_1 is measured. The cable under test is connected to the output of a RF-generator, the output of the coupling tube is connected to the measuring input of a RF-receiver. Generator and receiver may be included in a sensitive network analyser (see Figure 45 and Figure 56).

The measuring tube shall be of a material, which is not ferromagnetic and good conductive (for example brass), with an inner diameter of about 40 mm to 50 mm and a length of 2 m to 4 m or more, where the total length of 2 m or more may be achieved by screwing together single parts of tubes (RF-tight).

One way to realise the short circuit at the near end of the CUT is to solder a braid of silvered copper wires to a punched disk of copper. This "contacting braid" is fixed on the outer conductor of the cable sample where the sheath is removed, e.g. with cable clamps. The electrical contact between this contacting braid and the measuring tube may then be achieved by a jam-disk, which is fixed by the clasp cap, which is screwed to the tube (see Figure 57).

The contacting braid, which is prepared once, may be used several times. Soldering of the screen of the cable sample to the tube – as usual at the classic triaxial – set-up is no longer required and the time to prepare the CUT is minimised.

The termination at the far end of the CUT is achieved by a resistor of the same value as the characteristic impedance of the CUT. Experience has shown that the best results are obtained with SMD resistors, respectively so called "mini-melf-resistors" with low mechanical dimensions and good RF-characteristics, which are soldered directly between the inner and the outer conductor of the CUT. To avoid radiation and to contact the outer conductor of the CUT, this termination is shielded by a case, which is well conductive (see Figure 45).

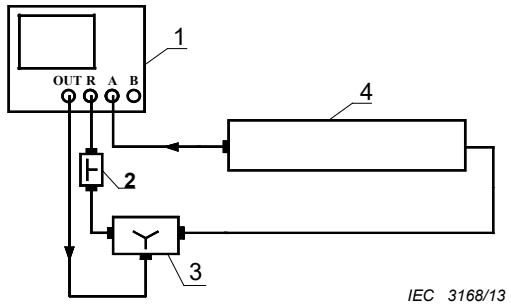

Key

1 Network analyser
2 Attenuator 20 dB
3 Power divider
4 Measuring tube

Figure 56 – Schematic for the measurement of the screening attenuation a_s

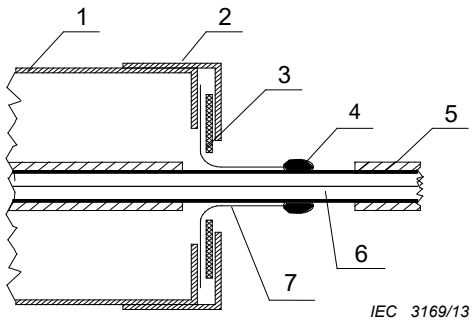

Key

1 tube of brass
2 clasp cap
3 jam disk
4 contact to the cable screen of CUT
5 sheath of cable sample
6 cable under test (CUT)
7 contacting braid

Figure 57 – Short circuit between tube and cable screen of the CUT

To obtain clear and reproducible results, the sample must be well centered in the measuring tube. A slackly mounted cable under test in the measuring tube will lead to deviations of the characteristic impedance Z_2 of the outer system over the coupling length and thus to additional reflections. Centering may be achieved by mounting the sample in punched polyethylene disks which are placed in the measuring tube, or better by stretching the sample under test, e.g. with a desk vice. Also, vertical mounting of the measuring tube is useful.

10.9 Influence of mismatches

10.9.1 Mismatch in the outer circuit

Mismatches in the outer circuit may result in significant errors. With the screening case of the terminating resistor, a mismatch is inserted into the outer circuit, which affect the results significantly depending on the mechanical dimensions [28]. The mean characteristic impedance of the outer circuit, formed by the cable screen and the measuring tube, respectively in the outer circuit at the screening case is given by:

$$Z_2 \approx \frac{60}{\sqrt{\varepsilon_{r2}}} \cdot \ln\left(\frac{D_m}{D_a}\right) \quad (65)$$

$$Z_3 \approx \frac{60}{\sqrt{\varepsilon_{r2}}} \cdot \ln\left(\frac{D_m}{D_{case}}\right) \quad (66)$$

where

D_a is the outer diameter of cable screen;

D_{case} is the outer diameter of screening case;

D_m is the inner diameter of measuring tube.

A deviation between D_{case} and D_a thus results in different impedances and therefore in additional reflections in the outer circuit. For example, a screening case with an outer diameter of $D_{case} = 1{,}2 \cdot D_a$ results in a impedance Z_3 which is 11 Ω less than Z_2 (ε_{r2}=1,0).

Figure 58 facilitates the understanding of the theoretical relationships.

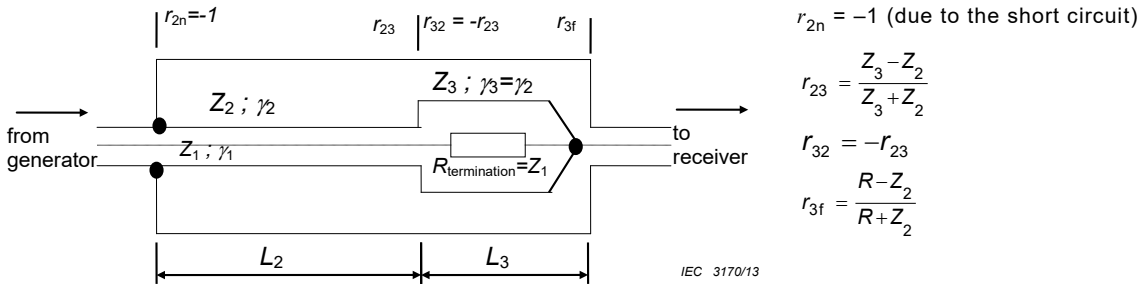

Figure 58 – Triaxial set-up, impedance mismatches

The outer circuit thus consists of two lines with different characteristic impedances. To calculate the voltage at the receiver, some additional variables have to be defined.

U_h is the voltage, which is coupled from the cable under test into the outer circuit (Z_2, γ_2, L_2), propagation to the far end, including the total reflection at the near end.

$$\frac{U_h}{U_1} = \frac{U_{2f}}{U_1} + \frac{U_{2n}}{U_1} \cdot r_{2n} \cdot e^{-\gamma_2 \cdot L_2} \tag{67}$$

Where U_{2f}, U_{2n} are the voltages in a matched outer circuit according to Equation (42) and Equation (44).

Multiple reflections of this wave between the short circuit at the near end of the outer circuit and the transition from Z_2 to Z_3 are described by T_{2f}.

$$T_{2f} = \frac{1 + r_{23}}{1 - r_{2n} \cdot r_{23} \cdot e^{-2 \cdot \gamma_2 \cdot L_2}} \tag{68}$$

The superposition of the wave which is propagating from the line Z_2, γ_2, L_2 to the far end (receiver) of the line Z_3, γ_3, L_3 – including the multiple reflections between the transitions from Z_3 to Z_2 and Z_3 to R (receiver input) – is described by T_{3f}.

$$T_{3f} = \frac{1 + r_{3f}}{1 - r_{32} \cdot r_{3f} \cdot e^{-2 \cdot \gamma_3 \cdot L_3}} \cdot e^{-\gamma_3 \cdot L_3} \tag{69}$$

The superposition of the wave which is propagating from line Z_3, γ_3, L_3 to line Z_2, γ_2, L_2 is described by T_{32}.

$$T_{32} = \frac{1 + r_{32}}{1 - r_{32} \cdot r_{3f} \cdot e^{-2 \cdot \gamma_3 \cdot L_3}} \cdot r_{3f} \cdot e^{-2 \cdot \gamma_3 \cdot L_3} \tag{70}$$

The superposition of the wave which is propagating from line Z_2, γ_2, L_2 to line Z_3, γ_3, L_3 is described by T_{23}.

$$T_{23} = \frac{1 + r_{23}}{1 - r_{2n} \cdot r_{23} \cdot e^{-2 \cdot \gamma_2 \cdot L_2}} \cdot r_{2n} \cdot e^{-2 \cdot \gamma_2 \cdot L_2} \quad (71)$$

In consideration of all these reflections, the voltage at the receiver is calculated by:

$$\frac{U_{receiver}}{U_1} = \frac{U_h}{U_1} \cdot \frac{T_{2f} \cdot T_{3f}}{1 - T_{32} \cdot T_{23}} \quad (72)$$

Figure 59 and Figure 60 show the calculated voltage ratio for a cable screen with the same characteristics as in Figure 49 but with different dimensions of the screening case.

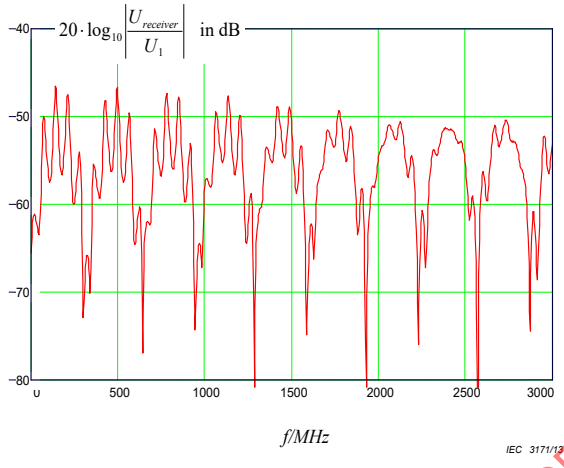

quantities used:

C_T = 0,02 pF/m

M_T = 0,4 nH/m

R = 50 Ω	Z_1 = 50 Ω	ε_{r1} = 2,3
Z_2 = 120 Ω	ε_{r2} = 1,1	L_2 = 2 m
Z_3 = 90 Ω	ε_{r2} = 1,1	L_3 = 0,03 m

Figure 59 – Calculated voltage ratio including multiple reflections caused by the screening case

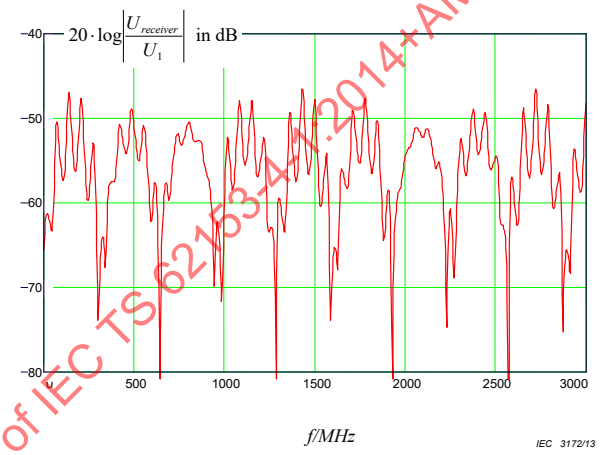

quantities used:

C_T = 0,02 pF/m

M_T = 0,4 nH/m

R = 50 Ω	Z_1 = 50 Ω	ε_{r1} = 2,3
Z_2 = 120 Ω	ε_{r2} = 1,1	L_2 = 2 m
Z_3 = 90 Ω	ε_{r2} = 1,1	L_3 = 0,1 m

Figure 60 – Calculated voltage ratio including multiple reflections caused by the screening case

To avoid the disturbing reflections at the screening case, the reflection factor r_{23} or (and) r_{3f} must be minimized. A worthwhile solution in practice is to design the screening case in a way that the characteristic impedance Z_3 is approximately of the same value as the input resistance of the receiver. In this case, the reflection factor $r_{3f} \approx 0$ and thus T_{3f}=1, T_{32}=0. This results in a voltage ratio which is equal to the ideal frequency response of Equation (48).

10.9.2 Mismatch in the inner circuit

10.9.2.1 General

A mismatch in the inner circuit, i.e. between the generator and the DUT or between the DUT and the load resistor, may result in significant errors.

The mismatch between the DUT and the load resistor can be reduced by choosing an appropriate load resistor. Theoretical and practical investigations [28] show that a mismatch of the terminating resistor in the inner circuit is of low influence as long as:

$$\frac{|R_{\text{termination}} - Z_1|}{Z_1} \cdot 100\ \% \leq 10\ \%$$

However, when measuring cables, especially multi-conductor cables having a "coaxial" impedance significantly different from the generator impedance, one has either to use impedance matching adapters or to take into account the reflection loss of the mismatch between generator and DUT.

Impedance matching adapters are only available for standard impedances like 60 Ω or 75 Ω. For other impedances, one would have to build homemade adapters. However, those adapters only work for frequencies up to some 10 MHz. This is illustrated in Figure 61. It shows the attenuation and return loss of a 50 Ω to 5 Ω impedance matching adapter. A DUT impedance of 5 Ω is typical when measuring multi-pair cables with individually screened pairs or when measuring high voltage cables for electrical vehicles.

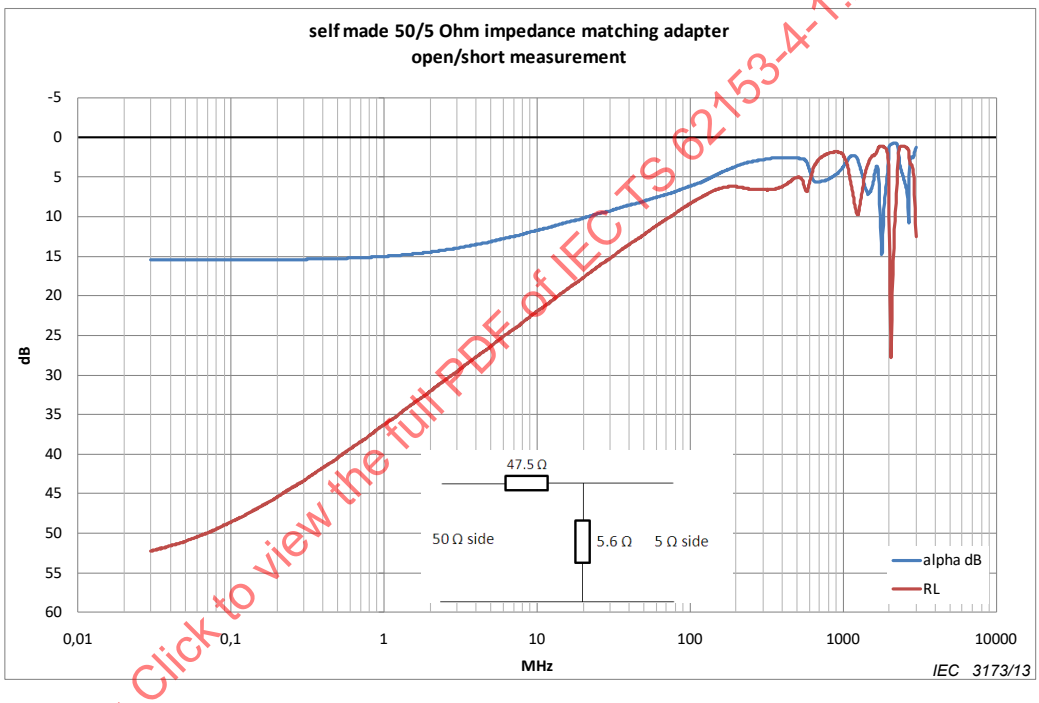

Figure 61 – Attenuation and return loss of a self-made 50 Ω to 5 Ω impedance matching adapter

Therefore it is recommended not to use self-made impedance matching adapters but to measure with mismatch between generator and DUT and to take into account the reflection loss of the mismatch:

$$a_s = 10 \times \log_{10} \left| \frac{P_1}{P_{\text{Smax}}} \right| = 10 \times \log_{10} \left| \frac{P_1}{P_{\text{2max}}} \times \frac{2 \times Z_{\text{S}}}{\text{R}} \right| \tag{73}$$

$$a_s = Env\left\{ -20 \times \log_{10} |S_{21}| + |\Gamma_s| + 10 \times \log_{10} \left| \frac{300}{Z_1} \right| \right\} \tag{74}$$

where

a_s is the screening attenuation related to the radiating impedance Z_s of 150 Ω in dB;

Env is the minimum envelope curve of the measured values in dB;

S_{21} is the scattering parameter S_{21} (complex quantity) of the set-up where the primary side of the two port is the DUT and the secondary side is the tube, i.e. the operational attenuation of the set-up;

Γ_s is the reflection loss of the junction between the generator and DUT.

The junction loss is obtained from the reflection coefficient (scattering parameter S_{11}) as described in 10.9.2.2. Where S_{11} could either be measured or calculated using the mean characteristic impedances for the purpose of simplification:

$$S_{11} = \frac{Z_1 - Z_0}{Z_1 + Z_0} \tag{75}$$

where

Z_1 is the nominal characteristic impedance of the cable under test in Ω;

Z_0 is the output impedance of the generator, i.e. system impedance of the network analyser, in Ω.

10.9.2.2 Reflection loss of a junction

In case a source with an inner resistance R_i feeds a load with a different resistance R_L, power is lost compared to the matched case due to the mismatch. If the source is connected to the junction by a transmission line with a characteristic impedance Z_1=R_i and the load is connected to the junction by a transmission line with a characteristic impedance Z_2=R_L, the equivalent circuit is as shown in Figure 62:

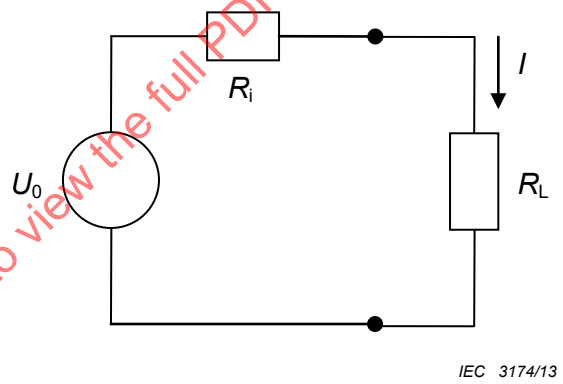

Figure 62 – equivalent circuit of a load resistance connected to a source

The power in the load resistance R_L is given by

$$P = I^2 R_L = \left(\frac{U_0}{R_i + R_L}\right)^2 R_L = U_0^2 \frac{R_L}{(R_i + R_L)^2} \tag{76}$$

In case of impedance matching R_L=R_i, the maximum power P_0 is fed:

$$P_0 = U_0^2 \frac{R_i}{4R_i^2} = \frac{1}{4} U_0^2 \frac{1}{R_i} \tag{77}$$

The ratio of Equations (76) and (77) describes the loss:

$$\frac{P}{P_0} = \frac{U_0^2 R_L}{(R_i + R_L)^2} \frac{4R_i}{U_0^2} = \frac{4R_L R_i}{(R_i + R_L)^2} \tag{78}$$

The following auxiliary calculation introduces the reflection coefficient r:

$$1 - r^2 = 1 - \left(\frac{R_L - R_i}{R_L + R_i}\right)^2 = \frac{(R_L + R_i)^2}{(R_L + R_i)^2} - \frac{(R_L - R_i)^2}{(R_L + R_i)^2} =$$
$$\frac{R_L^2 + 2R_L R_i + R_i^2 - R_L^2 + 2R_L R_i - R_i^2}{(R_L + R_i)^2} = \frac{4R_L R_i}{(R_L + R_i)^2} \tag{79}$$

Using Equation (79), the power ratio (Equation (78)) becomes:

$$\frac{P}{P_0} = 1 - r^2 \tag{80}$$

The magnitude in dB therefore is (see also IEC/TR 62152 Equation C.67)

$$\Gamma_s = -10 \log_{10} \left|1 - r^2\right| \tag{81}$$

11 Background of the shielded screening attenuation test method for measuring the screening effectiveness of feed-throughs and electromagnetic gaskets (IEC 62153-4-10)

11.1 General

The proper function of modern communication equipment is strongly influenced by the proper EMI shielding of electrical components. Feed-through configurations with poor ground connections can contribute significantly to the overall EMI level of communication equipment [1]. Electromagnetic gaskets like contact springs or conducting polymers can dramatically reduce conducted and radiated emissions, respectively. A cross-sectional sketch of the typical configuration of a feed-through is shown in Figure 63. The connector body is soldered onto the circuit board and thus electrically connected to the ground potential or equipotential of the electronic circuitry.

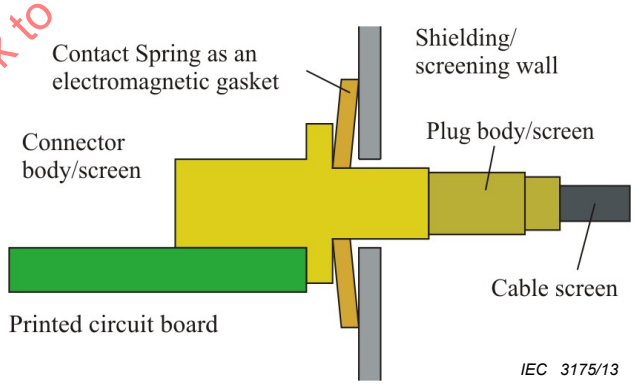

Figure 63 – Cross-sectional sketch of a typical feed-through configuration

At higher frequencies, the potential of the circuit board's ground plane is usually not equal to that of the shielding box. A contact spring short circuits this potential difference. If the contact spring were not present in the setup of Figure 63, excessive radiation of electromagnetic waves along the cable's outer conductor will be the result.

It is usually a very time-consuming task to evaluate the shielding or screening effectiveness of a feed-through or electromagnetic gasket (EMI or EMC gasket) in a test configuration as e.g. is recommended in CISPR 25. The measurement setups that are described there are generally based on some kind of free space measurement, which requires an anechoic chamber.

The introduction of well-defined electrically conducting boundaries in a test fixture would greatly simplify the measurement procedure. This is possible by application of a coaxial test setup based on the experience in measuring shielding effectiveness of cables, cable assemblies and connectors with the standardized shielded triaxial screening effectiveness test methods [5], [7] and [10] by IEC and CENELEC.

11.2 Theoretical background of the test Fixtures and their equivalent circuit

A cross-sectional view of the test fixture is shown in Figure 64. The left section represents the inner area of a shielding box. A signal is fed to the outer conductor of the connector under test by means of the coaxial line's inner and outer conductor. The amount of RF leakage that can be detected on the opposite side of the shielding wall is picked up by the coaxial line to the right. A separate EMI gasket can be tested with the configuration in Figure 64a).

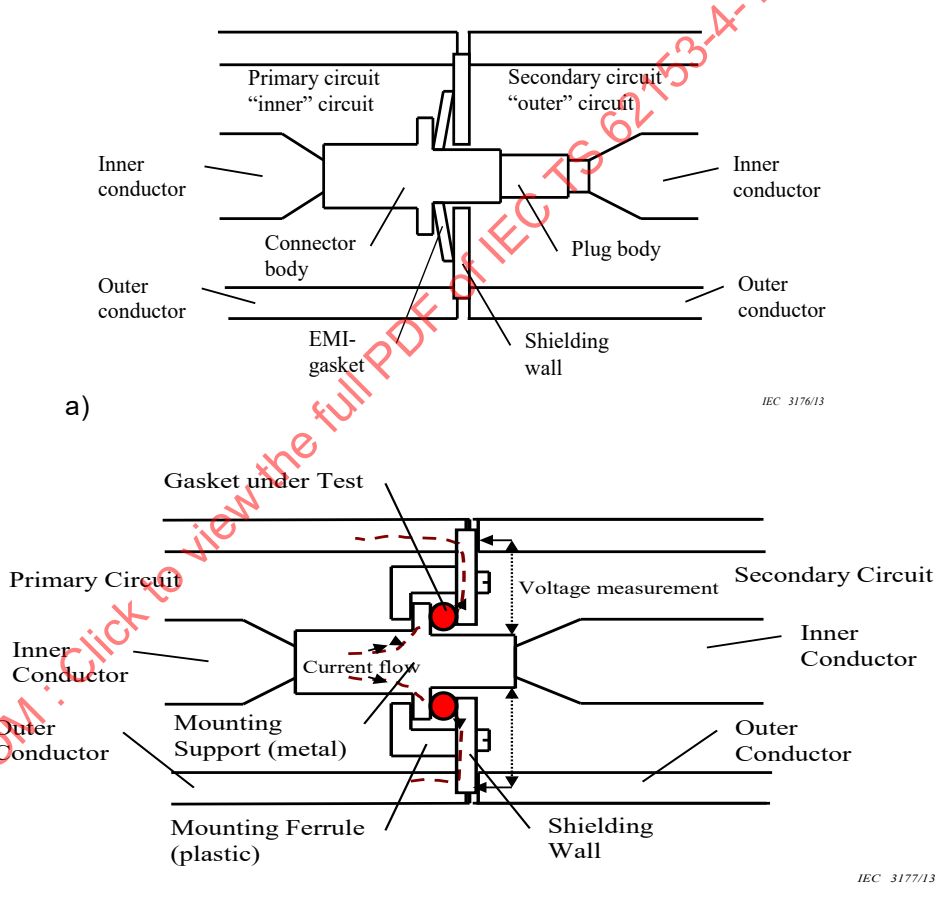

Figure 64 – Cross-sectional sketch of the test fixture with a feed-through connector (a) and EMI gasket (b) under test

The test fixture consists of cascaded two-ports formed by a primary and a secondary transmission line separated with an isolating metallic plate to mount the test objects. The equivalent circuit of the test fixtures is shown in Figure 65.

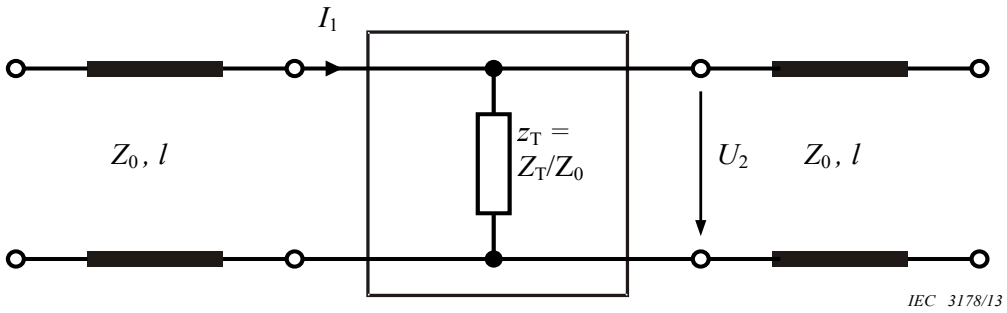

Key

$z_T=Z_T/Z_0$	*normalised transfer impedance*
Z_T	*transfer impedance of the device under test*
Z_0	reference impedance (generator and receiver impedance)
I_1	current in the primary transmission line
U_2	coupled voltage to the secondary circuit
l	length of the coaxial line section

Figure 65 – Equivalent circuit of the test fixture

In the case of a two-port scattering parameter S_{21} or forward transfer function measurement, where the two ports of the network analyzer are connected to both coaxial line sections, S_{21} is a direct measure for the shielding efficiency of a feed-through or EMI gasket tested in well-defined circumstances that make repeatable and comparable tests possible.

In an equivalent circuit of the measurement of a feed-through or gasket, the transfer impedance is shunt impedance Z_T between the primary and secondary circuit.

The transfer impedance of an electrically short screen is defined as the quotient of the open circuit voltage U_2 induced to the secondary circuit by the current I_1 fed into the primary circuit or vice versa. Z_T of an electrically short screen is expressed in ohms [Ω] or decibels in relation to 1 Ω.

Operational (Betriebs) transfer function in the forward direction H_{B21} or the forward Operational (Betriebs) scattering parameter S_{21} of a two-port (see Figure 66) is defined as

$$S_{21} = \frac{V_{r2}}{V_{i1}}\bigg|_{V_{i2}=0} = \frac{2U_2}{E_1}\sqrt{\frac{Z_A}{Z_B}} = H_{B21} \tag{82}$$

where V_{i1} and V_{r1} are the square roots of incident (unreflected) and reflected complex power waves at port 1, and V_{i2} and V_{r2} are those at port 2. See Annex C of IEC TR 62152:2009.

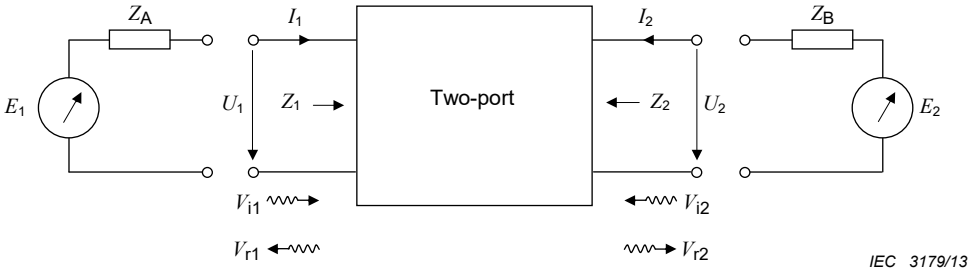

Figure 66 –Two-port network

A two port network containing the normalized transfer impedance $Z_T = Z_T/Z_0 = (U_2/I_1)/Z_0$ can be described by the scattering matrix $\underline{S}$ when placed between equal impedances Z_0 equal to the characteristic impedances Z_0 of the transmission lines of the fixture

$$\underline{S} = \begin{pmatrix} S_{11} & S_{12} \\ S_{21} & S_{22} \end{pmatrix} = \begin{pmatrix} \frac{-1}{1+2z_T} & \frac{2z_T}{1+2z_T} \\ \frac{2z_T}{1+2z_T} & \frac{-1}{1+2z_T} \end{pmatrix} \tag{83}$$

Equation (83) indicates that the transfer impedance Z_T of the feed-through or gasket may be estimated from the measured S parameter S_{21} by:

$$\begin{aligned} Z_T &= \frac{U_2}{I_1} = z_T Z_0 = \frac{S_{21} Z_0}{2(1-S_{21})} \\ &\approx \frac{S_{21}}{2} Z_0 = \frac{H_{B21} Z_0}{2} \quad \text{for} \quad |S_{21}| << 1 \end{aligned} \tag{84}$$

The operational forward transfer function S_{21} or H_{B21} is a measure of screening effectiveness and the corresponding screening transfer function Γ_S consisting of the screening attenuation α_s and screening phase β_s is then

$$\begin{aligned} \Gamma_s &= \alpha_s + j\beta_s = \ln \frac{1}{S_{21}} \\ &= 20 \log_{10} \left| \frac{1}{S_{21}} \right| [\text{dB}] - j \arg S_{21} [\text{rad}] \end{aligned} \tag{85}$$

$$\begin{aligned} \alpha_s &= 20 \log_{10} \left| \frac{Z_0}{2Z_T} \right| [\text{dB}] \\ |Z_T| &= \frac{|Z_0|}{2} 10^{-\frac{\alpha_s / \text{dB}}{20}} \end{aligned} \tag{86}$$

Equation (86) gives the relationship between the transfer impedance Z_T and the screening attenuation a_s. The screening attenuation is dependent on the characteristic impedances of the test fixture. Only the transfer impedance is independent on the test fixture and is therefore a primary parameter of the screening effectiveness. The smaller Z_T the better is the screening or shielding.

Equation (86) gives the Z_T corresponding to a screening attenuation measured in a configuration with the nominal impedance Z_0 of the inner and outer "world" formed by the test fixture. In real life Equation (86) gives only the true values in an operating system within the characteristic impedance $Z_{Aop} = Z_{Bop} = Z_0$. Bringing the feed-through or gasket into an operating system with different primary or secondary circuit impedances Z_{Aop} and Z_{Bop}, the true operating screening attenuation a_{sop} can now be recalculated according to Equation (87) by the use of the transfer impedance Z_T determined by Equation (86) (see 11.4).

$$\alpha_{sop} = 20 \log_{10} \frac{\sqrt{Z_{Aop} \cdot Z_{Bop}}}{2Z_T} \tag{87}$$

The market likes to talk about shielding or screening effectiveness in decibels without really defining the operative conditions. Therefore, for example in cable and connector shielding, the outer circuit impedance has been normalized to 150 Ω. If the measurements are done in a test fixture which has feeding and receiving line impedances of 50 Ω, the relation between shielding attenuation and transfer impedance is:

$$\alpha_{sn} \approx 20 \log_{10} \left| \frac{43\,\Omega}{Z_T / \Omega} \right| [\text{dB}] \tag{88}$$

α_{sopn} is the normalized screening attenuation (for feed-throughs or gaskets) when measured in a fixture with a transmission line characteristic impedance Z_0.

$$\alpha_{sopn} = 20 \log_{10} \left| \frac{\sqrt{150 \cdot Z_0}}{2Z_T} \right| \text{ [dB]} \quad (89)$$

11.3 Pictures and measurement results

11.3.1 Characteristic impedance uniformity

The uniformity of the characteristic impedances is important. Line sections with deviations from the nominal characteristic impedance will cause impedance transformations, resulting in measurements that will generate erroneous calculations of the transfer impedance.

Cable measurement with shielded screening effectiveness test method has shown that to get test results which correspond to the theory unintended reflection points in the test fixture must be avoided. Time domain reflectometer (TDR) in Figure 67 shows that the impedance of the test object inserted in the test fixture is about 110 Ω, which leads to a return loss of only 8,5 dB in the 50 Ω test fixture. The length of the test object area is about 7,5 cm. It is predicted that an improvement in impedance uniformity in the test fixture will considerably increase the upper frequency limit.

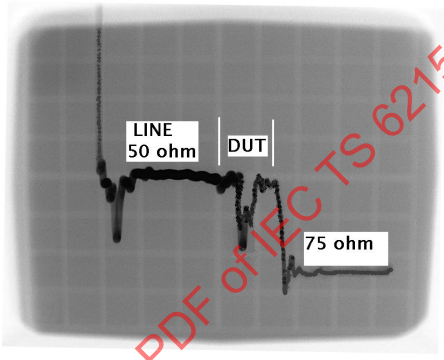

IEC 3180/13

rise time 200 ps

time (horizontal) scale 2 ns/div (about 20 cm/div)

impedance (vertical) scale 10 Ω/div

50 Ω feeding line (0,5 m)

75 Ω termination

Figure 67 – TDR measurement of the text-fixture with inserted "Teflon-through" sample

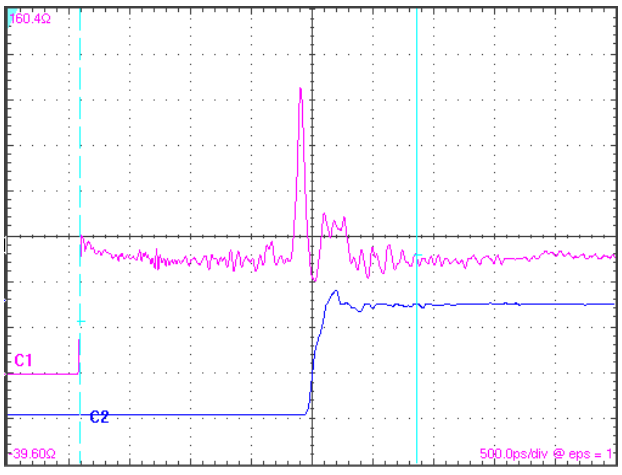

IEC 3181/13

rise time ≤12 ps

upper trace (C1) shows the reflection step response when the far end is terminated with 50 Ω

lower trace (C2) shows the (through) transmission step response

time (horizontal) scale 0,5 ns/div or 8,5 cm/div

impedance (vertical) scale 20 Ω/div

Figure 68 – TDR step response from A (Input)-port of test fixture with inserted "Teflon-through" sample

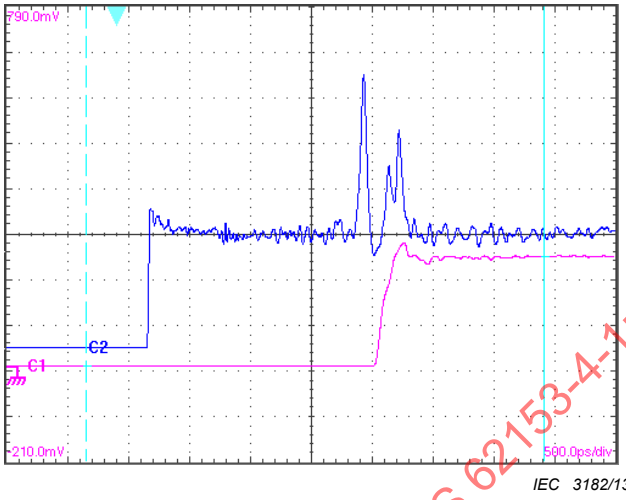

rise time ≤12 ps

upper trace (C2) shows the reflection step response when the far end is terminated with 50 Ω

lower trace (C1) shows the (through) transmission step response

time (horizontal) scale 0,5 ns/div or 8,5 cm/div

impedance (vertical) scale 20 Ω/div

Figure 69 – TDR step response from B (Output)-port of test fixture with inserted "Teflon-through" sample

In Figure 67, measurements are made with 200 ps rise time step from A end with the far-end terminated in 75 Ω. The shorter rise time, below 12 ps TDR responses in Figure 68 and Figure 69 show more exactly the impedance variations in the test fixture with a "Teflon through" sample. Measurements were made in both directions. In the same Figures are the through transmission step responses. Observe the fact that the transmission in both directions is identical as also the theory of passive two-ports assumes.

The S-parameters in the frequency domain of the "Teflon-through" sample are shown in Figure 70 and Figure 71. The time domain and frequency domain measurements support each other. The "Teflon-through" behaves as a low-pass filter with a limiting frequency of about 2,5 GHz. The deformation of the through step response is caused by reflections and limited bandwidth.

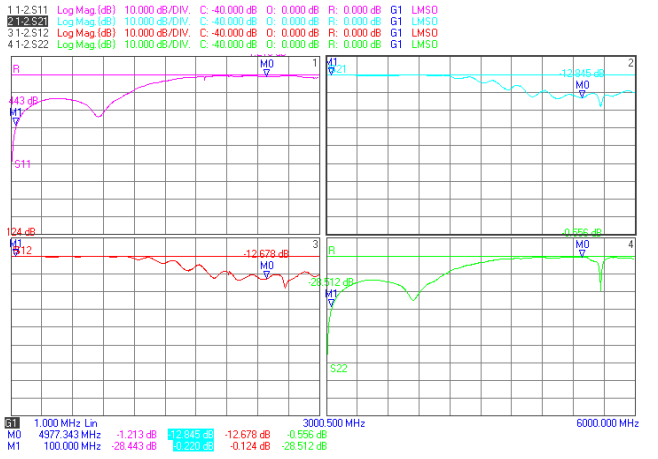

IEC 3183/13

frequency (horizontal) scale 1 MHz to 6 000 MHz linear sweep

vertical scale 10 dB/div

Figure 70 – S-parameter measurement (linear sweep): "Teflon-through" sample

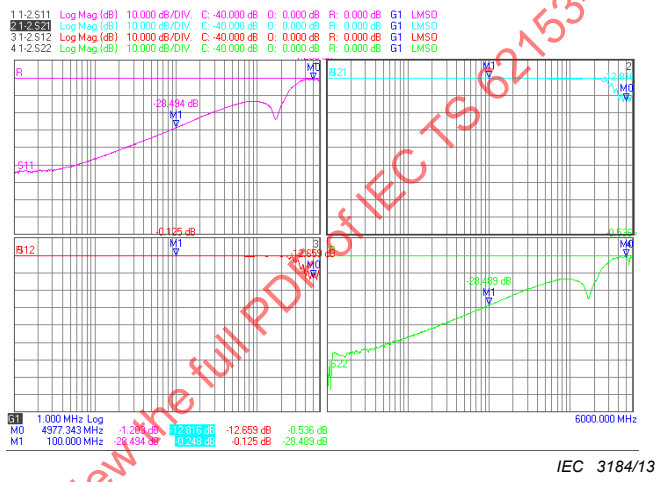

IEC 3184/13

frequency (horizontal) scale 1 MHz to 6 000 MHz logarithmic sweep

vertical scale 10 dB/div

Figure 71 – S-parameter measurement (logarithmic sweep): "Teflon-through" sample

11.3.2 Measurements of shielding effectiveness

Figure 72 and Figure 73 show pictures of the test fixture and measurement set-up. Figure 74 and Figure 75 are detailed views of the contact area. To investigate the noise level (the lower trace in Figure 76) of the network analyzer, port one was connected to the test fixture and port two was terminated by a 50 Ω load. The upper trace in Figure 76 shows measurement results when a metal plate is mounted in the test fixture instead of a feed-through. The measured amplitude of S_{21} is comparable to the case where only the noise limit of the network analyzer was measured. Therefore, we expect to be able to measure shielding/screening attenuations above 100 dB at frequencies up to approximately 4 GHz and above. Further investigations have shown that with improving the impedance uniformity and shortening the test area, considerable increases in the upper frequency can be achieved. Also a dynamic range of 125 dB has been demonstrated.

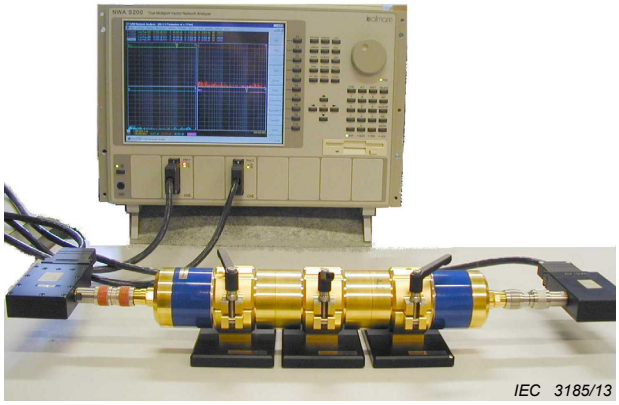

Figure 72 – *S* parameter test setup

Figure 73 – TDR test setup

Figure 74 – Test fixture assembled

Figure 75 – Detailed views of the contact area the test fixture and the secondary side of side opened

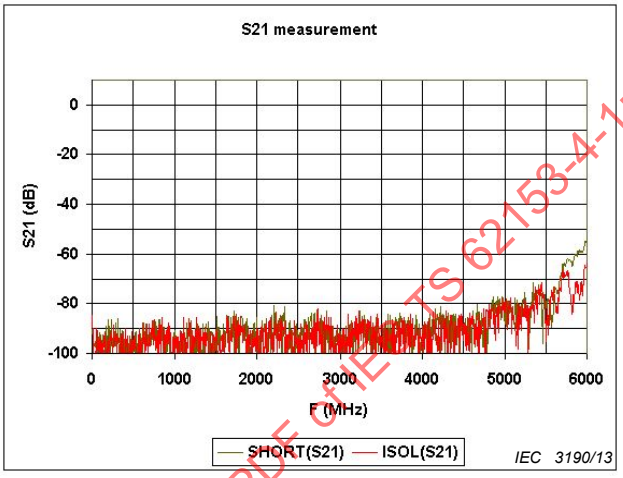

Lower trace (red): Isolation of NWA; port 2 (receiving port) of the NWA terminated by a 50 Ω load

Upper trace (brown) Isolation of the test fixture when characterizing an ideal short-circuit with metal plate

Figure 76 – S_{21} measurements

11.3.3 Calculation of transfer impedance

The calculation of the transfer impedance out of the measured S_{21} according to Equation (84) demands a de-embedding of the transmission lines of the test-fixture (see Figure 65). This moves the reference plane of the calibrated coaxial NWA ports towards the location of the transfer impedance and assures a phase correct representation.

Figure 77 shows the measured screening attenuation of the feed-through “Sonnenscheibe” gasket sample and Figure 78 the calculated transfer impedance. The slope shows that the leakage is not purely inductive but has also a resistive component. The “Sonnenscheibe” has simple stamped spring contacts which give considerable improvement to the feed-through shielding attenuation but they have radial slices which cause the leakage.

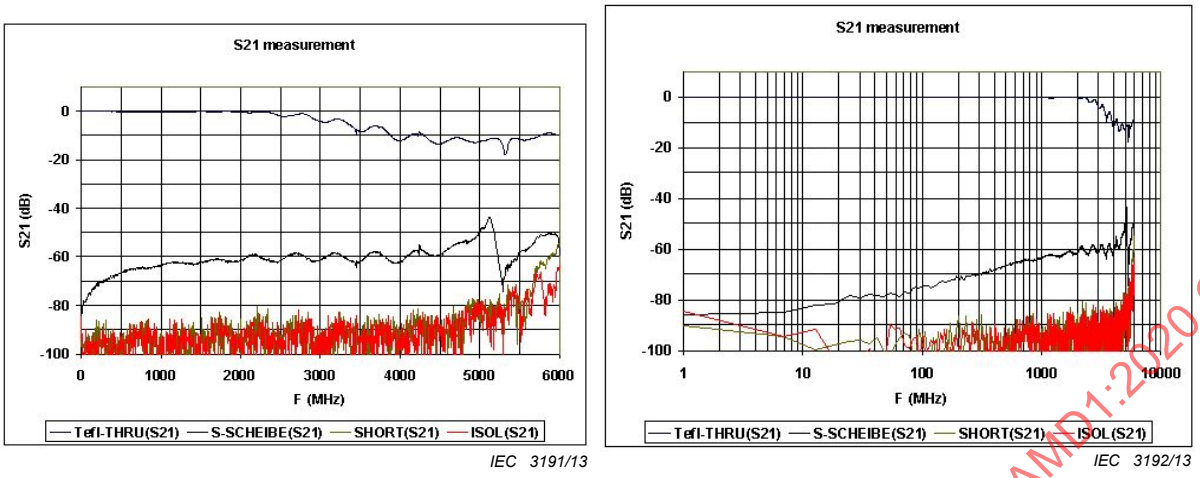

a) linear frequency sweep

b) logarithmic frequency sweep

frequency sweep 1 MHz to 6 000 MHz

S_{21} (vertical) scale 10 dB/div

upper trace is the “Teflon-through“ sample

middle trace is the “Sonnenscheibe” feed-through sample

two lower traces short circuit (brown) and Isolation (red) traces

Figure 77 – S_{21} measurements of “Teflon-through” and “Sonnenscheibe” feed-through

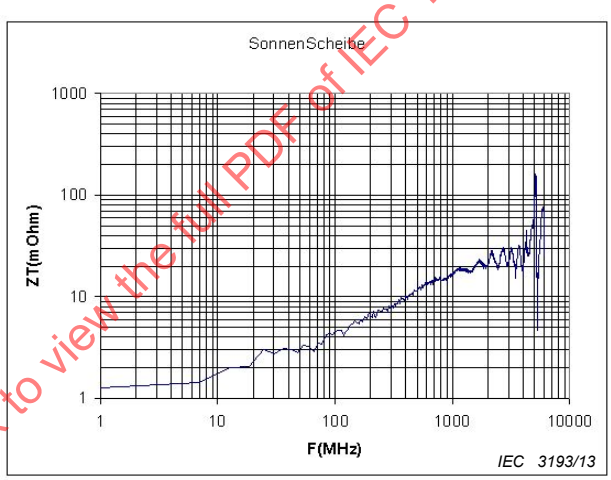

Figure 78 – Transfer impedance ZT of a “Sonnenscheibe” feed-through based on the S_{21} measurement in Figure 77

Figure 79 shows the screening attenuation of a conducting plastic gasket. It has a shielding level of about 60 dB and in contrast to the “Sonnenscheibe”, it increases with the frequency. The explanation is the uniformity of the gasket and the eddy currents. Both frequency domain and time domain measurement give about the same shielding attenuation level. The level of transfer impedance is about 20 mΩ decreasing with frequency (see Figure 80).

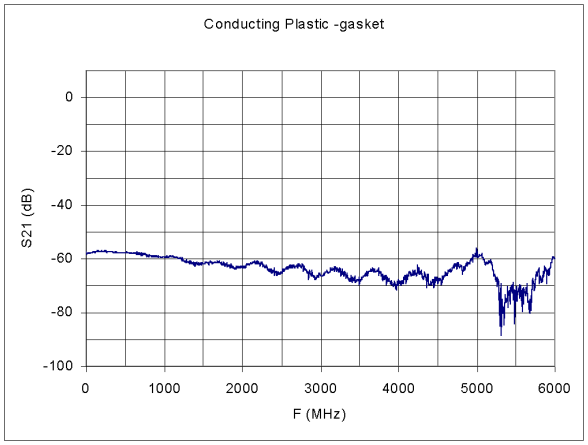

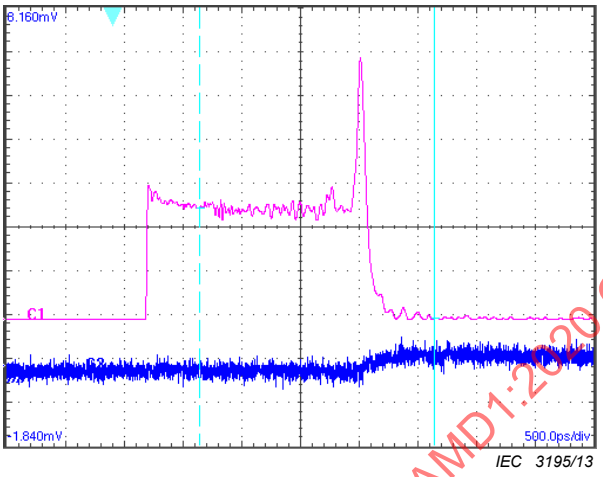

a) frequency domain

1 MHz to 6 000 MHz, 10 dB/div

S_{21} measurement

b) time domain

0,5 ns/div and 20 Ω/div

upper trace (C1): TDR step response

lower trace (C2): through transmission step response (TDT)

Figure 79 – measurements of a conducting plastic gasket

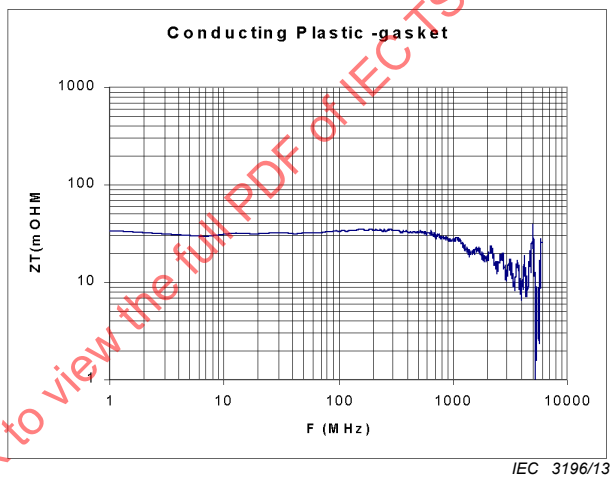

Figure 80 – Z_T of the conducting plastic gasket based on the S_{21} measurement in Figure 79

11.4 Calculation of screening attenuation for feed-through when the transfer impedance Z_T is known

a) Reference (see Figure 81)

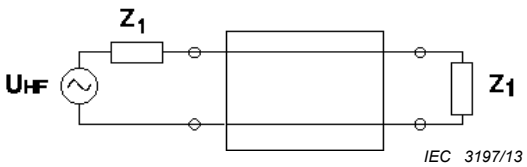

Figure 81 – equivalent circuit of the set-up without DUT

Maximum unreflected power:

$$P_{av} = \frac{U_{HF}}{2} \cdot \frac{U_{HF}}{2Z_1} = \frac{1}{4} \cdot \frac{U_{HF}}{Z_1} \tag{90}$$

b) Measurement (see Figure 82)

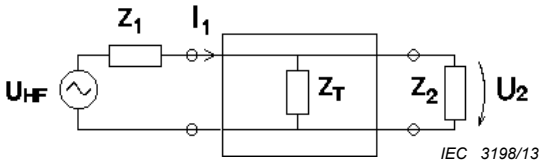

Figure 82 – equivalent circuit of the set-up with inserted DUT

$$I_1 = \frac{U_{HF}}{Z_1} \qquad for\ Z_T << Z_1 \tag{91}$$

$$U_2 = I_1 Z_T = U_{HF} \cdot \frac{Z_T}{Z_1} \qquad for\ \ Z_T << Z_2 \tag{92}$$

$$I_2 = \frac{U_2}{Z_2} \tag{93}$$

$$\begin{aligned} P_2 = U_2 I_2 &= \left(U_{HF} \cdot \frac{Z_T}{Z_1} \right) \cdot \frac{U_{HF} Z_T / Z_1}{Z_2} \\ &= U_{HF}^2 \cdot \frac{Z_T^2}{Z_1^2 Z_2} \end{aligned} \tag{94}$$

Power attenuation (= screening attenuation):

$$\begin{aligned} \alpha_S &= 10 \cdot \lg \left(\frac{P_{av}}{P_2} \right) \\ &= 10 \cdot \lg \left(\frac{1}{4} \cdot \frac{U_{HF}^2}{Z_1} \cdot \frac{Z_1^2 Z_2}{U_{HF}^2 Z_T^2} \right) \\ &= 10 \cdot \lg \left(\frac{1}{4} \cdot \frac{Z_1 Z_2}{Z_T^2} \right) = 20 \cdot \lg \left(\frac{\sqrt{Z_1 Z_2}}{2Z_T} \right) \end{aligned} \tag{95}$$

12 Background of the shielded screening attenuation test method for measuring the screening effectiveness of RF connectors and assemblies (IEC 62153-4-7)

12.1 Physical basics

12.1.1 Surface transfer impedance Z_T

The surface transfer impedance Z_T [Ω] of an electrically short screen is defined as the quotient of the longitudinal voltage induced to the inner circuit by the current fed into the outer

circuit or vice versa (see Figure 83). In case of cables, Z_T of an electrically short cable screen is expressed in milli-ohms per length [mΩ/m] or in decibels in relation to 1 Ω.

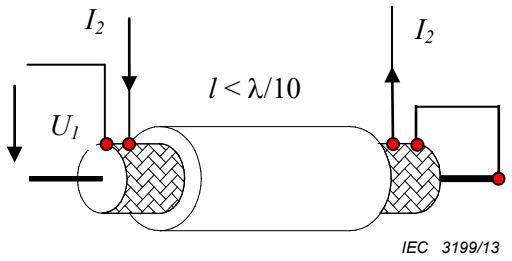

Figure 83 – Definition of Z_T

$$Z_T = \frac{U_1}{I_2} \text{ [m}\Omega\text{/m]} \qquad (96)$$

$$Z_T \text{ dB}(\Omega) = +20 \cdot \log_{10}\left(\frac{|Z_T|}{1\Omega}\right) \qquad (97)$$

In the case of single units like connectors or connecting hardware, the transfer impedance is expressed as the transfer impedance of the unit.

12.1.2 Screening attenuation a_S

For coaxial elements respectively in the common mode of screened balanced elements, the logarithmic ratio of the feeding power P_1 and the periodic maximum values of the power $P_{r,max}$ which may be radiated due to the peaks of voltage U_2 in the outer circuit is termed screening attenuation a_S.

The screening attenuation a_S of electrically long elements, e.g. coaxial cables is defined as the logarithmic ratio of the power fed into the cable and the radiated maximum peak power:

$$a_S = 10 \cdot \log_{10}\left(Env\left|\frac{P_{feed}}{P_{rad,max}}\right|\right) \qquad (98)$$

12.1.3 Coupling attenuation a_C

For screened balanced cables or connectors, the coupling attenuation a_C is the sum of the unbalance attenuation a_U of the pair and the screening attenuation a_S of the screen.

For electrically long devices, i.e. above the cut-off frequency, the coupling attenuation a_C is defined as the logarithmic ratio of the feeding power P_1 and the periodic maximum values of the coupled power $P_{r,max}$ in the outer circuit.

$$a_C = 10 \cdot \log_{10}\left(Env\left|\frac{P_{feed}}{P_{r,max}}\right|\right) \qquad (99)$$

12.1.4 Coupling transfer function

The coupling transfer function $T_{n,f}$ (see Figure 84) gives the relation between the screening attenuation a_S and the transfer impedance Z_T of a screened element like a coaxial cable or a coaxial connector (n = near end, f = far end). In the lower frequency range, where the samples are electrically short, the transfer impedance Z_T can be measured up to the cut-off frequencies $f_{cn,f}$. Above these cut off frequencies $f_{cn,f}$ in the range of wave propagation, the screening attenuation a_S is the measure of screening effectiveness. In the case of cables, the

cut-off frequencies $f_{cn,f}$ may be moved towards higher or lower frequencies by variable length of the cable under test.

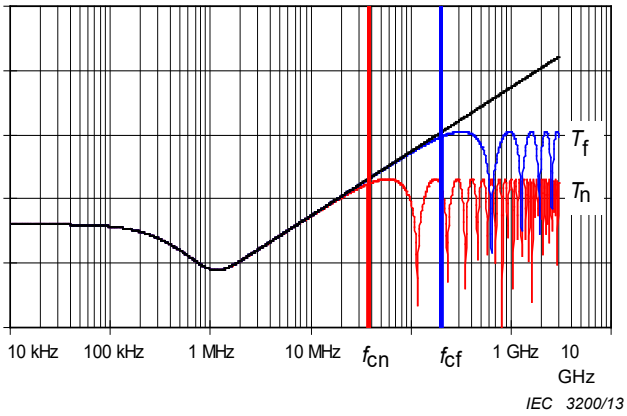

Figure 84 – Calculated coupling transfer function

12.1.5 Relationship between length and screening measurements

The relationship between the effective coupling length of the device under test and the electrical wave length is important for the characteristic curve of the screening measurements. In the frequency range of electrically short coupling lengths, the measured screening effectiveness decreases with increasing length. Therefore it is necessary to define the related length. In the case of cables, the measured value is related to 1 m by dividing the measured value by the length under test and the value is given in milli-ohms per meter [mΩ/m]. In the case of fixed elements like connectors or connecting hardware, the measured value is the value of the unit and will not be related to length. When measuring connectors or connecting hardware, care should be taken with connecting cables and contact resistances, because they add to the test result.

With electrically long lengths respectively in the range of wave propagation, the screening attenuation formed by the maximum envelope curve is the measure of the screening effectiveness. Therefore the screening attenuation is defined only at high frequencies, above the cut-off frequencies.

The point of intersection between the asymptotic values for low and high frequencies is the so called cut-off frequency f_c. This frequency gives the condition for electrical long samples:

$$f_c \cdot l \geq \frac{c_0}{\pi \cdot \left| \sqrt{\varepsilon_{r1}} \pm \sqrt{\varepsilon_{r2}} \right|} \qquad (100)$$

where $\varepsilon_{r1,2}$ are the relative dielectric permittivity of the inner and the outer system and l is the cable length respectively the length of the unit under test.

Usual RF connectors have mechanical dimensions in the longitudinal axis in the range of 10 mm to 50 mm. With Equation (100), i.e. the definition of electrical long elements, we get cut-off frequencies of about 3 GHz or higher for standard RF-connectors. Above the cut-off frequency they are considered to be electrically long.

The screening attenuation is by definition only valid in the frequency range above the cut-off frequencies, where the elements are electrically long. Thus the screening attenuation of a RF connector itself can only be measured at frequencies above about 3 GHz.

But customers and users of RF connectors and assemblies like to have the screening attenuation also in the MHz range, because it is more illustrative than the transfer impedance and can be used for direct calculation of emission and radiation.

The problem can be solved by using the tube in tube procedure, based on the shielded screening attenuation test set-up according IEC 62153-4-4 (triaxial method).

12.2 Tube in tube set-up (IEC 62153-4-7)

12.2.1 General

By extending the electrical short RF-connector by a RF-tight closed metallic tube, one is building a cable assembly which is electrically long. Thus the cut-off frequency respectively the lower frequency limit to measure the screening attenuation is extended towards lower frequencies.

The tube in tube procedure allows the measurement of the connector (and its mated adapter) together with its connecting cables. If one connects the extension tube to the connecting cable close to the connector(see Figure 85), one is measuring the screening attenuation of the combination of the connector (and its mated adapter) and the transition between the cable and the connector under test. This measurement reproduces the practical application of a connector; the measurement of the naked connector without connecting cable is worthless.

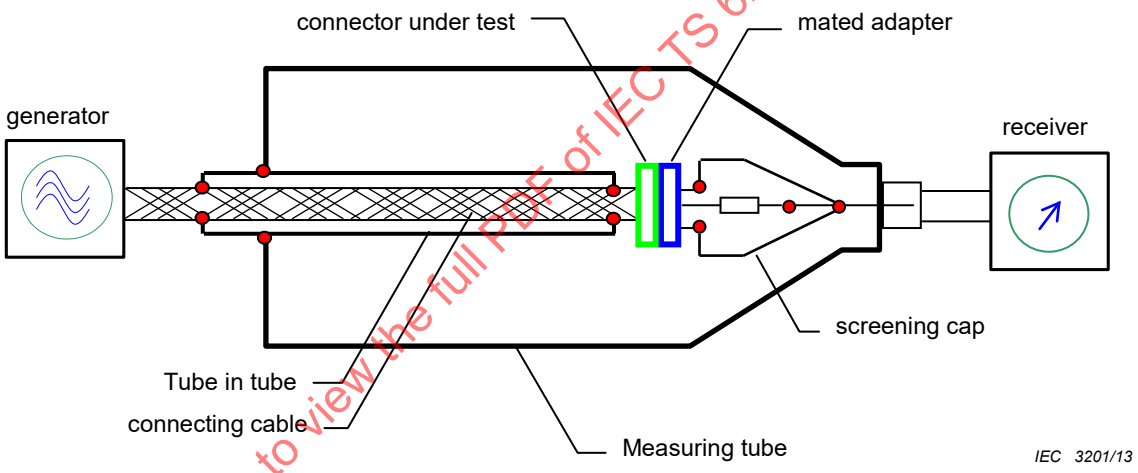

Figure 85 – Principle test set-up for measuring the screening attenuation of a connector with the tube in tube procedure

12.2.2 Procedure

The connector respectively the assembly under test is connected to the connecting cable and mounted together with the RF-tight extension tube into the measuring tube. The connector under test is connected to its mating connector in the test head and is fed via the connecting cable with RF energy by the generator.

In the case of coaxial connectors, the mating connector is matched with its characteristic impedance. In the case of screened balanced or multiconductor cables, the pair under test is matched with a symmetrical/asymmetrical load (see Figure 86 for the general set-up and Figure 87 for the preparation of the connector). In this way, the transfer impedance as well as the screening and the coupling attenuation of the pair under test may be measured with one test set-up.

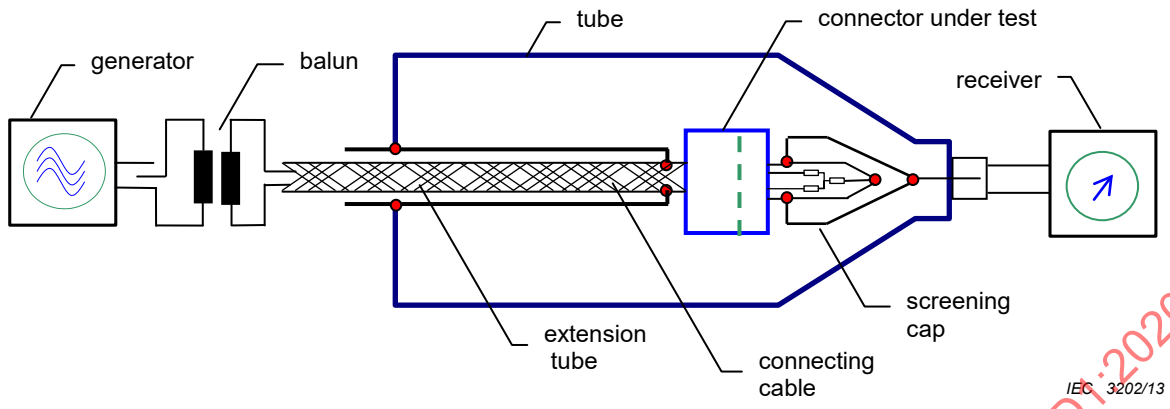

NOTE The balun transformer is not required in case of multiport VNA with mixed mode capabilities, see Annex A.

Figure 86 – Principle test set-up for measuring the coupling attenuation of screened balanced or multipin connectors

With the test set-up according to Figure 87, one can measure the coupling attenuation a_C, when the device under test (DUT) is fed in the differential mode as well as the screening attenuation a_S, when the DUT is fed in the common mode. The difference between the measurement of the screening attenuation a_S and the measurement of the coupling attenuation a_C is the unbalance attenuation a_U.

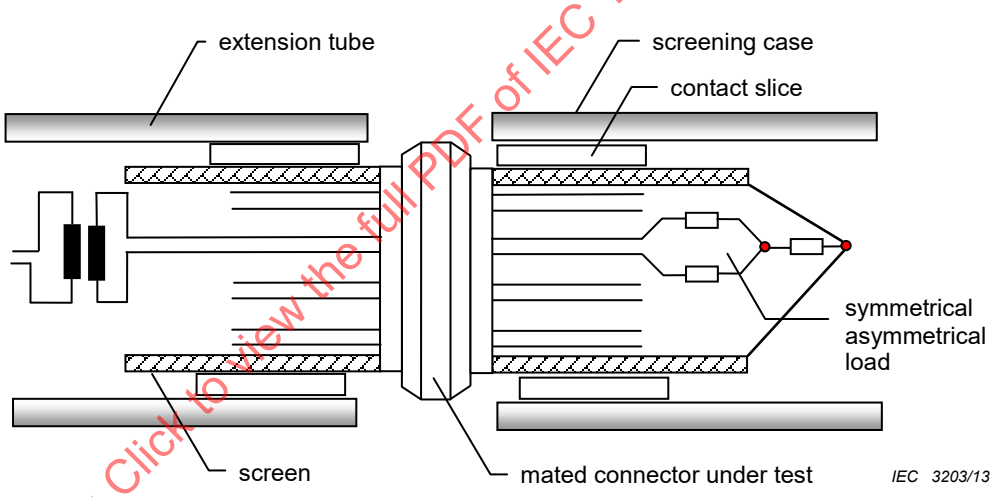

Figure 87 – Principle preparation of balanced or multiconductor connectors for coupling attenuation

The connector under test forms together with the connecting cable and the tube in tube the inner system, where the electrical short connector is enlarged by the RF-tight tube in tube. The outer system is formed by the outer conductor of the connector under test, enlarged by the tube in tube and the measuring tube.

The energy, which couples from the inner system into the outer system, propagates in both directions. At the short circuit at the near end it will be reflected, so that at the far end the superimposition of both waves can be measured. The logarithmic ratio of the feeding voltage to the measured voltage at the far end is the measure of the screening attenuation, respectively the coupling attenuation.

With the same test set-up also the transfer impedance may be measured with only one sample preparing.

During the measurement, the connector under test is connected to its mating part. It is not possible to separate the influence of the device under test from its mating part or to make a calibration of the mating part alone.

Therefore the type of the mating connector should be reported in the test report. Different mating parts or mating parts from different manufacturers may lead to different test results.

The sensitivity of the system depends on the RF-tightness of the tube in tube and the connection technique. The sensitivity respectively the ground floor of the system may be determined while measuring a semi rigid cable instead of a connector. With the triaxial set-up, a sensitivity of >125 dB up to 3 GHz was measured.

12.2.3 Measurements and simulations

In a first approach, one has measured short cable pieces instead of a connector. The advantage is that the results are not influenced by a mating adapter or the transition between cable and connector. The cable has been a coaxial cable with an impedance of 75 Ω, foam PE dielectric and a single braid screen (not optimised, i.e. under-braided).

For the calculation, the sample under test has been divided into two parts, the extension tube and the cable piece. The transfer impedance and capacitive coupling impedance of the extension tube can be neglected. The second section is the cable piece under test with the parameters of Table 13.

Table 13 – Cable parameters used for simulation

DC resistance	8 mΩ/m
magnetic coupling	0,6 mH/m
capacitive coupling	0,02 pF/m
impedance:	75 Ω
dielectric permittivity	1,35

The comparison of the simulation with the measurement results (see Figure 88 and Figure 89) shows a good correspondence. In the lower frequency range, when the samples are electrically short one gets the same results. However, in the higher frequency range, one can see the influence of the extension tube.

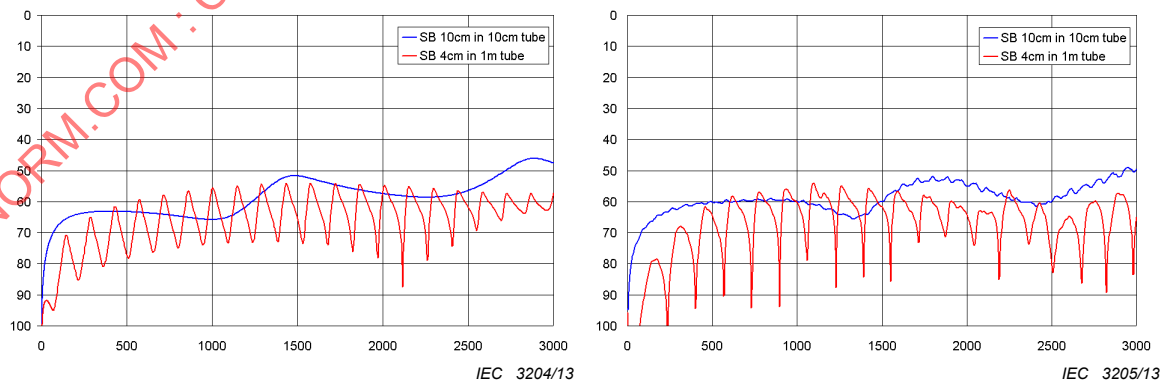

a) simulation b) measurement

Figure 88 – Comparison of simulation and measurement, linear frequency scale

The 10 cm sample is electrically short over the whole frequency range, as the cut-off frequency is 5,9 GHz. Thus the coupled power is increasing with increasing frequency. However, the quasi cable assembly composed of the connector and the extension tube is electrically long above 590 MHz, which results in a constant maximum coupled power.

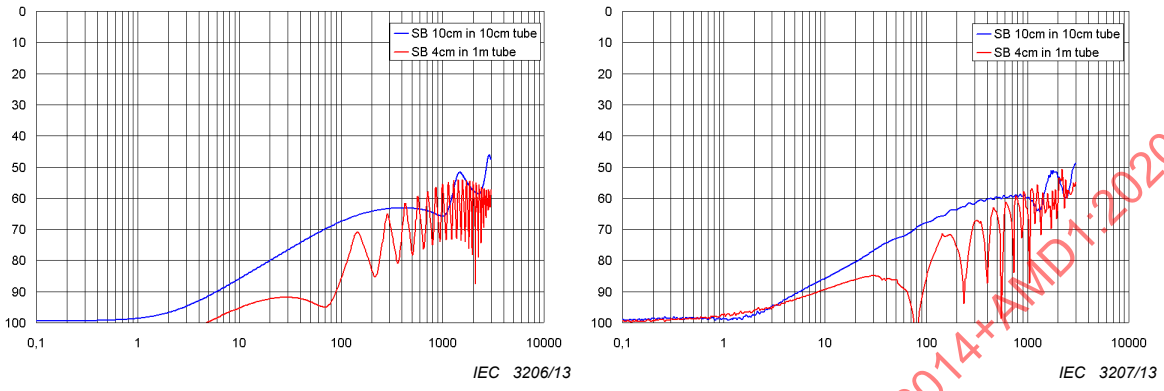

a) simulation b) measurement

Figure 89 – Comparison of simulation and measurement, logarithmic frequency scale

One characteristic of an electrically long object is also that the maximum coupled power is independent of the sample length (see envelope curve of Figure 88, single braid 4 cm in 1 m tube above 590 MHz).

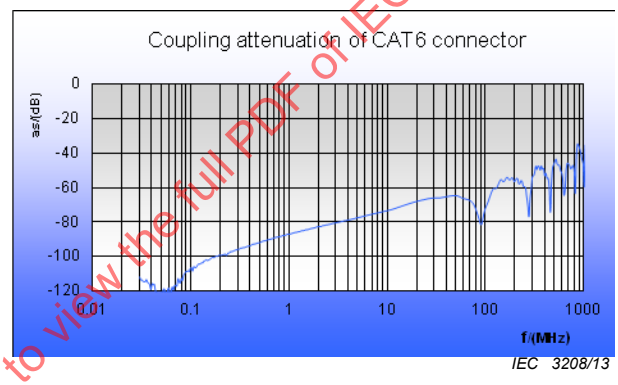

Figure 90 – Measurement of the coupling attenuation of a CAT6 connector

Figure 90 shows the measurement of the coupling attenuation of a CAT6 connector with the tube in tube procedure with 1 m extension tube.

12.2.4 Influence of contact resistances

Contact resistances between the feeding cable and the extension tube respectively the screening case in the test head may influence the test result. Contacts in the test set-up shall be prepared carefully with low resistance, respectively with low impedance. Contacts shall be achieved over the complete circumference of the screen. Critical contacts are shown in Figure 91.

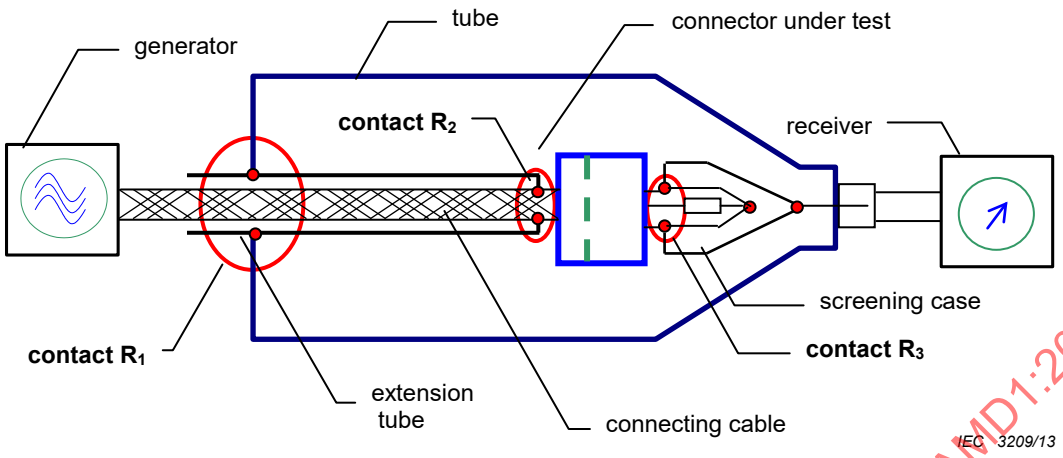

Figure 91 – Contact resistances of the test set-up

The equivalent circuit of the complete test set-up including the contact resistances is given in Figure 92. The test set-up shall be designed such that contact resistances of the extension tube are in series with the input impedance of the receiver and the contact resistance of the screening case including the matching load of the DUT is in series with the generator.

In this case, contact resistances of a few milli-ohms in series with the 50 Ω input resistance of the generator, respectively the output impedance receiver are negligible.

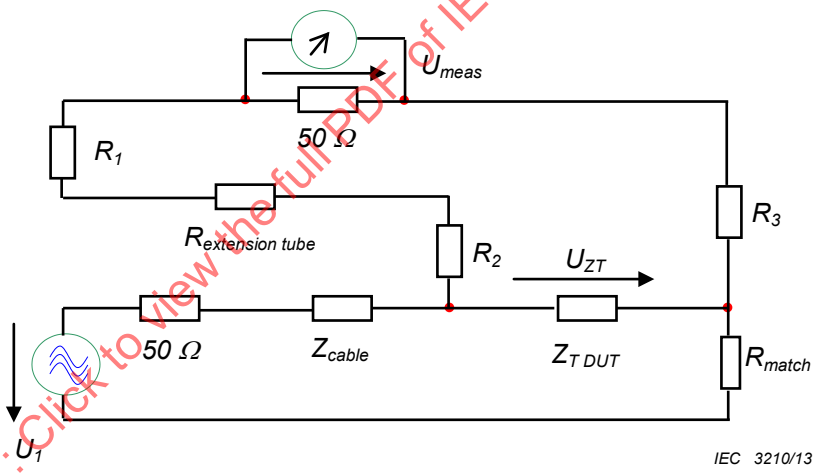

Figure 92 – Equivalent circuit of the test set-up with contact resistances

If contact resistances are in series with the transfer impedance of the DUT, they will influence the result considerably.

Annex A
(normative)

Mixed mode S-parameter

A.1 General

To measure the parameters like unbalance attenuation, coupling attenuation etc. of balanced cables, connectors and components, a differential signal is required. This can, for example, be generated by using a balun which converts the unbalanced signal of a 50 Ω network analyser into a balanced signal.

Alternatively, a balanced signal may be obtained by using a vector network analyser (VNA) having two generators with a phase shift of 180°. Another alternative is to measure with a multi-port VNA (virtual balun).

The properties of balanced pairs are determined mathematically from the measured values of each single conductor of the pair against reference ground. The coverable frequency range for the determination of the reflection and transmission characteristics of symmetrical pairs is no longer limited by the balun but by the VNA and the connection technique.

A.2 Definition of mixed mode S-parameters

The transmission characteristics of four poles or two ports, such as coaxial cables, may be described by the scattering parameter or abbreviated “S-parameter”, see Figure A.1. In matrix notation it is written:

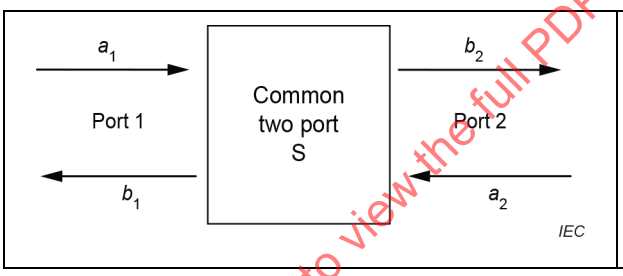

$$\begin{pmatrix} b_1 \\ b_2 \end{pmatrix} = (S) \cdot \begin{pmatrix} a_1 \\ a_2 \end{pmatrix} = \begin{pmatrix} S_{11} & S_{12} \\ S_{21} & S_{22} \end{pmatrix} \cdot \begin{pmatrix} a_1 \\ a_2 \end{pmatrix} \quad \text{(A.1)}$$

where *a* and *b* are the normalized power waves of the input and output ports.

Figure A.1 – Common two-port network

The definition of the scattering matrix can be easily extended to arbitrary N gates, see Figure A.2. For a four-port, this results in:

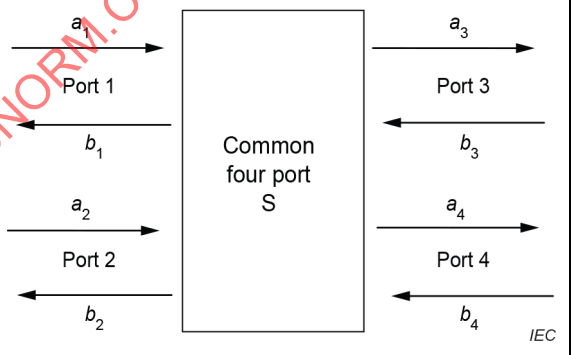

$$\begin{pmatrix} b_1 \\ b_2 \\ b_3 \\ b_4 \end{pmatrix} = \left(S^{\text{std}}\right) \begin{pmatrix} a_1 \\ a_2 \\ a_3 \\ a_4 \end{pmatrix} = \begin{pmatrix} S_{11} & S_{12} & S_{13} & S_{14} \\ S_{21} & S_{22} & S_{23} & S_{24} \\ S_{31} & S_{32} & S_{33} & S_{43} \\ S_{41} & S_{42} & S_{43} & S_{44} \end{pmatrix} \cdot \begin{pmatrix} a_1 \\ a_2 \\ a_3 \\ a_4 \end{pmatrix}$$

(A.2)

Figure A.2 – Common four port network

A.3 Mixed mode S-parameter nomenclature

For the measurement of symmetrical two-ports, the physical ports of the multi-port VNA are combined into logical ports, see Figure A.3:

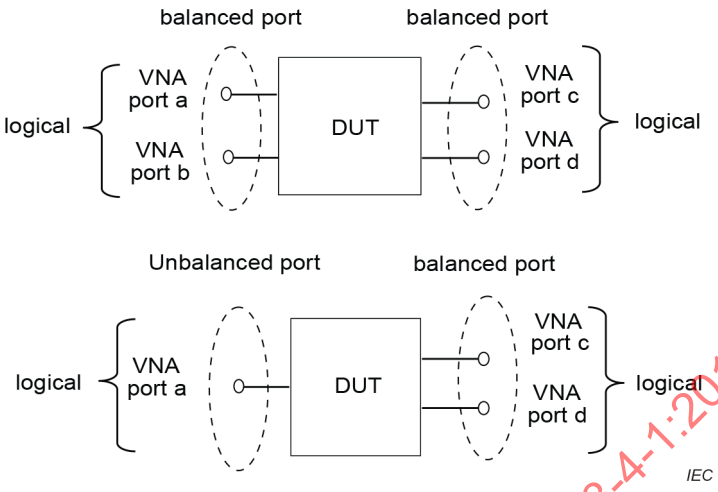

Figure A.3 – Physical and logical ports of a VNA

According to Figure A.4, the following nomenclature is used:

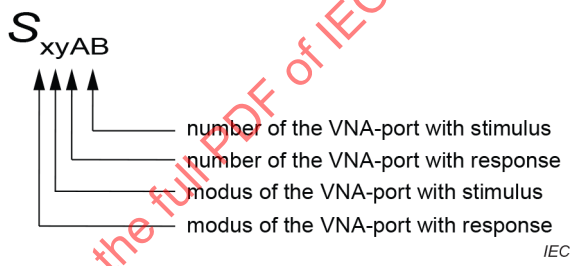

Modus	s: Single ended
	d: Differential mode
	c: Common mode

Figure A.4 – Nomenclature of mixed mode S-parameters

Accordingly, the S-parameters can be understood as ratios of power waves.

$$S_{xyAB} = \frac{input\ signal\ at\ VNA\text{-}port\ A\ at\ modus\ x}{input\ signal\ at\ VNA\text{-}port\ B\ at\ modus\ y} \quad (A.3)$$

The conversion of the asymmetrical four-port scattering parameters S^{std} to mixed mode scattering parameters S^{mm} for a symmetrical two-port network is given by:

$$S^{mm} = M \times S^{std} \times M^{-1} \quad (A.4)$$

where

$$M = \frac{1}{\sqrt{2}} \begin{bmatrix} 1 & -1 & 0 & 0 \\ 0 & 0 & 1 & -1 \\ 1 & 1 & 0 & 0 \\ 0 & 0 & 1 & 1 \end{bmatrix} \tag{A.5}$$

$$S^{mm} = \begin{bmatrix} \begin{bmatrix} S_{dd11} & S_{dd12} \\ S_{dd21} & S_{dd22} \end{bmatrix} & \begin{bmatrix} S_{dc11} & S_{dc12} \\ S_{dc21} & S_{dc22} \end{bmatrix} \\ \begin{bmatrix} S_{cd11} & S_{cd12} \\ S_{cd21} & S_{cd22} \end{bmatrix} & \begin{bmatrix} S_{cc11} & S_{cc12} \\ S_{cc21} & S_{cc22} \end{bmatrix} \end{bmatrix} \tag{A.6}$$

The derivation of the mixed mode parameters (Formulae (A.4) to (A.6)) is described in Annex B.

For the measurement of a two-port with an unbalanced port (single ended) and a balanced port, e.g. to measure coupling attenuation according to IEC 62153-4-5 or to IEC 62153-4-9, the measurement configurations according to Table A.1 arise:

Table A.1 – Measurement configurations unbalanced – balanced

			Stimulus		
			Single ended	Differential mode	Common mode
			Logical port 1	Logical port 2	Logical port 2
Response	Single ended	Logical port 1	S_{ss11}	S_{sd12}	S_{sc12}
	Differential mode	Logical port 2	S_{ds21}	S_{dd22}	S_{dc22}
	Common mode	Logical port 2	S_{cs21}	S_{cd22}	S_{cc22}

The measurement of the coupling attenuation corresponds to a stimulus in the differential mode and to a response in the unbalanced (coaxial) mode (single ended), i.e. a measurement of the S-parameter S_{sd12}. The measurement of the screening attenuation corresponds to a stimulus in the common mode and to a response in the unbalanced (coaxial) mode (single ended), i.e. a measurement of the S-parameter S_{sc12}, see Figure A.5.

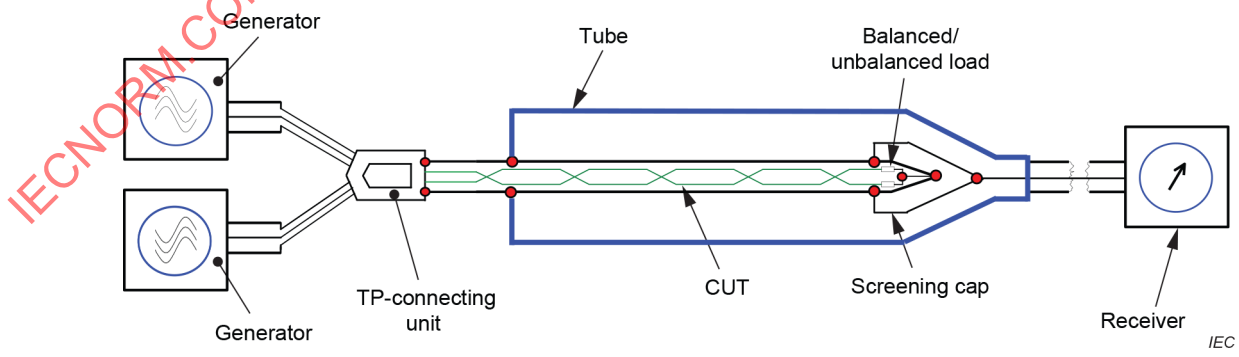

Figure A.5 – Balunless measuring of coupling attenuation, principle set-up with multiport VNA and standard head

For the measurement of a two-port, the test configurations according to Table A.2 are obtained:

Table A.2 – Measurement configurations balanced – balanced

			Stimulus			
			Differential mode		Common mode	
			Logical port 1	Logical port 2	Logical port 1	Logical port 2
Response	Differential mode	Logical port 1	S_{dd11}	S_{dd12}	S_{dc11}	S_{dc12}
		Logical port 2	S_{dd21}	S_{dd22}	S_{dc21}	S_{dc22}
	Common mode	Logical port 1	S_{cd11}	S_{cd12}	S_{cc11}	S_{cc12}
		Logical port 2	S_{cd21}	S_{cd22}	S_{cc21}	S_{cc22}

The measurement of the attenuation of a balanced pair corresponds to a stimulus and a response in differential mode, i.e. a measurement of the S-parameter S_{dd21}. The measurement of the unbalance attenuation with stimulus in differential mode and common mode response corresponds at the near end with the S-parameter S_{cd11} or S_{cd21} when measured at the far end.

A.4 Termination

A differential mode termination according to Figure A.6 and Figure A.7 is required for each pair at the near and far end of the cable.

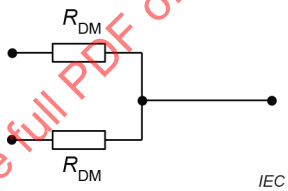

Figure A.6 – Termination network

$$R_{DM} = \frac{Z_{diff}}{2} \quad \text{(A.7)}$$

The termination of the common mode is 25 Ω (R_{CM} = 0).

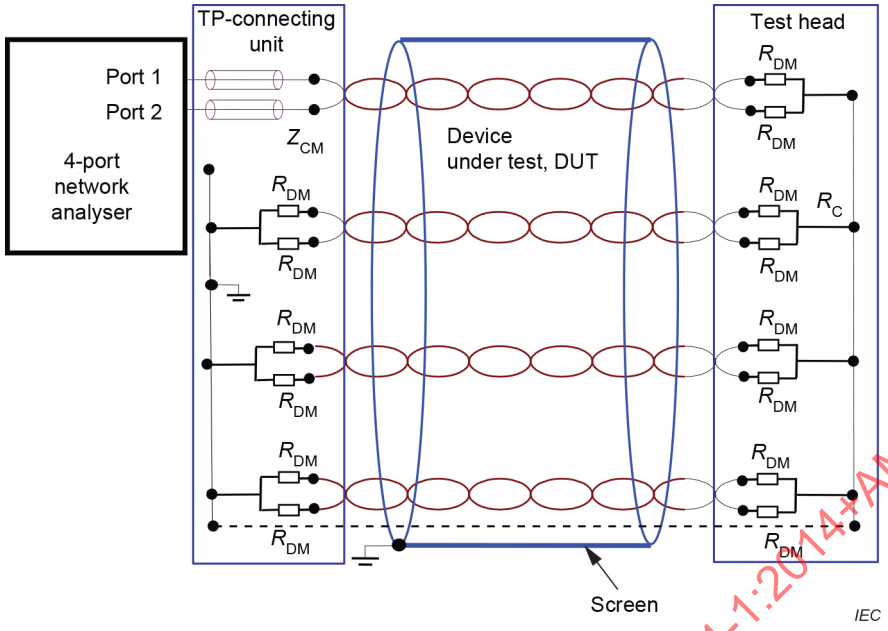

Figure A.7 – Termination of a screened symmetrical cable, principle

NOTE Since mixed mode VNAs use a 50 Ω generator and receiver impedance as default value, the common mode value results in 25 Ω.

A.5 Reference impedance of a VNA

When measuring with a 4 port VNA with mixed mode parameters, a full 4-port calibration, e.g. with electronic calibration units shall be applied. The VNA (Z_0 = 50 Ω physical analyser ports) sets the default values reference impedances for the differential mode Z_{0d} = 100 Ω (= 2 × Z_0) and for the common mode Z_{0c} = 25 Ω (= Z_0/2).

A.6 TP-connecting unit

When measuring balunless respectively with “virtual balun”, a TP connecting unit is required. The TP-connecting unit performance requirements are given in Table A.3.

Table A.3 – TP-connecting unit performance requirements (100 kHz to 2 GHz)

Parameter	Value
Characteristic impedance, primary side (single ended)[a]	50 Ω
Characteristic impedance, secondary side (differential)[a]	1 × 100 Ω (differential)
Return loss, differential mode[b]	> 20 dB
Attenuation, differential mode[c]	< 0,3 dB
Unbalance attenuation (TCTL)[d]	> 60 dB-10*log (*f*), 40 dB max.

[a] Two ports with single ended impedances of 50 Ω generate a common mode impedance of 25 Ω and a differential mode impedance of 100 Ω.

[b] To be measured e.g. with a 4 port mixed mode network analyser. One logical port is generated by the combination of two single ended ports. A second logical port is generated by the combination of two other single ended ports. The absolute dB value of the S-parameter S_{dd11} then represents the return loss of the differential mode.

NOTE With the test set-up according to b), the absolute dB value of the S-parameter S_{cd11} then represents the unbalance attenuation (TCL). The TP connecting unit is used also for the measurement of coupling attenuation.

[c] With the test set-up according to [b)], the absolute dB value of the S-parameter S_{dd21} then represents the attenuation of the differential mode.

[d] With the test set-up according to [b)], the absolute dB value of the S-parameter S_{cd21} then represents the unbalance attenuation (TCTL).

Annex B
(informative)

Example derivation of mixed mode parameters using the modal decomposition technique

It is not a requirement of this document that a full derivation is produced, and any method of extracting the required S-parameters is acceptable. This may be achieved by the use of network analyser hardware functions, specific mathematical software, or by circuit simulation tools.

Annex B presents a summary of how to derive mixed mode parameters from 4-port measurements of S-parameters, where *V* is the voltage and *I* is the current, see Figure B.1:

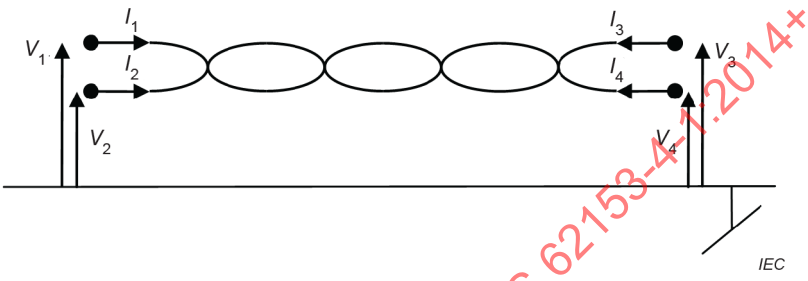

Key

V voltage

I current

Figure B.1 – Voltage and current on balanced cable or cabling under test (CUT)

An impedance matrix (Z) of the cable or cabling under test (CUT) can be calculated based on Equation (B.1).

$$\begin{bmatrix} V_1 \\ V_2 \\ V_3 \\ V_4 \end{bmatrix} = \begin{bmatrix} Z_{11} & Z_{12} & Z_{13} & Z_{14} \\ Z_{21} & Z_{22} & Z_{23} & Z_{24} \\ Z_{31} & Z_{32} & Z_{33} & Z_{34} \\ Z_{41} & Z_{42} & Z_{43} & Z_{44} \end{bmatrix} \begin{bmatrix} I_1 \\ I_2 \\ I_3 \\ I_4 \end{bmatrix} \quad \text{(B.1)}$$

The modal domain impedance matrix [Z^m] is then calculated from Equation (B.2) below, using the conversion matrices given in Equation (B.3) and Equation (B.4).

$$Z^m = P_e^{-1} Z Q_e \quad \text{(B.2)}$$

$$P_e^{-1} = \begin{bmatrix} P^{-1} & 0 \\ 0 & P^{-1} \end{bmatrix} \quad \text{(B.3)}$$

$$Q_e = \begin{bmatrix} Q & 0 \\ 0 & Q \end{bmatrix} \quad \text{(B.4)}$$

In the case of a 1 pair cable or cabling under test (CUT), the size of the conversion matrices becomes 4 × 4 with the values given in Equation (B.5) and Equation (B.6).

$$P = \begin{bmatrix} \frac{1}{2} & 1 \\ -\frac{1}{2} & 1 \end{bmatrix} \tag{B.5}$$

$$Q = \begin{bmatrix} 1 & \frac{1}{2} \\ -1 & \frac{1}{2} \end{bmatrix} \tag{B.6}$$

The conversion matrices replace the Balun transformers and are referred to as mathematical baluns, producing Equation (B.7) and Equation (B.8).

$$\begin{bmatrix} V_1 \\ V_2 \\ V_3 \\ V_4 \end{bmatrix} = P_e \begin{bmatrix} V_{D1} \\ V_{C1} \\ V_{D2} \\ V_{C2} \end{bmatrix} \tag{B.7}$$

$$\begin{bmatrix} I_1 \\ I_2 \\ I_3 \\ I_4 \end{bmatrix} = Q_e \begin{bmatrix} I_{D1} \\ I_{C1} \\ I_{D2} \\ I_{C2} \end{bmatrix} \tag{B.8}$$

Substituting Equation (B.7) and Equation (B.8) into Equation (B.1), we obtain Equation (B.9), which is equivalent to a set of hybrid transformers attached at each end of the cable pair as described in Figure B.2.

$$\begin{bmatrix} V_{D1} \\ V_{C1} \\ V_{D2} \\ V_{C2} \end{bmatrix} = \begin{bmatrix} Z_{11}^{m} & Z_{12}^{m} & Z_{13}^{m} & Z_{14}^{m} \\ Z_{21}^{m} & Z_{22}^{m} & Z_{23}^{m} & Z_{24}^{m} \\ Z_{31}^{m} & Z_{32}^{m} & Z_{33}^{m} & Z_{34}^{m} \\ Z_{41}^{m} & Z_{42}^{m} & Z_{43}^{m} & Z_{44}^{m} \end{bmatrix} \begin{bmatrix} I_{D1} \\ I_{C1} \\ I_{D2} \\ I_{C2} \end{bmatrix} \tag{B.9}$$

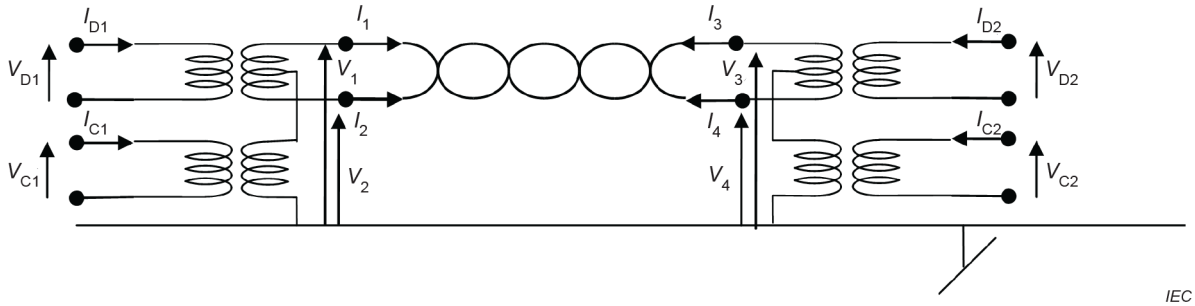

Figure B.2 – Voltage and current on unbalanced DUT

For the measurements concerned in this document, S-parameters are measured and converted into *Z*-parameters. The *Z*-parameter matrix of a 2*n*-port circuits can be derived using Equation (B.10).

$$Z = R^{\frac{1}{2}}[E+S][E-S]^{-1}R^{\frac{1}{2}} \tag{B.10}$$

where E is a $2n \times 2n$ unit matrix and $R^{\frac{1}{2}}$ is given by Equation (B.11).

$$R^{\frac{1}{2}} = \begin{bmatrix} \sqrt{r_1} & 0 & \dots & 0 \\ 0 & \sqrt{r_2} & 0 & M \\ M & 0 & 0 & 0 \\ 0 & \dots & 0 & \sqrt{r_{2n}} \end{bmatrix} \tag{B.11}$$

Where r_x is the impedance of the measurement port, typically 50 Ω, giving Equation (B.12).

$$R^{\frac{1}{2}} = \begin{bmatrix} \sqrt{50} & 0 & \dots & 0 \\ 0 & \sqrt{50} & 0 & M \\ M & 0 & 0 & 0 \\ 0 & \dots & 0 & \sqrt{50} \end{bmatrix} \tag{B.12}$$

The S-parameters in the modal domain are then calculated using Equation (B.13), giving Equation (B.14).

$$S^{\mathrm{m}} = R_{\mathrm{m}}^{-\frac{1}{2}}\left[Z^{\mathrm{m}} - R_{\mathrm{m}}\right]\left[Z^{\mathrm{m}} + R_{\mathrm{m}}\right]^{-1}R_{\mathrm{m}}^{\frac{1}{2}} \tag{B.13}$$

$$R_{\mathrm{m}}^{\frac{1}{2}} = \begin{bmatrix} \sqrt{r_{\mathrm{m1}}} & 0 & \dots & 0 \\ 0 & \sqrt{r_{\mathrm{m2}}} & 0 & M \\ M & 0 & 0 & 0 \\ 0 & \dots & 0 & \sqrt{r_{\mathrm{m2}n}} \end{bmatrix} \tag{B.14}$$

By this method, it is possible to convert unbalance network analyser measurements into mixed mode S-matrices which contain both balanced and unbalanced parameters, as in Equation (B.15).

$$\begin{bmatrix} S_{11} & S_{12} & S_{13} & S_{14} \\ S_{21} & S_{22} & S_{23} & S_{24} \\ S_{31} & S_{32} & S_{33} & S_{34} \\ S_{41} & S_{42} & S_{43} & S_{44} \end{bmatrix} \Rightarrow \begin{bmatrix} S_{DD11} & S_{DC11} & S_{DD12} & S_{DC12} \\ S_{CD11} & S_{CC11} & S_{CD12} & S_{CC12} \\ S_{DD21} & S_{DC21} & S_{DD22} & S_{DC22} \\ S_{CD21} & S_{CC21} & S_{CD22} & S_{CC22} \end{bmatrix} \quad \text{(B.15)}$$

Bibliography

[1] HALME, L., SZENTKUTI, B.: *The Background for electromagnetic screening measurements of cylindrical screens*, *Teletiedotuksia 1987* of the Finnish PTT, Helsinki (Special English Edition), pp. 29-37, or *PTT, Technische Mitteilungen* No 3, 1988, pp. 105 -115, Swiss PTT, Bern

[2] VANCE E.F.: *Coupling to shielded cables*, J. Wiley and Sons, Inc., New York, London 1978, pages 183

[3] SCHELKUNOFF, S.A.: *The electromagnetic theory of coaxial transmission lines and cylindrical shields*, *Bell System Technical Journal*. Vol. 13, pp. 552-579, Oct. 1934

[4] KADEN, H.: *Wirbelströme und Schirmung in der Nachrichtentechnik*, Springer-Verlag, Heidelberg 1959, 354 p. (in German)

[5] IKRATH, K.: *Leakage of electromagnetic* energy *from coaxial cable structures*, US Army and Signalling Engineering Laboratories, Fort Monmouth, New Jersey, Dec. 1957

[6] FOWLER, E.P.: Superscreened cables, *Radio and Electronic Engineer*, Vol. 49, No. 1, pp. 28-44, Jan. 1979, IERE, UK

[7] TYNI, M.: *The transfer impedance of coaxial cables with braided outer conductor*, *3rd Wroclaw Symposium on EMC*, 1976, pp. 410-418

[8] EICHER, B., STAEGER, Ch., SZENTKUTI, B., FAHRNI, H.: *Simple and accurate screening measurements of RF cables up to 3 GHz, PTT, Technische Mitteilungen* No 4, 1988, Swiss PTT, Bern

[9] Super-screened coaxial cables for the nuclear power industry: Part I. General requirements and tests; Part II. Cable data sheets', Atomic Energy Standard Specification AESS(TRG)71181

[10] MADLE, P.J.: *Cable and connector attenuation and transfer impedance measurements using quadraxial and quintaxial test methods*, IEEE 1975 *EMC Symposium Record*, paper 75CH 1002-5 EMC pp. 4B 16.1.5

[11] STAEGER, C., BOLINGER, W.: *Screening effectiveness of coaxial connectors and measuring methods at high frequency and microwave*, *PTT, Technische Mitteilungen* No 9, 1988, pp. 374-379, Swiss PTT, Bern

[12] SMITHERS, B.W.: *The Screening characteristics of coaxial cables and connectors*, ERA Report No 83-0030 (Part 1), 1982, 320 p.

[13] FOWLER, E.P.: *Screening measurements in the time domain and their conversion into the frequency domain*, *Journal IERE*, Vol. 55, No 4, pp. 127-132, Apr. 1985

[14] EICHER, B.: *Cable screening measurements in the frequency range 1-20 GHz: line injection method versus mode stirred chamber*, *Record of the Zürich EMC Symposium* 1991, pp. 159-162

[15] EICHER, B., BOILLOT, L.: *Very low frequency to 40 GHz screening measurement on cables and connectors: Line injection method and mode stirred chamber*, *IEEE EMC Symposium* 1992, pp. 302-307

[16] BREITENBACH, O., HÄHNER, T.: *Kabelschirmung im Übergang von MHz- zu GHz-Frequenzen, Erweiterte Anwendung eines einfachen Messverfarens*, NTZ Bd.46, 1993, Heft 8, pp. 602-608

[17] TC 46/WG 5(Fowler)9, 22 Oct. 1995: Transfer impedance (ZT) test method for multi-pin 1745 (D-type) connectors, (N23)

[18] JUNGFER, H., Die Messung des Kopplungswiderstandes von Kabelschirmungen bei hohen Frequenzen, NTZ, 1956, Heft 12

[19] KLEY, T., Optimierte Kabelschirme Theorie und Messung, Diss. ETH Nr. 9354, 1991

[20] HALME, L., SZENTKUTI, B., *The background for electromagnetic screening measurements of cylindrical screens*, Techn. Mitteilung PTT Nr. 3, 1988

[21] MEINKE, H., *Einführung in die Elektrotechnik höherer Frequenzen*, Springer Verlag 1961

[22] KLEIN, W., *Die* Theorie *des Nebensprechens auf Leitungen*, Springer Verlag 1965

[23] KADEN, H., *Die elektromagnetische Schirmung in der Fernmelde- und HF-Technik.* Springer Verlag 1950

[24] MERZ, C., *Untersuchung des Einflusses verschiedener Störfaktoren bei der Messung der Schirmdämpfung mit Hilfe des Triaxialen Meßverfahren*, Praktikumsbericht WS 95/96,FH Gießen-Friedberg

Additional reading

[25] CRAWFORD, M.L., RIDDLE, B.F.: *A proposed TEM-driven mode-stirred chamber for large system radiated EMC/V testing, 10 kHz – 40 GHz*, Record of the Zürich EMC Symposium 1991, pp. 431-437

[26] FOWLER, E.P.: *Test methods for cable screening effectiveness – A review*, Proc. IERE conf. on EMC, York 1988, IERE Publication No 81, pp. 259-267

[27] FOWLER, E.P., HALME, L.K.: *State of art in cable screening measurements*, Record of the Zürich EMC Symposium 1991, pp. 151-158

[28] FOWLER, E.P.: *Cables and connectors – Their contribution to electromagnetic compatibility*, IEEE EMC Symposium 1992, pp. 329-333.

[29] HÄHNER T., MUND B., *EMV-Verhalten symmetrischer Kabel*, emc journal 4/97

[30] HALME, L.K.: *Development of IEC cable shielding effectiveness standards*, IEEE EMC Symposium 1992, pp. 321-328.

[31] SZENTKUTI, B.T.: *Shielding quality of cables and connectors: Some basics for better understanding of test methods*, Record of IEEE International EMC Symposium, Anaheim, California, August 17-21, 1992, pp. 294-301.

[32] BOKELMANN D., EISENSTADT W., *Combined Differential and Common-Mode Scattering Parameters: Theory and Simulation, IEEE Transactions on Microwave Theory and Techniques, Vol 43, No 7, July 1995 ON MICROWAVE THEORY AND TECHNIQUES, VOL. 43, NO. 7, JULY 1995*

[33] HÄHNER T., MUND B., *Balunless Measurement of Coupling Attenuation of Balanced Cables & Components, Wire and Cable Technology International, July 2013*

[34] HÄHNER T., *Messung der Übertragungseigenschaften symmetrischer Kabel bis in den GHz Frequenzbereich, Technische Akademie Esslingen [TAE], 15. October 2013*

[35] MUND B., PFEILER C., *Balunless measurement of coupling attenuation of screened balanced cables up to 2 GHz, IWCS, 64rd International Cable Connectivity Symposium, October 05-10, 2015, Atlanta, GA, USA*

[36] EN 50289-1-1:2017, *Communication cables – Specifications for test methods – Part 1-1: Electrical test methods – General requirements*

IEC TS 62153-4-1

Edition 1.1 2020-05

FINAL VERSION

colour inside

Metallic communication cable test methods – Part 4-1: Electromagnetic compatibility (EMC) – Introduction to electromagnetic screening measurements

IEC TS 62153-4-1:2014-01+AMD1:2020-05 CSV(en)

CONTENTS

FOREWORD 7
1 Scope 9
2 Normative references 9
3 Symbols interpretation 10
4 Electromagnetic phenomena 12
5 The intrinsic screening parameters of short cables 14
5.1 General 14
5.2 Surface transfer impedance, Z_T 14
5.3 Capacitive coupling admittance, Y_C 15
5.4 Injecting with arbitrary cross-sections 17
5.5 Reciprocity and symmetry 17
5.6 Arbitrary load conditions 17
6 Long cables – coupled transmission lines 17
7 Transfer impedance of a braided wire outer conductor or screen 25
8 Test possibilities 31
8.1 General 31
8.2 Measuring the transfer impedance of coaxial cables 31
8.3 Measuring the transfer impedance of cable assemblies 32
8.4 Measuring the transfer impedance of connectors 32
8.5 Calculated maximum screening level 32
9 Comparison of the frequency response of different triaxial test set-ups to measure the transfer impedance of cable screens 37
9.1 General 37
9.2 Physical basics 37
9.2.1 Triaxial set-up 37
9.2.2 Coupling equations 39
9.3 Simulations 41
9.3.1 General 41
9.3.2 Simulation of the standard and simplified methods according to EN 50289-1-6, IEC 61196-1 (method 1 and 2) and IEC 62153-4-3 (method A) 41
9.3.3 Simulation of the double short circuited methods 47
9.4 Conclusion 55
10 Background of the shielded screening attenuation test method (IEC 62153-4-4) 55
10.1 General 55
10.2 Objectives 56
10.3 Theory of the triaxial measuring method 56
10.4 Screening attenuation 61
10.5 Normalised screening attenuation 63
10.6 Measured results 64
10.7 Comparison with absorbing clamp method 66
10.8 Practical design of the test set-up 67
10.9 Influence of mismatches 68
10.9.1 Mismatch in the outer circuit 68
10.9.2 Mismatch in the inner circuit 70

11 Background of the shielded screening attenuation test method for measuring the screening effectiveness of feed-throughs and electromagnetic gaskets (IEC 62153-4-10) 73
11.1 General 73
11.2 Theoretical background of the test Fixtures and their equivalent circuit 74
11.3 Pictures and measurement results 77
11.3.1 Characteristic impedance uniformity 77
11.3.2 Measurements of shielding effectiveness 79
11.3.3 Calculation of transfer impedance 81
11.4 Calculation of screening attenuation for feed-through when the transfer impedance Z_T is known 83
12 Background of the shielded screening attenuation test method for measuring the screening effectiveness of RF connectors and assemblies (IEC 62153-4-7) 84
12.1 Physical basics 84
12.1.1 Surface transfer impedance Z_T 84
12.1.2 Screening attenuation a_S 85
12.1.3 Coupling attenuation a_C 85
12.1.4 Coupling transfer function 85
12.1.5 Relationship between length and screening measurements 86
12.2 Tube in tube set-up (IEC 62153-4-7) 87
12.2.1 General 87
12.2.2 Procedure 87
12.2.3 Measurements and simulations 89
12.2.4 Influence of contact resistances 90
Annex A (normative) Mixed mode S-parameter 92
A.1 General 92
A.2 Definition of mixed mode S-parameters 92
A.3 Mixed mode S-parameter nomenclature 93
A.4 Termination 95
A.5 Reference impedance of a VNA 96
A.6 TP-connecting unit 96
Annex B (informative) Example derivation of mixed mode parameters using the modal decomposition technique 98
Bibliography 102

Figure 1 – Total electromagnetic field $(\vec{E}_t, \vec{H}_t)$ 13
Figure 2 – Defining and measuring screening parameters – A triaxial set-up 14
Figure 3 – Equivalent circuit for the testing of Z_T 16
Figure 4 – Equivalent circuit for the testing of $Y_c = j\,\omega C_T$ 16
Figure 5 – Electrical quantities in a set-up that is matched at both ends 16
Figure 6 – The summing function $S\{L \cdot f\}$ for near and far end coupling 21
Figure 7 – Transfer impedance of a typical single braid screen 21
Figure 8 – The effect of the summing function on the coupling transfer function of a typical single braid screen cable 22
Figure 9 – Calculated coupling transfer functions T_n and T_f for a single braid – $Z_F = 0$ 22
Figure 10 – Calculated coupling transfer functions T_n and T_f for a single braid – $\mathrm{Im}(Z_T)$ is positive and $Z_F = +0{,}5 \times \mathrm{Im}(Z_T)$ at high frequencies 23

Figure 11 – Calculated coupling transfer functions T_n and T_f for a single braid – Im(Z_T) is negative and Z_F = –0,5 × Im(Z_T) at high frequencies 24
Figure 12 – $L \cdot S$: the complete length dependent factor in the coupling function T 25
Figure 13 – Transfer impedance of typical cables 26
Figure 14 – Magnetic coupling in the braid – Complete flux 27
Figure 15 – Magnetic coupling in the braid – Left-hand lay contribution 27
Figure 16 – Magnetic coupling in the braid – Right-hand lay contribution 27
Figure 17 – Complex plane, Z_T = *Re* Z_T + j *Im* Z_T, frequency *f* as parameter 28
Figure 18 – Magnitude (amplitude), | Z_T (*f*) | 28
Figure 19 – Typical Z_T (time) step response of an overbraided and underbraided single braided outer conductor of a coaxial cable 29
Figure 20 – Z_T equivalent circuits of a braided wire screen 30
Figure 21 – Comparison of signal levels in a generic test setup 33
Figure 22 – Triaxial set-up for the measurement of the transfer impedance Z_T 37
Figure 23 – Equivalent circuit of the triaxial set-up 38
Figure 24 – Simulation of the frequency response for *g* 42
Figure 25 – Simulation of the frequency response for *g* 42
Figure 26 – Simulation of the frequency response for *g* 43
Figure 27 – Simulation of the frequency response for *g* 43
Figure 28 – Simulation of the 3 dB cut off wavelength (L/λ_1) 44
Figure 29 – Interpolation of the simulated 3 dB cut off wavelength (L/λ_1) 44
Figure 30 – 3 dB cut-off frequency length product as a function of the dielectric permittivity of the inner circuit (cable) 45
Figure 31 – Measurement result of the normalised voltage drop of a single braid screen on a solid PE dielectric in the triaxial set-up 46
Figure 32 – Measurement result of the normalised voltage drop of a single braid screen on a foam PE dielectric in the triaxial set-up 47
Figure 33 – Triaxial set-up (measuring tube), double short circuited method 48
Figure 34 – Simulation of the frequency response for *g* of a cable having solid PE dielectric (ε_{r1}=2,3) 49
Figure 35 – Simulation of the frequency response for *g* of a cable having foamed PE dielectric (ε_{r1}=1,6) 49
Figure 36 – Simulation of the frequency response for *g* of a cable having foamed PE dielectric (ε_{r1}=1,3) 50
Figure 37 – Simulation of the frequency response for *g* of a cable having PVC dielectric (ε_{r1}=5) 50
Figure 38 – Interpolation of the simulated 3 dB cut off wavelength (L/λ_1) 51
Figure 39 – 3 dB cut-off frequency length product as a function of the dielectric permittivity of the inner circuit (cable) 52
Figure 40 – Simulation of the frequency response for *g* 53
Figure 41 – Interpolation of the simulated 3 dB cut off wavelength (L/λ_1) 54
Figure 42 – 3 dB cut-off frequency length product as a function of the dielectric permittivity of the inner circuit (cable) 54
Figure 43 – Definition of transfer impedance 56
Figure 44 – Definition of coupling admittance 56
Figure 45 – Triaxial measuring set-up for screening attenuation 57

Figure 46 – Equivalent circuit of the triaxial measuring set-up 57
Figure 47 – Calculated voltage ratio for a typical braided cable screen 59
Figure 48 – Calculated periodic functions for ε_{r1} = 2,3 and ε_{r2} = 1,1 60
Figure 49 – Calculated voltage ratio-typical braided cable screen 60
Figure 50 – Equivalent circuit for an electrical short part of the length Δl and negligible capacitive coupling 62
Figure 51 – a_s of single braid screen, cable type RG 58, L = 2 m 64
Figure 52 – a_s of single braid screen, cable type RG 58, L = 0,5 m 65
Figure 53 – a_s of cable type HF 75 0,7/4,8 2YCY (solid PE dielectric) 65
Figure 54 – a_s of cable type HF 75 1,0/4,8 02YCY (foam PE dielectric) 66
Figure 55 – a_s of double braid screen, cable type RG 223 66
Figure 56 – Schematic for the measurement of the screening attenuation a_s 68
Figure 57 – Short circuit between tube and cable screen of the CUT 68
Figure 58 – Triaxial set-up, impedance mismatches 69
Figure 59 – Calculated voltage ratio including multiple reflections caused by the screening case 70
Figure 60 – Calculated voltage ratio including multiple reflections caused by the screening case 70
Figure 61 – Attenuation and return loss of a self-made 50 Ω to 5 Ω impedance matching adapter 71
Figure 62 – equivalent circuit of a load resistance connected to a source 72
Figure 63 – Cross-sectional sketch of a typical feed-through configuration 73
Figure 64 – Cross-sectional sketch of the test fixture with a feed-through connector (a) and EMI gasket (b) under test 74
Figure 65 – Equivalent circuit of the test fixture 75
Figure 66 –Two-port network 75
Figure 67 – TDR measurement of the text-fixture with inserted “Teflon-through” sample 77
Figure 68 – TDR step response from A (Input)-port of test fixture with inserted “Teflon-through” sample 78
Figure 69 – TDR step response from B (Output)-port of test fixture with inserted “Teflon-through” sample 78
Figure 70 – S-parameter measurement (linear sweep): “Teflon-through” sample 79
Figure 71 – S-parameter measurement (logarithmic sweep): “Teflon-through” sample 79
Figure 72 – S parameter test setup 80
Figure 73 – TDR test setup 80
Figure 74 – Test fixture assembled 80
Figure 75 – Detailed views of the contact area the test fixture and the secondary side of side opened 81
Figure 76 – S_{21} measurements 81
Figure 77 – S_{21} measurements of “Teflon-through” and “Sonnenscheibe” feed-through 82
Figure 78 – Transfer impedance ZT of a “Sonnenscheibe” feed-through based on the S_{21} measurement in Figure 77 82
Figure 79 – measurements of a conducting plastic gasket 83
Figure 80 – Z_T of the conducting plastic gasket based on the S_{21} measurement in Figure 79 83
Figure 81 – equivalent circuit of the set-up without DUT 83

Figure 82 – equivalent circuit of the set-up with inserted DUT 84
Figure 83 – Definition of Z_T 85
Figure 84 – Calculated coupling transfer function 86
Figure 85 – Principle test set-up for measuring the screening attenuation of a connector with the tube in tube procedure 87
Figure 86 – Principle test set-up for measuring the coupling attenuation of screened balanced or multipin connectors 88
Figure 87 – Principle preparation of balanced or multiconductor connectors for coupling attenuation 88
Figure 88 – Comparison of simulation and measurement, linear frequency scale 89
Figure 89 – Comparison of simulation and measurement, logarithmic frequency scale 90
Figure 90 – Measurement of the coupling attenuation of a CAT6 connector 90
Figure 91 – Contact resistances of the test set-up 91
Figure 92 – Equivalent circuit of the test set-up with contact resistances 91
Figure A.1 – Common two-port network 92
Figure A.2 – Common four port network 92
Figure A.3 – Physical and logical ports of a VNA 93
Figure A.4 – Nomenclature of mixed mode S-parameters 93
Figure A.5 – Balunless measuring of coupling attenuation, principle set-up with multiport VNA and standard head 94
Figure A.6 – Termination network 95
Figure A.7 – Termination of a screened symmetrical cable, principle 96
Figure B.1 – Voltage and current on balanced cable or cabling under test (CUT) 98
Figure B.2 – Voltage and current on unbalanced DUT 100

Table 1 – The coupling transfer function *T* (coupling function)[a] 19
Table 2 – Screening effectiveness of cable test methods for surface transfer impedance Z_T 35
Table 3 – Load conditions of the different set-ups 39
Table 4 – Parameters of the different set-ups 41
Table 5 – Cut-off frequency length product 45
Table 6 – Typical values for the factor *v*, for an inner tube diameter of 40 mm and a generator output impedance of 50 Ω 48
Table 7 – Cut-off frequency length product 51
Table 8 – Material combinations and the factor *n* 53
Table 9 – Cut-off frequency length product 54
Table 10 – Cut-off frequency length product for some typical cables in the different set-ups 55
Table 11 – Δa in dB for typical cable dielectrics 64
Table 12 – Comparison of results of some coaxial cables 67
Table 13 – Cable parameters used for simulation 89
Table A.1 – Measurement configurations unbalanced – balanced 94
Table A.2 – Measurement configurations balanced – balanced 95
Table A.3 – TP-connecting unit performance requirements (100 kHz to 2 GHz) 97

INTERNATIONAL ELECTROTECHNICAL COMMISSION

_____

METALLIC COMMUNICATION CABLE TEST METHODS –

Part 4-1: Electromagnetic compatibility (EMC) – Introduction to electromagnetic screening measurements

FOREWORD

1) The International Electrotechnical Commission (IEC) is a worldwide organization for standardization comprising all national electrotechnical committees (IEC National Committees). The object of IEC is to promote international co-operation on all questions concerning standardization in the electrical and electronic fields. To this end and in addition to other activities, IEC publishes International Standards, Technical Specifications, Technical Reports, Publicly Available Specifications (PAS) and Guides (hereafter referred to as "IEC Publication(s)"). Their preparation is entrusted to technical committees; any IEC National Committee interested in the subject dealt with may participate in this preparatory work. International, governmental and non-governmental organizations liaising with the IEC also participate in this preparation. IEC collaborates closely with the International Organization for Standardization (ISO) in accordance with conditions determined by agreement between the two organizations.
2) The formal decisions or agreements of IEC on technical matters express, as nearly as possible, an international consensus of opinion on the relevant subjects since each technical committee has representation from all interested IEC National Committees.
3) IEC Publications have the form of recommendations for international use and are accepted by IEC National Committees in that sense. While all reasonable efforts are made to ensure that the technical content of IEC Publications is accurate, IEC cannot be held responsible for the way in which they are used or for any misinterpretation by any end user.
4) In order to promote international uniformity, IEC National Committees undertake to apply IEC Publications transparently to the maximum extent possible in their national and regional publications. Any divergence between any IEC Publication and the corresponding national or regional publication shall be clearly indicated in the latter.
5) IEC itself does not provide any attestation of conformity. Independent certification bodies provide conformity assessment services and, in some areas, access to IEC marks of conformity. IEC is not responsible for any services carried out by independent certification bodies.
6) All users should ensure that they have the latest edition of this publication.
7) No liability shall attach to IEC or its directors, employees, servants or agents including individual experts and members of its technical committees and IEC National Committees for any personal injury, property damage or other damage of any nature whatsoever, whether direct or indirect, or for costs (including legal fees) and expenses arising out of the publication, use of, or reliance upon, this IEC Publication or any other IEC Publications.
8) Attention is drawn to the Normative references cited in this publication. Use of the referenced publications is indispensable for the correct application of this publication.
9) Attention is drawn to the possibility that some of the elements of this IEC Publication may be the subject of patent rights. IEC shall not be held responsible for identifying any or all such patent rights.

This consolidated version of the official IEC Standard and its amendment(s) has been prepared for user convenience.

IEC TS 62153-4-1 edition 1.1 contains the first edition (2014-01) [documents 46/465/DTS and 46/492/RVC] and its amendment 1 (2020-05) [documents 46/726/DTS and 46/748/RVDTS].

This Final version does not show where the technical content is modified by amendment 1. A separate Redline version with all changes highlighted is available in this publication.

The main task of IEC technical committees is to prepare International Standards. In exceptional circumstances, a technical committee may propose the publication of a technical specification when

- the required support cannot be obtained for the publication of an International Standard, despite repeated efforts, or
- the subject is still under technical development or where, for any other reason, there is the future but no immediate possibility of an agreement on an International Standard.

Technical specifications are subject to review within three years of publication to decide whether they can be transformed into International Standards.

IEC TS 62153-4-1, which is a technical specification, has been prepared by IEC technical committee 46: Cables, wires, waveguides, R.F. connectors, R.F. and microwave passive components and accessories.

This first edition of technical specification IEC TS 62153-4-1 constitutes a technical revision. This edition includes the following significant technical changes with respect to IEC TR 62153-4-1:

a) comparison of the frequency response of different triaxial test set-ups to measure the transfer impedance of cable screens;
b) background of the shielded screening attenuation test method (IEC 62153-4-4);
c) background of the shielded screening attenuation test method for measuring the screening effectiveness of feed-throughs and electromagnetic gaskets (IEC 62153-4-10);
d) background of the shielded screening attenuation test method for measuring the screening effectiveness of RF connectors and assemblies (IEC 62153-4-7).

This publication has been drafted in accordance with the ISO/IEC Directives, Part 2.

A list of all parts of the IEC 62153 series, under the general title: *Metallic communication cable test methods*, can be found on the IEC website.

The committee has decided that the contents of the base publication and its amendment will remain unchanged until the stability date indicated on the IEC web site under "http://webstore.iec.ch" in the data related to the specific publication. At this date, the publication will be

- reconfirmed,
- withdrawn,
- replaced by a revised edition, or
- amended.

IMPORTANT – The 'colour inside' logo on the cover page of this publication indicates that it contains colours which are considered to be useful for the correct understanding of its contents. Users should therefore print this document using a colour printer.

METALLIC COMMUNICATION CABLE TEST METHODS –

Part 4-1: Electromagnetic compatibility (EMC) – Introduction to electromagnetic (EMC) screening measurements

1 Scope

This part of IEC 62153 deals with screening measurements. Screening (or shielding) is one basic way of achieving electromagnetic compatibility (EMC). However, a confusingly large number of methods and concepts is available to test for the screening quality of cables and related components, and for defining their quality. This technical specification gives a brief introduction to basic concepts and terms trying to reveal the common features of apparently different test methods. It is intended to assist in correct interpretation of test data, and in the better understanding of screening (or shielding) and related specifications and standards.

2 Normative references

The following documents, in whole or in part, are normatively referenced in this document and are indispensable for its application. For dated references, only the edition cited applies. For undated references, the latest edition of the referenced document (including any amendments) applies.

IEC 60096-1:1986, *Radio-frequency cables – Part 1: General requirements and measuring methods*[1]

IEC 60096-4-1, *Radio-frequency cables – Part 4: Specification for superscreened cables – Section 1: General requirements and test methods*[1]

IEC 60169-1-3, *Radio-frequency connectors - Part 1: General requirements and measuring methods - Section Three: Electrical tests and measuring procedures: Screening effectiveness*

IEC 61196-1:2005, *Coaxial communication cables - Part 1: Generic specification - General, definitions and requirements*

IEC 61726, *Cable assemblies, cables, connectors and passive microwave components - Screening attenuation measurement by the reverberation chamber method*

IEC 62153-4-2, *Metallic communication cable test methods - Part 4-2: Electromagnetic compatibility (EMC) - Screening and coupling attenuation - Injection clamp method*

IEC 62153-4-3, *Metallic communication cable test methods - Part 4-3: Electromagnetic compatibility (EMC) - Surface transfer impedance - Triaxial method*

IEC 62153-4-4, *Metallic communication cable test methods - Part 4-4: Electromagnetic compatibility (EMC) - Shielded screening attenuation, test method for measuring of the screening attenuation as up to and above 3 GHz*

IEC 62153-4-5, *Metallic communication cables test methods - Part 4-5: Electromagnetic compatibility (EMC) - Coupling or screening attenuation - Absorbing clamp method*

---

[1] This publication has been withdrawn.

IEC 62153-4-6, *Metallic communication cable test methods - Part 4-6: Electromagnetic compatibility (EMC) - Surface transfer impedance - Line injection method*

IEC 62153-4-7, *Metallic communication cable test methods - Part 4-7: Electromagnetic compatibility (EMC) - Test method for measuring the transfer impedance and the screening - or the coupling attenuation - Tube in tube method*

IEC 62153-4-9, *Metallic communication cable test methods – Part 4-9: Electromagnetic compatibility (EMC) – Coupling attenuation of screened balanced cables, triaxial method*

IEC 62153-4-10, *Metallic communication cable test methods - Part 4-10: Electromagnetic compatibility (EMC) - Shielded screening attenuation test method for measuring the screening effectiveness of feed-throughs and electromagnetic gaskets double coaxial method*

IEC/TR 62152:2009, *Transmission properties of cascaded two-ports or quadripols – Background of terms and definitions*

EN 50289-1-6: 2002, *Communication cables – Specifications for test methods Part 1-6: Electrical test methods – Electromagnetic performance*

CISPR 25, *Vehicles, boats and internal combustion engines – Radio disturbance characteristics – Limits and methods of measurement for the protection of on-board receivers*

3 Symbols interpretation

This clause gives the interpretation of the symbols used throughout this specification.

α_1, α_2 attenuation constants of primary and secondary circuit

a_s screening attenuation

a_{sn} normalized screening attenuation with phase velocity difference not greater than 10 % and 150 Ω characteristic impedance of the injection line (Z_s=150 Ω and $|\Delta v/v_1|$=10 % or $\varepsilon_{r1}/\varepsilon_{r2n}$=1,21)

c_o velocity of light in free space $c_o = 3 \times 10^8$ m/s

C_T through capacitance of the braided cable

CUT cable or component under test

E e.m.f.

f frequency

f far end

f_c cut-off frequency

f_{cf} far end cut-off frequency

f_{cn} near end cut-off frequency

Φ_1 the total flux of the magnetic field induced by the disturbing current I_1

Φ'_{12} the direct leaking magnetic flux

Φ''_{12} complete magnetic flux in the braid

I_1, U_1 current and voltage in the primary circuit (feeding system)

I_F current coupled by the feed through capacitance to the secondary system (measuring system)

ε_{r1} relative permittivity of the injection line (feeding system)

ε_{r2} relative permittivity of the cable (measuring system)

L cable length, coupling length

L_1 (external) inductance of the outer circuit

L_2 (external) inductance of the inner circuit

M'_{12} mutual inductance related to direct leakage of the magnetic flux Φ'_{12}

M''_{12} mutual inductance related to the magnetic flux Φ''_{12} (or ½ Φ''_{12}) in the braid

$$M'_{12} = \frac{\Phi'_{12}}{j\omega I_1} \text{ and } M''_{12} = \frac{1}{2} \cdot \frac{\Phi''_{12}}{j\omega I_1}$$

M_T effective mutual inductance per unit length for braided screens

$M_T = M'_{12} - M''_{12}$

where M'_{12} relates to the direct leakage of the magnetic flux and M''_{12} relates to the magnetic flux in the braid [24]

n near end

P_1 sending power

P_{2f} far end measured power

P_{2n} near end measured power

P_r radiated power in the environment of the cable, which is comparable to $P_{2n}+P_{2f}$ of the absorbing clamp method of 12.4 of IEC 61196-1:1995

P_s radiated power in the normalised environment of the cable under test (Z_s=150 Ω and $|\Delta v/v_1|$=10 % or $\varepsilon_{r1}/\varepsilon_{r2n}$=1,21)

R load resistance of secondary circuit (input resistance of receiver)

R_T screen resistance per unit length

T coupling transfer function

T_f far end transfer function

T_n near end transfer function

U'_2 the disturbing voltage induced by Φ'_{12}

U''_{rh} the disturbing voltage induced by ½ Φ''_{12} of the right hand lay contribution

U''_{lh} the disturbing voltage induced by ½ Φ''_{12} of the left hand lay contribution

U''_2 is equal to U''_{rh} and U''_{lh} (= the disturbing voltage induced by ½ Φ''_{12})

v phase velocity

v_1 phase velocity of the "primary" system (feeding system)

v_2 phase velocity of the "secondary" system (measuring system)

v_{r1} relative phase velocity of the "primary" system (feeding system)

v_{r2} relative phase velocity of the "secondary" system (measuring system)

Z_1 characteristic impedance of the "primary" system (feeding system or line (1))

Z_2 characteristic impedance of the cable under test (CUT) (measuring system or line (2))

Z_{1f} terminating impedance of the line (1) in the far end

Z_{2n} terminating impedance of the line (2) in the near end

Z_{2f} terminating impedance of the line (2) in the far end (in a matched set-up $Z_{1f} = Z_1$ and $Z_{2n} = Z_{2f} = Z_2$)

$$Z_{12} = \sqrt{Z_1 Z_2}$$

Z_a surface impedance of the braided cable

Z_F capacitive coupling impedance per unit length

Z_f capacitive coupling impedance

Z_T surface transfer impedance per unit length

Z_{Th} transfer impedance of a tubular homogeneous screen per unit length

Z_t surface transfer impedance

Z_{TEn} effective transfer impedance (= $| Z_F + Z_T |$) per unit length in the near end

Z_{TEf} effective transfer impedance (= $| Z_F - Z_T |$) per unit length in the far end

$Z_{TEn,f}$ effective transfer impedance (= $| Z_F \pm Z_T |$) per unit length in the near end or in the far end

Z_{TE} effective transfer impedance (= max $| Z_{TEn}, Z_{TEf} |$) per unit length

Z_{te} effective transfer impedance (= max $| Z_f \pm Z_t |$)

Z_{ten} normalized effective transfer impedance of a cable (Z_1 = 150 Ω and $| v_1 - v_2 | / v_2 \leq 10$ % velocity difference in relation to velocity of CUT

4 Electromagnetic phenomena

It is assumed that if an electromagnetic field is incident on a screened cable, there is only weak coupling between the external field and that inside, and that the cable diameter is very small compared with both the cable length and the wavelength of the incident field. The superposition of the external incident field and the field scattered by the cable yields the total electromagnetic field $(\vec{E}_t, \vec{H}_t)$ in Figure 1. The total field at the screen's surface may be considered as the source of the coupling: electric field penetrates through apertures by electric or capacitive coupling; also magnetic fields penetrate through apertures by inductive or magnetic coupling. In addition, the induced current in the screen results in conductive or resistive coupling.

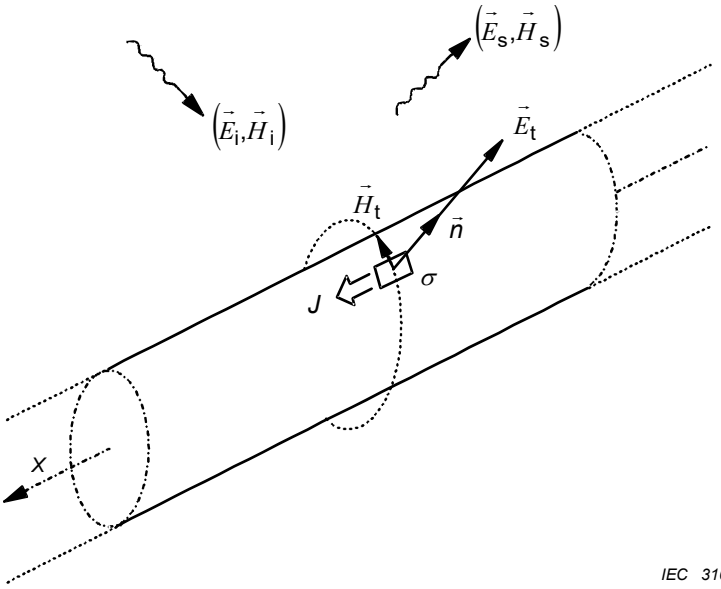

Key

$(\vec{E}_i,\vec{H}_i)$	incident electromagnetic field
$(\vec{E}_s,\vec{H}_s)$	scattered electromagnetic field
$(\vec{E}_t,\vec{H}_t)$	total electromagnetic field
x	positive axial cable direction
σ	induced surface charge density- (C/m^2)
$\vec{n}$	unit vector normal to the surface
ε_o, ε_r	permittivity, free space and relative

Figure 1 – Total electromagnetic field $(\vec{E}_t,\vec{H}_t)$

$$(\vec{E}_t,\vec{H}_t)=(\vec{E}_i,\vec{H}_i)+(\vec{E}_s,\vec{H}_s) \quad (1)$$

$$J=\vec{n}\cdot\vec{H}_t \quad (2)$$

$$\sigma=\vec{n}\cdot\vec{E}_t\varepsilon_o\varepsilon_r \quad (3)$$

where the symbols are described in the key of Figure 1.

As the field at the surface of the screen is directly related to density of surface current and surface charge, the coupling may be assigned either to the total field $(\vec{E}_t,\vec{H}_t)$ or to the surface current- and charge- densities (J and σ). Consequently, the coupling into the cable may be simulated by reproducing, through any suitable means, the surface currents and charges on the screen. Because the cable diameter is assumed to be small, the higher modes may be neglected and it is possible to use an additional coaxial conductor as the injection structure, as shown in Figure 2.

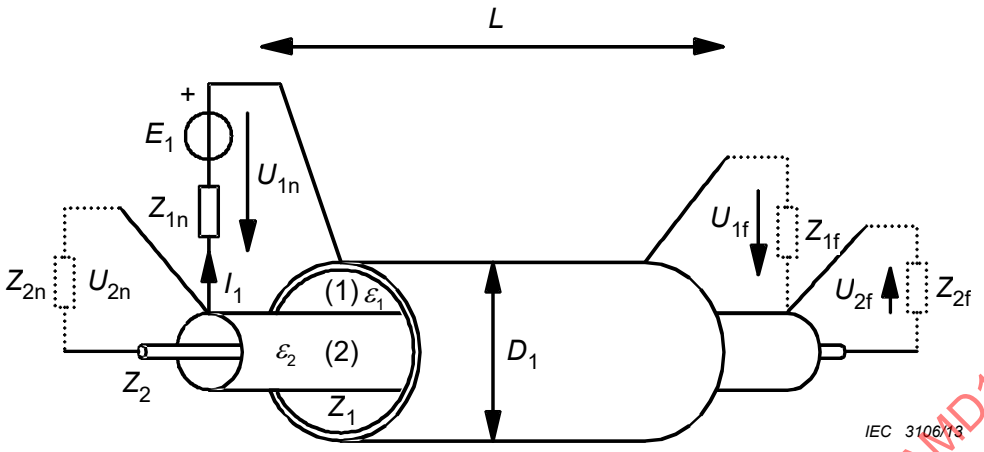

Key (for Figures 2,3,4,5)

(1), (2)	outer circuit (1), tube, respectively inner circuit (2), cable
$Z_{1,2}$	characteristic impedance of the outer circuit (1), tube, respectively inner circuit (2), cable
$\varepsilon_{1,2}$	dielectric permittivity of the outer circuit (1), tube, respectively inner circuit (2), cable
$\beta_{1,2}$	phase constant of the outer circuit (1), tube, respectively inner circuit (2), cable
$\lambda_{1,2}$	wave length of the outer circuit (1), tube, respectively inner circuit (2), cable
L	coupling length
D_1	diameter of injection cylinder-tube
V	voltmeter
A	ammeter
Z_{1n}, Z_{1f}	load resistance at the near end, respectively far end of the outer circuit (1), tube
Z_{2n}, Z_{2f}	load resistance at the near end, respectively far end of the inner circuit (2), cable
E_1	EMF of the generator
I_1, I_2	current in the outer circuit (1), tube, respectively inner circuit (2), cable
U_{1n}, U_{1f}	voltage at the near end, respectively far end of the outer circuit (1), tube
U_{2n}, U_{2f}	voltage at the near end, respectively far end of the inner circuit (2), cable

Figure 2 – Defining and measuring screening parameters – A triaxial set-up

Figure 2 shows the concept of a triaxial set-up. The outer circuit (1) is formed by an injection cylinder-tube and the screen under test, with an characteristic impedance Z_1. The inner circuit (2) is formed by the screen under test, and centre conductor, with an characteristic impedance Z_2. The screening at the ends of circuit (2) is not shown. Observe the conditions Z_{1f}, Z_{2n}, Z_{2f} and λ in Figure 3 and Figure 4. Also note that diameter of the injection cylinder tube (D1) shall be much smaller than the coupling length (L).

5 The intrinsic screening parameters of short cables

5.1 General

The intrinsic parameters refer to an infinitesimal length of cable, like the inductance or capacitance per unit length of transmission lines. Assuming electrically short cables, with $L << \lambda$ which will always apply at low frequencies, the intrinsic screening parameters are defined and can be measured as indicated in the subclauses 5.2 and 5.3.

5.2 Surface transfer impedance, Z_T

As shown in Figure 3, where Z_{1f} and Z_{2f} are zero, the surface transfer impedance (Z_T in Ω/m) is given:

$$Z_T = \frac{U_{2n}}{I_1 \cdot L} \tag{4}$$

where

Z_T is the transfer impedance,

U_{2n} is the voltage at the near end of the inner circuit (2),

L is the coupling length

I_1 is the current in the outer circuit (1).

The dependence of Z_T on frequency is not simple and is often shown by plotting log Z_T against log frequency. Note that the phase of Z_T may have any value, depending on braid construction and frequency range.

NOTE In circuit (2) of Figure 3, the voltmeter and short circuit may also be interchanged.

5.3 Capacitive coupling admittance, Y_C

As shown in Figure 4, where Z_{1f} and Z_{2f} are open circuit, the capacitive coupling admittance (Y_C in S/m) is given by:

$$Y_C = \mathrm{j} \cdot \omega C_T = \frac{I_2}{U_{1n} \cdot L} \tag{5}$$

where

Y_C is the coupling admittance

C_T is the through capacitance;

ω is the radian frequency;

j is the imaginary operator

L is the coupling length

I_2 is the current in the inner circuit (2).

The through capacitance C_T is a real capacitance and has usually a constant value up to 1 GHz and higher (with aperture $a << \lambda$).

While Z_T is independent of the characteristics of the coaxial circuits (1) and (2), C_T is dependent on those characteristics. There are two ways of overcoming this dependence:

a) The normalized through elastance K_T (with units of m/F) derived from C_T is independent of the size of the outer coaxial circuit (2), but it depends on its permittivity:

$$K_T = C_T / (C_1 \cdot C_2) \tag{6}$$

$$K_T \sim 1/(\varepsilon_{r1} + \varepsilon_{r2}) \tag{7}$$

where C_1 and C_2 are the capacitance per unit length of the two coaxial circuits.

b) The capacitive coupling impedance Z_F (with units of Ω/m) again derived from C_T is also independent of the size of the outer coaxial circuit (2) and, for practical values of ε_{r1}, is only slightly dependent on its permittivity:

$$Z_F = Z_1 Z_2 Y_C = Z_1 Z_2 \mathrm{j}\omega C_T \tag{8}$$

$$Z_F \sim \sqrt{(\varepsilon_{r1} \cdot \varepsilon_{r2})}/(\varepsilon_{r1} + \varepsilon_{r2}) \tag{9}$$

Compared with Z_T, Z_F is usually negligible, except for open weave braids. It may, however, be significant when Z_{2n} and $Z_{2f} >> Z_2$ (audio circuits).

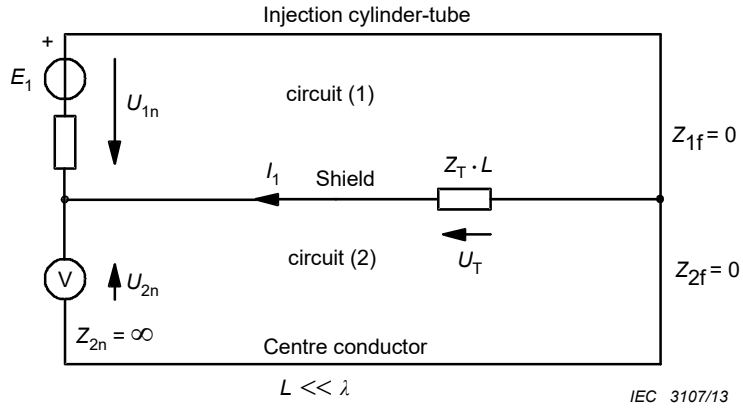

Key

See Figure 2.

Figure 3 – Equivalent circuit for the testing of Z_T

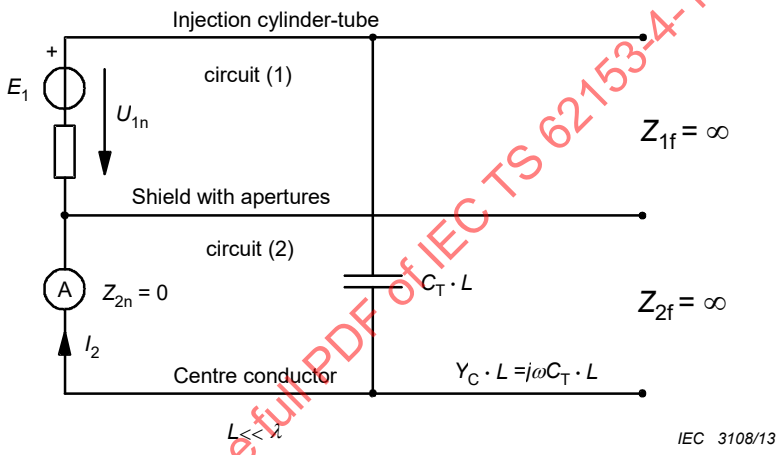

Key

See Figure 2.

Figure 4 – Equivalent circuit for the testing of $Y_c = j\ \omega C_T$

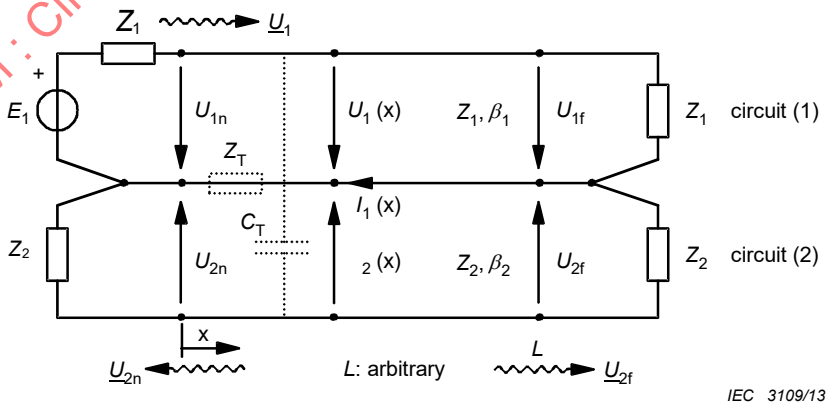

Key

See Figure 2.

NOTE Z_T and C_T are distributed (not correctly shown here). The loads Z_1, Z_2 at the ends may represent matched receivers.

Figure 5 – Electrical quantities in a set-up that is matched at both ends

5.4 Injecting with arbitrary cross-sections

A coaxial outer circuit (2) has been assumed so far in this report, but it is not essential because of the invariance of Z_T and Z_F. Using a wire in place of the outer cylinder, the injection circuit (2) becomes two-wire with the return via the screen of the cable under test. Obviously the charge and current distribution become non-uniform, but the results are equivalent to coaxial injection, especially if two injection lines are used opposite to each other, and may be justified for worst-case testing. Note that the IEC line injection test uses a wire.

5.5 Reciprocity and symmetry

Assuming linear shield materials, the measured Z_T and Z_F values will not change when interchanging the injection circuit (1) and the measuring circuit (2). Each of the two conductors of the two-line circuit can be interchanged, but in practice the set-up will have to take into account possible ground loops and coupling to the environment.

5.6 Arbitrary load conditions

When the circuit ends of Figure 3 and Figure 4 are not ideally a short or open circuit, Z_T and Z_F will act simultaneously. Their superposition is noticeable in the low frequency coupling of the matched circuit (1) and circuit (2) (see Figure 5 and Table 1).

6 Long cables – coupled transmission lines

The coupling over the whole length of the cable is obtained by summing up (integrating) the infinitesimal coupling contributions along the cable while observing the correct phase. The analysis utilizes the following assumptions and conventions:

– matched circuits considered with the voltage waves $\underline{U}_1$, $\underline{U}_{2n}$, $\underline{U}_{2f}$, see Figure 5,

– representation of the coupling, using the normalized wave amplitudes $U/\sqrt{Z}\left[\sqrt{Watt}\right]$, instead of voltage waves. i.e. the coupling transfer function, in the following denoted by "coupling function", will be defined as

$$T_n = \frac{\underline{U}_{2n}/\sqrt{Z_2}}{\underline{U}_1/\sqrt{Z_1}} \qquad (10)$$

$$T_f = \frac{\underline{U}_{2f}/\sqrt{Z_2}}{\underline{U}_1/\sqrt{Z_1}} \qquad (11)$$

The square of the coupling transfer function, $|T|^2$, is the ratio of the power waves travelling in circuits (2) and (1). Due to reciprocity and assuming linear screen (shield) materials, T is reciprocal, i.e. invariant with respect to the interchange of injection and measuring circuits (1) and (2). The quantity $|1/T|^2$ or in logarithmic quantities

$$a_s = -20 \times \log_{10}|T| \qquad (12)$$

may be considered as the "screening attenuation" of the cable, specific to the set-up.

Performing the straight forward calculations of coupled transmission line theory, the coupling function T, given in Table 1, is obtained. The term $S\{L \cdot f\}$ is the "summing function" S, being dependent on L and f. (The wavy bracket just indicates that the product $L \cdot f$ is the argument of the function S and not a factor to S). S represents the phase effect, when summing up the infinitesimal couplings along the line, and is:

$$S_{\underset{f}{n}}\{L\cdot f\} = \frac{\sin\frac{\beta L\pm}{2}}{\frac{\beta L\pm}{2}}\exp\left(-j\cdot\frac{\beta L+}{2}\right) \tag{13}$$

$$\beta L+ = (\beta_2 + \beta_1)\cdot L \tag{14}$$

$$\beta L\pm = (\beta_2 \pm \beta_1)\cdot L \tag{15}$$

$$\beta L\pm = 2\pi L f\cdot(1/v_2 \pm 1/v_1) \tag{16}$$

$$\beta L\pm = 2\pi L f\cdot\left(\sqrt{\varepsilon_{r2}} \pm \sqrt{\varepsilon_{r1}}\right)/c \tag{17}$$

subscript ± refers to near/far end respectively; i.e. + indicates the near end and – indicates the far end;

\+ refers to both near/far ends.

Note that weak coupling, i.e. $T << 1$, has been assumed. This case, including losses, is given in [1][2].

Equation (18) and the representation in Table 1 illustrate the contributions of the different parameters to the coupling function T:

$$T_{\underset{f}{n}} = (Z_F \pm Z_T)\cdot\frac{1}{\sqrt{Z_1\cdot Z_2}}\cdot\frac{L}{2}\cdot S_{\underset{f}{n}}\{L\cdot f, \varepsilon_{r1}, \varepsilon_{r2}\} \tag{18}$$

2 Figures in square brackets refer to the bibliography.

Table 1 – The coupling transfer function *T* (coupling function)[a]

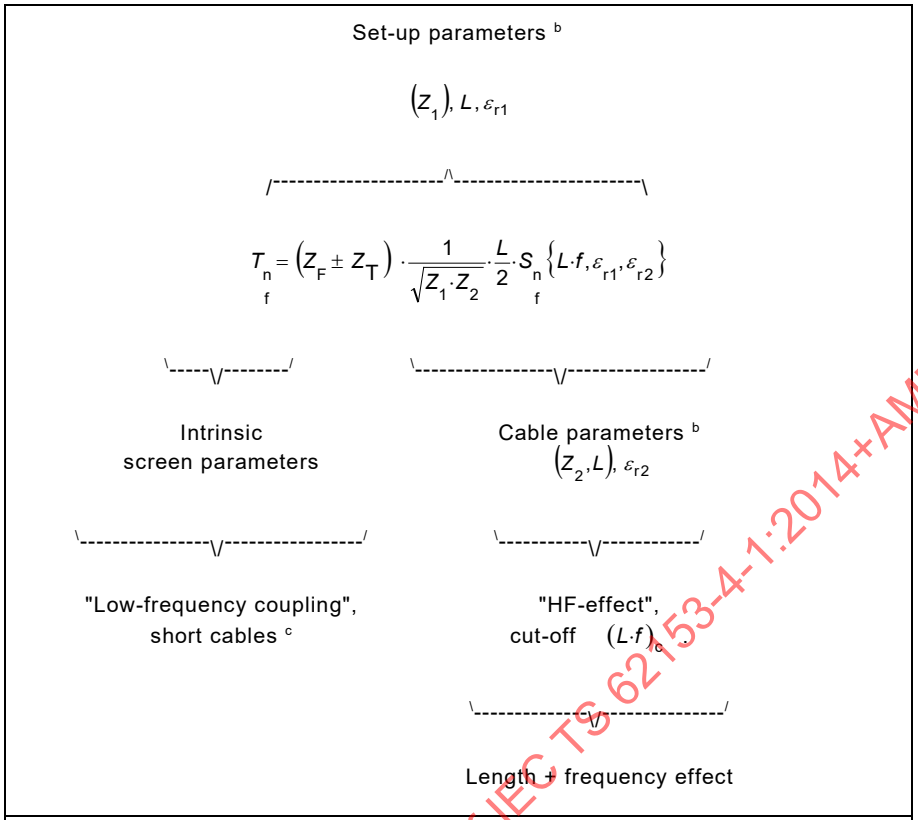

a T^2 is the power coupling from circuit (1) to circuit (2).
The stacked subscripts $\substack{n\\f}$ are associated to the stacked operation symbols ± in the obvious way: upper subscript → upper operation, lower subscript → lower operation.

b ε_{r1} and ε_{r2} contained in S as parameters.

c for $L << \lambda$: $S\{L \cdot f\} \rightarrow 1$.

Note especially the following points.

a) There may be a directional effect ($T_n \neq T_f$) in the whole frequency range if Z_F is not negligible. (But Z_F is usually negligible except with loose, single braid shields.)

b) Up to a constant factor, T is the quantity directly measured in a set-up.

c) For low frequencies, i.e. for short cables ($L << \lambda$), the trivial coupling formula is obtained that is directly proportional to L:

$$T_{\substack{n\\f}} = (Z_F \pm Z_T) \cdot \frac{1}{Z_{12}} \cdot \frac{L}{2} \tag{19}$$

where

$$Z_{12} = \sqrt{Z_1 \cdot Z_2}$$

d) The summing function $S\{L \cdot f\}$ is presented in Figure 6.

e) $S\{L \cdot f\}$ has a sin(*x*)/*x* behaviour. A cut-off point may be defined as $(L \cdot f)_c$:

$$(L \cdot f)_{c_{\substack{n\\f}}} = \frac{c}{\pi \left| \sqrt{\varepsilon_{r1}} \pm \sqrt{\varepsilon_{r2}} \right|} \tag{20}$$

f) The exact envelope of $S\{L \cdot f\}$ is

$$\operatorname{Env}\left|\underset{f}{S_n}\{L\cdot f\}\right| = \frac{1}{\sqrt{1+\dfrac{(L\cdot f)^2}{(L\cdot f)^2_{cn}}}} \qquad (21)$$

g) The first minimum (zero) of $S\{L\cdot f\}$ occurs at

$$(L\cdot f)_{min} = \pi(L\cdot f)_c \qquad (22)$$

h) As seen from Equations (13) and (21), below the cut-off points $\underset{f}{(L\cdot f)_{cn}}$ is $S\{L\cdot f\} \approx 1$ and above them it starts to oscillate and its envelope drops asymptotically 20 dB/decade,

$$\operatorname{Env}\left|\underset{f}{S_n}\{L\cdot f\}\right| \approx \frac{\left(\underset{f}{(L\cdot f)_{cn}}\right)}{(L\cdot f)} \qquad (23)$$

i) S is symmetrical in L and f, i.e. L and f are interchangeable. For a fixed length a cut-off frequency f_c and vice versa, for a fixed frequency a cut-off length L_c may be defined. Substituting c/λ_o for f, we obtain the cut-off length as

$$\underset{f}{L_{c_n}} = \frac{\lambda_o}{\pi\left|\sqrt{\varepsilon_{r1}} \pm \sqrt{\varepsilon_{r2}}\right|} \qquad (24)$$

j) The effect of S in the frequency range (L = constant) is illustrated in Figure 8. The coupling function is proportional to Z_T, only if $f < f_c$. Note also the typical values indicated for f_c.

k) The minima and maxima of S are not resonances, they are due to cancelling and additive effects of the coupling along the line.

l) The far end cut-off frequency is significantly influenced by the permittivity of the outer system (ε_{r1}). Selecting $\varepsilon_{r1} \to \varepsilon_{r2}$ we obtain $(L\cdot f)_{cf} \to \infty$, i.e. no cut-off at the far end. Due to practical aspects (tolerances, homogeneity, etc.), an ideal phase matching $(\varepsilon_{r1} \equiv \varepsilon_{r2})$ is not feasible.

m) The effects of Z_T and Z_F on the coupling transfer functions T_n and T_f are shown in Figure 8.

n) The total effect of L on the coupling is not contained in S alone, but in the product $L\cdot S\{L\cdot f\}$. The product $L\cdot S$ is presented in Figure 12 for f = constant. The coupling function T which can be measured in a set-up is proportional to L if $L < L_c$. However, for appropriately long cables ($L > L_c$), the maximum coupling is independent of L and we obtain a length independent shielding attenuation above the cut-off point $(L\cdot f)_c$. But we should remember that $(L\cdot f)_c$ as well as A_s are still dependent on the set-up parameters (ε_{r1}, Z_1).

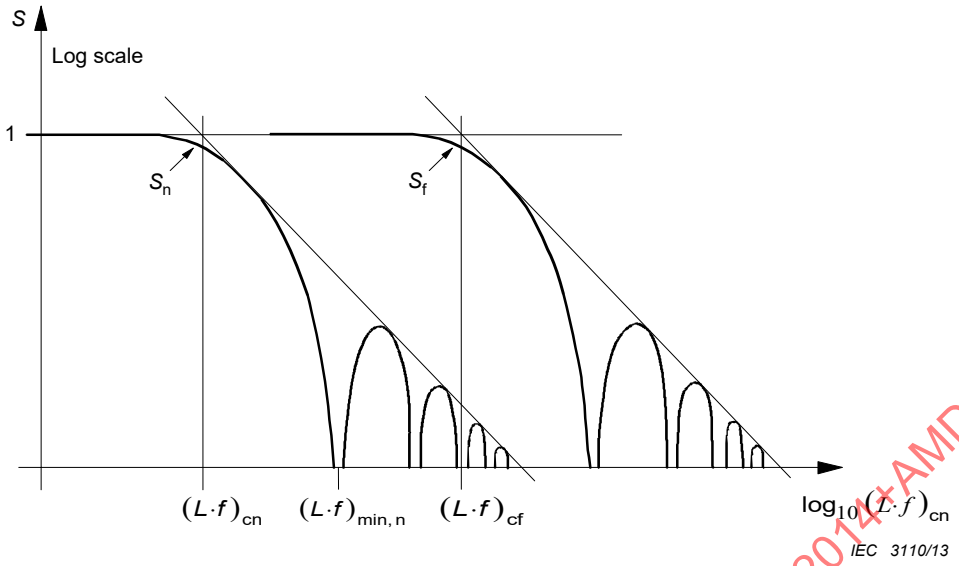

Key

$(L \cdot f)_{cn,f}$ cut-off point at near (n) respectively far (f) end

$S_{n,f}$ summing function at the (n) respectively far (f) end

NOTE $S_f > S_n$ above near end cut-off, yielding a directive effect.

Figure 6 – The summing function $S\{L \cdot f\}$ for near and far end coupling

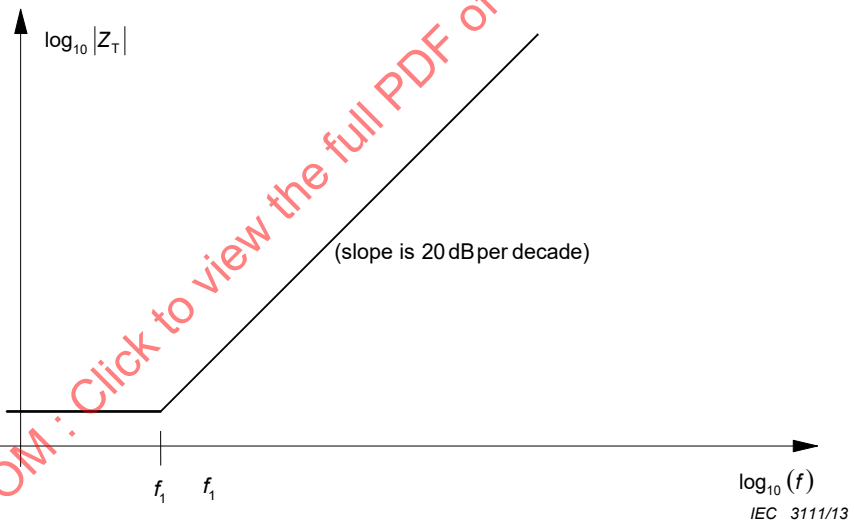

Key

$\log_{10}|Z_T|$ magnitude of the transfer impedance drawn on a logarithmic scale

$\log_{10}(f)$ frequency drawn on a logarithmic scale

f_1 frequency of the intersection of the DC resistance of the screen and the 20dB slope at higher frequencies

Figure 7 – Transfer impedance of a typical single braid screen

Figure 8 gives the result of adding (on a log scale) the frequency responses from Figure 6 and Figure 7. It is assumed the cable has a negligible capacitive coupling impedance Z_F ($Z_F << Z_T$).

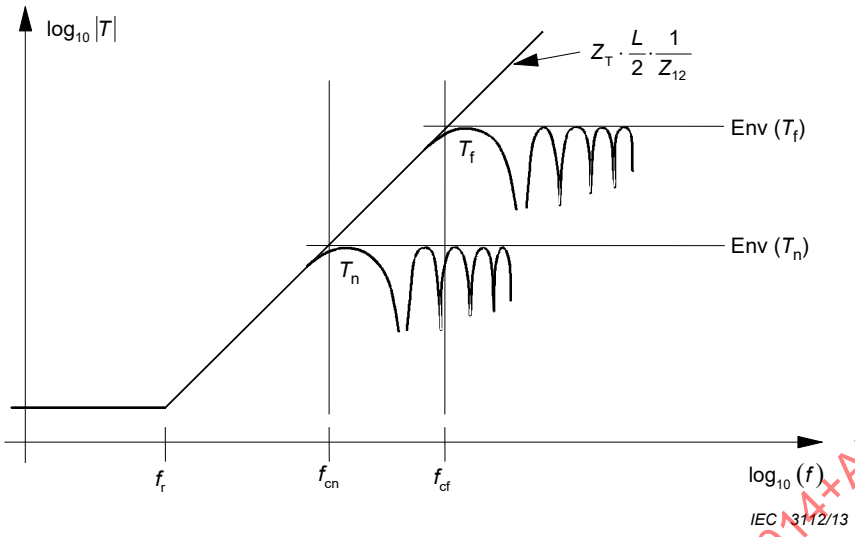

Key

$T_{n,f}$	coupling transfer function at the (n) respectively far (f) end
Env($T_{n,f}$)	envelope of the coupling transfer function at the (n) respectively far (f) end
$f_{cn,f}$	cut-off frequency at the (n) respectively far (f) end

Example: ε_{r1} = 1 (set-up), ε_{r2} = 2,2 (cable), L = 1 m; results in f_{cn} = 40 MHz; f_{cf} = 200 MHz

Figure 8 – The effect of the summing function on the coupling transfer function of a typical single braid screen cable

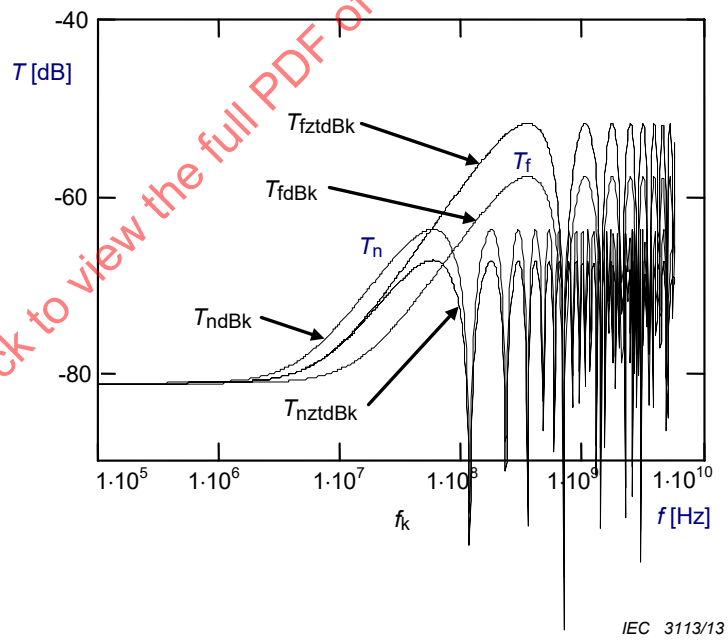

In calculations the following parameters are used:

Z_T (d.c.) =15 mΩ/m and Z_T (10 MHz) = 20 mΩ/m increasing 20 dB/decade (see Figure 7), cable length 1 m, and velocities of the outer and inner line: v_1 = 200 Mm/s and v_2 = 280 Mm/s corresponding to a velocity difference of 40 %.

Figure 9 – Calculated coupling transfer functions T_n and T_f for a single braid – Z_F = 0

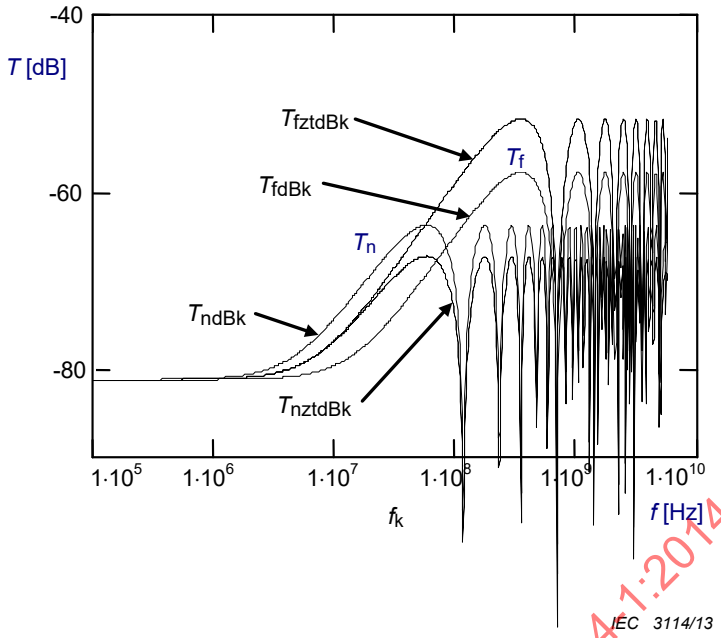

T_n is 3,5 dB higher and T_f is 6 dB lower than in reference Figure 9 because

$T_n \sim | Z_F + Z_T | = 1{,}5 \times Z_T$ and

$T_f \sim | Z_F - Z_T | = 0{,}5 \times Z_T$

Figure 10 – Calculated coupling transfer functions T_n and T_f for a single braid – Im(Z_T) is positive and Z_F = +0,5 × Im(Z_T) at high frequencies

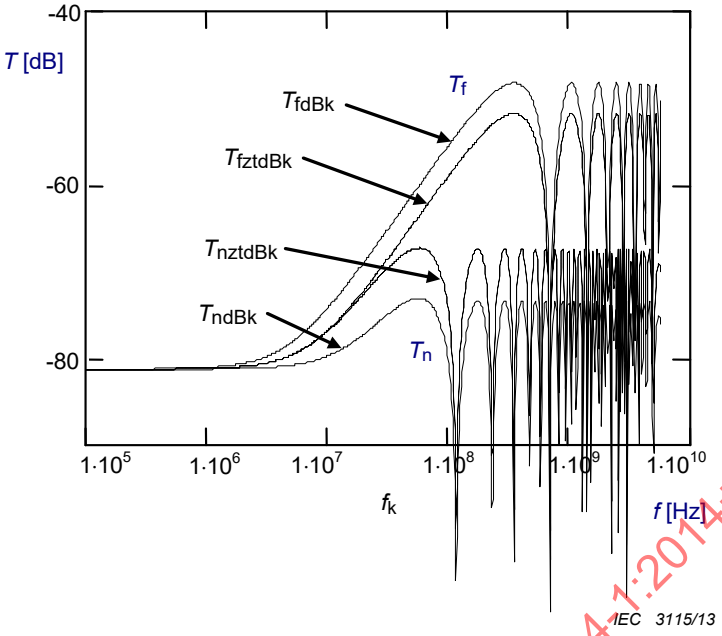

T_f is 3,5 dB higher and T_n is 6 dB lower than in reference Figure 9 because

$T_f \sim |Z_F - Z_T| = 1{,}5 \times |Z_T|$ and

$T_n \sim |Z_F + Z_T| = 0{,}5 \times |Z_T|$

Figure 11 – Calculated coupling transfer functions T_n and T_f for a single braid – Im(Z_T) is negative and $Z_F = -0{,}5 \times$ Im(Z_T) at high frequencies

In Figure 9, $Z_F = 0$ and Z_T is positive.

In Figure 10 and Figure 11, Z_F is significant ($Z_F = (1/2) \times Z_T$).

In Figure 11, the imaginary part of Z_T is negative at high frequencies.

The following notes apply to Figure 9 to Figure 11.

NOTE 1 T_n for near-end, T_f for far-end and dB means that $T_{n,f}$ are calculated in dB ($20 \times \log_{10} | T_{n,f} |$).

NOTE 2 T_n dB: near-end when $Z_F = (1/2) \times Z_T$ and T_{nzt} dB: near-end when $Z_F = 0$.

NOTE 3 T_f dB: far-end when $Z_F = (1/2) \times Z_T$ and T_{fzt} dB: far-end when $Z_F = 0$.

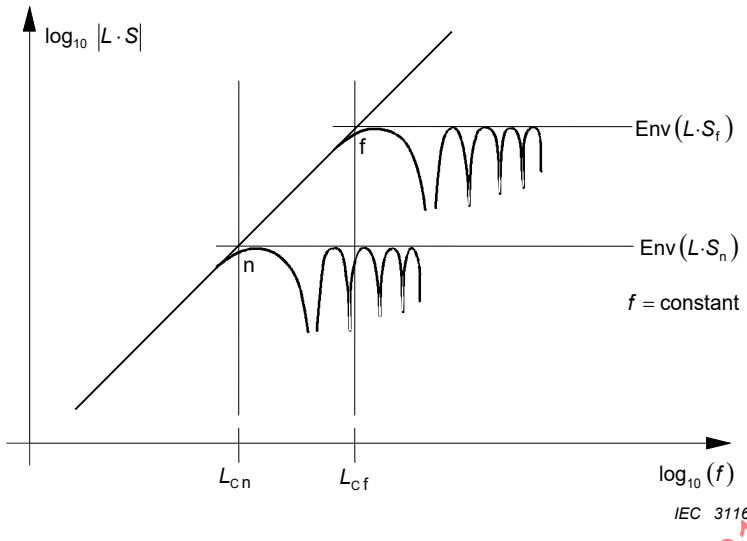

NOTE 1 For $L > L_c$, the maximum value of T is attained, i.e. the maximum coupling (or the screening attenuation) is not dependent on L.

NOTE 2 L_{cf} strongly depends on ε_{r1}.

NOTE 3 See also Table 1 and list item n)

Figure 12 – $L \cdot S$: the complete length dependent factor in the coupling function T

7 Transfer impedance of a braided wire outer conductor or screen

Typical transfer impedances of cables with braided wire screens are shown in Figure 13. The constant Z_T value at the low-frequency end is equal to the DC resistance of the screen, the 20 dB per decade rise at the high-frequency end is due to the inductive coupling through the screen and the dip at the middle frequencies is caused by eddy currents or skin effect of the braid. Some braided cables may behave anomalously having less than a 20 dB per decade rise at high frequencies. By using an extrapolation of 20 dB per decade we are in most cases on the conservative side. This extrapolation can be used up to several GHz.

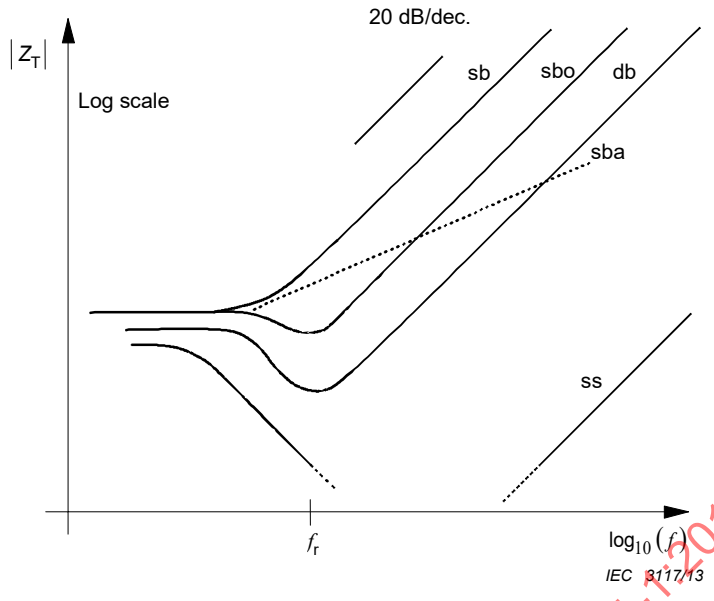

Key

f_r: typically 1....10 MHz
sb: single braid
sbo: single braid optimized
sba: single braid 'anomalous'
db: double braid
ss: superscreen

Figure 13 – Transfer impedance of typical cables

An electrically short piece of braided coaxial cable (2) is considered to be placed in a triaxial arrangement as in Figure 2.

It is assumed that the outer circuit (1) is the disturbing one. As stated, a braided cable has a transfer impedance Z_T that increases proportionally to frequency at high frequencies, because of the leakage of the magnetic field through holes in the braid.

The total flux of the magnetic field induced by the disturbing current I_1 is Φ_1. A part of it, Φ'_{12} leaks directly through the holes and includes a disturbing voltage U'_2 in the inner circuit. However, a part Φ''_{12} of Φ_1 flows in the braid and complicates the mechanism of the total magnetic leakage by the following additional phenomenon.

The braiding wires alternate between the outer and inner layer. It means that the inner and outer braid wires are likewise ingredients of both the inner (2) and outer (1) circuit of Figure 14.

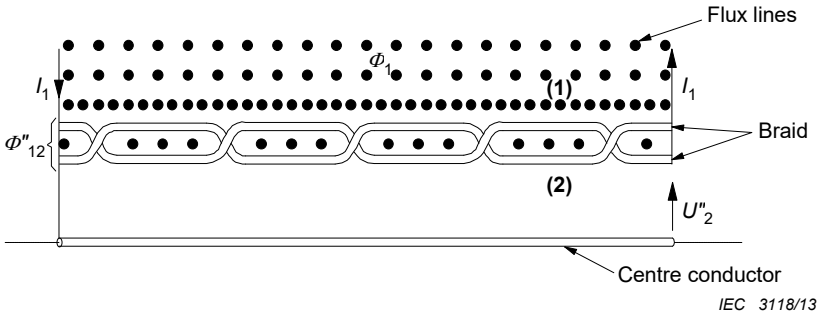

Figure 14 – Magnetic coupling in the braid – Complete flux

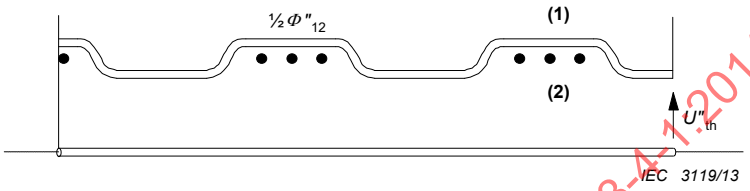

Figure 15 – Magnetic coupling in the braid – Left-hand lay contribution

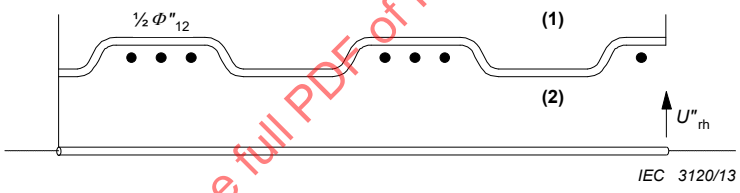

Figure 16 – Magnetic coupling in the braid – Right-hand lay contribution

Therefore it is necessary and unavoidable that Φ''_{12} is partly also in the inner circuit (see Figure 14). Both the left hand (lh) (see Figure 15) and right hand (rh) lay (see Figure 16) of the braiding wires bring into the inner circuit (2) an equal disturbing voltage U''_2 induced by Φ''_{12} / 2. The voltages are in parallel:

$$U''_{rh} = U''_{lh} = U''_2 = ½j\omega\Phi''_{12} \quad (25)$$

This phenomenon is similar to the "magnetic part" of the coupling through a homogeneous screen.

The two induced disturbing voltages oppose each other.

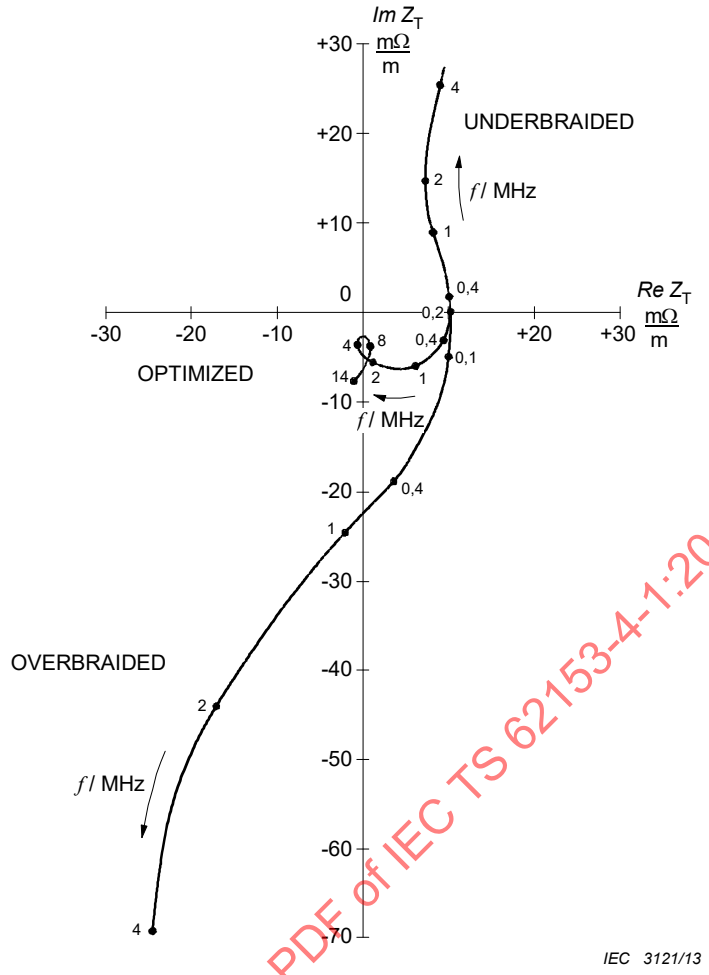

Figure 17 – Complex plane, Z_T = *Re* Z_T + j *Im* Z_T, frequency *f* as parameter

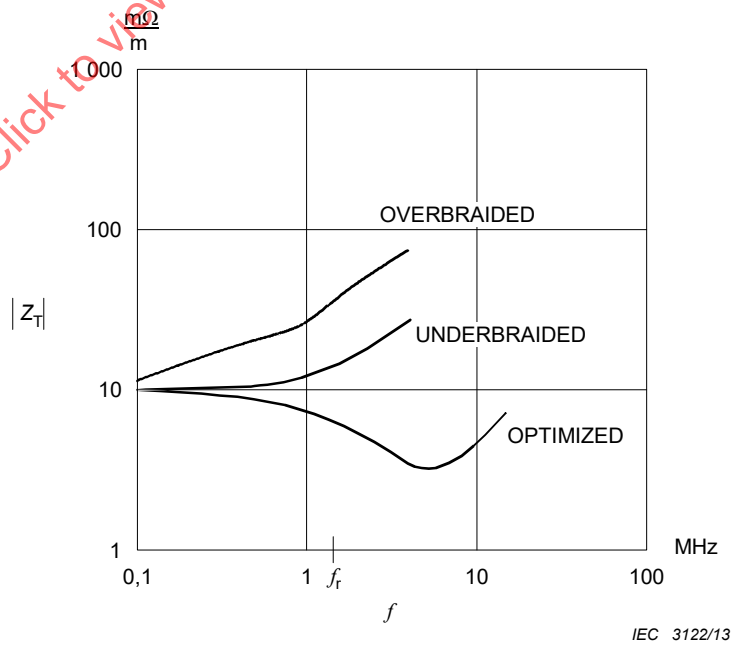

Figure 18 – Magnitude (amplitude), | Z_T (*f*) |

In Figure 17 and Figure 18, the d.c., resistance Z_T (d.c.), is set to the value of 10 mΩ/m.

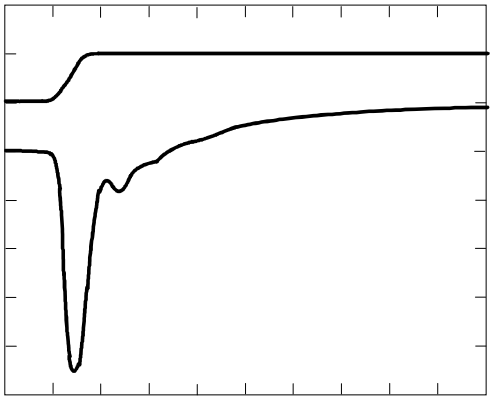

Figure 19a – Overbraided cable

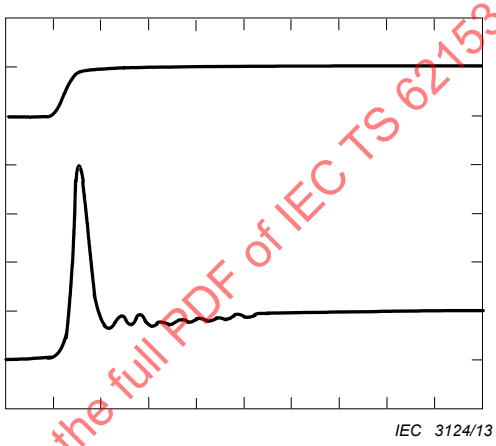

Figure 19b – Underbraided cable

Top trace: Injection step current (100 mA/div)

Time base: 50 ns/div

Amplifier gain: 30 dB, therefore Z_T (time) = 12,5 mΩ/m/div

Lower trace: The height of the spike corresponds to

a) – Z_T (3 MHz) = –4,7 × 12,5 mΩ/m = –59 mΩ/m;

b) – Z_T (3 MHz) = +4 × 12,5 mΩ/m = +50 mΩ/m.

Figure 19 – Typical Z_T (time) step response of an overbraided and underbraided single braided outer conductor of a coaxial cable

Braid optimization is based on these important physical facts. Both leakage phenomena can be described by mutual inductances:

$$M'_{12} = \frac{\Phi'_{12}}{\mathrm{j}\omega I_1} \tag{26}$$

$$M''_{12} = \frac{1}{2} \times \frac{\Phi''_{12}}{\mathrm{j}\omega I_1} \tag{27}$$

Clearly it is possible to make braided-wire screens where either M'_{12} or M''_{12} are dominant or where they cancel each other. Therefore, underbraided, overbraided or optimized braids may be considered. Figure 17 shows measured transfer impedances in the complex plane of such screens and the main transfer impedance components of a braided screen can be observed. From the optimized case, it can be concluded that at low frequencies the braid behaves approximately as a homogeneous tubular screen. The same can be concluded from Figure 18 where the transfer impedance amplitudes are shown as a function of frequency, but from it cannot be seen directly if the screen is underbraided or overbraided.

The transfer impedance of a braided wire screen consists of the following three main components (mentioned above).

a) At low and medium frequencies, the tubular screen coupling behaviour (Z_{Th}) varies with eddy currents and decreasing Z_T. In [2] it is stated that a good approximation for Z_{Th} is a tubular homogeneous screen [3] with the thickness of one wire diameter and the same d.c. resistance as the braid.

b) The mutual inductance M'_{12} is related to direct leakage of the magnetic flux Φ'_{12}.

c) The mutual inductance M''_{12} (negative) is related to the magnetic flux Φ''_{12} in the braid.

By adding these components, a good approximation is obtained for the transfer impedance Z_T of a braided wire screen:

$$Z_T \approx Z_{Th} + \mathrm{j}\,\omega\,(M'_{12} - M''_{12}) \tag{28}$$

and the first approximation of the equivalent circuit is shown in Figure 20a.

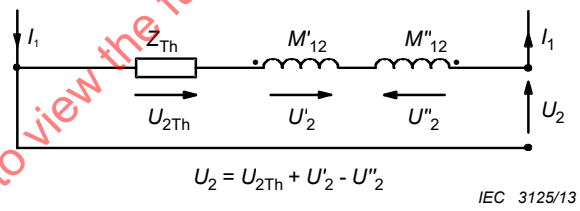

Figure 20a – Contributions to the transfer impedance

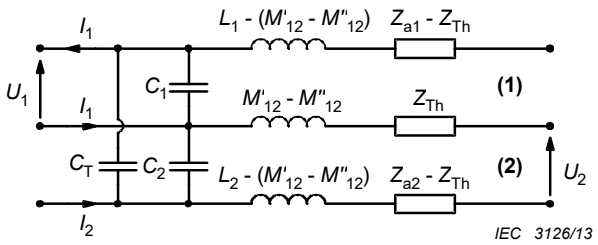

Figure 20b – Significant elements of circuits (1) and (2)

Figure 20 – Z_T equivalent circuits of a braided wire screen

A more complete equivalent circuit where the through capacitance C_T and surface impedances Z_a of the braided cable are incorporated is shown in Figure 20b. L_1 and L_2 are the (external) inductances of the outer and inner circuit.

Many attempts have been made to calculate the transfer impedance of a braided coaxial cable. Most of the literature ([2], [4], [5]) have concentrated on models of braided screens and calculation of direct leakage of the magnetic field induced by I_1, and of M'_{12}. Satisfactory results have been achieved.

There exists very little literature ([6], [7]) on M''_{12} but the matter has been studied by experts of standardization bodies. Especially the calculation and stability of M''_{12} have been shown to be very problematic because of so many uncertain and unstable parameters, e.g. the resistance of the crossover points of the wires, which have an effect on the magnetic field distribution in the braid. Also the pressure of the jacket has an effect on the small space between the right hand lay and left-hand lay of the braided wires. Not to mention the number of wire ends per carrier and the braid angle and the tightness and optical coverage of the braid.

After understanding the magnetic coupling mechanisms, it is not surprising that the transfer impedances of braided wire screens vary considerably and are unstable for many braid and cable constructions whether or not they are optimized. It is also clear that a perforated tube cannot be used as a model for a braided screen.

It is clear that a loose highly optimized braid can have a very unstable Z_T during bending, twisting and/or pressing. An overbraided screen with a high filling factor or optical cover normally has a (pure) negative transfer impedance at high frequencies because of a large M''_{12} coupling through the mutual "space" between the left and right lays of the braid in comparison with a small leakage through the braid M'_{12}. Pressure on the jacket would improve the screening performance by diminishing the mutual "space" and decrease the Z_T.

The manufacture of a good stable optimized cable requires the control of braid parameters such as:

– braid angle, tension (and lubricant) of the strands;
– number of strand in a spindle;
– wire diameter;
– plating;
– pressure of the jacket on the braid in manufacturing.

8 Test possibilities

8.1 General

A number of test procedures are used to test cables for their screening properties, some of which will be found in IEC standards. Each procedure has benefits for some users which for historical reasons may not be widely appreciated. Table 2 summarizes the test procedures available, some of which will be discussed here, with special reference to their applicability to cables, cable assemblies and connectors.

8.2 Measuring the transfer impedance of coaxial cables

All tests listed in Table 2 can be used on coaxial cables, but if a single test is needed to cover frequencies above and below 100 MHz, tests 1, 4, 7, 9 and 10 can be dismissed. Of the others, those with 's' under 'grouping' (column 3) have better intrinsic isolation between measuring and injection circuits, while in those with 'o' under grouping the injection circuit is unscreened. The difference is the line interchange referred to in 4.5 above. One benefit of an unscreened injection line is that better access may be obtained for inspection of the cable under test, which may be useful if the sample is in any way flawed. The two test methods with unscreened injection lines are test 3 and test 8. The latter, with its wide frequency coverage is recommended for future testing.

8.3 Measuring the transfer impedance of cable assemblies

Even with a restricted frequency range, many of the tests listed in Table 2 are not suited to tests on cable assemblies. Tests 1, 4, and 6 are unsuitable because an electrically short sample may be needed to achieve the upper frequencies, while test 10 is still limited to frequencies above 100 MHz. Tests with screened injection wires (test 2 and test 5) are difficult to set up due to the varying cross section of the assembly, a difficulty which also applies to test 3. Such objections leave tests 7, 8 and 9. To set against its low (effective) upper frequency limit, with test 7 it is easy to distinguish between connector and cable contributions, so it is ideal in a diagnostic role. Test 9 works only above 30 MHz, which may be restrictive. Test 8 will require several measurements on each sample, as it is unreasonable to assume that a cable assembly has circular symmetry.

It is only fair to state that in any frequency domain test on cable assemblies where signal phase is not recorded, a test is only valid if the sample length is not varied (tests carried out on a sample of one length cannot be used to assess a sample of another length – whether it be longer or shorter). Of the transfer impedance tests being discussed, only test 7 can be used in this way.

Multi-conductor cable assemblies are more complex, because the 'core' cannot be considered to be coaxial. A test for such cable assemblies has not yet been addressed.

8.4 Measuring the transfer impedance of connectors

In principle, all the tests in Table 2 can be used on coaxial connectors.

As with tests on cable assemblies, there is much benefit to be gained from using a test with an unscreened injection circuit, though other tests will remain in the standard, because they have become accepted. If it is possible to distinguish the screening of a connector from that of the attached cable, this will considerably ease the test procedure.

Multi-pin connectors are far more numerous and varied than coaxial connectors. However, non-circular connectors cannot be tested by the means implied by the test procedures of Table 2, though by suitable variation test 7 and test 10 would become appropriate. This problem is under study.

NOTE These methods give only an outline for measurement of symmetrical multicore cables, multipin connectors and cable assemblies made with these components.

The problems to be addressed come from the fact that:

a) a connector is electrically short, while the parameters of a cable are distributed, and it may be electrically long;

b) multi-core cables rarely have circular symmetry. This applies both physically and to the signal paths on their conductors;

c) most multi-pin connectors have no circular symmetry; nor are they equally spaced from other conductors, which might couple to them;

d) economics will dictate that a cable assembly test should apply to other assemblies using the same components, even though of differing overall length.

8.5 Calculated maximum screening level

It is important to know the exact theoretical limitation of the test equipment. By knowing the limitations, it is possible to calculate the maximum measurable screening effectiveness. This should be calculated to check the strengths and weaknesses of the test setup or even to optimize the test setup.

The following test equipment specifications are required for the calculation:

- minimum input (noise floor);
- maximum input;

- amplification/attenuation;
- maximum output.

Figure 21 gives a comparison of the different signal levels in a generic test setup. The maximum screening is the difference between the maximum obtainable input signal to the DUT and the minimum detectable signal from the DUT, in this case 131 dB. The noise floor level (*NL*) of the measuring system must be low enough to allow the measurement. In this case, lower than –122 dBm. Measurements at the noise floor result in a maximum error of 3 dB. When measured 6 dB above the noise floor, the error is only about 1 dB.

The triaxial tube column is divided in two to show both the loss in the tube and the actual maximum screening.

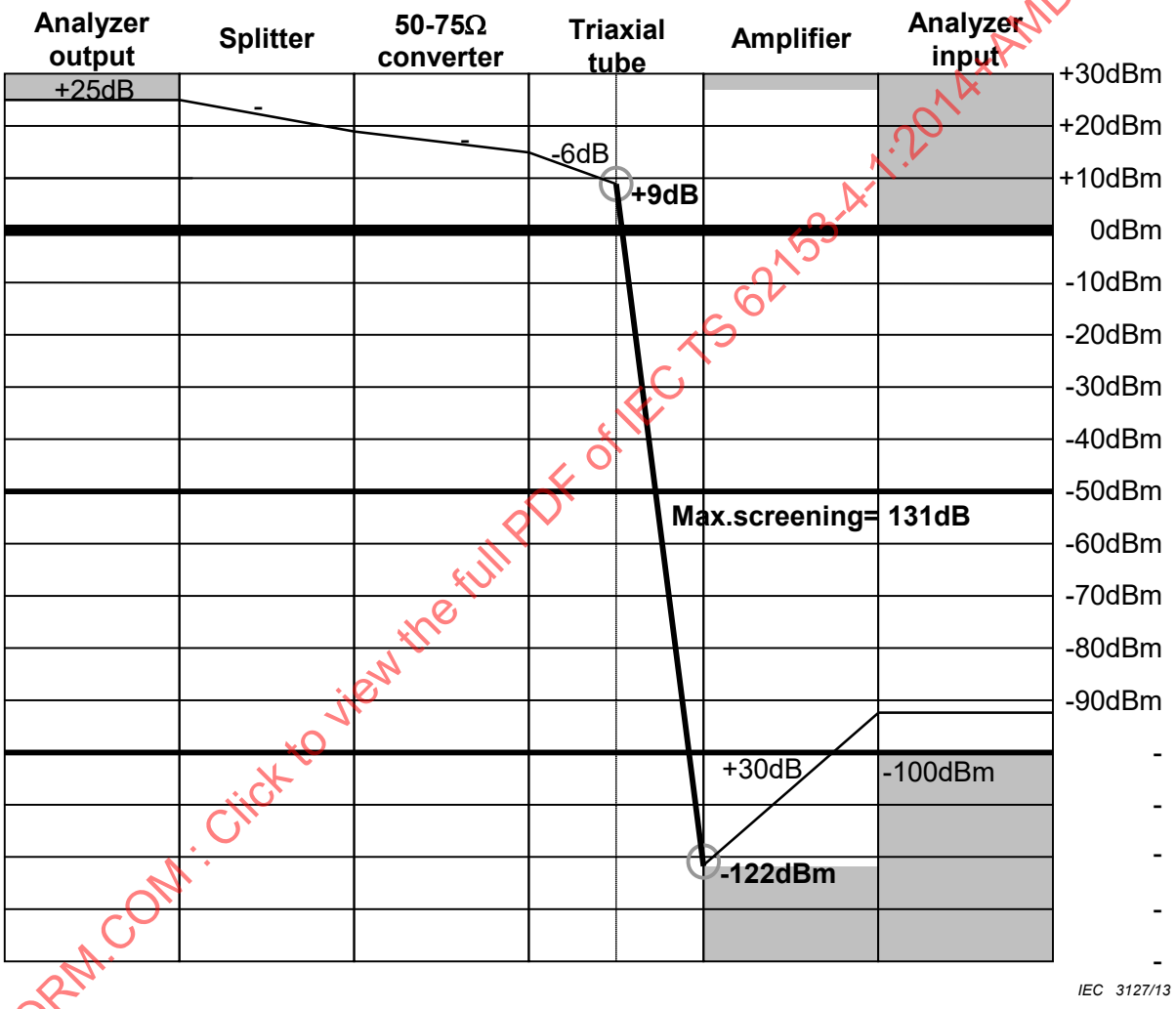

Figure 21 – Comparison of signal levels in a generic test setup

Taking into consideration the noise level of 1 Hz bandwidth at room temperature being –173 dBm, (increase 10 × log(bandwidth) dB) and adding the noise figure of the amplifier, we get the theoretical noise level of the test setup. Assuming that the amplifier in the Figure 21 example has a noise figure of 11 dB, we can then calculate that the bandwidth (Δf) of the network analyzer shall be smaller than 10 kHz.

This can be expressed as a general formula:

$$NL = (-173 + F + 10 \times \log_{10} \Delta f) \quad (29)$$

where

NL is the noise floor level of receiving side of the measuring system in dBm;

F is the noise figure of the pre amplifier in dB;

Δf is the bandwidth of the receiver in Hz.

Table 2 – Screening effectiveness of cable test methods for surface transfer impedance Z_T

	Short title	Reference	Grouping (see Note 1)	Frequency range		Injection N or F (see Note 2)	Advantages or shortcomings
				Possible	Actually used		
1	IEC triaxial	IEC 62153-4-3	kf s	d.c. to 50 MHz	10 kHz to 30 MHz	F	Rigid test rig or flexible (milked on braid)
2	Terminated triaxial (Simons)	Figure A5 of IEC 60096-1:1986 [32]	m s	10 kHz to 1 GHz	100 kHz to 500 MHz	N F	Flexible test jig relies on ferrites
3	Braid injection (Fowler)	[9]	m o	d.c. to 500 MHz	10 kHz to 500 MHz	N F	Flexible test needs good screening on measuring system
4	Quadraxial	[10]	m s	100 kHz to 50 MHz	100 kHz to 1 GHz	N	Deep resonances make use above 50 MHz theoretically impossible. The test has been used for assessing screening at frequencies up to 1 GHz
5	Matched T triaxial (Staegar)	IEC 60169-1-3 [11]	m s	1 kHz to 12 GHz	100 MHz to 10 GHz 10 kHz to 100 MHz	N F	Rigid test jig needs good screening
6	ERA triaxial (Smithers)	[12]	kf s	d.c. to 400 MHz	10 kHz to 300 MHz	F	Very short CUT requires amplifier or phase locked loop
7	Line injection (time domain)	IEC 60096-4-1 [33] [13]	m o	d.c. to 100 MHz	1 kHz to 80 MHz (note 3)	N F	Very easy to use. Needs good screening in measuring amplifier
8	Line injection (frequency domain)	IEC 62153-4-6 [14]	m o	d.c. to 20 GHz	10 kHz to 3 GHz	N F	Flexible and cheap measuring set-up, equipment needs to be well shielded
9	Open screening attenuation test method (absorbing clamp)	IEC 62153-4-5	m o	30 MHz to 2,5 GHz	30 MHz to 1 GHz 300 MHz to 2,5 GHz	N F	Poor sensitivity. Measuring of a_S is dependent on the surroundings
10	Reverberation chamber method	IEC 61726 [15]	kn kf	0,1 GHz →	0,3 GHz to 40 GHz	N & F	Flexible in use, but a complex and expensive computer controller with sophisticated test software needed
11	Shielded screening attenuation test method	IEC 62153-4-4 [16] (note 4)	m s	d.c. to 5 GHz	10 kHz to 3 GHz	F	High-sensitivity measurements can be made without a screened room. Transfer impedance and screening attenuation can be measured with one set-up
12	Open multipin connector screening test method	[17]	o	d.c. to 1 GHz	10 kHz to 700 MHz	N	Low cost and flexible

Short title	Reference	Grouping (see Note 1)	Frequency range		Injection N or F (see Note 2)	Advantages or shortcomings
			Possible	Actually used		
13 Coupling attenuation measurements of balanced cables, cable-assemblies, connecting hardware						
13.1 Current clamp injection method	IEC 62153-4-2		50 MHz to 1 GHz	50 MHz to 1 GHz		High sensitivity but a screened room is recommended
13.2 Shielded triaxial test method	IEC 62153-4-9 [22]		d.c. to 3 GHz	d.c. to 1 GHz		High-sensitivity measurements can be made without a screened room
13.3 Absorbing clamp method	IEC 62153-4-5 IEC 62153-4-11 IEC 62153-4-12 IEC 62153-4-13		50 MHz to 2,5 GHz	50 MHz to 2,5 GHz		Poor sensitivity
14 Shielded screening attenuation, test method for measuring the transfer impedance Z_T and the screening attenuation a_S of RF connectors up to and above 3 GHz; tube in tube method	IEC 62153-4-7	m s	d.c. to 20 GHz	d.c. to 3 GHz		High-sensitivity measurements can be made without a screened room Transfer impedance and Screening attenuation with one test set-up
15 Shielded screening attenuation test method for measuring the screening effectiveness of feedtroughs and electromagnetic gaskets – double coaxial method	IEC 62153-4-10	m s	d.c. to 4 GHz	d.c. to 3 GHz		High-sensitivity measurements can be made without a screened room

NOTE 1 Grouping by condition of 'primary circuit':

kn = short circuit at near end;

kf = short circuit at far end;

m = matched with characteristic impedance;

o = open on unscreened;

s = screened or shielded.

NOTE 2 N denotes near end feeding of primary relative to secondary circuit. F denotes far end feeding of primary relative to secondary circuit.

NOTE 3 Effective frequencies tested. Actually pulse with T_R = 3,5 ns and duration up to 160 µs.

NOTE 4 Secondary circuit near end short circuited.

9 Comparison of the frequency response of different triaxial test set-ups to measure the transfer impedance of cable screens

9.1 General

Different triaxial test set-ups for the measurement of the transfer impedance exist as described in EN 50289-1-6 and the IEC 62153-4 series. All of them are based on the same principle but are using different load conditions. In one method for example the cable under test is matched, while in the other the cable is short circuited at the far end. Furthermore, generator and receiver may be interchanged in the different set-ups. The following investigation analyses the frequency response of the different set-ups and their influence on the cut-off frequency up to which the transfer impedance could be measured.

9.2 Physical basics

9.2.1 Triaxial set-up

9.2.1.1 General

The triaxial set-up is of the “triple coaxial” form, see Figure 22 and Figure 23. A short length of the screen under test forms both, the inner conductor of the outer system and at the same time the outer conductor of the inner system. The coupling between the two coaxial systems is caused by the transfer impedance and the capacitive coupling admittance of the screen. The matching circuit, load resistor and series resistor are used to change the load conditions of the set-up. Also the generator and receiver may be interchanged between the different methods.

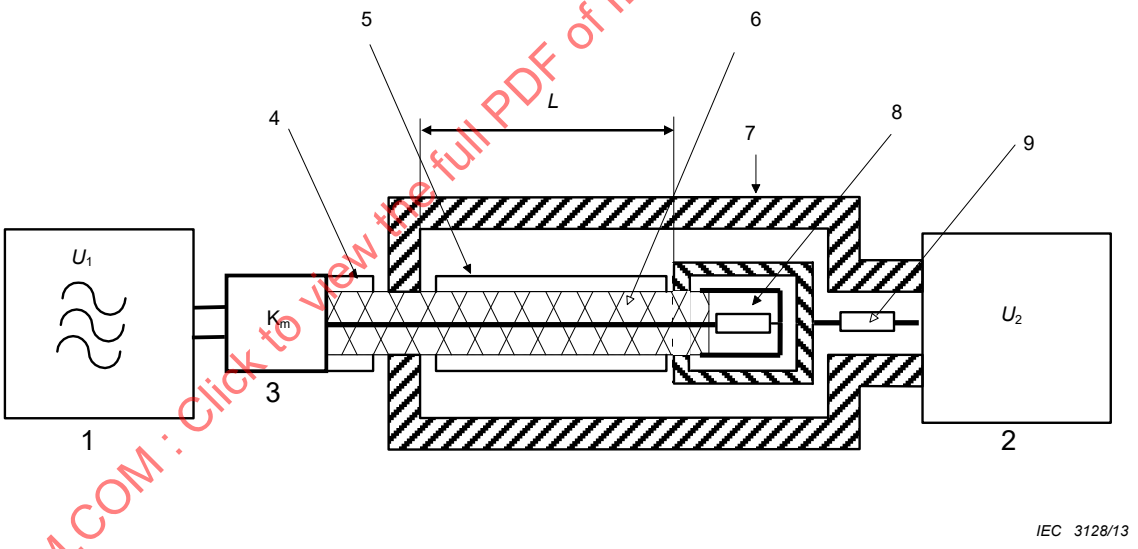

Key

1	Signal generator	6	Cable screen
2	Calibrated receiver or network analyzer	7	Tube
3	Matching circuit	8	Terminating resistor
4	Cable under test	9	Series resistor
5	Cable sheath		

Figure 22 – Triaxial set-up for the measurement of the transfer impedance Z_T

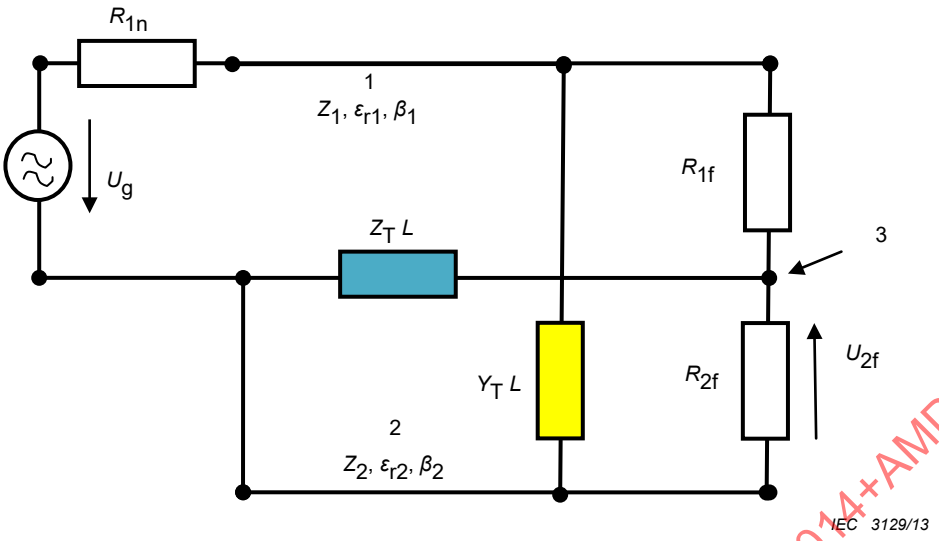

Key

1	inner circuit, cable
2	outer circuit, tube
3	screen
$Z_{1,2}$	characteristic impedance of the inner circuit, cable, respectively outer circuit, tube
$\varepsilon_{1,2}$	dielectric permittivity of the inner circuit, cable, respectively outer circuit, tube
$\beta_{1,2}$	phase constant of the inner circuit, cable, respectively outer circuit, tube
L	coupling length
Z_T	transfer impedance
Y_T	capacitive coupling admittance
R_{1n}	load resistance at the near end of the inner circuit, cable. Equal to the output impedance of the generator respectively input impedance of the receiver including an eventually used feeding resistor
R_{1f}	load resistance at the far end of the inner circuit, cable. Depending on the used method either equal to the characteristic impedance of the cable or a short circuit.
R_{2f}	load resistance at the far end of the outer circuit, tube. Equal to the output impedance of the generator respectively input impedance of the receiver including an eventually used feeding resistor
U_g	EMF of the generator
U_{2f}	voltage at the far end of the outer circuit

Figure 23 – Equivalent circuit of the triaxial set-up

9.2.1.2 Load conditions of the different set-ups

EN 50289-1-6 is using a method, where the cable under test and the far end of the secondary circuit are matched. The signal is fed to the cable under test and the disturbing voltage is measured at the far end of the outer circuit. A simplified method is to neglect the matching resistor at the far end of the outer circuit, which results in a higher dynamic range.

IEC 61196-1 describes two methods:

Method 1: Feeding through a resistance, where the signal is fed via a resistance into the outer circuit and the disturbing voltage is measured at the far end of the cable under test.

Method 2: Direct feeding, where the signal power is fed directly into the outer circuit and the disturbing voltage is measured at the far end of the cable under test.

With the revision of IEC 61196-1, the standard IEC 62153-4-3 has been published which also describes several methods:

Method A “Matched-Short” is equal to EN 50289-1-6.

Method B “Short-Short” is the double short circuited method, where the load resistance of the cable is replaced by a short circuit, thus having two short circuits in the set-up. One is at the near end of the outer circuit (between the cable screen and the tube) and the other is at the far end of the cable. The advantage of this method is the simplification of the sample preparation. A short circuit is easier to make than to solder a resistor, especially if the sample is a multi-conductor cable. Furthermore, the measurement sensitivity is improved. Compared to the “matched-short” method, the dynamic range is improved by about 16 dB. In the “milked on braid” method, an additional braid, the measuring braid, is pulled over the cable sheath instead of using the measuring tube. The advantage is that the sample could be bent under test, however the preparation is more laborious than with the measuring tube.

The load conditions of the different methods are given in Table 3. The impedance of the outer circuit, Z_2 is varying with the diameter of the screen under test. Using the measuring tube Z_2 is in general higher, and in the “milked on braid” method Z_2 is lower, than the input impedance of the receiver.

Table 3 – Load conditions of the different set-ups

Method	Generator	Receiver	R_{1n}/Z_1	R_{1f}/Z_1	Z_2/R_{2f}
EN 50289-1-6					
Standard	IC	OC	1	1	0,71
simplified	IC	OC	1	1	1…5 depending on the tube diameter
IEC 61196-1					
Method 1: feeding through a resistance	OC	IC	1	1	0,71
Method 2: direct feeding	OC	IC	1	1	1…5 depending on the tube diameter
IEC 62153-4-3 Double short circuit methods					
With tube	OC	IC	1*	0	1…5 depending on tube diameter
With milked on braid	IC	OC	1*	0	0,1…0,4 depending on screen and sheath diameter of the cable
IC: inner circuit (cable under test) OC: outer circuit (tube)					
* only if the cable impedance is equal to the generator impedance. For other cable impedances, the value may vary, e.g. 0,67 for cables with an impedance of 75 Ω.					

9.2.2 Coupling equations

The equations for the coupling between the inner circuit and outer circuit for any load conditions are described in [18] and [19]. By taking into account the short circuit at the near end of the outer circuit (between the cable screen and the measuring tube), neglecting the attenuation of the disturbing and disturbed line, assuming non ferromagnetic materials and introducing further variables, the following equations are defined.

$$\frac{u_{2f}}{u_q} = \frac{L}{R_{1f} + R_{1n}} \cdot [Z_T \cdot g + Z_F \cdot h] \quad (30)$$

$$g = \frac{1}{N} \cdot \frac{1}{1-n^2} \cdot \frac{j}{x} \cdot \{ r \cdot [\cos x - \cos nx] - j \cdot n \cdot \sin nx + j \cdot \sin x \} \quad (31)$$

$$h = \frac{1}{N} \cdot \frac{1}{1-n^2} \cdot \frac{j}{x} \cdot \{ n \cdot r \cdot [\cos x - \cos nx] - j \cdot \sin nx + j \cdot n \cdot \sin x \} \quad (32)$$

$$N = \left\{ \cos x + \frac{j \cdot \sin x}{r + w} \cdot [1 + r \cdot w] \right\} \cdot \{ \cos nx + j \cdot v \cdot \sin nx \} \quad (33)$$

$$x = \beta_1 \cdot L = 2\pi \cdot \frac{L}{\lambda_1} \quad (34)$$

$$n = \frac{\beta_2}{\beta_1} = \frac{\lambda_1}{\lambda_2} = \sqrt{\frac{\varepsilon_{r2}}{\varepsilon_{r1}}} \quad (35)$$

$$r = \frac{R_{1f}}{Z_1} \quad (36)$$

$$v = \frac{Z_2}{R_{2f}} \quad (37)$$

$$w = \frac{R_{1n}}{Z_1} \quad (38)$$

where

$Z_{1,2}$ is the characteristic impedance of the inner circuit (cable) respectively outer circuit (tube);

$\varepsilon_{1,2}$ is the dielectric permittivity of the inner circuit (cable) respectively outer circuit (tube);

$\beta_{1,2}$ is the phase constant of the inner circuit (cable) respectively outer circuit (tube);

$\lambda_{1,2}$ is the wave length in the inner circuit (cable) respectively outer circuit (tube);

L is the coupling length;

Z_T is the transfer impedance;

Y_T is the capacitive coupling admittance;

$R_{1,n}$ is the load resistance at the near end of the inner circuit (cable). Equal to the output impedance of the generator respectively input impedance of the receiver including an eventually used feeding resistor;

$R_{1,f}$ load resistance at the far end of the inner circuit (cable). Depending on the used method either equal to the characteristic impedance of the cable or a short circuit.

The factors g and h (see Equations (31) and (32)) describe the frequency response of the test set-up. At low frequencies, when $\lambda >> L$, the factors g and h are equal to 1. However, with increasing frequency, the factors g and h start to oscillate and thus also the measurement results. The maximum frequency to which the transfer impedance could be measured without oscillations, caused by the set-up, is defined as the 3 dB deviation from the linear interpolation of the measurement results. Or in other words, the maximum frequency is reached when the factor g respectively h becomes $> \sqrt{2}$ respectively $< 1/\sqrt{2}$.

9.3 Simulations

9.3.1 General

For the following investigations, simulations have been chosen rather than a pure mathematical solution because they are easier to grasp and clearly illustrate the differences in the set-ups given in Table 4. In general, the capacitive coupling can be neglected compared to the magnetic coupling ($Z_F << Z_T$). i.e. the cut-off frequency is mainly determined by the frequency behaviour of the factor *g*. Thus the following simulations are limited to the factor *g*.

Due to the reciprocity of the materials, it is possible to interchange the generator and receiver without changing the results. Thus the standard EN 50289-1-6 method gives the same results as IEC 61196-1, method 1: "feeding through a resistance" and the simplified EN 50289-1-6 method gives the same results as IEC 61196-1, method 2: "direct feeding".

Table 4 – Parameters of the different set-ups

Method	$w=R_{1n}/Z_1$	$r=R_{1f}/Z_1$	$v=Z_2/R_{2f}$	$n=\sqrt{\varepsilon_{r2}}/\sqrt{\varepsilon_{r1}}$
EN 50289-1-6, IEC 62153-4-3 method A				
Standard	1	1	0,71	0,66 (0,45)...0,91
Simplified	1	1	1...5 depending on the tube diameter	
IEC 61196-1				
Method 1: feeding through a resistance	1	1	0,71	0,66 (0,45)...0,91
Method 2: direct feeding	1	1	1...5 depending on the tube diameter	
IEC 62153-4-3 Double short circuit methods				
With tube	1[a]	0	1...5 depending on tube diameter	0,66 (0,45)...0,91
With milked on braid	1[a]	0	0.1...0,4 depending on screen and sheath diameter of the cable	1,02...2,0

[a] only if the cable impedance is equal to the generator impedance. For other cable impedances, the value may vary, e.g. 0,67 for cables with an impedance of 75 Ω.

In the tube methods, the factor *n* is given by the dielectric permittivity of the cable (inner circuit) as the dielectric permittivity of the outer circuit is nearly independent on the sheath material and can be assumed to be 1. However, in the "milked on braid method", the factor *n* is dependent on both the dielectric permittivity of the cable insulation and the sheath, as the "measuring braid" is directly put on the sheath of the sample. The values for the factor *n* are given for typical insulation materials (PE, foam PE, PTFE ...). The values in brackets are given for an insulation material of PVC, which may be used in multi-pair/conductor cables. For the "milked on braid" method, typical combinations of insulation and sheath materials (PE/PVC, PE/LSZH, PTFE/FEP...) are taken into account, resulting in a value $n > 1$.

9.3.2 Simulation of the standard and simplified methods according to EN 50289-1-6, IEC 61196-1 (method 1 and 2) and IEC 62153-4-3 (method A)

In EN 50289-1-6, IEC 61196-1 method 1: "feeding through a resistance" and IEC 62153-4-3 method A: "Matched-Short", the factor $v=Z_2/R_{2f}$ is specified at $1/\sqrt{2}$. The following simulations show that this factor is a good compromise with respect to the maximum frequency to which the transfer impedance could be measured.

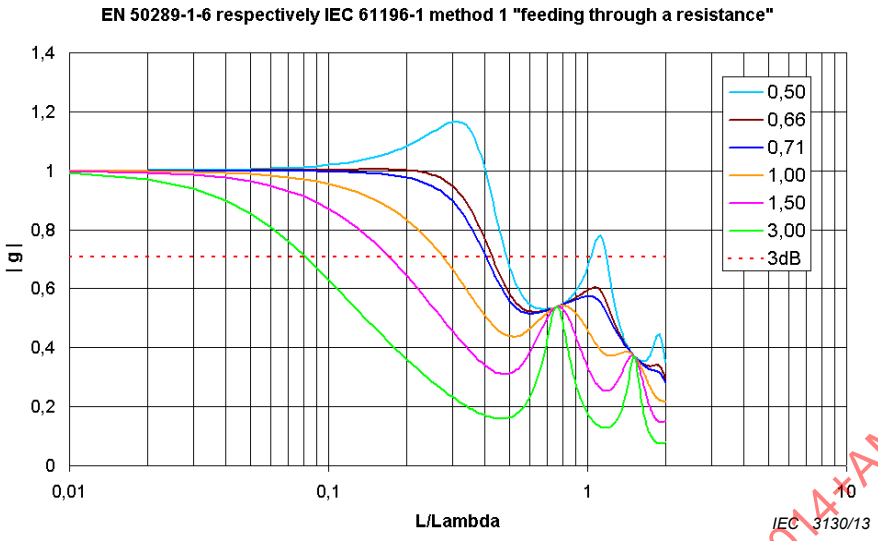

Key

Coloured lines correspond to indicated factors of $v=Z_2/R_{2f}$.

Simulation parameters		
ε_{r1}	ε_{r2}	n
2,3 (solid PE)	1,0	0,569

Figure 24 – Simulation of the frequency response for *g*

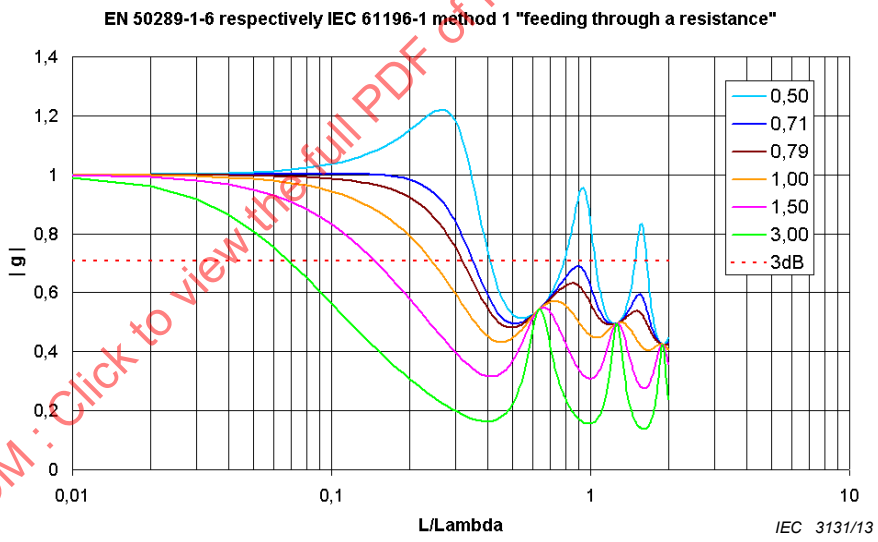

Key

Coloured lines correspond to indicated factors of $v=Z_2/R_{2f}$.

Simulation parameters		
ε_{r1}	ε_{r2}	n
1,6 (foam PE)	1,0	0,791

Figure 25 – Simulation of the frequency response for *g*

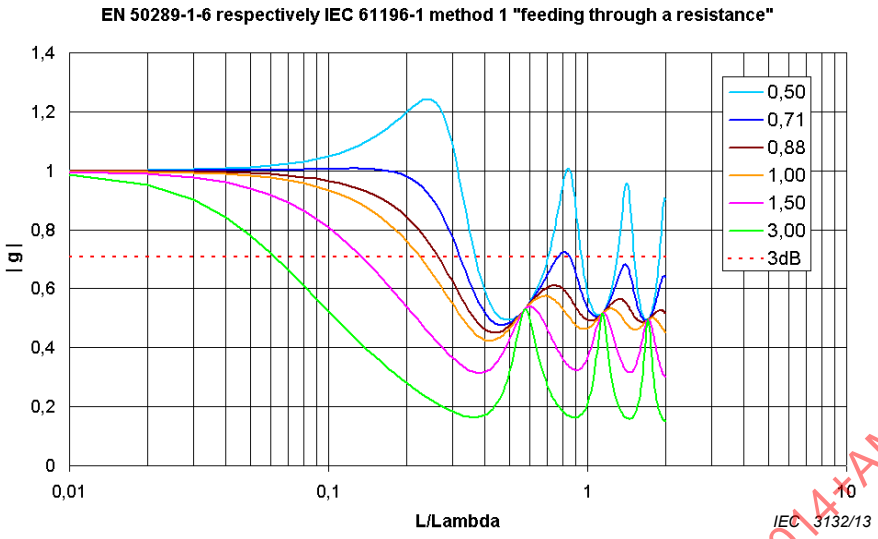

Key

Coloured lines correspond to indicated factors of $v=Z_2/R_{2f}$.

Simulation parameters		
ε_{r1}	ε_{r2}	n
1,3 (foam PE)	1,0	0,877

Figure 26 – Simulation of the frequency response for *g*

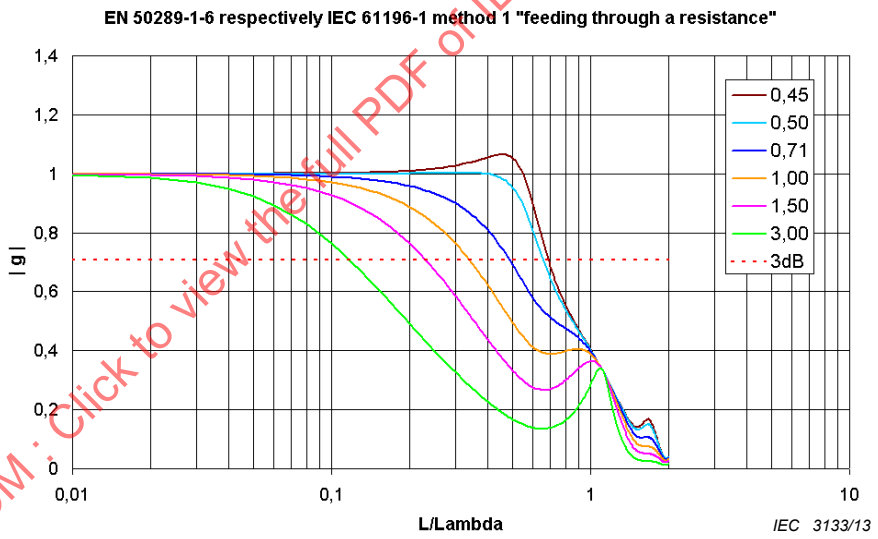

Key

Coloured lines correspond to indicated factors of $v=Z_2/R_{2f}$.

Simulation parameters		
ε_{r1}	ε_{r2}	n
5 (PVC)	1,0	0,447

Figure 27 – Simulation of the frequency response for *g*

The highest frequencies (respectively shortest wavelengths) are obtained if the factor $v=1/\sqrt{2}$ respectively $v=n$, whichever is smaller. In Figure 24 and Figure 27, the highest frequency is obtained for $v=n$ (=0,659 respectively 0,447). But in Figure 25 and Figure 26, the highest frequency is obtained for $v=1/\sqrt{2}=0,71$. Below that value, the factor g overshoots, i.e. becomes higher than one. Above that value, the cut-off frequency is decreasing.

Figure 28 gives the calculated, by iteration, 3 dB cut-off wavelength (L/λ_1) at which the factor $|g|$ becomes $1/\sqrt{2}$. The graph is given as a function of the factor $n=\sqrt{\varepsilon_{r2}}/\sqrt{\varepsilon_{r1}}$ and for different factors $v=Z_2/R_{2f}$. The curves show a linear behaviour and could be interpolated by straight line.

This has been done in Figure 29 for $v=1/\sqrt{2}$, $v=1$, $v=1{,}8$ and $v=3{,}6$. The factor $v=1/\sqrt{2}$ corresponds to the set-up according to EN 50289-1-6, IEC 61196-1 method 1 "feeding through a resistance" and IEC 62153-4-3 method A "Matched-Short". The other values of the factor v correspond to the simplified set-up, i.e. direct feeding. For common diameters of the measuring tube (around 40 mm) and common cable screen diameter (2 mm to 9 mm), the impedance in the outer circuit is 90 Ω to 180 Ω and $v=1{,}8\ldots3{,}6$.

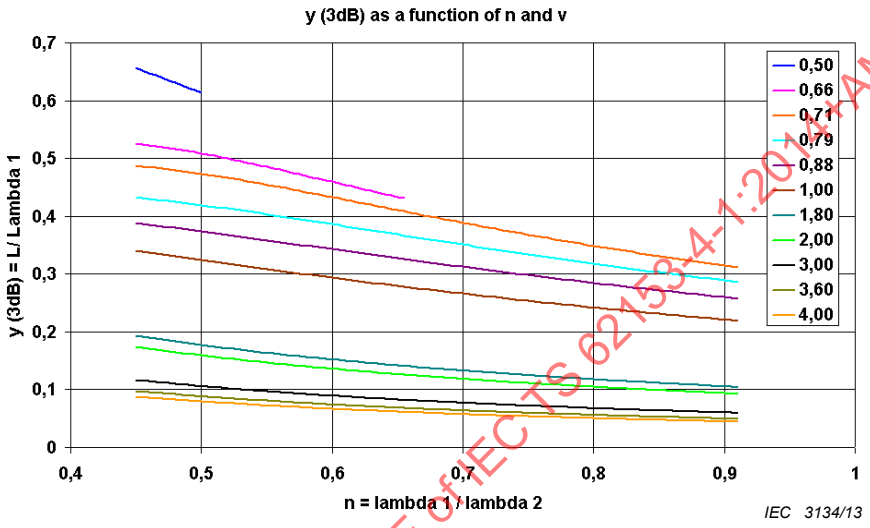

Key

Coloured lines correspond to indicated factors of $v=Z_2/R_{2f}$.

Figure 28 – Simulation of the 3 dB cut off wavelength (L/λ_1)

The graphs for $v=0{,}5$ and $v=0{,}66$ are only given for n up to 0,5 respectively 0,66 because otherwise the factor g oversoots as described above.

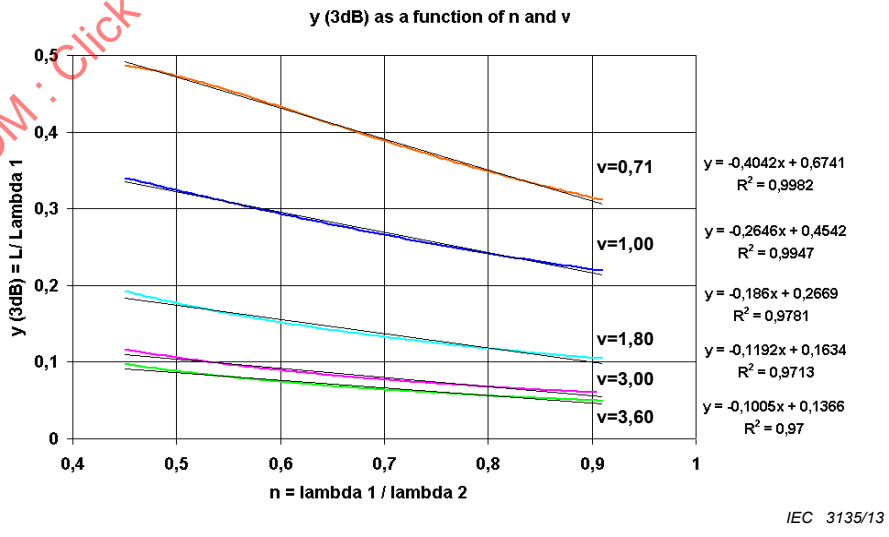

Key

Coloured lines correspond to indicated factors of $v=Z_2/R_{2f}$.

Figure 29 – Interpolation of the simulated 3 dB cut off wavelength (L/λ_1)

The linear interpolation equation is used to derive an equation to calculate the cut-off frequency length product up to which the transfer impedance could be measured in a given triaxial test set-up.

Table 5 – Cut-off frequency length product

Triaxial test set-up	v	Cut-off equation
EN 50289-1-6 IEC 61196-1 method 1 “feeding through a resistance IEC 62153-4-3 method A “matched-short”	v=1/√2	$(f \cdot L)_{3\ dB} \approx \left[\frac{200}{\sqrt{\varepsilon_{r1}}} - \frac{120}{\varepsilon_{r1}}\right] \cdot MHz \cdot m$
Simplified EN 50289-1-6 IEC 61196-1 method 2 “direct feeding”	v=1	$(f \cdot L)_{3\ dB} \approx \left[\frac{135}{\sqrt{\varepsilon_{r1}}} - \frac{80}{\varepsilon_{r1}}\right] \cdot MHz \cdot m$
	v=1,8	$(f \cdot L)_{3\ dB} \approx \left[\frac{80}{\sqrt{\varepsilon_{r1}}} - \frac{55}{\varepsilon_{r1}}\right] \cdot MHz \cdot m$
	v=3	$(f \cdot L)_{3\ dB} \approx \left[\frac{50}{\sqrt{\varepsilon_{r1}}} - \frac{35}{\varepsilon_{r1}}\right] \cdot MHz \cdot m$
	v=3,6	$(f \cdot L)_{3\ dB} \approx \left[\frac{40}{\sqrt{\varepsilon_{r1}}} - \frac{30}{\varepsilon_{r1}}\right] \cdot MHz \cdot m$

The equations given in Table 5 are drawn in the graphs of Figure 30.

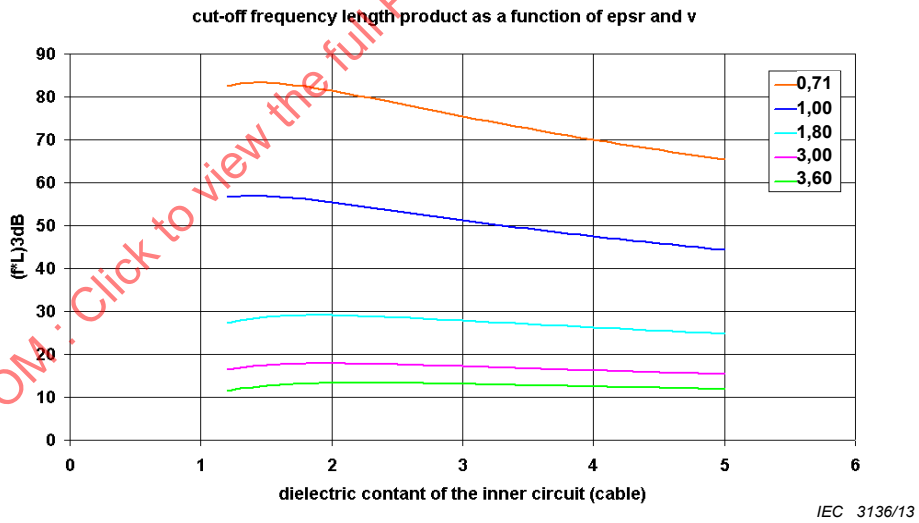

Key

Coloured lines correspond to indicated factors of $v=Z_2/R_{2f}$.

Figure 30 – 3 dB cut-off frequency length product as a function of the dielectric permittivity of the inner circuit (cable)

For example, if a cable with a PE insulation – dielectric permittivity of, ε_{r1} = 2,3, and a screen diameter of 3,5 mm is measured in a triaxial set-up according to EN 50289-1-6 or IEC 61196-1 method 1 “feeding through a resistance” with v=0,71, then the cut-off frequency length product is about 80 MHz·m. Therefore for a coupling length of 0,5 m, the maximum frequency to which the transfer impedance could be measured is around 160 MHz.

If the same cable is measured in a triaxial set-up according to IEC 61196-1 method 2 “direct feeding” or the simplified set-up according to EN 50289-1-6 where v=3, then the cut-off frequency length product is about 18 MHz·m. For a coupling length of 0,5 m, the maximum frequency to which the transfer impedance could be measured is around 36 MHz.

Figure 31 and Figure 32 show the measurement results of the normalised voltage drop – i.e. the attenuation caused by the series resistor has been taken into account – in the triaxial set-up for different factors of v. Both figures show the results of the same screen design, however one with a solid PE insulation (ε_{r1}=2,3), the other with a foam PE insulation (ε_{r1}=1,6). The measurement results confirm the simulations. From the equations given in Table 5 one obtains cut-off frequency length products for v=3 of about 18 MHz·m and for v=1 of about 55 MHz·m for both the solid PE and the foam PE. This is also found from the measurement results.

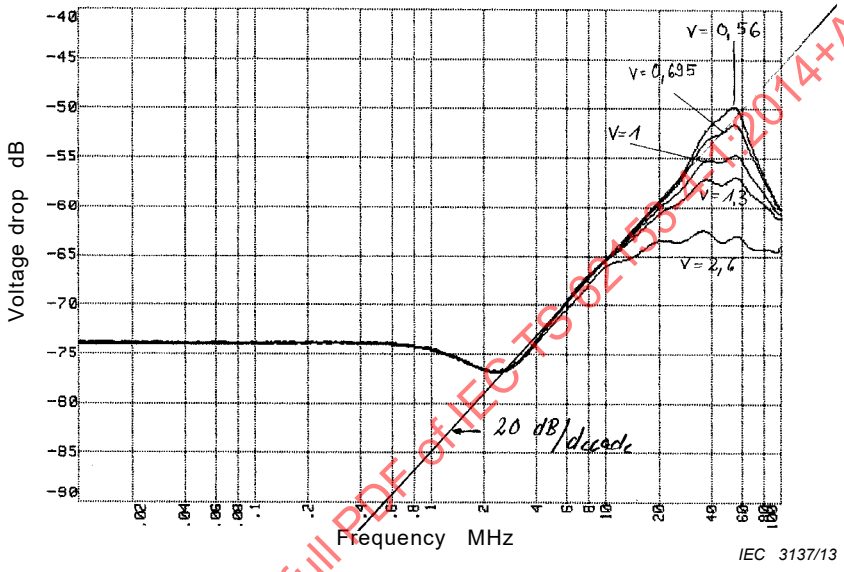

Key

Indicated lines correspond to factors of $v=Z_2/R_{2f}$

Measurement set-up parameters				
ε_{r1}	ε_{r2}	n	Z_2	L
2,3 (PE)	1,0	0,659	130 Ω	1 m

Figure 31 – Measurement result of the normalised voltage drop of a single braid screen on a solid PE dielectric in the triaxial set-up

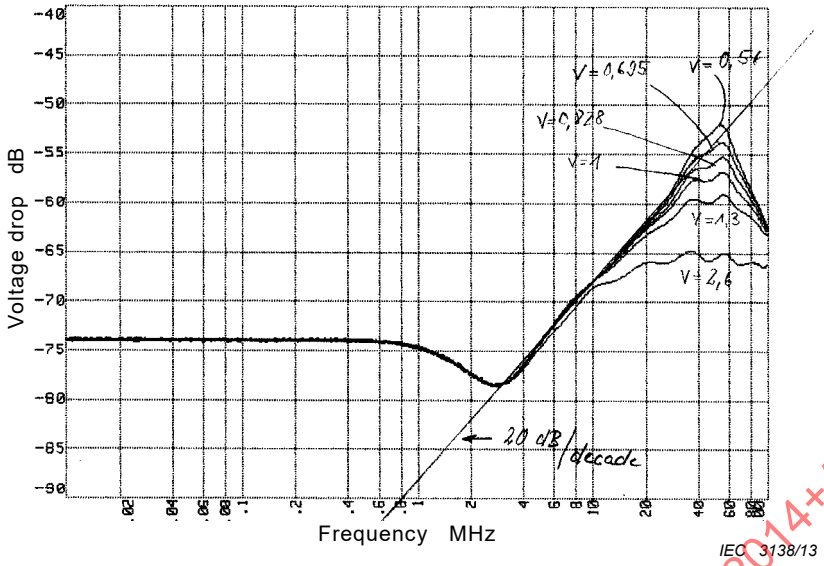

Key

Indicated lines correspond to factors of $v = Z_2/R_{2f}$

Measurement set-up parameters				
ε_{r1}	ε_{r2}	n	Z_2	L
1,6 (foam PE)	1,0	0,791	130 Ω	1 m

Figure 32 – Measurement result of the normalised voltage drop of a single braid screen on a foam PE dielectric in the triaxial set-up

9.3.3 Simulation of the double short circuited methods

9.3.3.1 General

For the double short circuited methods, one has either a measuring tube or a “milked on braid”. When using a measuring tube, the dielectric permittivity of the outer circuit (tube) is nearly independent on the sheath material and could be assumed to be 1. However in the “milked on braid” method, the dielectric permittivity is given by the sheath material. Thus the factor n is different for both methods. Also the impedance of the outer circuit is different for both methods, first due to the different dimensions, second due to the different permittivities.

9.3.3.2 Simulation of the double short circuited method using a measuring tube

The double short circuited method using a measuring tube is shown in Figure 33. The outer circuit is fed over a fixed – i.e. the same value for all cable types – feeding resistor, the value of which is equal to the output impedance of the generator (e.g. 50 Ω). Thus the load impedance of the outer circuit at the far end is equal to 2 times the output impedance of the generator. The factor v is then only dependent on the diameters of the screen and of the measuring tube.

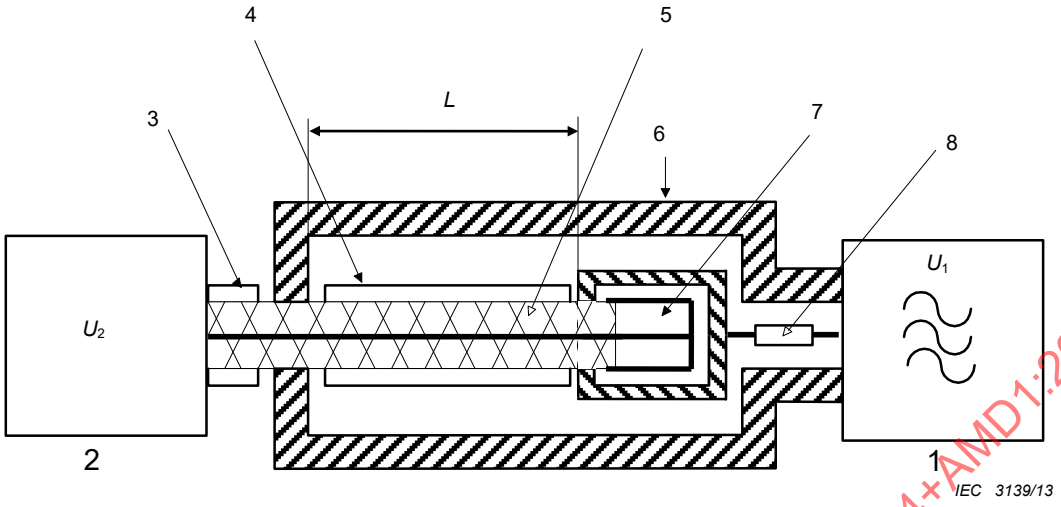

Key

1 signal generator
2 calibrated receiver or network analyzer
3 cable under test
4 cable sheath
5 cable screen
6 tube
7 short circuit
8 series resistor (50 Ω)

Figure 33 – Triaxial set-up (measuring tube), double short circuited method

Table 6 – Typical values for the factor *v*, for an inner tube diameter of 40 mm and a generator output impedance of 50 Ω

Screen diameter mm	**Z_2** Ω	***v*= Z_2/R_{2f}**
9	89	0,89
8	97	0,97
5	125	1,25
3,5	146	1,46
2	180	1,80

Those values have been used in the following simulations. The graphs in Figure 34 to Figure 37 show the simulated frequency response for different dielectric permittivities of the cable and for the different factors of *v* given in Table 6.

Figure 38 plots the results of calculation by iteration for the 3 dB cut-off wavelength (L/λ_1) at which the factor $|g|$ becomes $1/\sqrt{2}$. The curves have then been interpolated by straight lines.

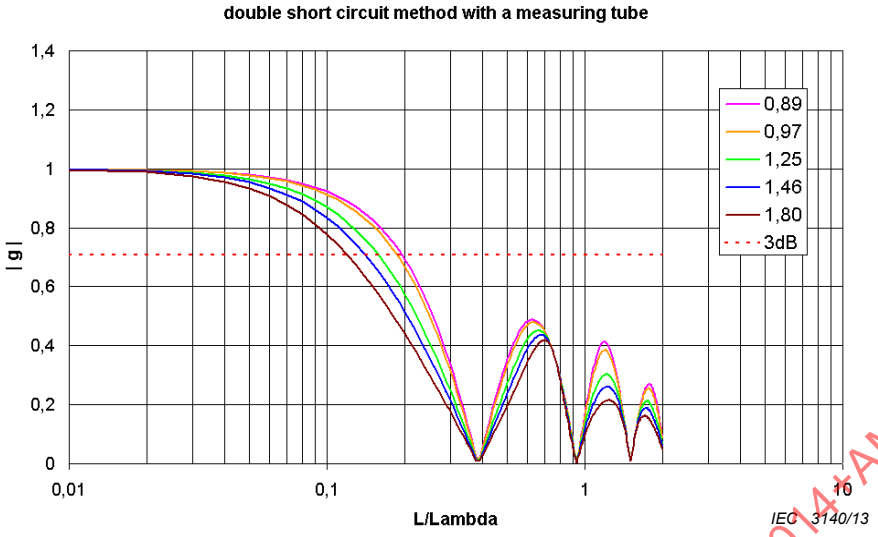

Key

Coloured lines correspond to indicated factors of $v=Z_2/R_{2f}$.

Simulation parameters		
ε_{r1}	ε_{r2}	n
2,3 (solid PE)	1,0	0,659

Figure 34 – Simulation of the frequency response for *g* of a cable having solid PE dielectric (ε_{r1}=2,3)

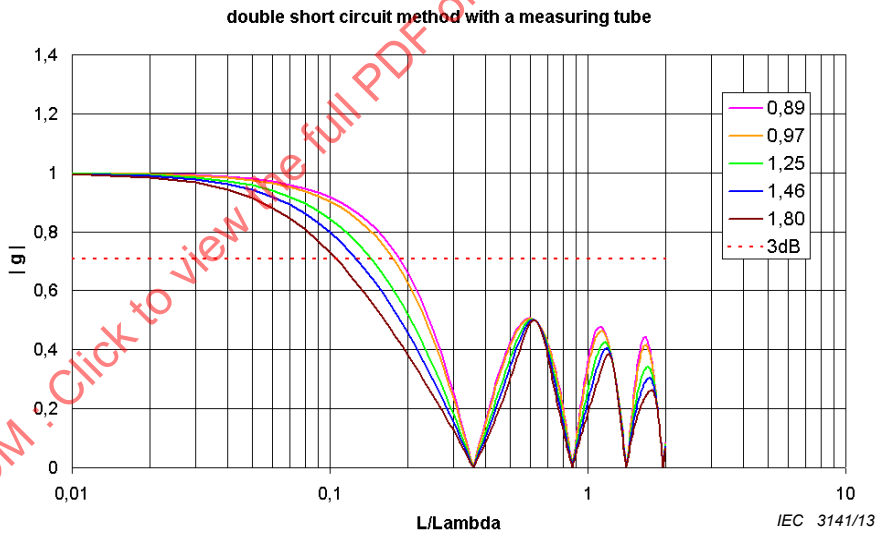

Key

Coloured lines correspond to indicated factors of $v=Z_2/R_{2f}$.

Simulation parameters		
ε_{r1}	ε_{r2}	n
1,6 (foam PE)	1,0	0,791

Figure 35 – Simulation of the frequency response for *g* of a cable having foamed PE dielectric (ε_{r1}=1,6)

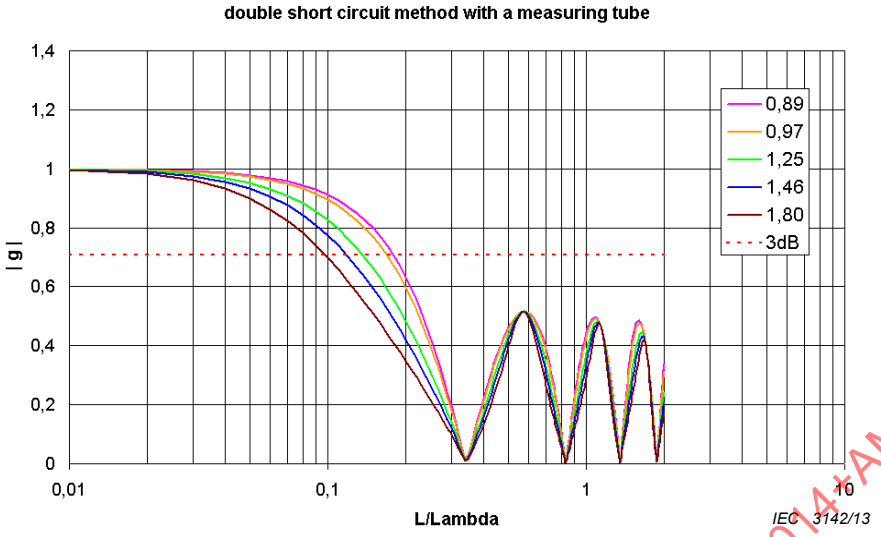

Key

Coloured lines correspond to indicated factors of $v = Z_2/R_{2f}$.

Simulation parameters		
ε_{r1}	ε_{r2}	n
1,3 (foam PE)	1,0	0,877

Figure 36 – Simulation of the frequency response for *g* of a cable having foamed PE dielectric (ε_{r1}=1,3)

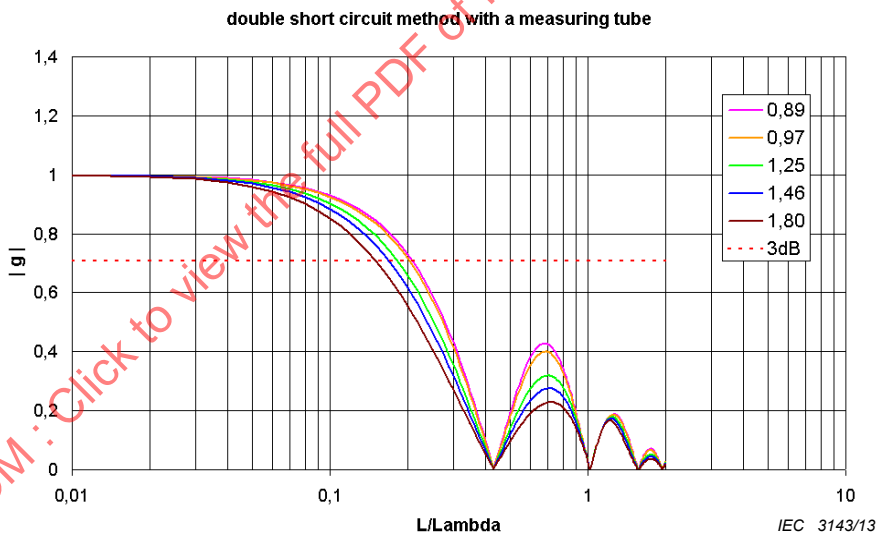

Key

Coloured lines correspond to indicated factors of $v = Z_2/R_{2f}$.

Simulation parameters		
ε_{r1}	ε_{r2}	n
5 (PVC)	1,0	0,447

Figure 37 – Simulation of the frequency response for *g* of a cable having PVC dielectric (ε_{r1}=5)

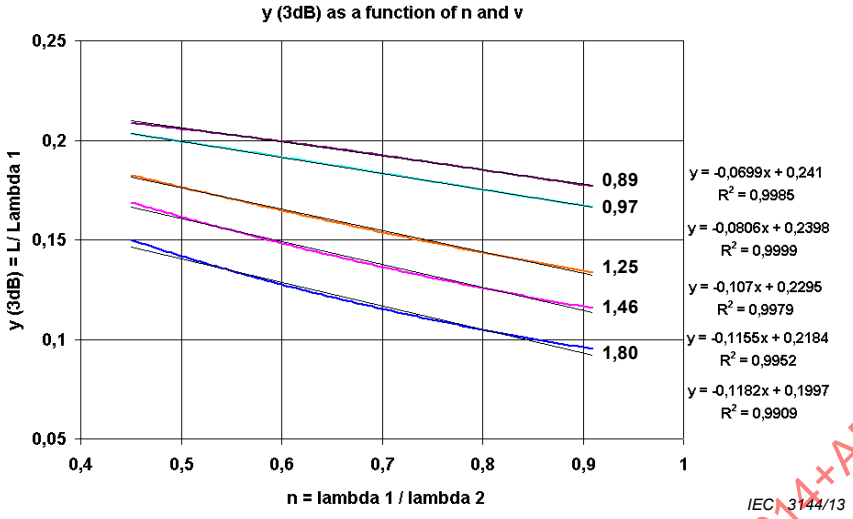

Key

Coloured lines correspond to indicated factors of $v=Z_2/R_{2f}$.

Figure 38 – Interpolation of the simulated 3 dB cut off wavelength (L/λ_1)

From the found linear interpolation, one can derivate following equations to calculate the cut-off frequency length product, to which the transfer impedance could be measured in the "double short circuit" triaxial set-up using a measuring tube.

Table 7 – Cut-off frequency length product

v=0,89	$(f \cdot L)_{3\ dB} \approx \left[\frac{70}{\sqrt{\varepsilon_{r1}}} - \frac{20}{\varepsilon_{r1}}\right] \cdot \text{MHz} \cdot \text{m}$
v=0,97	$(f \cdot L)_{3\ dB} \approx \left[\frac{70}{\sqrt{\varepsilon_{r1}}} - \frac{25}{\varepsilon_{r1}}\right] \cdot \text{MHz} \cdot \text{m}$
v=1,25	$(f \cdot L)_{3\ dB} \approx \left[\frac{68}{\sqrt{\varepsilon_{r1}}} - \frac{32}{\varepsilon_{r1}}\right] \cdot \text{MHz} \cdot \text{m}$
v=1,46	$(f \cdot L)_{3\ dB} \approx \left[\frac{65}{\sqrt{\varepsilon_{r1}}} - \frac{35}{\varepsilon_{r1}}\right] \cdot \text{MHz} \cdot \text{m}$
v=1,80	$(f \cdot L)_{3\ dB} \approx \left[\frac{60}{\sqrt{\varepsilon_{r1}}} - \frac{35}{\varepsilon_{r1}}\right] \cdot \text{MHz} \cdot \text{m}$

The equations given in Table 7 are plotted in the graphs of Figure 39. For example, if a cable with a PE insulation – dielectric permittivity of ε_{r1}=2,3 – is measured in a triaxial set-up with v=1,46 (screen diameter=3,5 mm, tube diameter=40 mm), then the cut-off frequency length product is about 27 MHz·m.: i.e. for a coupling length of 0,5 m, the maximum frequency to which the transfer impedance could be measured is around 60 MHz. If the same cable is measured in a triaxial set-up according to IEC 61196-1 method 2 "direct feeding" or the simplified set-up according to EN 50289-1-6 where v=3, then the cut-off frequency length product is about 18 MHz·m: i.e. for a coupling length of 0,5 m, the maximum frequency to which the transfer impedance could be measured is around 36 MHz. That is to say, that the

double short circuit method (using a measuring tube) facilitates the sample preparation, has a 6 dB higher dynamic range and also allows to measure the transfer impedance up to higher frequencies, compared to the simplified EN 50289-1-6 or IEC 61196-1 method 2 "direct feeding".

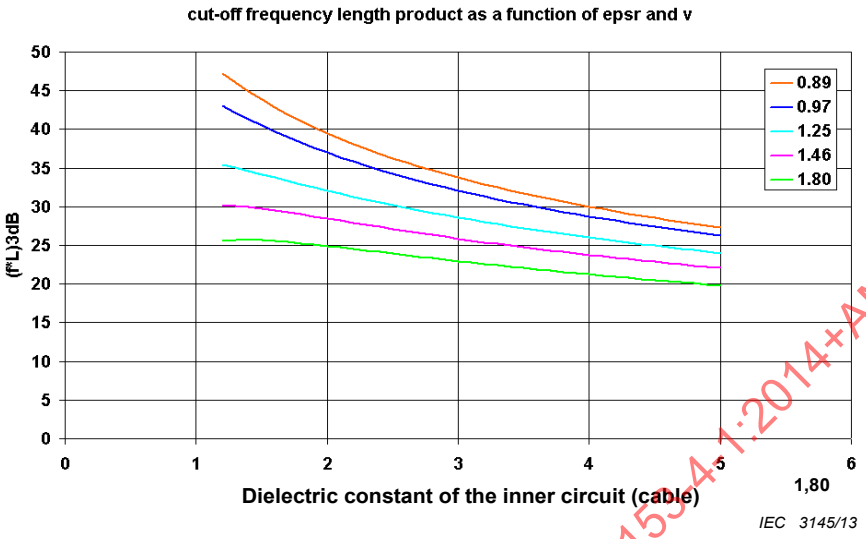

Key

Coloured lines correspond to indicated factors of $v=Z_2/R_{2f}$.

Figure 39 – 3 dB cut-off frequency length product as a function of the dielectric permittivity of the inner circuit (cable)

9.3.3.3 Simulation of the double short circuited method using a "milked on braid"

In the "milked on braid" method, a measuring braid is used instead of a measuring tube. The measuring braid is put directly over the sheath of the sample. Thus the dielectric permittivity of the outer circuit is given by the dielectric permittivity of the sheath (ε_{r2}=2…5), and the impedance of the outer circuit is given by the dielectric constant and the diameter over the sheath of the sample.

In this method, the inner circuit is fed over a 10 dB attenuation pad instead of a 50 Ω feeding resistor while using a measuring tube. However, using a 10 dB attenuation pad instead of a feeding resistor doesn't affect the cut-off frequency, as described below.

For cable screen diameters between 1 mm to 10 mm, sheath thickness between 0,2 mm to 1 mm and ε_{r2} between 2 and 5, the impedance in the outer circuit is between 5 Ω and 20 Ω, i.e. v between 0,1 and 0,4.

A closer look on the coupling equations (Equation (30) to Equation (38)) shows that for small values of the factor v and at low frequencies, the frequency response of the test set-up (factor g) becomes nearly independent of it. The worst case with respect to the 3 dB cut-off is reached if v=0. This is drawn out in the equations below and in Figure 40. Thus, in the following, the simulations are done for v=0.

$$N = \left\{ \cos x + \frac{\mathrm{j} \cdot \sin x}{r + w} \cdot \left[1 + r \cdot w \right] \right\} \cdot \left\{ \cos nx + \mathrm{j} \cdot v \cdot \sin nx \right\} \tag{39}$$

for small values of v, i.e. v<<1 and low frequencies, i.e. x<<1 one gets

$$N = \left\{\cos x + \frac{\mathrm{j}\cdot\sin x}{r+w}\cdot\left[1+r\cdot w\right]\right\}\cdot\left\{e^{\mathrm{j}\cdot nx} - \mathrm{j}\cdot(1 - v\cdot\sin nx)\right\} \tag{40}$$

$$\approx \left\{\cos x + \frac{\mathrm{j}\cdot\sin x}{r+w}\cdot\left[1+r\cdot w\right]\right\}\cdot\left\{e^{\mathrm{j}\cdot nx} - \mathrm{j}\right\}$$

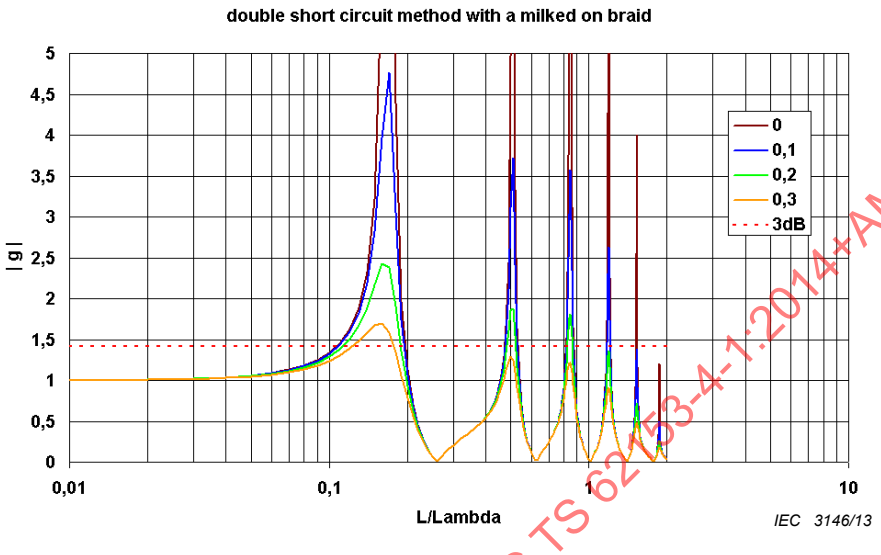

Key

Coloured lines correspond to indicated factors of $v=Z_2/R_{2f}$.

Simulation parameters		
ε_{r1}	ε_{r2}	n
2,3 (PE)	5 (PVC)	1,474

Figure 40 – Simulation of the frequency response for *g*

Taking into account typical combinations of insulation and sheath materials (PE/PVC, PE/LSZH, PTFE/FEP…), one gets values for the factor n between 1,02 and 2. Those values in Table 8 have been used for the iteration of the 3 dB cut-off wavelength (L/λ_1) shown in Figure 41.

Table 8 – Material combinations and the factor *n*

ε_{r1}	ε_{r2}	$n=\sqrt{\varepsilon_{r2}}/\sqrt{\varepsilon_{r1}}$
2,3 (PE)	5 (PVC)	1,47
	3 (LSZH)	1,14
1,6 (foam PE)	5 (PVC)	1,77
	3 (LSZH)	1,37
1,3 (foam PE)	5 (PVC)	1,96
	3 (LSZH)	1,52
2,0 (PTFE)	2,1 (FEP)	1,02
1,3 (expanded PTFE)	2,1 (FEP)	1,27

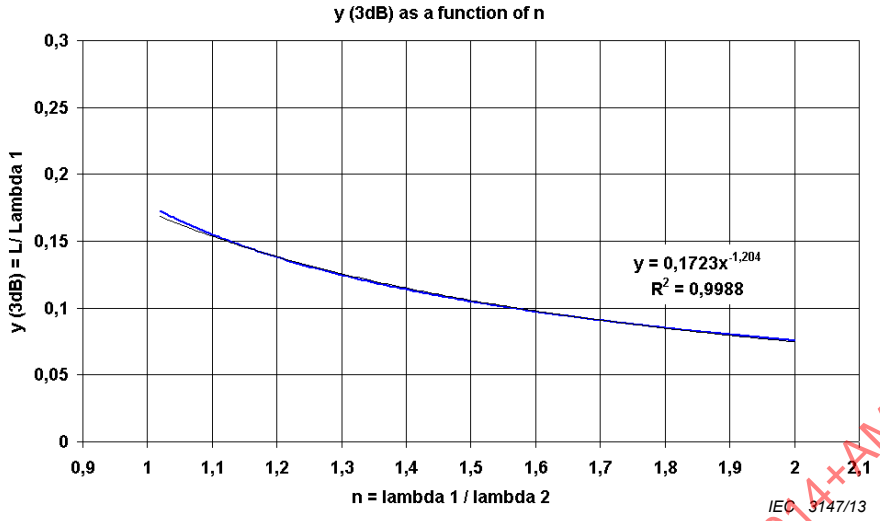

Key

Plotted line is for $v=Z_2/R_{2f} << 1$.

Figure 41 – Interpolation of the simulated 3 dB cut off wavelength (L/λ_1)

From the interpolation, one can derive following equation given in Table 9 for the 3 dB cut-off frequency length product. The equation in Table 9 is plotted in Figure 42.

Table 9 – Cut-off frequency length product

$v<<1$	$(f \cdot L)_{3\,\mathrm{dB}} \approx \left[\frac{50 \times n^{-1,204}}{\sqrt{\varepsilon_{r1}}}\right] \cdot \mathrm{MHz} \cdot \mathrm{m}$

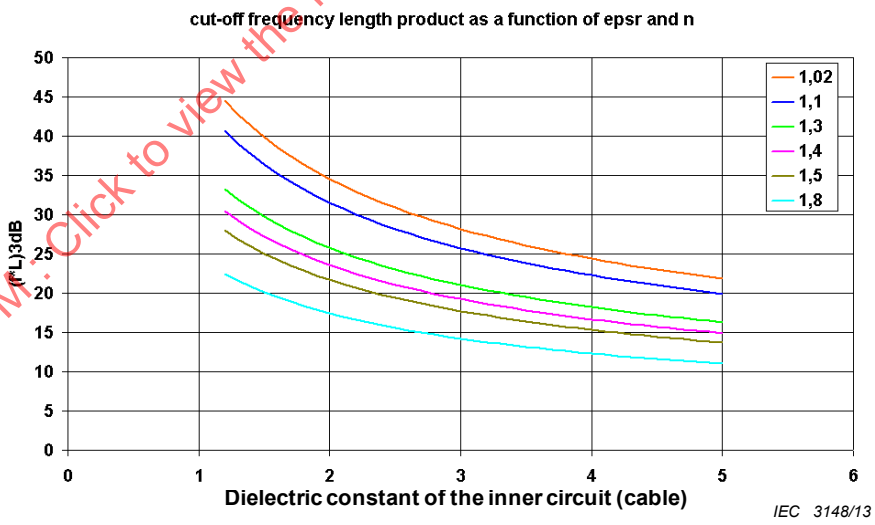

Key

Coloured lines correspond to indicated factors of $n=\sqrt{\varepsilon_{r2}}/\sqrt{\varepsilon_{r1}}$, for $v=Z_2/R_{2f} << 1$.

Figure 42 – 3 dB cut-off frequency length product as a function of the dielectric permittivity of the inner circuit (cable)

For example, a cable with PE insulation and PVC sheath (n=1,47) with the dimensions of a RG 58 (screen diameter around 3,5 mm) measured with the “milked on braid” method results in a cut-off frequency length product of 20 MHz·m. The same cable measured in the double

short circuit method with a measuring tube results in a cut-off length product of 27 MHz·m. If measured in the simplified EN 50289-1-6 method respectively one gets a cut-off frequency length product of 18 MHz·m. Thus the major advantage of the “milked on braid” method is that it allows for bending of the sample under test.

9.4 Conclusion

The best compromise between a simple test set-up and the cut-off frequency is given for the “double short circuit” method using a measuring tube. It covers the usually required frequency range of 100 MHz (see Table 10) for the transfer impedance measurement (using a 30 cm tube) and has the highest dynamic range of all triaxial methods.

The “milked on braid” method has a limited frequency range, requires a long sample preparation but allows for bending of the sample under test.

The matched method according to EN 50289-1-6, IEC 62153-4-3 method A “matched-short” respectively IEC 61196-1 method 1 “direct feeding” has the highest cut-off frequency but also the lowest dynamic range. An additional error source in that method is the accuracy of the series resistor which might have unknown frequency behaviour and thus an unknown attenuation.

Table 10 – Cut-off frequency length product for some typical cables in the different set-ups

Cable type	Sheath	EN 50289-1-6 IEC 61196-1 method 1 IEC 62153-4-3 method A	Double short circuit method using a tube	Double short method using a milked on braid
RG 58 (ε_{r1}=2,3)	PVC	80 MHz·m (v=0,71)	28 MHz·m (v=1,46)	20 MHz·m (n=1,47)
	LSZH			28 MHz·m (n=1,14)
Thin Ethernet (ε_{r1}=1,6)	PVC	83 MHz·m (v=0,71)	30 MHz·m (v=1,46)	20 MHz·m (n=1,77)
	LSZH			28 MHz·m (n=1,37)
RG 214 (ε_{r1}=2,3)	PVC	80 MHz·m (v=0,71)	35 MHz·m (v=0,97)	20 MHz·m (n=1,47)
	LSZH			28 MHz·m (n=1,14)
RG 8 (ε_{r1}=1,3)	PVC	83 MHz·m (v=0,71)	42 MHz·m (v=0,97)	20 MHz·m (n=1,96)
	LSZH			26 MHz·m (n=1,52)

10 Background of the shielded screening attenuation test method (IEC 62153-4-4)

10.1 General

In many cases, above all in the lower frequency range, the screening effectiveness of cables is described by the transfer impedance Z_T. It is, for an electrically short length of cable, defined (see Figure 43) as the quotient of the longitudinal voltage measured on the secondary side of the screen to the current in the screen, caused by a primary inducing circuit, related to unit length [23]. Although the transfer impedance Z_T covers only the galvanic and magnetic couplings, it is common practice to use it also as a quantity which includes the effect of the coupling capacitance C_T through the cable screen [24]. In this case, it is named equivalent

transfer impedance Z_{TE} which includes the effects of galvanic, magnetic and capacitive coupling.

For the determination of the proper coupling capacitance there is, as standardised quantity, the capacitance coupling admittance Y_T. The coupling admittance (see Figure 44) for an electrically short peace of cable is defined as the quotient of the current in the screen caused by the capacitive coupling in the secondary circuit to the voltage in the primary circuit related to unit length [23].

With electrically short cables, where wave propagation can be neglected, the screening quantities related to unit length can directly be used to calculate an induced disturbing voltage. In the higher frequency range, the implications get similar complicated as the transmission characteristics of a simple line, dependent on the impedance and admittance per unit length as well as on the terminating resistors.

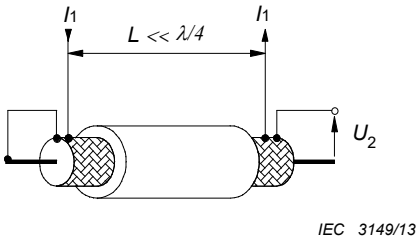

$$Z_T = \frac{U_2}{I_1 \cdot L}$$

Figure 43 – Definition of transfer impedance

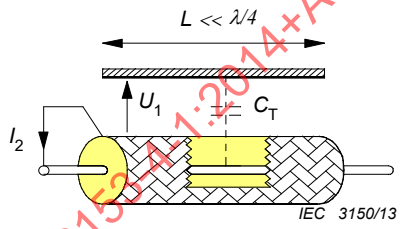

$$Y_T = \frac{I_2}{U_1 \cdot L} = \mathrm{j} \cdot \omega \cdot C_T$$

Figure 44 – Definition of coupling admittance

10.2 Objectives

It is desirable to measure and evaluate the screening efficiency of cable screens also in the wave propagation frequency range such that its characteristics can be directly applied. This requires a closer examination of the conditions of such applications.

In general, a system of electromagnetic induction consists of a transmission circuit in the cable, which is assumed to be fully defined, and of a surrounding transmission system, which is assumed to be universal with respect to the definition of cable screening. The screening effectiveness may be universally described by the maximum power output into the surroundings of the cable related to the power propagating in the cable. The power ratio is best expressed logarithmically as screening attenuation.

An often used procedure to determine the screening attenuation is the well-known “absorbing clamp method“ given in IEC 62153-4-5. The drawback of this method is that the set-up requires relatively much space, does not exclude environmental effects – unless the measuring area is enclosed in a shielded cabin –, and that the available absorbing clamp transformers considerably limit the measurement sensitivity.

It suggests itself to limit the free space such that the said problems don’t occur but wave propagation near the cable surface is not significantly changed. A triaxial measuring set-up is the solution. It has a one-sided short circuit between the metal tube and the cable screen. Power is fed into the terminated inner circuit of the cable and the disturbing power is measured at the opposite end of the outer circuit.

10.3 Theory of the triaxial measuring method

On the basis of the known reversibility of primary and secondary measuring circuits, the proposed measuring set-up, presented in Figure 45, is similar to the triaxial set-up for measuring the transfer impedance. The benefits of feeding the inner system, which is

terminated by its characteristic impedance, are the matching of the generator and reflection free wave propagation over the cable length.

The characteristic impedance of the outer circuit depends on the diameter of the measuring tube and the cable design. The effect of the mismatch in the outer circuit is discussed later on.

The equivalent circuit using lumped circuit elements (shown in Figure 46) facilitates the understanding of the theoretical relationships.

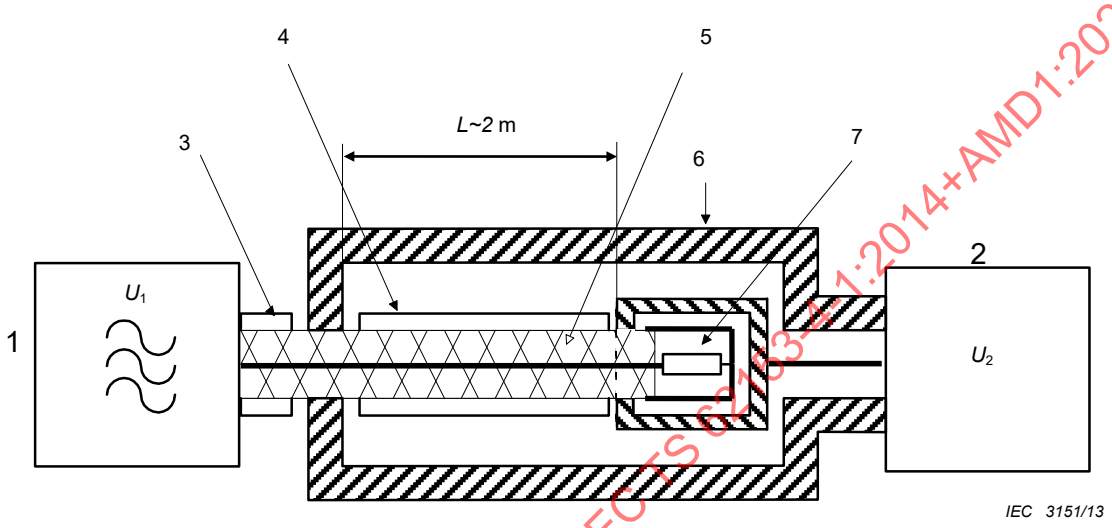

Key

1 signal generator
2 calibrated receiver or network analyzer
3 input voltage to cable under test
4 cable sheath
5 cable screen
6 tube
7 terminating resistor $R_1=Z_1$

Figure 45 – Triaxial measuring set-up for screening attenuation

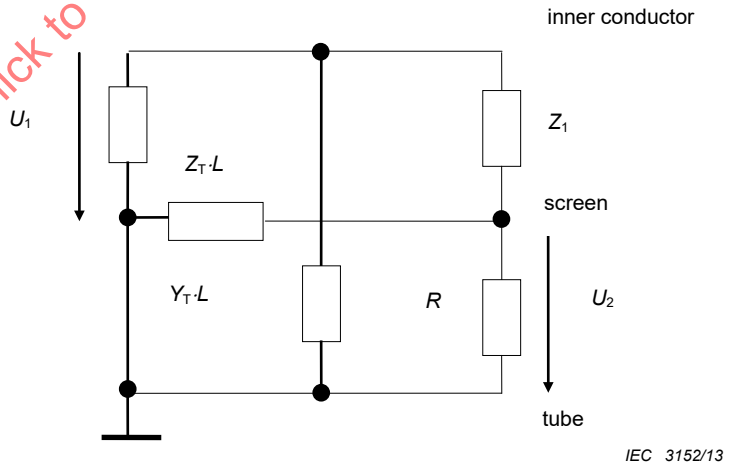

Figure 46 – Equivalent circuit of the triaxial measuring set-up

Based on the conditions of the objects to be measured, it is assumed that the transfer impedance Z_T is low and the reciprocal quantity of the coupling admittance Y_T is high in comparison with the characteristic impedances Z_1 and Z_2 and the load resistance R. Therefore, the feedback of the secondary circuit on primary circuit can be neglected.

When the frequency is low, one may consider the primary circuit shown in Figure 46 as a voltage divider and read the disturbing voltage ratio directly. The one-sided short circuit in the measuring circuit prevents the efficiency of the capacitance coupling admittance Y_T.

$$\frac{U_2}{U_1} \approx \frac{Z_T \cdot L}{Z_1} \tag{41}$$

In the high frequency range, where wave propagation has to be considered, one may expect the transfer impedance to be proportional to the frequency in most cases. Therefore it is expedient to use the following equation:

$$Z_T = R_T + j \cdot \omega M_T \approx j \cdot \omega M_T \tag{42}$$

and consider the effective mutual inductance per unit length M_T at high frequencies as an approximated constant quantity as it is usually done with the through capacitance C_T.

It is common practice to describe the capacitive coupling in the form of the capacitive coupling impedance Z_F, which is nearly invariant with respect to the geometry of the outer circuit (tube). [24], [27].

$$Z_F = Z_1 Z_2 Y_T = Z_1 Z_2 \cdot j \cdot \omega C_T \tag{43}$$

Furthermore, the attenuation constants α_1 and α_2 of the circuits may generally be neglected as, for example, the value of nearly 1 dB/m of the common cable type RG 58 at 3 GHz is relatively small compared to the usual measuring uncertainty.

In the relevant literature it is common practice to describe wave propagation in the form of phase constant [24], [25]. If the ratio between effective length and wave length is used instead of the phase constant, the periodic phenomena become clearer. With wave length λ_0 in free space or λ_1, λ_2 in the circuits 1 and 2, the following relation exists:

$$\beta_{1,2} \cdot L = 2\pi \cdot \sqrt{\varepsilon_{r1,2}} \cdot \frac{L}{\lambda_0} = 2\pi \frac{L}{\lambda_{1,2}} \tag{44}$$

According to the theory of wave propagation [25] and line crosstalk [26], a wave propagates in the matched inner circuit towards the matched end. In the outer circuit, a part of the induced wave propagates forwards to the measuring receiver and the other part is moving backwards to the short circuit. The total reflection at the short circuit reverses this backward wave and superposes it to the original forward wave, i.e. the sum can be obtained as measured value.

If the second circuit is matched at both ends, the backward wave would be measured at the generator end (near end) and the forward wave at the opposite end (far end) separately.

Hence equations for the near end are derived from [24]:

$$\frac{U_{2n}}{U_1} = \frac{Z_T + Z_F}{2Z_1} \frac{c_0}{j \cdot \omega\left(\sqrt{\varepsilon_{r1}} + \sqrt{\varepsilon_{r2}}\right)} \left\{1 - e^{-j2\pi\left(\sqrt{\varepsilon_{r1}} + \sqrt{\varepsilon_{r2}}\right)\frac{L}{\lambda_0}}\right\} \tag{45}$$

and for the far end:

$$\frac{U_{2f}}{U_1} = \frac{Z_F - Z_T}{2Z_1} \frac{c_0}{j \cdot \omega\left(\sqrt{\varepsilon_{r1}} - \sqrt{\varepsilon_{r2}}\right)} \cdot \left\{1 - e^{-j \cdot 2\pi\left(\sqrt{\varepsilon_{r1}} - \sqrt{\varepsilon_{r2}}\right)\frac{L}{\lambda_0}}\right\} \cdot e^{-j \cdot 2\pi \frac{L}{\lambda_2}} \quad (46)$$

Equations (47) and (48) are depicted in Figure 47 with the indicated parameters.

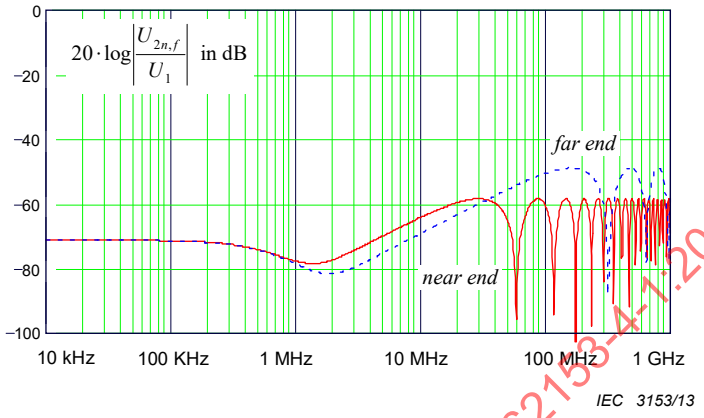

Calculation parameters

C_T	=	0,02	pF/m	M_T	=	0,4	nH/m
R	=	50	Ω	L	=	2	m
Z_1	=	50	Ω	ε_{r1}	=	2,3	
Z_2	=	120	Ω	ε_{r2}	=	1,1	

Figure 47 – Calculated voltage ratio for a typical braided cable screen

With a short circuit and an unmatched measuring receiver, these original voltage waves cause additional voltage portions. The sum of all voltage portions is zero at the shorted end (near end) and U_2 at the receiver end (far end). By use of the wave parameter and reflection factors or terminating resistors, it is possible to calculate all voltage portions and the voltage U_2 from the primary induced voltage waves, see Equation (45) and Equation (46):

$$\left|\frac{U_2}{U_1}\right| \approx \left| \frac{Z_T - Z_F}{\sqrt{\varepsilon_{r1}} - \sqrt{\varepsilon_{r2}}} \left[1 - e^{-j \cdot \varphi_1}\right] + \frac{Z_T + Z_F}{\sqrt{\varepsilon_{r1}} + \sqrt{\varepsilon_{r2}}} \cdot \left[1 - e^{-j \cdot \varphi_2}\right] \right| \cdot \left| \frac{1}{\omega \cdot Z_1} \right| \left| \frac{c_0}{2 + (Z_2 / R - 1) \cdot \left(1 - e^{-j\,\varphi_3}\right)} \right| \quad (47)$$

or in consideration of Equations (42) and Equation (43)

$$\left|\frac{U_2}{U_1}\right| \approx \left| \frac{M_T / Z_1 - C_T Z_2}{\sqrt{\varepsilon_{r1}} - \sqrt{\varepsilon_{r2}}} \left[1 - e^{-j \cdot \varphi_1}\right] + \frac{M_T / Z_1 + C_T Z_2}{\sqrt{\varepsilon_{r1}} + \sqrt{\varepsilon_{r2}}} \left[1 - e^{-j \cdot \varphi_2}\right] \right| \cdot \left| \frac{c_0}{2 + (Z_2 / R - 1) \cdot \left(1 - e^{-j \cdot \varphi_3}\right)} \right| \quad (48)$$

where

$$\varphi_1 = 2\pi\left(\sqrt{\varepsilon_{r1}} - \sqrt{\varepsilon_{r2}}\right)\frac{L}{\lambda_0} \qquad \varphi_2 = 2\pi\left(\sqrt{\varepsilon_{r1}} + \sqrt{\varepsilon_{r2}}\right)\frac{L}{\lambda_0} \qquad \varphi_3 = \varphi_2 - \varphi_1 = 4\pi\sqrt{\varepsilon_{r2}}\,\frac{L}{\lambda_0}$$

Calculated results for a typical braided cable screen are given in Figure 49. Another way to obtain the related induced voltage is given in [21].

The functional equation (see Figure 48)

$$\left|1 - e^{-j\cdot\varphi}\right| = \left|2 \times \sin(\varphi/2)\right| \quad \text{with } \varphi = \varphi_1, \varphi_2, \varphi_3 \tag{49}$$

shows that the equation of the voltage ratio contains three periodic partial functions of the ratio effective length L to wave length λ_0:

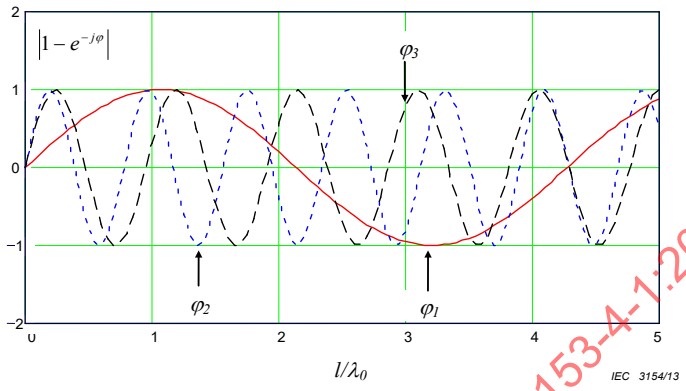

Figure 48 – Calculated periodic functions for ε_{r1} = 2,3 and ε_{r2} = 1,1

For low frequencies, when $L << \lambda_0$ and, consequently, $\sin(\varphi) \approx \varphi$, Equation (48) changes into Equation (42), the result of the common measuring method for the transfer impedance.

An example of the theoretical curve of the voltage ratio is shown in Figure 49 in two diagrams: The left one, a) with a logarithmic scale to extend the lower frequency range and the right one b) with a linear scale up to very high frequencies.

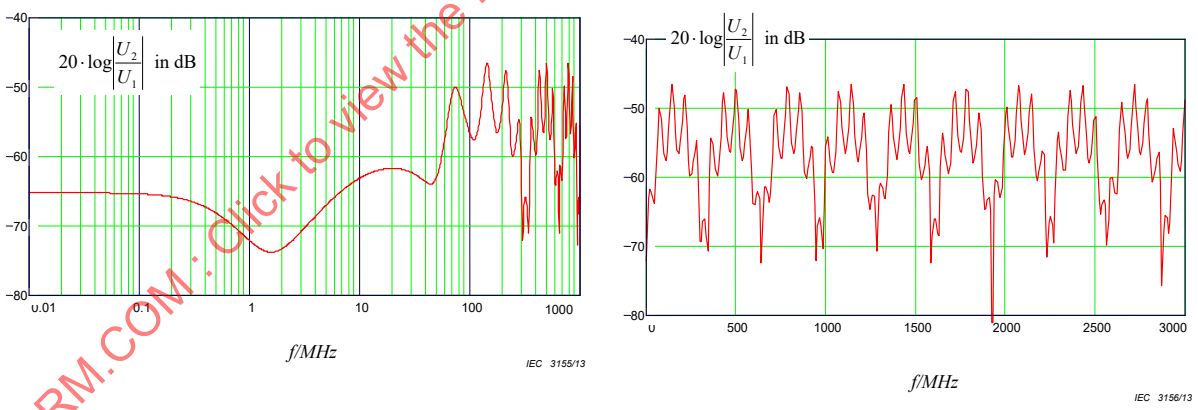

a) Logarithmic frequency scale

b) Linear frequency scale

Calculation parameters

C_T	=	0,02	pF/m	M_T	=	0,4	nH/m
R	=	50	Ω	L	=	2	m
Z_1	=	50	Ω	ε_{r1}	=	2,3	
Z_2	=	120	Ω	ε_{r2}	=	1,1	

Figure 49 – Calculated voltage ratio-typical braided cable screen

It is not useful to specify the induced power for an exact length of cable at a single frequency, anywhere between a minimum and maximum of the function. Only the periodic maximum voltage is important for the evaluation of the screening effectiveness. In the outer circuit, the wave propagation shall be nearly the same as in free space. Therefore, the characteristic

impedance Z_2 is higher than the common input resistance R of the measuring receiver, i.e. 50 Ω or sometimes 75 Ω.

Consequently, periodic maximum values of the voltage ratio are obtained from Equation (47) and Equation (48), which are independent of the input resistance of the receiver R and of effective cable length L:

$$\left|\frac{U_2}{U_1}\right|_{\max} \approx \frac{C_0}{\omega Z_1} \cdot \left| \frac{Z_T - Z_F}{\sqrt{\varepsilon_{r1}} - \sqrt{\varepsilon_{r2}}} + \frac{Z_T + Z_F}{\sqrt{\varepsilon_{r1}} + \sqrt{\varepsilon_{r2}}} \right| \tag{50}$$

or in consideration of Equation (42) and Equation (43):

$$\left|\frac{U_2}{U_1}\right|_{\max} \approx \left| \frac{M_T / Z_1 - C_T Z_2}{\sqrt{\varepsilon_{r1}} - \sqrt{\varepsilon_{r2}}} + \frac{M_T / Z_1 + C_T Z_2}{\sqrt{\varepsilon_{r1}} + \sqrt{\varepsilon_{r2}}} \right| \cdot c_0 \tag{51}$$

At first sight, C_T, Z_2, ε_{r2} and Z_F appear as random quantities which depend on freely chosen dimensions of the measuring tube. In reality, however, the voltage ratio is independent of the characteristic impedance of the outer circuit since $C_T \cdot Z_2$ and Z_F are practically invariant with respect to the dimensions of the measuring tube [24], [27]. Furthermore, the influence of the cable sheath on the resulting relative permittivity ε_{r2} is negligible if the design of the measuring tube takes into account the requirement for a wave propagation which is approximately the same as in the free space; in consequence $\varepsilon_{r2} \approx 1{,}0$.

The periodic maximum value is independent of the effective length L and frequency f or wave length λ. A measured frequency response would hint at a frequency-related quantity rather than the pure mutual inductance M_T.

As it is seen from Figure 48 and Figure 49, the envelope rise is reached with the first maximum of the wide period at:

$$\frac{\lambda_0}{L} \leq 2 \cdot \left| \sqrt{\varepsilon_{r1}} - \sqrt{\varepsilon_{r2}} \right| \quad \text{or} \quad f > \frac{C_0}{2 \cdot L \cdot \left| \sqrt{\varepsilon_{r1}} - \sqrt{\varepsilon_{r2}} \right|} \tag{52}$$

In this frequency range, Z_T can be calculated if Z_F is negligible:

$$|Z_T| \approx \frac{\omega \cdot Z_1 \cdot |\varepsilon_{r1} - \varepsilon_{r2}|}{2 \cdot c_0 \cdot \sqrt{\varepsilon_{r1}}} \cdot \left|\frac{U_2}{U_1}\right|_{\max} \tag{53}$$

10.4 Screening attenuation

The screening attenuation is defined as the logarithmical ratio of the maximum power in the secondary (outer) circuit to the power propagating in the primary (inner) circuit.

$$a_s = -10 \times \log_{10}\left(\mathrm{Env} \left| \frac{P_{r,\max}}{P_1} \right| \right) \tag{54}$$

The power coupled into the outer circuit depends on Z_2 although the peak voltage is independent of it. Thus a normalised value of the characteristic impedance of the outer circuit Z_s must be defined. It is common practice to define Z_s = 150 Ω [24].

In the standardised "absorbing clamp method" (see IEC 62153-4-5), the outer circuit is matched with Z_2, and the radiated power is the sum of the near end and far end crosstalk. From the comparison of that measuring circuit with the measuring circuit of the triaxial method results the relation of the measured power to the radiated power.

The equivalent circuit for an electrical short part of the length ΔL and for a negligible capacitive coupling illustrates the circumstances in Figure 50.

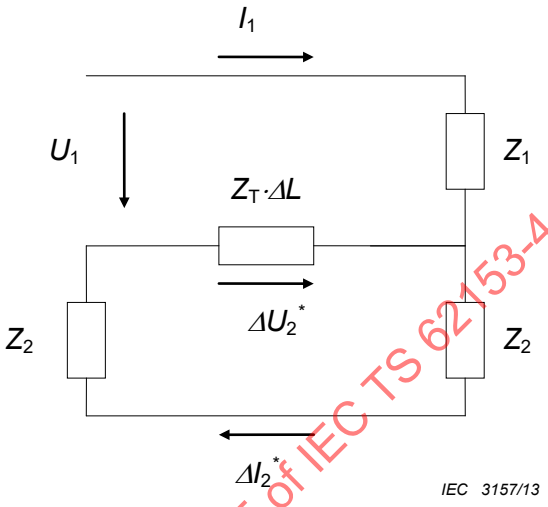

Figure 50 – Equivalent circuit for an electrical short part of the length Δl and negligible capacitive coupling

The power in the primary circuit is:

$$P_1 = U_1 \cdot I_1 = \frac{U_1^2}{Z_1} = I_1^2 \cdot Z_1 \tag{55}$$

The power in the secondary circuit, which is coupled by the transfer impedance Z_T is

$$P_2{}^* = \Delta U_{2^*} \cdot \Delta I_{2^*} \quad \Delta U_{2^*} = I_1 \cdot Z_T \cdot \Delta L \tag{56}$$

$$\Delta I_2^* = \frac{\Delta U_2^*}{2 \cdot Z_2} \tag{57}$$

Thus

$$\frac{P_2^*}{P_1} = \frac{\left(\Delta U_2^*\right)^2}{2 \cdot Z_2} \cdot \frac{1}{I_1^2 \cdot Z_1} = \frac{\left(Z_T \cdot \Delta L\right)^2}{2 \cdot Z_1 \cdot Z_2} \tag{58}$$

If the secondary circuit is short circuited at one end and terminated by R at the other end, the power measured at R is

$$\frac{P_2}{P_1} = \frac{(Z_T \cdot \Delta L)^2}{Z_1 \cdot R} \tag{59}$$

Thus

$$\frac{P_2^*}{P_2} = \frac{R}{2Z_2} \tag{60}$$

or in the case of radiation due to the normalised characteristic impedance of the environment

$$\frac{P_r}{P_2} = \frac{P_{r,max}}{P_{2,max}} = \frac{R}{2Z_s} \tag{61}$$

Thus the screening attenuation is calculated by:

$$\begin{aligned} a_s &= 10 \times \log_{10} \left| \frac{P_1}{P_{r,max}} \right| = 10 \times \log_{10} \left| \frac{P_1}{P_{2,max}} \cdot \frac{2Z_s}{R} \right| \\ &= 10 \times \log_{10} \left| \left(\frac{U_1}{U_{2,max}} \right)^2 \cdot \frac{2Z_s}{Z_1} \right| \\ &= 20 \times \log_{10} \left| \frac{U_1}{U_{2,max}} \right| + 10 \times \log_{10} \left| \frac{300}{Z_1} \right| \end{aligned} \tag{62}$$

10.5 Normalised screening attenuation

From Equation (50), it is seen that the maximum voltage ratio and therefore the screening attenuation is a function of the velocity difference between the primary and secondary circuit. Therefore the test results may also be presented for normalised conditions where Z_s = 150 Ω and the velocity difference $|\Delta v/v_1|$ = 10 % or $\varepsilon_{r1}/\varepsilon_{r2,n}$ = 1,21.

The normalised screening attenuation is calculated by:

$$a_{s,n} = 20 \times \log_{10} \left| \frac{\omega \cdot \sqrt{Z_1 \cdot Z_s} \cdot \left| \sqrt{\varepsilon_{r1}} - \sqrt{\varepsilon_{r2,n}} \right|}{Z_T \cdot c_0} \right| \tag{63}$$

With respect to Equation (50), Equation (62) and Equation (63) and assuming negligible Z_F, the difference Δa of the normalised and the measured screening attenuation is given by:

$$\Delta a = a_{sn} - a_s = 20 \times \log_{10} \left(\sqrt{2} \cdot \frac{\left| 1 - \sqrt{\frac{\varepsilon_{r2,n}}{\varepsilon_{r1}}} \right|}{\left| 1 - \frac{\varepsilon_{r2,t}}{\varepsilon_{r1}} \right|} \right) \tag{64}$$